





Overland flood modelling in data sparse regions

By

Olumese Gibson Efeovbokhan

May 2022

Abstract

Flood events pose significant threats to urban areas necessitating the development of effective flood risk management strategies. In many low-income countries, inadequate policies on flood disaster management, coupled with the large population of inhabitants that reside at strategic locations such as the coastal regions of such dwellings, make flood forecasting an important decision-making tool and policy driver. The flood risk that threatens these coastal cities is exacerbated by climate change-induced weather conditions such as an increased frequency of storm events, high humidity, and sea level rise. The devastation caused by such weather events is aggravated by high runoffs that occur in urbanised areas and saturated soils. Unfortunately, most of these coastal cities in these low-income countries, have a large population exposed to flooding. They also lack accurate meteorological and readily available topographical data, which poses numerous challenges when attempting to understand the dynamics of floods in such countries. This study focuses on enhancing the effectiveness and accuracy of pluvial flood modelling in data-sparse regions of the developing world by investigating validation criteria, low-cost data generation methods, sub-catchment representation of hydrological processes, and a comparative analysis of UAV photogrammetry and LiDAR terrain data. The study area consists of 3 sub-catchments in Lagos State and is from parts of Lagos Island, Ikoyi, and Victoria Island. In this study, the Digital Terrain Model (DTM) used was derived from LiDAR data captured by Gemini 167 ALTM equipment in March 2009 with 1m spatial resolution. This study also utilised photogrammetry point-cloud acquisition using a vertical take-off and landing UAV to generate DTM. The rainfall data used in this study was the daily rainfall depth measurements obtained from the weather monitoring station at the Nigeria Meteorological Agency (NiMET), and the 5-hour crowd-sourced rainfall depth obtained on July 8th, 2017, was 176.5 mm. A specific methodology was used for manipulating the terrain data to generate a DTM, assessing the DTM's suitability for hydrological modelling and conducting hydrological analysis of the DTM to delineate the sub-catchments that were used for the model calibration process. In a bid to ascertain the suitability of generating flood forecasts for data-sparse regions, some criteria were developed to suit these regions, and the sparse data available was utilised for hydrological model simulations of the historical flood event using a simple and complex modelling approach. This was achieved using two flood models, FloodMap hydro-inundation 2D and City Catchment Analysis Tool, in their simplified and complex forms, respectively, for the simulation of the historical flood event. The outcome of the results for the two hydrological models was further compared using their point depths and validation data obtained. The research also sought alternative ways of generating terrain data for flood forecasting and utilized photogrammetric data obtained by unoccupied aerial vehicles for this purpose. The results from this study showed that the drainage capacity of a catchment area had the greatest influence on modelled flood extent over all other model parameters (hydraulic conductivity and Manning's roughness). This posits that the drainage capacity of a catchment area greatly affects the flooding that such catchments are susceptible to. Therefore, the formulation of flood policies required to build flood resilience in such catchment areas need to focus on improving the drainage capacity of such regions by

maintaining the hydrological function in such terrain and also reducing runoff resulting from storm events in these areas by adopting blue-green city concepts. The principle here is that the smaller the amount of water resulting in runoff, the less susceptible such catchment areas would be to flooding. Alternative approaches for generating data for flood forecasting were examined in this study, especially the role that unoccupied aerial vehicles could play in bridging these gaps caused by data unavailability. The results show good promise in the application of photogrammetric data obtained by unoccupied aerial vehicles for flood modelling, despite some differences in comparing the terrain output with data generated from high-tech LiDAR approaches. This approach marks a remarkable shift in the way flood risk management can be conducted in such data-sparse regions and is a possible approach to overcome the terrain data sparsity in flood modelling and greatly assist in forecasting floods. Continuous challenges of flooding in data-sparse regions would linger unabated if proactive approaches to forecasting floods are not sought. The study also confirmed that Nigeria had no defined flood policy where plans, research, and resources aimed specifically at reducing flood risk were clearly outlined. The country only has a National Disaster Response Plan to guide its activities during a disaster and this covers about 13 disasters that Nigeria was susceptible to. The absence of a specific flood policy for Nigeria further aggravates the problem of enacting favourable flood risk management strategies for the country. A flood policy in Nigeria would allocate resources to drive favourable flood risk management and also result in a shift from the reactive approach to managing floods in the country to a proactive flood risk management strategy. A flood policy would further curb the current lax building regulations in the country that result in increased runoff, including the blockage of drainage lines, and evolve approaches to prevent the alteration of the hydrological function of such urban landscapes, such as the adoption of blue-green city concepts to build the resilience of these societies to flooding.

Dedication

This PhD research is dedicated to my dear mother, Mrs Justina Omonsefe Efeovbokhan (1957-2016) and my darling wife, Dr Sharon Gibson Efeovbokhan (1984-2020).

Acknowledgement

I am indeed indebted to numerous people and establishments for being able to successfully submit this PhD thesis. I was granted a scholarship for this PhD from the Petroleum Technology Development Fund (PTDF) Nigeria. I thank the organisation for the scholarship considering the economic hardship currently faced in my country. I also thank the Nigerian Military for granting my application for study leave and the subsequent extensions I applied for. I intend to ensure the outcome of this research drives favourable flood risk management policies to justify the resources and time I spent undertaking the study.

My profound gratitude goes to the University of Nottingham for providing the stimulating intellectual environment for this study. I am specifically grateful to my first supervisor Dr Nick Mount who guided me even before I came to Nottingham to commence the PHD and throughout the duration of the study. Nick, you have been a mentor whose positive criticism and strive for perfection spurred me into going the extra mile to produce this work, worthy to be submitted as a PhD thesis. You were fully interested in my welfare during challenging times and have been an inspiration to me. I am most grateful to you Nick and appreciate all your efforts. My gratitude extends to my second supervisor, Prof Doreen Boyd for all her guidance and direction throughout the PhD. You constantly shared numerous materials to guide my work and also sacrificed valuable time to peruse my drafts to ensure my works measured up to acceptable standards. Your candid concern for my success and personal wellbeing as a doctoral student is indescribable. Doreen, I thank you for the constant motivation and direction you gave me throughout this PhD. I am indeed blessed to have you both as my supervisors for this PhD. My thanks extend to Prof Dapeng Yu and Dr Steve Birkinshaw of Loughborough and Newcastle Universities respectively. I was introduced to both of you my first supervisor Dr Nick Mount and I used hydrological models from your universities for my PhD. I appreciate the guidance and direction you both gave me throughout my PhD.

I humbly thank my dear dad, Major General Mathias Efeovbokhan (retired) for all his prayers, support and assistance throughout this PhD, especially during the challenging times I had. Dad, you indeed proved to be a father like no other as you sacrificed everything to ensure the wellbeing of my kids and myself. I am most grateful to you for all your contribution towards the completion of this PhD. I say ‘obilu aba’ ‘obulu aba’ and ‘obebhalu eramwen’ in our native dialect to show my gratitude. My thanks extend to my dear brothers, Drs’ Elvis and Nosa Efeovbokhan and their families. I am grateful to you guys for the constant support throughout this PhD. We were indeed raised as a team and will always remain ‘Team Efeovbokhan’. I specially thank my darling wife of blessed memory Dr Sharon Gibson Efeovbokhan. You were indeed my pillar when I took on this PhD and I am proud to tell you it is finally complete. Keep watching over us from above until we meet to part no more. I thank my dear kids, Zuriel and Medad Efeovbokhan for all the emotional support throughout this research work. The constant whispers of ‘everything’s gonna be okay dad’ sure kept me going. I am indeed blessed to have such wonderful kids. God bless you guys. I wish to acknowledge the efforts of my fieldwork assistant Yemi for all the support and sacrifice when I went to the study area

for my fieldwork. I am most grateful for all the ideas and contribution to ensure I got the relevant data required for my research. My thanks extend to my relatives, aunts, uncles, the Izunyons and my in-laws for all the support throughout the duration of this PhD.

I cannot end this acknowledgement without thanking the Cornerstone Church community, superior officers, and my friends for all their support. I am grateful to Major General C Airhiavbere (rtd) and Major General AB Omozoje for all the support throughout this PhD. I also thank Dr Ephraim, Tim, Drs' Seun, Victor and Emma, the Edimes', Mr Caleb and the entire Overseas Fellowship of Nigerian Christians for all the support throughout this PhD. I am indeed grateful.

Above all, I give thanks to God Almighty for keeping me safe and giving me the strength to complete this PhD thesis.

Declaration

I declare that no portion of the work referred to in this thesis has been submitted in support of an application for any other degree or qualification in this university or any other institute of learning. The results and findings embodied in this thesis are the works of the named candidate.

Abbreviations

ALOS	Advanced Land Observing Satellite
CityCAT	City Catchment Analysis Tool
CRED	Centre for Research on the Epidemiology of Disasters
DC	Drainage Capacity
DEFRA	Department for Food, Environment and Rural Affairs
DGPS	Differential Global Positioning System
DRU	Disaster Response Unit
DTM	Digital Terrain Model
EA	Environmental Agency
ESA	European Space Agency
FCERM	Flood and Coastal Erosion and Risk Management
FDM	Flood Disaster Management
FFWS	Flood Forecasting and Warning System
FGN	Federal Government of Nigeria
FloodMap	FloodMap Hydro-inundation 2D Model
FME	Federal Ministry of Environment
FRM	Flood Risk Management
FWMA	Flood and Water Management Act
GCP	Ground Control Point
GIS	Geographical Information System
HC	Hydraulic Conductivity
ICRC	International Community of the Red Cross
IDP	Internally Displaced Persons
IPCC	Intergovernmental Panel on Climate Change
LGA	Local Government Area
LiDAR	Light Detection and Ranging
LULC	Land Use Land cover

MAE	Mean Absolute Error
MC	Mannings Coefficient
NASRDA	National Space Research and Development Agency
NDRP	National Disaster Response Plan
NEMA	National Emergency Management Agency
NESERA	National Environmental Standards and Regulations Enforcement Agency
NIHSA	Nigeria Hydrological Services Agency
NiMET	Nigerian Meteorological Agency
NIOMR	Nigerian Institute for Oceanography and Marine Research
NOA	National Orientation Agency
OSGOF	Office of the Surveyor General of the Federation
RF	Random Forest
RMSE	Root Mean Square Error
ROC	Receiver Operating Characteristics
SfM	Structure-from-Motion
SRTM	Shuttle Radar Topography Mission
TIN	Triangulated Integrated Network
UAV	Unoccupied Aerial Vehicles
WFI	World Flood Index

Table of Contents

Abstract ii
Dedication iv
Acknowledgement v
Declaration vii
Abbreviations viii
Chapter 1: Introduction 1
1.1 Background 1
1.2 Aim 4
1.3 Research Questions 4
1.4 Objectives 5
1.5 Research structure 5
Chapter 2: A review of data required for flood modelling and flow routing processes 8
2.1 Overview of Flood Models 8
2.2 Data requirements for flood modelling 11
2.2.1 Topographical/Terrain data for flood modelling 14
2.2.2 Meteorological data for flood modelling 16
2.3 Hydraulic and hydrological processes in flood modelling 18
2.3.1 Surface roughness 18
2.3.2 Infiltration/Hydraulic conductivity 19
2.3.3 Evapotranspiration 20
2.4 Flood modelling at large and small scales 21
2.5 Factors affecting choice of flood models for simulating flood. 21
2.6 Defining criteria for testing the meaningfulness of flood forecasting in urbanized data sparse regions 23
2.7 Testing the validity of flood forecasts in data sparse coastal regions 26
2.7.1 Model parameterization 26
2.7.2 Accuracy 26
2.7.3 Reliability of flood forecasts 28
2.7.4 Replicability of flood forecasts 28
2.7.5 Simplicity 28
2.7.6 Computational demand 29
2.7.7 Robustness 29
2.7.8 Transferability 30

2.7.9 Sustainability 30
2.8 Summary of Chapter 2 30
Chapter 3: Flood risk management in the study area and data available for pluvial flood modelling 31
3.1 Overview of flooding in Nigeria 31
3.2 Study area and flood risk management 36
3.3 Nexus of the geography of Lagos and flooding 38
3.4 Flood risk management in Nigeria 39
3.5 Flood risk management in regions with varying data availabilities 40
3.5.1 FRM in the Netherlands 40
3.5.2 FRM in the United Kingdom 41
3.5.3 FRM in Bangladesh 42
3.5.4 FRM in Beira, Mozambique 43
3.6 Challenges of flood risk management in the study area 44
3.6.1 Lack of a Policy on flood risk management. 44
3.6.2 Insufficient Budget Allocation for Disaster Management. 44
3.6.3 Insufficient Skilled Personnel for FRM and Unavailable Data for Analysis. 45
3.6.4 Flood disaster management minimal at the local level. 45
3.6.5 Poor urban development regulations and lax regulations 46
3.7 Summary of Chapter 3 48
Chapter 4: Methodology for data processing, model parameterization and pluvial modelling in data sparse regions 49
4.1 Overview of Chapter 4 49
4.2 Methodology for processing data and flood modelling 49
4.2.1 Terrain Data and Analysis 51
4.2.2 DTM Generation and Validation 51
4.2.3 Accuracy assessment of Generated DTM for Hydrological Modelling 53
4.3 Terrain analysis 56
4.4 Rainfall Data Manipulation 58
4.5 Description of FloodMap-HydroInundation 2D 60
4.5.1 Modelling surface flow 61
4.5.2 Modelling infiltration 61
4.5.3 Representing drainage 62
4.5.4 Flood loss from evapotranspiration 62

4.6 Parameter Representation in FloodMap-HydroInundation 2D 63
4.6.1 Representing buildings in FloodMap 63
4.6.2 Mannings roughness coefficient 63
4.6.3 Hydraulic conductivity 65
4.6.4 Drainage loss 65
4.6.5 Evapotranspiration 66
4.7 Parameters adopted for the FloodMap model 66
4.8 Pluvial Flood Modelling using FloodMap 67
4.9 Description of CityCAT 71
4.9.1 Modelling Surface Flow 71
4.9.2 Depicting Buildings in CityCAT 71
4.9.3 Modelling Infiltration in CityCAT 71
4.9.4 Modelling roof Drainage in CityCAT 72
4.10 Parameter representations in CityCAT 72
4.10.1 Representing Rainfall in CityCAT 72
4.10.2 Representing buildings in CityCAT 73
4.10.3 Modelling surface flow 75
4.10.4 Modelling infiltration 75
4.10.5 Flood loss from evapotranspiration 75
4.10.6 Representing green areas in CityCAT 75
4.11 Parameters adopted for CityCAT 75
4.12 Pluvial Flood Simulation using CityCAT 77
4.13 Summary of Chapter 4 81
Chapter 5: Generation of validation data for flood models in data sparse regions 82
5.1 Overview of Chapter 5 82
5.2 Generating low-cost flood model validation data in regions affected by data sparcity 82
5.2.1 Filtering crowdsourced information 84
5.2.2 Extracting flood depth from crowd sourced information 84
5.3 Application of crowd sources in generating flood validation data 90
5.3.1 Defining the Strata 90
5.3.2 Determining the Sample Size 90
5.3.3 Hybrid Stratified Random/Convenience Sampling 92
5.3.4 Combining the Samples 92

5.3.5 Generation of Validation Data 92
5.4 Summary of Chapter 5 96
Chapter 6: Flood modelling results and model validation 97
6.1 Methodology 97
6.2 Modelling Results for FloodMap 97
6.2.1 Validation Point Flood Depth for Sub-catchments 97
6.2.2 Validation Flood Extent for Sub-Catchments 97
6.2.3 Sensitivity Analysis 99
6.2.4 Calibration using ROC Curve 99
6.2.5 Catchment area flood modelling using FloodMap. 101
6.3 Replicating historical flood event 103
6.3.1 Replicating historical flood event using FloodMap 104
6.4 Modelling Results for CityCAT 107
6.4.1 Validation Point Flood Depth for Sub-catchments 107
6.4.2 Validation Flood Extent for Sub-Catchments 107
6.4.3 Sensitivity Analysis 107
6.4.4 CityCAT Calibration using ROC Curve 108
6.4.5 Catchment area flood modelling using CityCAT 110
6.4.6 Replicating historical flood event 112
6.5 Comparison of FloodMap and CityCAT modelling outputs 114
6.5.1 Model parameterization 115
6.5.2 Accuracy 115
6.5.3 Reliability 115
6.5.4 Robustness 116
6.5.5 Replicability 116
6.5.6 Transferability 117
6.5.7 Simplicity 117
6.5.8 Computational demand 117
6.6 Summary of Chapter 6 118
Chapter 7: Suitability of photogrammetric data from UAV for generating terrain data for flood modelling 119
7.1 Overview of Chapter 7 119
7.2 Introduction 119
7.3 Photogrammetry point cloud acquisition using a vertical take-off and landing UAV 122

7.3.1 Pre-flight assessment 122
7.3.2 Obtaining DGPS Points 122
7.3.3 UAV flights 122
7.4 Processing UAV imagery using Pix 4D 124
7.4.1 Alignment of photos and quality assessment 124
7.4.2 Building photogrammetry point cloud 124
7.4.3 DTM Extraction from photogrammetry point cloud data using LAStools 124
7.4.4 Tiling of point clouds. 125
7.4.5 Classifying noise. 125
7.4.6 Classifying ground and non-ground points. 126
7.4.7 Ground point extracting. 126
7.4.8 DTM generation. 126
7.4.9 Accuracy assessment of DTMs generated using UAV imagery 130
7.5 Comparison of DTMs generated using UAV photogrammetry and LiDAR 133
7.6 Flood Modelling using UAV generated DTMs 135
7.6.1 Comparison of flood simulations between the DTMs generated from UAV photogrammetry and LiDAR DTMs 139
7.6.2 Sub-catchment 1 flood simulation comparison 139
7.6.3 Sub-catchment 2 flood simulation comparison 141
7.6.4 Sub-catchment 3 flood simulation comparison 143
7.7 Summary of Chapter 7 145
Chapter 8: Analysis and discussion 147
8.1 Overview of Chapter 8 147
8.2 Outcome of Research Objective 1. 147
8.2.1 Sensitivity analysis of modelling results 148
8.2.2 Drainage Capacity 148
8.2.3 Roughness 148
8.2.4 Hydraulic conductivity 149
8.2.5 Model Calibration 150
8.3 Outcome of Research Objective 2. 150
8.4 Outcome of Research Objective 3 151
8.5 Outcome of Research Objective 4. 152
8.5.1 Suitability of UAV's for generating data for FRM 152
8.6 Research outcomes and implications on FRM in data sparse regions 154

8.6.1 Plausibility of flood modelling in data sparse regions 154
8.6.2 Outcome for researchers on flood modelling in data sparse regions 154
8.6.3 Types of flood models suitable for flood inundation modelling in data sparse regions 155
8.6.4 Investment to ensure greatest improvement in model performance 156
8.6.5 Establishment of a flood policy for Nigeria 157
8.7 Research challenges and Limitations 158
8.7.1 Dearth of observed validation data 158
8.7.2 Distance to study area 159
8.7.3 Difficulty in obtaining data for flood inundation extent modelling 159
8.7.4 Limitations on the use of UAV's in urban area 159
8.8 Recommendations for further research 159
8.8.1 Flood Policy for Nigeria 159
8.8.2 Generating weather data at higher temporal resolution 160
8.8.3 Application of UAV's for disaster management 160
8.8.4 Hydrological modelling at catchment and sub-catchment scales 160
8.8.5 Flood forecasting 161
8.9 Summary of Chapter 8 161
Chapter 9: Conclusion 163

List of Figures

Figure 1: Overview of PhD research 7
Figure 2: Map of Nigeria showing areas at risk of coastal flooding. Source: NEMA, Nigeria. .35
Figure 3: Map of Nigeria showing areas at risk of pluvial floods. Source: NEMA, Nigeria. 35
Figure 4: Map of Nigeria showing areas at risk of riverine flooding. Source: NEMA, Nigeria. 36
Figure 5: The study area top left-map of Africa showing the location of Nigeria; Bottom left-map of Nigeria showing the location of Lagos State; Right- The 3 sub-catchments under study in Lagos. 37
Figure 6: Methodology for data processing, parameterization and flood simulation using the FloodMap Model.....50
Figure 7: Path of a LASER pulse illustrating how LiDAR works (Fernandez-Diaz et al., 2014). 51
Figure 8: Process for DTM generation and validation 52
Figure 9: Generated DTM of the study area from LiDAR point clouds.....53
Figure 10: Linear regression chart validating the generated DTM 54
Figure 11: DGPS Locations within the study area 55
Figure 12: A- Fill, B-Flow direction, C- Flow accumulation, D-Basins, E-Drainage network, F-Delineated drainage network for sub-catchments under study 58
Figure 13: Locations of weather monitoring stations in relation to the sub-catchments.....59
Figure 14: Rainfall intensity chart 60
Figure 15: Land cover classification of the study area.....64
Figure 16: DSM of Sub-catchment 1 used for the FloodMap modelling. 68
Figure 17: DSM of Sub-catchment 2 used for the FloodMap modelling. 69
Figure 18: DSM of Sub-catchment 3 used for the FloodMap modelling. 70
Figure 19: Rainfall intensity chart for the CityCAT model 72
Figure 20: Procedure for converting shapefiles in .dwg to CityCAT recognisable format 74
Figure 21: DTM of sub-catchment 1 used for the CityCAT modelling 78
Figure 22: DTM of sub-catchment 2 used for the CityCAT modelling 79
Figure 23: DTM of sub-catchment 3 used for the CityCAT modelling. 80
Figure 24: Generating flood depth and extent from social media information. 83
Figure 25: The 3 sub-catchment areas for the study showing their point flood locations 85
Figure 26: The 3 crowd sourced flooded areas of interest within their drainage basins and the DGPS locations 86
Figure 27: left: Pole identified during flood for validation: Right- Object used to generate flood depth 87
Figure 28: A: Fence identified during flood for validation, B- Fence used to generate flood depth, C-Car tyre used to validate flood depth, D-Configuration of car tyre.....88
Figure 29: Left: Fence identified during flood for validation: Right- Same fence used to generate flood depth 89
Figure 30: Methodology for the generation of 3D reconstructed flood extents from respondents for the 3 sub-catchments. 91
Figure 31: Catchment 1 validation flood extent 93
Figure 32: Sub-catchment 2 flood validation extent 94
Figure 33: Sub-catchment 3 validation flood Extent 95

Figure 34: Methodology for the comparison of historical flood modelling results 98
Figure 35: Correlation plots of Depth and model parameters for sub-catchments 1-3 (L-R) .99
Figure 36: ROC Curve for sub-catchment 1 100
Figure 37: ROC Curve for sub-catchment 2. 100
Figure 38: ROC Curve for sub-catchment 3. 101
Figure 39: Flood depth for the entire catchment area using FloodMap. 103
Figure 40: Rainfall intensity for 19th October 2019 for FloodMap 104
Figure 41: Picture showing the tyres of a Toyota Highlander 2006 used to determine the depth of the flood 105
Figure 42: Map showing the flood depth for the 19th October 2019 flood simulation using FloodMap 106
Figure 43: CityCAT Correlation plots of Depth and model parameters for sub-catchments 1-3 (L-R) 107
Figure 44: ROC Curve for sub-catchment 1. 108
Figure 45: ROC Curve for sub-catchment 2. 109
Figure 46: ROC Curve for sub-catchment 3. 109
Figure 47: Flood depth for the entire catchment area using CityCAT 111
Figure 48: Rainfall intensity for 19th October 2019 for CityCAT 112
Figure 49: Map showing the flood depth for the 19th October 2019 flood simulation using CityCAT 113
Figure 50: photogrammetric data from UAV for generating terrain data for flood modelling. 121
Figure 51: Location of DGPS in the various Sub-catchments 123
Figure 52: Process for DTM extraction and validation 125
Figure 53: DTM of sub-catchment 1 127
Figure 54: DTM of sub-catchment 2 128
Figure 55: DTM of sub-catchment 3 129
Figure 56: RMSE and MAE for the assessment of the accuracy of the DTM for sub-catchment 1 130
Figure 57: RMSE and MAE for the assessment of the accuracy of the DTM for sub-catchment 2. 131
Figure 58: RMSE and MAE for the assessment of the accuracy of the DTM for sub-catchment 3. 131
Figure 59: Map of catchments showing areas the UAV DTMs intersect in the 3 catchments. 132
Figure 60: Line chart for the comparison of UAV and LiDAR DTMs for sub-catchment 1 depicting their RMSE and MAE 133
Figure 61: Line chart for the comparison of UAV and LiDAR DTMs for sub-catchment 2 depicting their RMSE and MAE 134
Figure 62: Line chart for the comparison of UAV and LiDAR DTMs for sub-catchment 3 depicting their RMSE and MAE 134
Figure 63: Flood point depth comparison between UAV and LiDAR DTMs 135
Figure 64: Flood extent for sub-catchment 1 using the UAV DTM.....136
Figure 65: Flood extent for sub-catchment 2 using the UAV DTM.....137

Figure 66: Flood extent for sub-catchment 3 using the UAV DTM.....138
Figure 67: Map showing the intersection (red polygon) of the LiDAR and UAV derived DTMs' flood extent for sub-catchment 1.....140
Figure 68: Chart comparing the flood extent obtained using the UAV DTM and the LiDAR DTMs for sub-catchment 1 with the RMSE and MAE values.....141
Figure 69: Map showing the intersection (red polygon) of the LiDAR and UAV derived DTMs' flood extent for sub-catchment 2.....142
Figure 70: Chart comparing the flood extent obtained using the UAV DTM and the LiDAR DTMs for sub-catchment 2 with the RMSE and MAE values.....143
Figure 71: Map showing the intersection (red polygon) of the LiDAR and UAV derived DTMs' flood extent for sub-catchment 3.....144
Figure 72: Chart comparing the flood extent obtained using the UAV DTM and the LiDAR DTMs for sub-catchment 3 with the RMSE and MAE values.....145

List of Tables

Table 1: Classification of 1-3D inundation models (Neelz & Pender, 2009).....9
Table 2: Overview of some flood models. 10
Table 3: Some data required for flood modelling. 11
Table 4: Research on flood modelling conducted in developed and developing countries ...12
Table 5: Satellites for obtaining terrain data for flood modelling. 15
Table 6: Satellites for generating precipitation data. 17
Table 7: Factors affecting the choice of hydrological models for various studies. 22
Table 8: Criteria for evaluating flood forecasts. 25
Table 9: Flooding in Nigeria (2000-2022) Source: EM-DAT 2022. 33
Table 10: Some flooding events that have occurred in Lagos. 38
Table 11: Challenges of FRM in Nigeria 47
Table 12: Selected range of Mannings values for the study area 65
Table 13: Range of values for parameterization of the FloodMap model 66
Table 14: Parameters adopted for FloodMap model 66
Table 15: Range of values for parameterization of the CityCAT model 76
Table 16: Parameters adopted for CityCAT simulations.....76
Table 17: FloodMap simulated flood depth from the entire catchment area compared to the observed flood depth.....101
Table 18: Comparison of FloodMap simulated flood depth from the 3 sub-catchment areas and the observed flood depth. 102
Table 19: CityCAT simulated flood depth from the entire catchment area compared to the observed flood depth.....110
Table 20: Comparison of CityCAT simulated flood depth from the 3 sub-catchment areas and the observed flood depth. 110
Table 21: FloodMap and CityCAT modelling processes.....114
Table 22: Accuracy of simulated historical event of FloodMap and CityCAT.....115
Table 23: List of some freely available global DEMs.....120
Table 22: Table showing the comparison of the UAV DTM and LiDAR DTM 151

Chapter 1: Introduction

1.1 Background

Flooding has been the most costly natural disaster in the world (Jenkins, 2016) which has resulted in loss of human lives, death of animals, destruction of property, escalation of the prices of goods and services, increased social insecurity, pollution of water, and spread of waterborne diseases and other epidemics (Dewan, 2015). The destruction caused by disasters, call for global concern, hence, the International Community of the Red Cross (ICRC) evolved Strategic Aim 1 of Vision 2020 "to save lives, protect livelihoods, and strengthen recovery from disasters and crises" (ICRC, 2011). In 2020, floods were the most common natural disaster worldwide with 201 reported flood events resulting in 6,171 deaths, affecting 33 million people and causing economic losses of $51.3 billion USD (CRED, 2021). Globally, flooding could be attributed to different causes such as sea level rise (Boettle et al., 2016), global temperature increase resulting from climate change (Somerville, 2020), urban development (Su et al., 2014), deforestation (Chakravarty et al., 2012), reduction in wetlands (EPA, 2012), illegal land use (Barbedo et al., 2014) as well as other causes. Population growth and alterations in land-use patterns have increased human vulnerability to floods with thousands of lives lost, millions rendered homeless with associated loss of properties and infrastructure (Dewan, 2015).

The Centre for Research on the Epidemiology of Disasters (CRED) compared disasters that occurred from 1980-1999 to those that occurred between 2000-2019 and the comparison confirmed that there was a 57% increase in disasters with associated loss of lives, affected population and economic losses; with flood hazards having the highest occurrence of all the natural hazards within the periods (CRED, 2020). The upsurge in the frequency of disasters worldwide has increased human vulnerability to disaster related threats and trends that have resulted in loss of lives, damages, losses of essential services and dislocations including disruption of services (Mani et al., 2003). With global average temperatures in 2019 being 1.1^{o}c above pre-industrial periods and the world on course for a temperature increase of 3.2^{o}c or more unless there are reductions in greenhouse gas emissions (CRED, 2020), there is the risk of increased frequency of extreme weather events with flooding being the hazard that is predicted to cause the most devastation. In order to enhance disaster risk reduction, the Sendai Framework for Disaster Risk Reduction 2015-2030, a United Nations conference on disaster risk reduction, had as one of its priorities for action as 'the enhancement of disaster preparedness for effective response and to build back better in recovery, rehabilitation and reconstruction'. With flooding being the most frequently occurring natural disaster, efforts to forecast flooding and build societies' resilience to floods will be invaluable in reducing vulnerability to flood risk. Risk is an interplay of the multiplier effect of hazard and vulnerability; with hazard being the probability associated with the occurrence of flooding events including their main drivers such as flow velocity, flood depth and duration (Cancado et al., 2008). Flood risk is thus determined by a combination of hazard threat and vulnerability.

Hence, effective flood risk management (FRM) will involve a detailed understanding of flooding a society is susceptible to in order to build the society's resilience to these floods and manage these floods whenever they occur. Flood management involves obtaining data and information, analysing risk and evaluation of decisions including the implementing and review of decisions to lessen flood risks; which is an iterative process of analysing, modification and adaptation of policies and actions (Sayers et al., 2017). In order to effectively manage floods, data is required to predict floods and drive favourable policies on FRM.

The process of FRM involves the ability to forecast flood events which will ultimately affect preparedness and response. Flood forecasting, as defined by the international glossary of hydrology is the 'prediction of stage, discharge, time of occurrence and duration of a flood, especially of the peak flood, at a specified point in a stream, resulting from precipitation and/or snowmelt' (WMO, 1992). For pluvial flooding, flash flood forecasting involves the combination of accurate rainfall prediction with useful lead times and the representation of the hydrologic and hydraulic processes to determine how flow accumulates (Hapuarachchi et al., 2011). A major setback in flood forecasting is the dearth of high-quality hydro-meteorological data of adequate spatial and temporal resolution for the estimation of modelling parameters and as real-time model forcings (Adams & Pagano, 2016). The process of flood forecasting is heavily reliant on the availability of weather predictions and terrain data. For countries that have access to adequate data for flood forecasting, their FRM plans can be better tailored to mitigate the envisaged flood hazard. However, for countries that are plagued by data sparsity, their FRM approaches may not adequately address the flood hazards that they are vulnerable to. Research by CRED revealed that for disasters from 2000-2017, in low-income countries, an average of 130 people died per million compared to 18 deaths per million in high income countries. This translates to people exposed to natural hazards in the poorest nations are more than seven times likely to perish from disasters compared to the equivalent populations in the richest nations. Furthermore, from 2000-2019, floods had the highest impact in Asia, with the next affected continent being Africa and then the Americas; with projections that many of these impacts could have been preventable (Mizutori & Guha-Sapir, 2020).

Africa has been affected with flood events varying in magnitude causing human, economic and social devastation. In 2020, flooding affected 7 million people in Africa causing 1,273 deaths which is the highest figure reported since 2006 (CRED, 2020). Flooding has been identified as one of the reasons that prevents Africa's increasing population from being elevated from poverty thus hindering the United Nations 2020 goal of positively affecting the lives of urban slum inhabitants (Hope Sr, 2009). Flood occurrences in Africa are unique because the impacts are usually devastating which are largely due to high flood vulnerability, high susceptibility and limited responses.

Nigeria, which is the most populous country in Africa, has also been affected by flood events. Indices used in generating the World Flood Index Report for 2017 and analyses countries using a World Risk Index (WRI), posits that a direct relationship exists between population and

impact of flooding. It further shows that an inverse relationship exists between the standard of living and risk of flooding. Countries with high vulnerability to flooding could have low susceptibility to flooding resulting from pragmatic and focused FRM efforts (Hilft, 2017). For example, in 1953, the North Sea Flood affected The Netherlands, Belgium and the United Kingdom resulting in 2,251 deaths with 1,893 casualties in the Netherlands alone (Gerritsen, 2005). With 55% of The Netherlands in danger of flooding and 25% of its landmass below sea level (Huizinga, 2012), the country has evolved diverse FRM strategies to reduce its risk of flooding and is currently rated 50th on the World Flood Index Report for 2017 (Hilft, 2017). Nigeria on the other hand is 53rd on the WRI despite having a much lower exposure to flood. The reason for Nigeria's high risk of flooding is that the country has high vulnerability to flooding, high susceptibility, lacks coping strategies and lacks adaptive capabilities. The Netherlands on the other hand has a higher exposure to flooding than Nigeria but much lower vulnerability, susceptibility and higher coping and adaptive capabilities. From this comparison, it is evident that successfully evolving focused FRM strategies would reduce these observed lapses and would ultimately improve the country's WRI rating. A good start to determining the impact the FRM strategies would be the identification of areas having high vulnerability to flooding and also to be able to forecast floods with an acceptable level of accuracy in order to drive focused FRM policies, but the unavailability of data poses a challenge to achieving this. In order to identify areas that are at risk of flooding, there is the need to determine the catchment characteristics of data sparse regions and the influence these parameters have on the hydrological cycle in that region. This is vital in flood forecasting as a good understanding of the hydrological cycles of these catchments will make it plausible to work with predicted precipitation events to evolve an efficient flood forecasting and early warning system.

Flood prediction has been found to be highly beneficial to FRM efforts especially in the areas of emergency response and community awareness (Borga et al., 2011). With continuous breakthroughs in computing, remote sensing capabilities, meteorological prediction and analysis including hydrological modelling advancement and supporting data; flood prediction is becoming more achievable with desirable results. Data sparse regions however face challenges in terms of data availability to conduct reliable research on flooding in order to enact favourable FRM policies. Global efforts to reduce the negative effects of flooding and evolve proactive mitigation strategies include the Sendai Framework for Action (2015-2030), which set goals to be achieved by Countries, set timelines for countries to conduct flood vulnerability mapping which would help drive policies that would reduce the impact of flooding in societies (Wahlstrom, 2015). While this may not be a problem for countries that have the adequate data and the resources to undertake this task, other less developed nations are not so fortunate.

This PhD thesis was thus undertaken to determine the feasibility of conducting flood modelling in data sparse regions as a prelude to forecasting floods in such regions. The research presents an approach to replicate a historical flood event with limited data availability and subsequently determining how plausible the results would be for FRM. The

quality of a hydrodynamic model depends on the ability of the model to be tested and validated against real historical events before it can be used operationally for flood forecasting (Henonin et al., 2013). In conducting the feasibility study on flood modelling, two hydrological models were employed. One of the models was used in its simplified form while the other model was used in its complex form and the outcomes were compared. The ability to calibrate a hydrological model to replicate a historical flood event for a sub-catchment serves as a springboard for the conduct of flood forecasting in that sub-catchment. This research also consolidated on advances in the acquisition of photogrammetric data from unoccupied aerial vehicles (UAVs) to generate a high-resolution Digital Terrain Models (DTM) which was compared with expensive and high-tech terrain data acquired using a LiDAR sensor. Hydrological modelling was conducted using the UAV generated DTM to confirm its suitability for replicating a historical flood event by comparing it with DTMs generated using LiDAR high-tech means.

1.2 Aim

The aim of this research is to assess the viability of conducting pluvial flood modelling in data-sparse urban regions of Nigeria.

1.3 Research Questions

This research was focused on enhancing FRM in a data sparse densely populated urbanised catchments by assessing the plausibility of conducting pluvial flood modelling in such areas. The achievement of this goal requires robust research approaches and the following research questions were addressed.

1. What are the opportunities and trade-offs associated with pluvial flood modelling in densely populated built-up areas characterized by data sparsity in developing cities?

2. How can modelled flood inundation extents be validated in data sparse regions?

3. How well does the hydrological process in sub-catchments represent the hydrological processes that occur in large catchment areas? What are the pros and cons of using sub-catchment compared to using entire catchment areas for hydrological modelling?

4. Can terrain data for flood modelling generated using photogrammetry point clouds obtained from UAVs be compared with terrain data generated using high-tech LiDAR point clouds? How well can such UAV derived terrain data be suitable for generating terrain data for flood modelling?

1.4 Objectives

The following research objectives were undertaken:

1. To determine if pluvial flood modelling can be meaningfully conducted in data-sparse regions of the developing world.

2. To determine the reliability of low-cost methods of generating flood model validation data in data sparse regions.

3. To determine how well sub-catchments are able to represent the hydrological processes of entire catchment areas for pluvial flood modelling.

4. To determine how well terrain data for pluvial flood modelling generated from UAV photogrammetry point clouds compares with terrain data generated from high-tech LiDAR point clouds.

1.5 Research structure

Chapter 1 gives a background to flooding with an overview of the global impact of flooding and the efforts undertaken to reduce its impact. It also highlights the impact of flooding in Africa and Nigeria. It showcases the impact flood modelling plays in flood forecasting and how this can be applied in the field of flood forecasting. The Chapter outlines the aim, research questions and objectives of this research. A synopsis of the research structure is also highlighted while an overview of the PhD research is at **Error! Reference source not found.**.

Chapter 2 is the literature review which conceptualized the main terminologies used in this research including past research that they had been applied in flood modelling. The chapter further gives an insight into hydrological models and the vital role they play in flood modelling and forecasting. The parameters that drive hydrological models are explained here, the date required to drive flood models and explains factors that guide the selection of hydrological models for flood modelling. The chapter compares research on FRM conducted in areas with relatively available areas and data sparse regions. It reviewed the FRM approaches by data sparse countries and how they were able to overcome their lack of data to enact plausible FRM strategies for their countries. It also defines criteria that can be used for testing the meaningfulness of flood forecasts.

The main focus of Chapter 3 is to give an overview of the study area and how its FRM strategies are affected by data sparsity and gives an insight into the impact of flooding on it. It compared FRM in the study area with FRM in countries with varying data availabilities. It finally outlines the challenges to FRM in the study area and sets the scene for processing of data in the data sparse region.

Chapter 4 focused on the main element of this research which was the flood modelling approaches using FloodMap-Hydro Inundation 2D (here in after referred to as FloodMap) and City Catchment Analysis Tool (CityCAT) to replicate a historical flood event for each of the 3

sub-catchments. It initially involved the manipulation of the point clouds to generate a DTM for the study area which was subsequently delineated to generate the 3 sub-catchments used for this study. It involved understanding the operating dynamics of FloodMap and CityCAT including their main drivers and parameter configurations required to simulate flow. It involved the effective use of sparse data for parameterizing the flood model and justifying the parameters selected for the study.

The main focus of Chapter 5 is the generation of low-cost flood validation data for flood modelling and how this can impact FRM in data sparse regions. It explains the approaches to generate validation data in data sparse regions using low-cost approaches including the role citizens' science can play in generating flood validation data. It further explains the approach used for the generation of flood extent to be used as validation data.

Chapter 6 analysed the results of the flood modelling and established how the outcomes fitted into wider research works conducted on similar studies. It involved a comparison of the results obtained from the FloodMap and CityCAT models including identifying the model which optimally represented the historical flood event. Sensitivity analysis and model calibration were also done here to determine which parameter configurations best represented each catchment area. The results comparing flood modelling in sub-catchments and whole catchment areas were presented here.

Chapter 7 looked at alternative means of generating terrain data for flood modelling and analysed the plausibility of adopting UAVS for the generation of DTMs required to drive flood forecasts. The Chapter exploits the successes recorded in Chapter 6 to utilize the calibrated model parameters for modelling the same historical flood event using a DTM generated from UAV photogrammetry. It also compared the flood model results from the DTM generated using UAV photogrammetry and that of the high-end LiDAR DTM. The potential of utilizing UAVS to plug data gaps for flood models especially in data sparse regions was showcased in this chapter.

Chapter 8 analysed the achievement of the research aim and objectives. It gave a synthesis of finding and drew lessons learnt for FRM in data sparse regions. The chapter showcased how the research findings fit into similar research at the international scene and areas where the research could be exploited. The chapter noted the absence of a detailed flood policy in Nigeria to drive the country's approach to FRM and outlined modalities for evolving a flood policy for the country. It also outlined how knowledge from the local communities can be harnessed and used to enact favourable FRM policies. The chapter identified the possibility of adopting blue-green cities for effective FRM. The lessons learnt, challenges and achievements of the research were outlined here including areas that require further research.

Chapter 9 is the concluding chapter where the achievements of the research were outlined along with the envisaged challenges of conducting flood forecasting in data sparse regions.

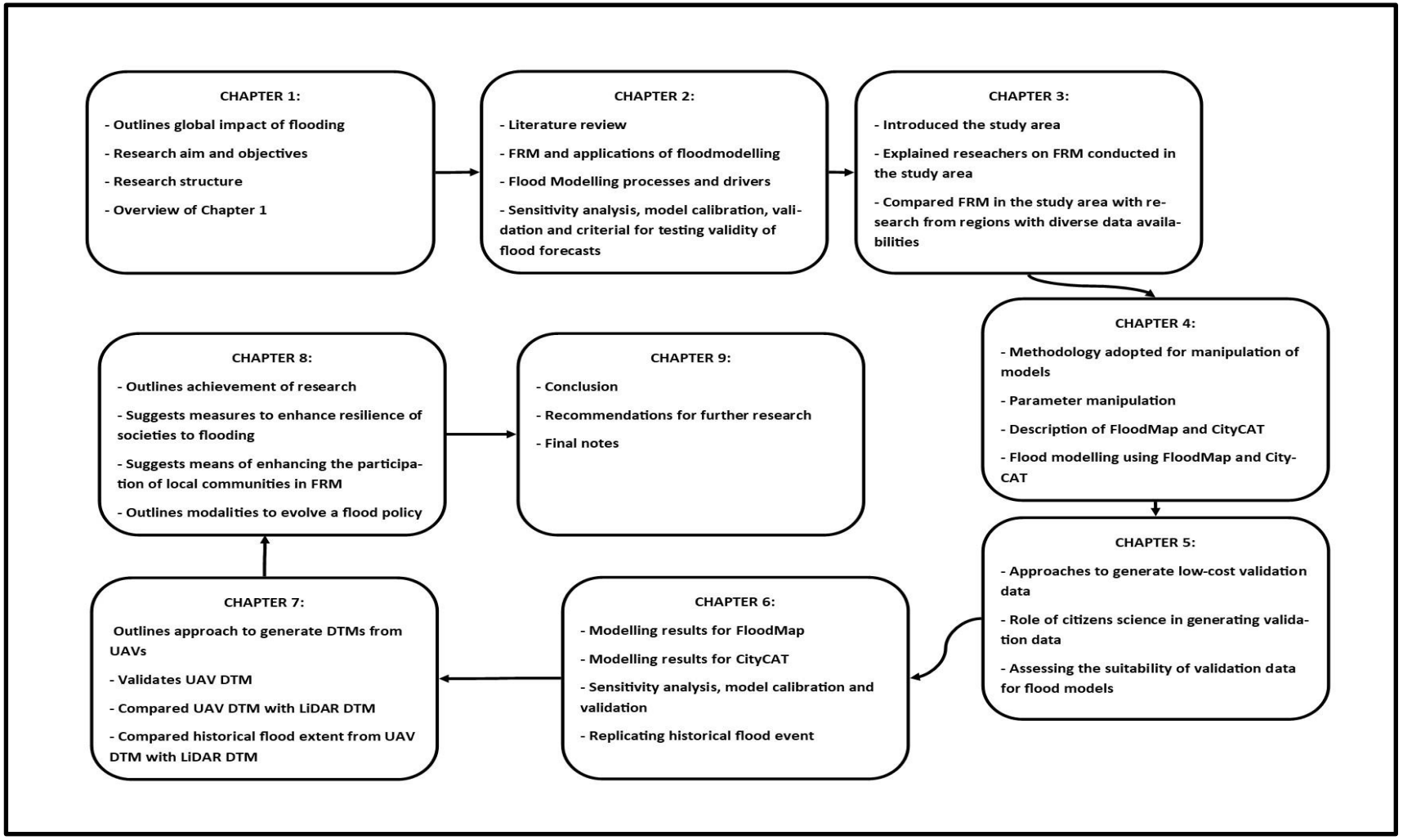


Figure 1: Overview of PhD research

Chapter 2: A review of data required for flood modelling and flow routing processes

2.1 Overview of Flood Models

Forecasting floods is currently becoming more probable resulting from advances in obtaining meteorological data, flood models, imagery from satellites, improved data and increased resources and computational power amongst other factors (Emerton et al, 2016). These advances have transcended to flood nowcasting which assists emergency responders in real-time during emergency situations (Yu and Wilby, 2017). Forecasting flood can be accomplished using inundation models to simulate flow accumulation resulting from forecasted weather conditions. These inundation models fall within the classifications of 1-3 Dimensions. A breakdown of the classification of models that fall within this range is at Table 1. 1D models are derived by integrating Navier-Stokes equations over the cross-sectional surface of the flow and are based on the St-Venant or shallow water equations and models flow in one direction which may result in errors (Neelz and Pender, 2009). The ID+ also known as the QUAVsi-2D or Pseudo-2D which is an improvement of the 1D but does not assume that flow is aligned with the river centre line and thus may be more accurate to model floodplains of higher dimensions (Pender & ELZ, 2011) (Kvocka, 2017). The setback of this model is that it does not include any momentum conservation on floodplains, hence water is being modelled to be transferred instantaneously from one end of the storage cells to the other and may produce errors (Neelz and Pender, 2009). 1D range of hydrological models are used for large scale modelling and their outputs range from forecasting water depths, cross sectional averaged velocity, inundation levels amongst other outputs as outlined in Table 1. The 2D range of hydrological models solve equations ranging from the 2D shallow water equations and some of them solve vertical velocities using continuity only (Bates et al., 2010). The 2D models involve equations that factor physical processes such as how velocity changes over time, inertia term, Coriolis force (the inertial *force* acting on an object in motion in relation to a rotating reference frame), gravity and bed resistance. It also includes atmospheric pressure, viscosity/turbulence and external forces such as wind waves etc (Syme, 2011). 1D views may not convey accurately, affected infrastructure while modelling urban areas while 3D views on the other hand, could present multidimensional visualizations of the floodplain and its effect on utilities to facilitate discussions with engineers, government and the public (Adda et al.,2010). The use of 3D maps generated from 3D flood inundation modelling have been used to plan relief works, damage assessment, flood patterns (flow, direction and velocity) amongst other uses (Feng et al, 2015). 3D simulation of flood risk is vital for scientific and intelligent management of flood disasters (Wu et al., 2019) but it requires high computational speeds to run and large amount of data to simulate.

Table 1: Classification of 1-3D inundation models (Neelz & Pender, 2009).

Serial	Method	Description	Application	Typical computation times	Output	Example models
(a)	(b)	(c)	(d)	(e)	(f)	(g)
1.	1D	Solution of the one-dimensional St-Venant equations.	Design scale modelling which can be of the order? of 10s to 100s of km depending on sub-catchment size.	Minutes	Water depth, cross-section averaged velocity, and discharge at each cross section. Inundation extent if Flood plains are part of 1D model, or through horizontal projection of water level.	Mike 11 HEC-RAS ISIS InfoWorks RS
2.	1D+	1D plus a storage cell approach to the simulation of floodplain flow.	Design scale modelling which can be of the order of 10s to 100s of km depending on sub-catchment size, also has the potential for broad scale application if used with sparse cross-section data.	Minutes	As for 1D models, plus water levels and inundation extent in floodplain storage cells	Mike 11 HEC-RAS ISIS InfoWorks RS
3.	2D-	2D minus the law of conservation of momentum for floodplain flow.	Broad scale modelling and applications where inertial effects are not important.	Hours	Inundation extent Water depths	LISFLOOD-FP JFLOW
4.	2D	Solution of the two-dimensional shallow water equations.	Design scale modelling of the order of 10s of km. May have the potential for use in broad scale modelling if applied with very coarse grids.	Hours or days	Inundation extent Water depths Depth-averaged velocities	TUFLOW Mike 21 TELEMAC SOBEK InfoWorks-2D
5.	2D+	2D plus a solution for vertical velocities using continuity only.	Predominantly coastal modelling applications where 3D velocity profiles are important. Has also been applied to reach scale river modelling problems in research projects.	Days	Inundation extent Water depths 3D velocities	TELEMAC 3D
6.	3D	Solution of the 3D Reynolds averaged Navier Stokes equations.	Local predictions of 3D velocity fields in main channels and floodplains.	Days	Inundation extent Water depths 3D velocities	CFX

The choice of a particular hydrological model depends on the objective of the modelling with respect to the study being conducted (Onyutha, 2016). For this research, one requirement is to be able to simulate inundation over roads and between buildings if possible, using the available data and with the computational speeds available. The attributes of a 2D hydrological model met the requirements of this research. Some hydrological models suitable for overland flood modelling of the study area were examined and a synopsis of their applications are at Table 2.

Table 2: Overview of some flood models.

Serial	Hydrological Model	Application
(a)	(b)	(c)
1.	ISIS 2D	-Shallow water flow model. - Predicts depths and velocities on a regular square grid. - Designed to model flows in coastal, estuary and floodplain environments. - Can model complex and simple hydraulics including fluvial, overland, estuarine and coastal modelling problems where the flow is not rapidly changing.
2.	HEC RAS	-Designed for 2D hydraulic calculations for natural and constructed channels. - Uses common geometric data representation, common geometric and hydraulic computation routines for 1. Steady flow water surface profile computations. 2. 1D and 2D unsteady flow simulation. 3. Movable boundary sediment transport computations. 4. Water quality analysis.
3.	MIKE	- Have a variety of MIKE Hydrological Models for various flood simulations. - Tool for understanding urban flooding, analysing scenarios and testing mitigation measures - Integrates flood plains, streets, rivers, coastal areas and sewer/storm water systems. - A versatile hydrological model capable of modelling flooding including erosion spanning sand and mud transport and also particle tracking.
5.	Infoworks 2D	- Utilizes irregular mesh so that size and orientation of the triangles are varied. - Heights at vertices of generated mesh elements calculated by interpolation from a specified Ground Model. - Independent rainfall profiles can be applied to selected areas and evaporation from the 2D mesh is factored. - Generated results can be exported to various interfaces including google maps for viewing.
6.	LisFlood	- Designed specifically to simulate floodplain inundation over complex topography. - Capable of simulating grids up to 10^6 cells for dynamic flood events. - Capable of simulating dynamic propagation of flood waves over fluvial, coastal and estuarine floodplains. - Non-commercial model aimed to enhance fundamental understanding of flood hydraulics, flood inundation prediction and flood risk assessment.
7.	FloodMap Hydro-inundation 2D (The model used for this study)	- Coupled 1D/2D flood inundation model. - Designed for fluvial flood inundation prediction in topographically complex floodplains. - Based on the sub-grid treatment approach and has been tested and verified with a range of boundary conditions and in a number of environments. - 1D model solves the full Saint-Vernant equations for unsteady open-channel flow using the Preissmann scheme based on the fixed bed model of Abbott and Basco (1989). - Has been applied in a range of dynamic environments from China, Spain, Turkey, Thailand and UK amongst others. In parts of the UK, the model has been used to generate a real-time flood map to aid flood response.
8.	CityCat (The model used for this study)	- Food modelling tool for hydrodynamic modelling, analysis and visualization of surface water flooding at city scale. - Provides solutions to shallow water equations using finite volume method where the computational domain is discretized into smaller sub-domains. - A versatile software with the ability to model and assess the effects of FRM measures within the study area.

2.2 Data requirements for flood modelling

The data required for flood models vary depending on the flood model requirement or the flood event to be modelled. However, flood modelling data generally fall into four categories spanning topographical data or DTM for the model grid, bulk flow data and outflow boundary conditions including meteorological data, an estimate of the grid square effective friction parameter for the model cells and finally data for validation (Smith et al., 2006). An overview of the data required for flood modelling is at Table 3.

Table 3: Some data required for flood modelling.

Data Type	**Purpose of Data**	**Details and Usage**
Digital Elevation Model	Defines terrain elevation for flow calculations	Essential for hydraulic modelling, determining water flow paths and flood extents.
Land Use/Land Cover Data	Identifies surface properties affecting runoff	Different land covers have varying runoff rates and permeability.
Hydrograph Data	Provides flow rate information from rainfall	Used to simulate inflow and outflow from rivers and channels.
Rainfall Data	Supplies precipitation values for runoff simulation	Key input for rainfall-runoff models to predict flood response.
River Network Data	Outlines watercourses and drainage pathways	Defines the network through which water flows during flooding.
Soil Data	Specifies soil characteristics influencing infiltration	Determines how much rainwater infiltrates the ground.
Roughness Coefficients	Represents surface roughness for flow resistance	Influences flow velocity and resistance in hydraulic models.
Flow Direction Data	Determines water flow directions on the terrain	Crucial for routing water and calculating flood propagation.
Hydraulic Structures Data	Represents dams, culverts, and other infrastructure	Incorporates man-made elements affecting water flow and storage.
Population Data	Identifies areas with potential human impact	Helps assess flood risk to people and infrastructure.
Land Use Vulnerability Data	Quantifies susceptibility of land uses to flooding	Identifies areas at higher risk due to urban development.

The differences between the data available for countries for FRM differs including the technical capabilities for conducting FRM research and studies. This is captured in the types of research that have been conducted in some developed countries compared to some developing countries and shown in Table 4.

Table 4: Research on flood modelling conducted in developed and developing countries

Serial	Research Title	Research Conducted	Major Findings	Source	Remarks
1.	Impact of hydraulic model resolution and loss of life model modification on flood fatality risk estimation: Case study of the Bommelerwaard, The Netherlands.	Flood modelling at resolutions of 5, 25 and 100 m.	Results displayed locally increased mortality rates in the higher resolution simulations nearby structures including road embankments, dikes, and culverts.	(Brussee et al., 2021)	Netherlands - Developed country
2.	Reconstructing the peak flow of historical flood events using a hydraulic model: The city of Bath, United Kingdom.	Reconstruction of historical flood events on the River Avon in the city of Bath using a 1D hydraulic model. Calibration of the model was done using two historical floods where the peak flow values were obtained from hydrological data of March 1947 and December 1960.	Annual maximum series of peak flow upstream of Bath city centre was created. Furthermore, a flow series consisting of data from 1866 to 2021 was generated by the research.	(Stamataki & Kjeldsen, 2021)	United Kingdom – Developed country
3.	Prediction of flood quantiles at ungauged catchments for the contiguous USA using Artificial Neural Networks	Used Artificial Neural Network (ANN) models for the estimation of 100- and 1500-year return levels for around 900,000 ungauged catchments. Models trained and validated using 4,079 gauges including selected catchment descriptors.	Research confirmed the applicability of ANN models for predicting ungauged flood quantiles across large geographic area. The importance of ANN in regional flood frequency analysis was recommended.	(Collins et al., 2022)	USA – Developed country
4.	Towards urban flood susceptibility mapping using data-driven models in Berlin, Germany	Research used 4333 flooded locations including 11 factors to implement convolutional neural network (CNN), ANN, random forest (RF) and support vector machine (SVM) for pluvial flood modelling.	Results showed that data-driven models were reliable tools for mapping susceptibility to urban pluvial flood but is dependent on availability of reliable flood inventory.	(Seleem et al., 2022)	Germany – Developed country
5.	Assessment of urban flood risk based on data-driven models: A case study in Fuzhou City, China	Used a coupled hydrological–hydrodynamic model and a developed integrated framework to assess flood vulnerability urbanized catchments under diverse flood hazard scenarios.	Results showed areas that were most susceptible to flooding and proposed plausible FRM approaches	(Ye et al., 2022)	China – Developed country

6.	Flood Management, Characterization and Vulnerability Analysis Using an Integrated RS-GIS and 2D Hydrodynamic Modelling Approach: The Case of Deg Nullah, Pakistan	Formulated a 2D hydrodynamic model to simulate an extreme flood event at a transboundary river of Deg Nullah in Pakistan that occurred in 2014. The flood extent images from MODIS and sparse observed flood extents were used to evaluate the model performance due to the absence of sufficient gauged data.	The 2D flood model simulation results showed a good agreement with the flood extents registered by MODIS and the sparsely observed ones.	(Yaseen et al., 2022)	Pakistan – Developing country
7.	The effects of changing land use and flood hazard on poverty in coastal Bangladesh	A combination of cellular automata (CA), logistic regression (LR), and Markov Chain models were combined to build a prediction model for future LULC from historical data. A spatial regression model was developed, incorporating multiple parameters to estimate the wealth index (WI) for present-day and future scenarios.	Flood risk correlated positively with the LULC and predicted annual damage	(Adnan et al., 2020)	Bangladesh – Developing Country
8.	Supervised and unsupervised machine learning approaches using Sentinel data for flood mapping and damage assessment in Mozambique	Sentinel-1 imagery (VH, VV) was used with supervised and unsupervised machine learning (Ojigi et al.) methods on a dataset comprising imagery from 13 countries worldwide for predicting and mapping floods in Mozambique	The predictions in Beira using VH imagery yielded an IoU Metric of 0.568. Approach was a reliable alternative for flood mapping, due to low cost and time effectiveness	(Nhangumbe et al., 2023)	Mozambique – Developing country
9.	Flood risks to urban development on a coastal barrier landscape of Lekki Peninsula in Lagos, Nigeria	Storm surges were modelled using a Planar GIS environment and the CAESAR model at Lagos Nigeria	The CAESAR model better represented the storm surges better but there was no validation data for the extents of the predicted storm surges	(Obiefuna et al., 2021)	Nigeria – Developing country

A comparison of these research on FRM show that some researches from developed countries have some level of data available to conduct experimental FRM studies at different scales while those in the developing world are mostly generic and are plagued with sparse data as well as inadequate technical capabilities for precision flood modelling. The developing countries sometimes have validation data for their simulations which enhances the reliability of the predictions. The simulations done at the developing countries mostly did not have validation data while those that used validation data focused on satellite data for their validation data with little observed data. This approach by the developing countries leaves room for bias and assumptions and does not test the reliability of the simulations undertaken. The ideal data availability would be able to model flood processes using high precision flood models but the realism especially in data sparse regions is that there are insufficient data to simulate these processes and also the unavailability of validation data to test model efficiency. An understanding of the hydraulic and hydrological processes of flood models would give better insights into the data required for flood models and the alternative approaches to ensure flood modelling as part of FRM drives can be embarked. The challenge of data availability to validate simulations was one problem in FRM this research tried to overcome.

2.2.1 Topographical/Terrain data for flood modelling

In modelling floods, an important input data is the geometric description of the terrain which could be referred to as the digital terrain model (DTM) (Md Ali et al., 2015). The approaches to generating DTMs include cartography (Zanardi et al., 2011) (Hutsul & Smirnov, 2017), ground survey (Kraus & Pfeifer, 2001), digital aerial photogrammetry (Escobar Villanueva et al., 2019; Uysal et al., 2015), Interferometric Synthetic Aperture Radar (SAR) (M. Ouarzeddine & Belhadj-Aissa) (Sukojo et al., 2021) (M. S. Ouarzeddine, 2002) and Light Detection and Ranging (LiDAR) (Muhadi et al., 2020) (Z. Chen et al., 2017) (Pfeifer & Mandlburger, 2017). An overview of the available satellites for obtaining terrain data for flood modelling is at **Error! Reference source not found.**. DTM which is usually made up of a triangularly integrated network (TIN), plays a very important role in the flood modelling process as it is utilized by a hydrological model to define flow routing and subsequently runoff routing paths of precipitation usually in relation to gravity. For floodplain modelling in rural areas, it is recommended that the DTM has a vertical accuracy of 0.5m and a spatial resolution of at least 10m (Ramsbottom & Wicks, 2003). For urban areas, 2D modelling at extremely high DTM resolution of 10cm provided an unprecedented level of detail in the representation of the dynamics of flood inundation over the urban terrain and depicted the extent to which low cost flood resilient urban surfaces could impact flood impacts (de Almeida et al., 2018). At smaller DTM resolutions, more detailed flow processes can be simulated and the impact of FRM approaches can be observed depending on the accuracy of the DTM. For example, on all roads in the UK, based on the UK Traffic Signs Manual (TSM) 2009, the absolute minimum road width is stipulated at 3m (TSM, 2009). For buildings in the UK, a minimum floor area for any new building is to be at least $37m^2$ (6.08m x 6.08m) as mandated by the Department for Communities and Local Government (DCLG, 2015).

Table 5: Satellites for obtaining terrain data for flood modelling.

Serial	Satellite	Technical details/Product	Resolution	Year Launched	Remarks
1.	ALOS-2	LiDAR and Optical satellite by JAXA	1m	2014	
2.	CBERS-4	Optical satellite	2.5m	2019	
3.	Deimos-1	Optical satellite by Deimos Imaging	70cm	2009	
4.	EROS A and B	Optical satellite by ImageSat International	1m	2000 and 2006	
5.	GeoEye-1	Optical satellite by DigitalGlobe	41cm	2008	Decommissioned in 2013
6.	ICESat-2	LiDAR satellite by NASA	30cm	2018	
7.	IKONOS	Optical satellite by GeoEye	1m	1999	
8.	KOMPSAT-3	Optical satellite	1m	2018	
9.	Landsat 8	Optical satellite	30m	2013	
10.	NigeriaCube 1,2 and 3	Cube Satellites operated by NASRDA		2021	
11.	NigeriaSAT 1 and 2	Optical Satellites by Surrey Satellite Technology	2.5m	2003	Decommissioned in 2011
12.	NigeriaSAT 1R	Optical Satellites by Surrey Satellite Technology	1m	2011	
13.	NigeriaSAT X and L	Optical Satellites by Surrey Satellite Technology	1m	2011	
14.	NigeriaSAT-2A and 2B	Optical Satellites by Surrey Satellite Technology	1m	2011	
15.	Planet Scope		3-5m	2016	
17.	Pleiades 1A and 1B	Optical satellite by CNES	50cm	2011	
18.	Quickbird	Optical satellite by DigitalGlobe	60cm	2011	Decommissioned in 2015
19.	Radarsat-2	SAR Satellite by MDA	3m	2007	
20.	RapidEye	5-Satellite constellation (Optical satellite) by Blackbridge	6m	2008	
21.	Sentinel 1	SAR Satellite	5-30m	2014	
22.	SPOT (CNES)	Optical satellite	20m	1986	
23.	SRTM	SAR Satellite	30m	2000	
24.	TanDEM-X	LiDAR Satellite by ESA	2m	2010	Decommissioned in 2019
25.	TerraSAR-X	SAR Satellite	3m	2007	
26.	WorldView-2	Optical satellite by DigitalGlobe	50cm	2009	
27.	WorldView-3	Optical satellite by DigitalGlobe	30cm	2014	

From the dimensions of road and buildings, in order for a model to capture the flow dynamics over these surfaces, a high resolution DTM is advantageous. A high resolution DTM is vital when small scale processes in the terrain need to be investigated especially when testing the effect of flood disaster management (FDM) measures. Using a lower resolution DTM while modelling pluvial flood in urban areas may result in the omission of vital routing processing over roads and buildings which could result in errors in the modelled flooding event. However, balancing DTM resolution and computational requirements for flood modelling is being given a lot of attention (Bates & De Roo, 2000) as larger catchment areas would ultimately demand higher computational power to drive the hydrological process (Haile & Rientjes, 2005). Researchers are inclined towards the use of DTM resolutions of 10m or less for flood modelling in urban areas when distinct constituents of the terrain are being investigated and they capture more channel morphology details.

2.2.2 Meteorological data for flood modelling

In pluvial flood modelling, precipitation is the most important meteorological parameter that influences modelled flood extent. Some temperate regions are affected by other forms of precipitation besides rainfall such as snow which results in snowmelt, where the modelling scenarios are different from normal rainfall. There are other meteorological factors that influence flow over terrain such as evapotranspiration, wind, etc but the most important parameter is precipitation, and it would be the focus of the meteorological factors considered. In tropical regions, precipitation is in the form of rainfall, and this would be the focus of this research. Rainfall within a catchment area usually expressed as rainfall depth but interpreted in hydrological models as rainfall intensity which greatly influences predicted flood output. As the flood intensity varies, it affects the responses of flood losses especially losses via drainages. Furthermore, the intensity of a flood is intricately linked to flood duration as losses via infiltration over time, has a direct relationship to rainfall intensity and duration. Accurately depicting the rainfall intensity over a catchment is vital in replicating an actual rainfall event. The introduction of weather monitoring stations with the capability of per second, per minute and possibly hourly rainfall measurements, enable precise modelling of such rainfall events. However, higher temporal rainfall measurements such as a couple of hour intervals, daily, monthly or annual rainfall depth are employed to generate rainfall intensities, but these have to be transformed to rainfall intensities usually by the use of intensity, duration, frequency (IDF) curves. The use of IDF curves has limitations and may however lead to the introduction of errors associated with the use of these IDF curves due to limited data availability, climate change, spatial variability of rainfall and stationary assumptions of IDF curves. Though there have been satellite generated rainfall intensities, their measurements are sometimes complemented by observed ground weather station measurements which are then interpolated across entire catchments. For example, Tropical Rainfall Measuring Mission, Multi-satellite Precipitation Analysis (TMPA) has freely available rainfall data for tropical regions at 0.25^0 spatial resolution at 3-hour intervals. Some other available sources of precipitation that could be utilized for flood modelling is at **Error! Reference source not found.**.

Table 6: Satellites for generating precipitation data.

Serial	Satellite	Technical details/Product	Date Launched	Remarks
1.	AMSR2	Uses a combination of microwave sensors to measure precipitation from space. Operated by JAXA	2012	
2.	AMSR2	Uses a combination of microwave sensors to measure precipitation from space. Operated by JAXA	2012	
3.	GCOM-W1	Uses a combination of microwave sensors to measure precipitation from space. Operated by JAXA	2012	
4.	Global Precipitation Measurement Microwave Imager	Uses a combination of microwave sensors to measure precipitation from space. Operated by NASA	2014	
5.	Global Precipitation Measurement (GPM)	Provides a global coverage of precipitation. It uses a combination of radar and radiometer sensors for the measurement of precipitation from space. Operated by NASA/JAXA	2014	
6.	GRACE-FO	Designed to measure changes in the Earth's gravitational field which can be applied to measure changes in water storage including precipitation and soil moisture. Operated by NASA and GFZ	2018	
7.	INSAT- 3D	Used for weather forecasting, storm monitoring, cyclone detection and warning systems, ocean state forecasting and atmospheric sounding. Operated by the INSAT.	2013	
8.	Megha-Tropiques	Uses a combination of microwave and infrared sensors to measure precipitation from space. Operated by ISRRO and CNES	2011	
9.	SMOS	Designed to measure soil moisture and ocean salinity. It can also provide information on precipitation. Operated by ESA	2009	
10.	Tropical Rainfall Measuring Mission (TRMM)	Uses a combination of radar and radiometer sensors for the measurement of precipitation from space. Operated by NASA/JAXA	1997	

2.3 Hydraulic and hydrological processes in flood modelling

Flow routing is used for predicting changes in magnitude, speed and shape of a flood wave over time at selected locations of a watercourse which generates a flow hydrograph or unsteady flow of the watercourse (Maidment, 1993). Runoff is the flow over land, of excess water that was not absorbed into the ground or evaporated (Critchley et al., 2013). Runoff routing (which is the focus of this research) is used to calculate from a rainfall event, the surface runoff hydrograph where losses from the rainfall are extracted and the excess rainfall is subsequently converted into a hydrograph (Kemp, 2002). Rainfall is subjected to several losses and hydraulic processes before excess rainfall results in runoff. These losses could be via absorption into the groundwater or infiltration (which depends on the permeability of the surface), evaporated directly or via plants (evapotranspiration) and losses from natural and/or artificial drainages. Runoff interacts differently with various obstructions to its flow such as buildings, trees, vegetation etc which are represented as hydraulic processes using various algorithms which can be classified as surface roughness or as obstructions. During an urban storm event, there are three major processes that drive the dynamics of surface water flow which are; the infiltration into pervious surfaces, discharges to storm sewer system and surface runoff of excess water (Liu et al., 2015). An overview of the hydraulic parameters (surface flow routing) and hydrological processes (infiltration, drainages and evapotranspiration) that interact with a rainfall event are explained in subsequent sub-paragraphs.

2.3.1 Surface roughness

Overland flow which is gravity driven is also influenced by the underlying surface that interacts with the flow. This underlying surface is referred to as the hydraulic roughness and hydrological modelling studies have been conducted using the roughness values to simulate such processes and one of them is Manning's roughness coefficient. The coefficient was first presented by an Irish Engineer, Robert Manning's in 1889 in its complicated form but was later simplified and has become one of the most widely used uniform flow formulas for open-channel flow computations (Chow, 1959). Though other formulas for roughness coefficients exist such as the Kutter's *n* which has similar values with the Manning's *n;* and the Pavlouskii formula proposed in USSR in 1925, the Manning's *n* still remains the preferred choice for inundation studies and its roughness values are accepted by the flood models that were used for this research. Specifically for flood modelling in urban areas, a uniform Manning's *n* of 0.01 – 0.1 was used to test sensitivity to mesh resolutions of 20m, 30m, 40m and 50m in Shanghai, China and results confirm the model being more sensitive to roughness than mesh resolution with increasing roughness sensitivity to more coarse resolutions (Yu et al, 2016). Still on studies in urban areas, hydrological model error was investigated using Manning's *n* values generated using manual inspection of aerial photographs and compared against values generated using land cover classes from the National Land Cover Dataset (Kalyanapu et al., 2009) The results from the National Datasets were found to be acceptable for medium to large watersheds. Manning's *n* has also been applied in hydrological modelling in urban areas

(Harun-ur-Rashid, 1990; Hessel et al., 2003; Yu & Coulthard, 2015) and have helped represent the interaction between flow and the underlying surface. Surface roughness can be applied as a uniform parameter over the entire catchment areas or as a distributed roughness value. The study area is urbanized, and a uniform roughness value may not fully capture the heterogeneous nature of the terrain. The use of distributed roughness parameterization can be applied for this study due to the high resolution DTM available, the diverse land use land cover (LULC) classes that define the study area and access to high-speed computers for the modelling tasks.

2.3.2 Infiltration/Hydraulic conductivity

Infiltration is the downward entry of water into the soil (Johnson, 1963) under the driving force of gravity and capillarity. The infiltration rate of a surface is the speed at which water enters the soil. Infiltration is usually affected by soil properties such as the texture and structure which affects it permeability. It is also affected by the temperature of water and sediments, the depth to ground water, length of time water is applied and atmospheric pressure (Johnson, 1963). Factors affecting infiltration capacity can be categorized into soil and soil profile, biologic and microstructures in the soil and vegetation (Horton, 1939). Water that cannot infiltrate the soil accumulates on it resulting in runoff with the runoff rate representing the difference between water and infiltration. Infiltration is measured on the ground using an infiltrometer which its measured infiltration rate is mm/hr. Hydrological models on the other hand, use equations to determine the infiltration rate when simulating a flood event. These equations are used to represent various infiltration models which are used to simulate the infiltration rate as water flows over a surface. This varying infiltration rate is represented as hydraulic conductivity in hydro-inundation models. An overview of some infiltration models includes the Green-Ampt Equation. This approach was developed by (W. H. Green & Ampt, 1911) for infiltration rates in uniform soils with the assumption that soil is characterized by a saturated wetting front and the water acts like a wetting front similar to a suction head. Other assumptions are that the wetting front advances at a constant rate, volumetric water remains constant above and below the wetting front as it moves, and with the soil suction below the wetting front remaining constant (Valette et al., 2006). It accounts for many variables that influence infiltration such as hydraulic conductivity, porosity of the soil, wetting point suction head and time, which delivers a method that can be implemented as the analytical solution to Richard's equation in a simplified case. Another infiltration models is Horton which is derived from the progression of a rainfall event noting that infiltration capacity decreases with rainfall duration at a defined intensity (Horton, 1939). The driving parameters of the Horton equation are infiltration capacity at the beginning of the rainfall and the minimum infiltration capacity reached with a constant which governs the time required under set conditions of infiltration capacity to change from the initial infiltration value to the final constant infiltration value (Diebold, 1942). The equation proved that it can be derived directly from fundamental principles (Horton, 1941) which is a favourable characteristic of a rational or semi rational equation. Darcy's Law is another equation that governs the flow of fluids through a permeable material or porous medium (Guest & Prévost,

2007; Joseph et al., 1982). A significant application of the formula is the ability to calculate the quantity of water flowing through the cross-section of an aquifer (Kumar & Jain, 2012). The equation is driven by the understanding that rate of flow through stratified beds of sand is directly proportional to energy loss and inversely proportional to the length of the path of flow. Despite the wide applications of Darcy's law, it has been found to be invalid for high values of Reynolds number (ratio of inertia forces to viscous forces) (Costa et al., 1999). It is also invalid at very low hydraulic gradient in materials characterised with little perviousness (Lederle et al., 2020). The Philip's Equation introduces sorptivity in infiltration studies which is the measure of a mediums capability to absorb or release fluid via capillarity (Philip, 1969) which has been adopted in defining the characteristics of soils and other permeable materials. In the equation, sorptivity is expressed as cumulative infiltration at a power series of time. The power series solution is only valid for a limited time span (Mollerup & Hansen, 2007) and the model has been applied for fitting purposes or for use in run-off simulations. Richard's equation is a nonlinear partial differentiation equation used to represent water movement in unsaturated soils. The equation is in one-dimension vertical flows, non-hysterical and non-swelling soils (Mollerup & Hansen, 2007). The equation is criticized as being computationally expensive and unpredictable (Short et al., 1995). Hydraulic conductivity (HC) is the property possessed by vascular vegetation, soils and rocks which defines the ease at which fluids percolate its openings, spaces and fractures (Ajibola et al., 2018). In hydrological models, HC is used to determine infiltration into the soil and also factor changes in the permeability of soils. HC values to be assigned for flood modelling are largely determined by the soil profile or terrain and the values can be obtained either empirically (from soil properties) or experimentally (from hydraulic experiments). The process of determining HC from hydraulic experiments in urban areas is not practicable, hence the adoption of correlation methods using the soil profile of the area is preferable (D. Yu et al., 2016). Though this method may be prone to errors, a range of HC parameters can be generated for different terrain types and sensitivity analysis of these HC values along with other identified model parameters will help in the choice of the optimal HC value that best describes the terrain under study. This adoption of the HC value determines the infiltration rate in the study area.

2.3.3 Evapotranspiration

Evapotranspiration in the context of hydrological modelling represents the combined flood losses resulting from evaporation from land/water bodies and transpiration from plants. It is affected by several factors such as the region under study (temperate or tropical), temperature, wind, humidity and land use type (urban, rural or vegetated). Evapotranspiration in urban areas can be neglected due to the short duration and atmospheric conditions of a storm event (Liu et al., 2015). Though flood losses from evapotranspiration are minimal compared to the flood event (Yu and Coulthard, 2015), it is still necessary to ensure that the other parameters the hydrological model depends on, optimally simulate the process that they were calibrated for; hence evapotranspiration will be used for this study. The process of determining evapotranspiration varies for a densely urban or a rural area

characterized by large vegetation cover. Measuring evapotranspiration is achieved using a lysimeter, field experiments, soil depletion studies and water balance method.

2.4 Flood modelling at large and small scales

Flood modelling at regional and global scale are currently feasible due to increased computational power, availability of data and the dynamic modelling approaches but the challenge is how well flood modelling at these large scales can represent flow processes at the local levels (Fleischmann et al., 2019). However, how well can regional and continental models represent local flood hazards? Flood modelling over urban terrain with a high level of precision, depends heavily on the resolution of the terrain data and this has a direct relationship with computational demand to simulate the flow processes. Large scale flood mapping is challenging without compromising spatiotemporal resolution, accuracy of modelling output, spatial scale and the hydrodynamics at the local scale level (Saksena et al., 2020). Furthermore, the representation of flood defence is relatively poor in large-scaled flood modelling and this hinders their ability to map floods accurately (Wing et al., 2019). The option of running flood modelling for large catchments in segmented smaller sub-catchments are options to reduce the computational demands and time required to run models at larger scales. In testing the ability of flood models at global and regional levels, the global approach had limitations in accurately estimating discharge and water levels due to its coarse DEM of 500m SRTM, while the regional model gave a better representation of the analysed variables compared to the global model (Fleischmann et al., 2019). Hydrological models were found to be the most effective tool in simulating flow pathways in shall catchments but were dependent on available data (Nasr & Hynds). The research further posited that most hydrological models appear to simulate large catchment hydrodynamics but do not perform well in smaller flashy catchments that are characterized by unique behaviours. The ability of a model to be able to simulate flow effectively at different catchments sizes with available data needs to be adequately researched into. The challenge of modelling flow in small sub-basins, there is the possibility of flows from neighbouring sub-basins especially when modelling extreme rainfall events and this could lead to inaccuracies in modelling flow at such smaller scales.

2.5 Factors affecting choice of flood models for simulating flood.

A model is a simulated representation of a real-world event. In hydrological modelling, a model simulates a real-world flow event. Keeping in mind that a model can never be “truth” or 100% correct; models can actually be ranked, depending on specific application as very useful, somewhat useful or essentially useless (Burnham & Anderson, 2002). The choice of a parsimonious models is preferred against a non-parsimonious one as a proper trade-off between bias and uncertainty is desired (Di Baldassarre et al., 2009). The selection of a flood model needs to be based on the scale on investment required, the flood context and the requirements needs for flood forecasting (Qi et al., 2021). The choice of a model for simulating a hydrological event depends on an interplay of several factors as shown in Table 7.

Table 7: Factors affecting the choice of hydrological models for various studies.

Serial	Factor	Research output/study area/Desired outcome	Challenge(s)	Recommendation(s)
1.	Type of modelling to be done (coastal, pluvial, fluvial or a combination)	Flood inundation modelling of a pluvial flood event	Densely urbanized study area with complex terrain	Urban drainage models comprise 4 components rainfall, rainfall-runoff, overland flow and sewer flow modules (Pina et al., 2014).
2.	Data available	Data availability defines the type of outcome desired	Limited data. Some models require specific data to run	Can simulate real-time event with limited data
3.	Desired output	Flood inundation map	Data accuracy important to reduce errors and uncertainty	Can be replicated without minimum fuss.
4.	Intended use of results	To drive favourable flood policies	To drive an informed flood policy	Applicable for flood forecasting.
5.	Expertise on model manipulation	Training and available support to be readily available	- Low human capacity - Training may be expensive	Simple to run, easy to teach hydrologists and model support available
6.	Versatility of model	Ability to account for diverse modelling processes	May result in additional errors and increase uncertainty	Can be applied to diverse sub-catchment areas and still generate acceptable results
7.	Computational requirement for model	Low computational power as research is in a data sparse region	Study area is data sparse and may not have high performance systems thereby taking a long duration to run	A model that doesn't require high computational power to run.
8.	Compatibility with other software	Ease of manipulating data between software and analysing results using various means	May need output in specific format for compatibility	Results to be in a format that can be easily transferred between softwares.
9.	Accuracy of results required	Simple process and reliability of results	An inaccurate model may result in driving the wrong FRM policies	Compromise between bias and uncertainty.
10.	Ease of manipulating model	Unambiguous model that generates desired results	- Data need to be in specific format - Ability to troubleshoot difficulties	A model that permits easy troubleshooting when necessary.
11.	Availability/Cost of model	Preferable free or at a minimal cost	Modelling may require technical support which may not be free	A free or affordable model noting that funds may be limited.
12.	Driving processes of the model	A model that can simulate pluvial flood. To represent flow processes and rout flow.	Complex approach to representing pluvial flow over a surface due to huge detain to be represented	Use an unambiguous model that can simulate flow within the study area with ease.

2.6 Defining criteria for testing the meaningfulness of flood forecasting in urbanized data sparse regions

Flood models are actively employed as tools to forecast floods, generate FFWS and drive FRM. The evaluation of flood forecasts depends on the efficiency and effectiveness of the early warning system to address two vital components namely: the reliability of the warning and the damage the warning prevents (Schröter et al., 2009). The ability to forecast floods is an interplay of the ability to predict rainfall in time and space, and the correct reproduction of the hydrological system specifically the reproduction of the dynamic behaviour of the flow over the terrain (Schröter et al., 2009). The reliability of a forecast thus depends on how effective the warning system is in relation to the uncertainty in the forecasting chain and the lead time it gives. Predictive uncertainty can be expressed in form of a predictive error which is expressed as a form of probability distribution function describing the variability between the simulated and observed values. The prediction error can thus be expressed as a time step variation between the observed and predicted discharge or depth values. In order to obtain a time step comparison of the observed and predicted values, there is the need to generate predicted time step hydrographs with different lead times which are then analysed against observed hydrograph. Before generating flood forecasts and then trying to evaluate their reliability, it is vital to calibrate the hydrological model and subsequently validate the predicted flood against observed flood extent. This usually involves a process of determining the sensitivity of modelling parameters that were used to generate the model to ensure a smooth calibration process. The overall aim is to be able to reproduce the entire process of forecasting floods and develop a warning system with sufficient lead time to be able to respond in good time.

Flood forecasting systems involves the predetermination of flood events in order to help drive best flood risk management policies (Adams & Pagano, 2016). Defining criteria for testing the meaningfulness of flood forecasts will assess the performance of existing FFWS and identify important outputs that drive the systems. In Australia, FFWS is delivered at the national level providing diverse hydrological services including the issuing of flood warning to particular catchments providing the specific heights of river information to emergency response agencies and other stakeholders (Pagano et al., 2016). **Accuracy** of the information provided, and the **reliability** of the forecast are thus important criteria that will trigger appropriate FRM approaches by stakeholders. In Russia, flooding is responsible for almost 30% of economic losses and the country's hydrological forecasting system (HFS) provides complete, effective and operational forecasts of the state of the country's inland waters (Borsch & Simonov, 2016). In order to achieve this, the HFS coordinates all meteorological and hydrology data flow in order to make the FFWS less complex and to speed up operations. The structure adopted for the Russian HFS (called Roshydromet) involves the collation of data down to the local levels which is then analysed to give early flood warning. The Roshydromet HFS adopts an **unambiguous** FFWS which is **robust** where the outputs are easily **transferrable** from the local level to the appropriate stakeholders. In Europe, the European Flood Awareness System

(EFAS) was launched in 2002 by the European Commission to have a common forecasting tool in Europe to eliminate the heterogeneity of national flood forecasting tools (Braud et al., 2018). In order for a unified FFWS to be adopted by many nations, a **simple** approach whose output can be easily **transferrable** and understood by FRM policy makers cutting across different nations needs to be pursued. This resulted in a FFWS that **simplifies** the representation of the hydrological process and easily transforms rainfall into discharge with the outputs regularly updated (Braud et al., 2018). The process of a FFWS is dependent on the **accuracy** of input data, the simulation of the flood event (suitable **computational power** is required) and the transmission of the flood forecast to appropriate stakeholders. In the United States, the National Weather Service arm of the National Oceanic and Atmospheric Administration (NOAA) is responsible for producing/disseminating public forecasts using a **robust** system of hydrological/hydraulic representations and modern forecasting technology (Adams III, 2016). However, the constraint the organisation faces is in their model inputs and **computational efficiency** of the models used. Generating a flood warning needs to be timely generated as well as disseminated. **Computational power** plays a vital role in the timely generation of flood warnings as a lot of the processes involve algorithm processing and mass storage space. A summary of major criteria that can be adopted to test the meaningfulness of flood forecasts in data sparse regions is at Table 8.

Table 8: Criteria for evaluating flood forecasts.

Serial	Criteria	Importance of desired attributes	Application at existing FFWS	Application to data sparse region
1	Parameterization	Ability to generate appropriate parameter values for adequate process representation	Parameterization of the integrate Flood Analysis System (IFAS) for the Indus River in Pakistan to generate sufficient lead time for the region (Aziz & Tanaka, 2011)	Defining the appropriate parameter values that optimally replicate a historical flood event and how well these parameters can represent other sub-catchment areas.
2	Accuracy	Ability to replicate historical/known events. Are the errors minimal?	Output from FloodMap UK helps improves the accuracy of forecasting surface water flooding in UK (D. Yu et al., 2017)	How accurate can the output be in relation to the sparse data available to drive selected hydrodynamic models?
3	Reliability	The lead period of a FFWS and the certainty at which forecasts are made	Provided medium-range flood warning using an integrated ensemble NWP and hydrological modelling for Europe (Werner et al., 2005)	What lead period can a FFWS provide for a data sparse region? What is the accuracy of such predictions?
4	Robustness	Ability of the FFWS to generate accurate outputs with uncertain inputs	The UrbanFlood FP7 Project with the capability of monitoring thousands of kilometres of flood defences is an integrated EWS (Krzhizhanovskaya et al., 2011)	To determine how the various parameters interact and which parameters influence the models the most.
5	Transferability	Interoperability of FFWS across diverse temporal and spatial contexts for which it was calibrated	Output from Australian Bureau of Meteorology easily transmitted among stakeholders (Borsch & Simonov, 2016).	How well will the parameter values calibrated from one sub-catchment be transferrable to other sub-catchments?
6	Replicability	Ability of FFWS to be used across different terrains	Incorporating StormSense into Tidewatch for mo	How easily can parameter values predict flooding in different sub-catchment areas?
7	Simplicity	Unambiguous FFWS which is easy to operate and manage	Applied a Mamdami Fuzzy Rule approach for flood early warning system using a GIS approach (Kurniyaningrum et al., 2019)	A simple FFWS will be easy to replicate and maintain in a data sparse region.
8	Computational demand	Ability to produce timely output with minimum computational power requirement	Used a hybrid of lumped hydrological models and logistic regression to save computational time (X. Li & Willems, 2020)	It will be encouraging for a FFWS to have minimum computational demands that doesn't compromise its reliability.
9	Sustainability	Ability to sustain the FFWS using minimal manpower, computational and financial demands	Output from HIDROMET proved to have desired sustainability and is being replicated across different sub-catchments (Henonin et al., 2013)	How can the forecasting system be sustained with limited manpower, computational and financial requirements?

2.7 Testing the validity of flood forecasts in data sparse coastal regions

Traditional means of testing the validity of flood forecasts utilize some form of observed flood event to evaluate against a flood forecast. Observed flood events can be obtained from satellite imagery (Bates et al., 2004; Dhara et al., 2020; Horritt, 2006); preferably from satellites with a high temporal resolution (Tiwari et al., 2020) to capture the flood event sufficiently, to be able to generate flood depths and extents at different intervals. Observed flood event can also be obtained from flood depths obtained from gauged catchments. Some cities have in place flood sensors that are able to measure the depth of a flood at intervals (Arshad et al., 2019; Mousa et al., 2016; Pengel et al., 2013). This approach is very effective in generating observed flood extent for pluvial floods as it will capture the flood event as it occurs and as it recedes making it easy to generate the flood hydrographs with a degree of certainty. These flood hydrographs can then be used as validation data against that generated by the forecasted flood event. Unfortunately, data sparse regions may not have any of the observed flood validation data which was the case of the study area. The crowd sourced means was only able to generate the flood event at the peak of the flood event using the videos and photos obtained. Problems will thus arise from parameterizing the model and also determining the accuracy of the modelled flood event. In data sparse regions, the ability to successfully parameterize a model, determine its accuracy, and be able to replicate the entire process of modelling a flood event in a data sparse region, will be termed as a successful flood modelling process in that region.

2.7.1 Model parameterization

Flood models require different parameters in varying formats and input values, hence, the process of determining parameter values differs from one model to another. As the parameters required by models differ, so do the parameters vary from one catchment area to another. Catchments have different infiltration rates and varying elevations. The drainage capacity of catchments also differs, including having different topography. These differences in catchments could result in misrepresentation of flow processes if the parameter values from one catchment area is adopted for use by another. However, catchments that are in close proximity may have similar catchment characteristics (Oudin et al., 2010) and the parameter values may suit the requirement to simulate the flow process in such a catchment area. In data sparse regions, the ability to parameterize a model is a vital requirement when forecasting flood in such regions. This is necessary to ensure that the process can be replicated in varying catchments within the data sparse region with a degree of certainty.

2.7.2 Accuracy

Rainfall data fed into a hydrological model plays a large role on the lead-time availed emergency responders (Looper & Vieux, 2012) and also the quality of the rainfall input is an important component of the modelling process (Hapuarachchi et al., 2011). Flood forecasts are prone to errors from both the input meteorological data and the modelling parameters. The accuracy of a flood forecast is largely an assessment of how well the flood forecast tends

towards a historical flood event. A detailed comparison of the forecasted and the observed flood event to determine the accuracy of a flood forecast has been achieved using statistical approaches (Hamby, 1994, 1995; Looper & Vieux, 2012; Vieux & Bedient, 2004), visual comparison (Petty et al., 2016), crowd sources/citizens science (Helmrich et al., 2021; Hung et al., 2016; D. Yu et al., 2016), or a combination of these methods. In defining the accuracy of these flood forecasts, the interaction of the parameters used by the models in generating the output can be determined which can be termed the sensitivity analysis of input parameters. The process of determining the optimal combination of parameters (calibration) including the assessment of the eventual model output (validation) can be used to determine the accuracy of the flood forecast. Dimensionless statistics give a relative model evaluation assessment (Moriasi et al., 2007) and these include Nash-Sutcliffe Efficiency (NSE), Index of Agreement (IA) and Prediction Efficiency (PE). The NSE is used to assess the predictive accuracy of a model by determining how well the plotted observed and simulated data fits the 1:1 line or in evaluating the residual variance. It indicates the relationship between the observed and simulated values of a model with the higher the NSE value indicating better model performance (Das et al., 2019). NSE values range from $-\infty$ to 1 (Nash & Sutcliffe, 1970) with NSE values ranging between $0.65 \geq 0.9$ indicating a models goodness-of-fit agreement ranging from acceptable, through good, to very good (Ritter & Munoz-Carpena, 2013). The IA evaluates the degree of model prediction error from the 2 models representing the ratio between mean square error and potential error which varies from 0 to 1 (Agrisoft, 2019). Agreement values of 1 indicate a perfect match while 0 depicts no agreement at all. The PE on the other hand, determines how well the probability distributions of the modelled simulation of the models and observed flood extent fit each other. PE tests the ability of a model to predict variation of fluxes around the mean and is a standard metric for tracking variations in models (G. Reeves et al., 2008). Mean absolute error (MAE.), Mean square error (MSE.) (G. D. Reeves et al.)(G. D. Reeves et al.) (G. D. Reeves et al.) (G. D. Reeves et al.) and root mean square error (RMSE) are valuable in model evaluation because they will indicate the errors in the parameters of interest which will aid in analysis (Moriasi et al, 2017). The Kling Gupta Efficiency (KGE) is also a widely used metric for evaluating the goodness-of-fit of -vectors of observations and corresponding model simulations. This metric rectifies some of the shortcomings of the coefficient of determination, also known to hydrologists as the efficiency of NSE (Vrugt & de Oliveira, 2022). Defining the uncertainty of the flood forecast as well as the ability to replicate the process of generating the forecast are vital. Various methods have been applied for calibrating models (H. V. Gupta et al., 2006), with mathematical models used for prediction in models but need sufficient input data (Taylor et al., 2010) but this approach may not be feasible in data sparse regions. Images of flood extent have been tested for calibrating flood models but showed significant differences between the uncertainty map and the observed flood event (Mason et al., 2009). The receiver operating characteristics (ROC) curve, is an approach used on a binary distribution to test its accuracy of prediction using the Area Under the curve (AUC) as a measure of diagnostic prediction (Hajian-Tilaki, 2013). The ROC curve (Schumann et al., 2014) (Manfreda et al., 2014; Manfreda et al., 2015;

Zhao et al., 2019) has been applied for model calibration where emphasis is placed on the how well calibrated flood parameters are able to replicate an observed flood event with the advantage of an accuracy assessment using the ROC curves which utilize a binary distribution of data for its analysis. In data sparse regions where model accuracy can be limited to inundation modelling and comparing with observed floods where there are flooded and non-flooded cells, the ROC curve is an invaluable tool for testing the accuracy of a model and also for determining the best combination of parameters that represent the observed flood event. Model calibration relies on the availability of observed data and inaccuracies in the observed data could lead to uncertainty in model predictions.

2.7.3 Reliability of flood forecasts

The reliability of a forecast is dependent on the accuracy of the rainfall forecast, the hydrodynamic model and its driving parameters, and the initial conditions (Kumar et al., 2020). A forecast's reliability also depends on the lead period of a FFWS and the certainty at which forecasts are made. The lead time determines the response time given to stakeholders and the longer the lead-time, the more reliable the FFWS is termed to be. In analysing the reliability of a forecast, the ability of a model to replicate a historical flood model will be used as a measure of how reliable the forecast can be as this will translate into the models ability to forecast floods with the appropriate weather forecast. The reliability of forecasts is a major constraint that hinders flood warnings in most societies (Parker et al., 2011).

2.7.4 Replicability of flood forecasts

The overall aim of a FFWS is the replicability of the processes involved in generating the output flood extent so that such approaches can be adopted for other areas. There cannot be two emergency situations that are alike, hence, different techniques need to be addressed to solve each situation (McCullough, 2011). When met with an upcoming flood event, responders need as much information about the event to enable planning to start as quickly as possible to trigger the appropriate response. Replicability of a forecast rests with the ability to optimally simulate the real-world event using the hydrological models and terrain characteristics which can then be adopted for predicted weather events. The model approach used to generate the forecast will need to be appropriately parameterized and accurate input fed into it. The process will need to be applicable over a range of scenarios and produce reliable results. An approach to test the validity of a flood forecast will thus include the ability to replicate the flood forecast in different locations within data sparse region. The question would be how well can forecasts be replicated in data sparse regions and how accurate can these forecasts be?

2.7.5 Simplicity

The process of generating a flood forecast is complex in terms of data generation, modelling forecast and dissemination of the forecast. The complex nature of generating forecasts can result in the introduction of errors. Advances in artificial intelligence have made it possible to replicate the way humans think and can extract crucial data from inputs and provide solutions

to complex problems (Chang & Guo, 2020). Uncertainty in flood forecasts can be amplified not only by model features but also from forcing data and observations (Tran et al., 2020). In order to ensure simplicity in flood forecast processes, an unambiguous process of representing the flow over the sub-catchment is advantageous. The underlying question is if simple modelling approaches can adequately represent complex processes? With the complex process resting on the number of parameters required to describe it.

2.7.6 Computational demand

Computational demands for flood forecasting depend on the catchment size, the resolution of the terrain representation over which the forecast is being made, the algorithms adopted by the model for forecasting and the scale at which the forecast is desired. Higher scales at the human action level, which are important for driving awareness and perception of flooding including driving favourable FRM decisions (Sanders et al., 2020), have requirements of high computational power. Flood modelling in large basins may be problematic due to the requirement of distributed hydrological models to estimate soil related and channel parameters on a cell by cell basis (Francés et al., 2002), hence the need for high computational power for such modelling. While non-parsimonious models may offer higher precision or capture more complex phenomena, they are often accompanied by increased uncertainties, data requirements, and computational challenges. In many cases, the added complexity does not necessarily lead to significantly improved flood predictions or management outcomes. Therefore, the preference for parsimonious flood models lies in their practicality, efficiency, interpretability, and their ability to provide reasonable flood predictions in data-sparse regions or situations where simplicity and accessibility are paramount (Ramadas et al., 2015). A parsimonious model is also in line with the Occams razor which favours a parsimonious model over a complex model (McSharry, 2018). Working in a data sparse region may be limited by the access to high computational systems and hydrodynamic models that can achieve actionable results within a defined time limit will be highly desirable for obtaining flood forecasts in these regions. Though the underlying algorithms and the input parameters affect computational time of hydrodynamic models, the time taken for these models to generate actionable flood extents for the same catchment, using the same computational system will determine the computational efficiency of the system.

2.7.7 Robustness

A robust flood model represents the ability of that model to generate accurate outputs with uncertain inputs. This attribute will be invaluable while working in a data sparse region as many hydrodynamic models require quite a number of input data which may not be available in such regions or if they are available, the data may be inaccurate. Input data requirement varies for different flood models but they can be ‘forced’ to run with a limited number of variables (Kauffeldt et al., 2016); the question will be how accurate are these modelled flood outputs?

2.7.8 Transferability

Parsimony of parameterized models is advantageous but they are limited by the lack of generality beyond the catchment for which they have been developed (Wainwright & Mulligan, 2013). This poses a challenge as transferability of parameter values from neighbouring catchments may not adequately represent the flood drivers of that catchment and result in errors in modelled output. A model that generates acceptable results over a range of catchments will be desired in a data sparse region and a particular hydrodynamic model can be used for flood forecasting within that catchment and reduce ambiguity whilst ensuring simplicity of the forecasting process.

2.7.9 Sustainability

Sustainability of a flood forecasting system defines the ability to keep replicating the FFWS using minimal manpower, computational and financial requirements. A sustainable FFWS can be easily implementable in other catchments areas as long as the process of generating forecasts is transferrable and produces accurate results. An example is the HIDROMET flood forecast system that was first implemented in one of Barcelona's catchments called Riera Blanca. The success and the sustainable nature of the flood forecasting process resulted in it being replicated in other catchment areas in Spain (Henonin et al., 2013). Evolving a sustainable process of forecasting flood in a data sparse region will be invaluable to the region as this will encourage the transfer of the process to other vital sub-catchment areas within the region.

2.8 Summary of Chapter 2

This chapter brought the entire research work into better perspective by introducing the dependent and independent variables in the study. A synopsis was made of 1 – 3 Dimension flood models highlighting on some flood models applied for FRM purposes. The important role data plays in driving flood modelling was showcased with comparison of the types of flood modelling research conducted at developed countries which have some level of data available for simulating the flood processes and developing countries with sparse data. The developed countries have the capability of simulating complex processes and have some capability of validating their simulations with observed data but the FRM research by developing countries mostly lack observed data for validation data and exploit satellite data to validate their simulations. The data required by flood models was highlighted with satellites that were available for the generation of terrain and meteorological data outlined. As flood models are driven by hydraulic and hydrological processes, an insight was provided into the various process representations by models in order to simulate a real-world event. The pros and cons of modelling floods at large and smalls scales were compared before looking into factors that affect the choice of models for diverse FRM applications. Vital model processes of sensitivity analysis, calibration and validation of models were outlined. As models are used for flood forecasting, criteria were defined that could be a guide when testing the meaningfulness of forecasts made by flood models especially in a data sparse region.

Chapter 3: Flood risk management in the study area and data available for pluvial flood modelling

3.1 Overview of flooding in Nigeria

Nigeria is located in West Africa within Latitudes 4° to 14° North of the Equator and Longitudes 4° to 15° East of the Greenwich Meridian. The country has a total landmass of 923,768 km^2, with 910,768 km² of this area being land, while the remaining 13 000 km² occupied by water. The Country has a coastline of 860km (Orupabo, 2008) and a population of 193,392,517 inhabitants (NBS, 2020). With coastlines being more populated than inland areas, this large coastline would pose huge threats if there were any coastal flood. Nigeria is the most populated nation in Africa with a population density of 204 inhabitants per square kilometre. Due to its proximity to the equator and the Atlantic Ocean, the country has a hot tropical climate with 2 major seasons namely, the wet (rainy), and the dry (harmattan) seasons. Rainfall decreases from over 4000mm in the Niger Delta to below 250mm in the extreme northeast. The North East Trade Winds which convey dry dust particles from the Sahara Desert is responsible for the dry season which lasts from about November to March while the South West Monsoon winds which carries moist air from the Atlantic Ocean results in the rainy season from April to October (Danlami et al., 2019). Reported cases of climate change have resulted in the disruption of some of these processes leading to increased desertification in the northern part of the country and higher frequencies of flash floods which are experienced in all the regions (Urama & Ozor, 2010). Nigeria has 2 major rivers namely the Rivers Niger and Benue which flow diagonally from the Northeast and Northwest respectively, converge at Lokoja and empty into the Atlantic Ocean in the south. The two rivers form the major drainage channels for the country with other smaller rivers emptying into the two rivers. In extremes of rainfall or dam releases from neighbouring countries, the rivers and some of their tributaries overflow their banks resulting in fluvial flooding (Olukanni & Salami, 2012). Nigeria is also affected by coastal flooding while some areas are affected by flash storms which result in pluvial flooding. A map of Nigeria depicting the drainage pattern of Rivers Niger and Benue which in turn drain into the Atlantic Ocean is at . Lagos state is located at the southwestern part of Nigeria and is directly affected by coastal dynamics due to its proximity to the Atlantic Ocean. The State is the commercial hub of the country having the largest seaport that serves the entire country.

Globally, climate change has resulted in increased rainfall and sea level rises which results in higher incidents of flood related disasters. Nigeria is not an exception from the impact of climate change as flooding is the most common natural disaster in the country (Ugwu et al., 2021) which has resulted in destruction of property including the loss of lives. In Nigeria, from 2000 to 2022, floods have affected 11,567,828 people and resulted in the death of 1,767 people (CRED, 2022) and the impact of flooding within this timeframe is at Table 9. Nigeria is bound to the South by the Atlantic Ocean and also has 2 major rivers that run from the east and west. The rivers confluence at a point called Lokoja and runs south into the Atlantic Ocean

– see Figure 5. Nigeria has a coastline of about 860km and is at risk of coastal floods as shown in Figure 2. The country is also at risk of pluvial floods especially in the Northern and southern parts of the country as depicted in Figure 3. Along the major rivers in the country, there have been cases of riverine flooding as shown in the riverine flood risk map at Figure 4, sometimes resulting from extreme rainfall events or release of water from dams in neighbouring countries. Some past flood events that have occurred in Lagos including their causes and the type of flood is at Table 10.

Floods are inevitable and enhancing the capability to live with floods by enhancing disaster resilient communities, is presently the focus of current FRM drives (De Bruijn, 2004; Liao, 2012). In order to be able to live with floods, there is the need to be able to identify vulnerable areas and predict floods. This is because the devastation caused by floods is exacerbated when the flooding event is unexpected and response to the flood is limited which is usually the case for floods that occur in Nigeria. FRM efforts are shifting from the usual grey approach by FRM to the integration of blue-green approaches to build flood resilient societies (Kapetas & Fenner, 2020). The study area is densely populated and highly urbanized resulting in high runoff whenever there is a precipitation event thus reducing water losses via infiltration. Another event that occurs in the study area is ponding caused by a combination of drainages that are blocked due to the illegal disposal of refuse resulting in the collecting of water within urban areas and buildings along drainage lines. Ponding also occurs where urban areas are designed without proper consideration of flow outlets for rainfall and have little infiltration (Prokic et al., 2019; Sholihah et al., 2020). The ability to identify vulnerable areas to flooding in Nigeria and evolve an efficient FFWS will greatly enhance the FRM capability of the country.

Table 9: Flooding in Nigeria (2000-2022) Source: EM-DAT 2022.

Disaster Number	Year	Disaster Type	Location
2000-0620-NGA	2000	Flood	Lagos province
2000-0364-NGA	2000	Flood	Sokoto North, Sokoto South districts (Sokoto province)
2000-0511-NGA	2000	Flood	Cross River province
2000-0547-NGA	2000	Flood	Zamfara province
2000-0596-NGA	2000	Flood	Gusau district (Zamfara province)
2000-0628-NGA	2000	Flood	Kebbi province
2001-0494-NGA	2001	Flood	Jigawa, Kano provinces
2001-0408-NGA	2001	Flood	Talata-Marafa district (Zamfara province)
2001-0276-NGA	2001	Flood	Oke-Ogun, Idimissa/olle-Oje, Ogbonmo, Oke-Idogbon, Ijebu-Owo, Post-Office, Oke-Ajama, Ilore, Iyere, Ishokun Oke, Ishokun Odo areas (Owo district, Ondo province)
2002-0238-NGA	2002	Flood	Bariga, Bode Joseh areas (Shomolu district, Lagos province), Lagos Mainland district (Lagos province)
2003-0455-NGA	2003	Flood	Kaduna, Kano, Niger, Jigawa provinces
2004-0413-NGA	2004	Flood	Adamawa province
2004-0434-NGA	2004	Flood	Gombe province
2004-0268-NGA	2004	Flood	Lagos province
2004-0315-NGA	2004	Flood	Jigawa province
2004-0402-NGA	2004	Flood	Ughelli North, Ughelli South districts (Delta province)
2005-0065-NGA	2005	Flood	Lagos province
2005-0423-NGA	2005	Flood	Jigawa, Bauchi, Taraba, Yobe provinces
2006-0556-NGA	2006	Flood	Gusau district (Zamfara province)
2006-0445-NGA	2006	Flood	Zamfara province
2006-0393-NGA	2006	Flood	Edo province
2007-0419-NGA	2007	Flood	Plateau, Adamawa, Borno, Anambra, Bauchi, Yobe, Ogun, Nassarawa, Lagos, Sokoto, Kebbi provinces
2007-0541-NGA	2007	Flood	Ogun province
2007-0595-NGA	2007	Flood	Ikorodu, Kosofe districts (Lagos province), Abeokuta North, Abeokuta South districts (Ogun province)
2009-0375-NGA	2009	Flood	Zamfara, Kaduna, Niger, Benue, Adamawa, Nassarawa, Sokoto, Jigawa, Abuja provinces
2009-0622-NGA	2009	Flood	Lagos province
2010-0509-NGA	2010	Flood	Jigawa, Sokoto, Kebbi, Niger, Katsina provinces
2011-0214-NGA	2011	Flood	Katsina, Lagos provinces

2011-0230-NGA	2011	Flood	Kano province
2011-0343-NGA	2011	Flood	Ibadan North, Ibadan South-West, Oluyole, Ido, Ibadan North-West, Egbeda, Ona Ara, Ibadan Northeast, Lagelu, Akinyele districts (Oyo province)
2011-0582-NGA	2011	Flood	Imo, Lagos provinces
2012-0366-NGA	2012	Flood	Nassarrawa, Niger, Plateau, Adamawa, Bauchi, Gombe, Taraba, Yobe, Jigawa, Kaduna, Kano, Katsina, Kebbi, Anambra, Ebonyi, Cross River, Lagos, Benue
2013-0386-NGA	2013	Flood	Abia, Bauchi, Ebonyi, Edo, Gombe, Jigawa, Kano, Katsina, Kebbi, Zamfara provinces
2014-0211-NGA	2014	Flood	Ibadan North, Ibadan North-East, Ibadan North-West, Ibadan South-East, Ibadan South-West districts (Oyo province)
2015-0448-NGA	2015	Flood	Kano, Katsina, Sokoto, Kebbi, Zamfara, Kaduna, Jigawa, Adamawa, Yobe, Gombe, Bauchi, Anambra, Benue, Delta, Niger, Ondo, Taraba provinces
2016-0337-NGA	2016	Flood	Gwaram, Dutse, Jahun, Ringim, Hadejia, Babura, Gumel, Malammadori, Birninkudu districts (Jigawa province)
2017-0272-NGA	2017	Flood	Ekiti, Osun, Akwa Ibom, Kebbi, Niger (Suleja, Tafa), Kwara, Ebonyi, Enugu, Abia, Oyo (Ibadan), Lagos (Victoria Island, Lekki, Oniru), Plateau, Sokoto, Edo, Bayelsa
2017-0378-NGA	2017	Flood	Benue (Makurdi), Kogi (Lokoja, Sarkin Noma suburbs, Ibaji, Igalamela-Odolu, Ajaokuta, Bassa, Koton-Karfe) states
2018-0238-NGA	2018	Flood	Jibia district; Yobe, Edo, Ogun, Katsina, Ondo, Baucho, Niger, Abuja states
2018-0365-NGA	2018	Flood	Kogi, Delta, Anambra, Niger
2019-0394-NGA	2019	Flood	Borno, Yobe, Jigawa, Kano State states
2019-0415-NGA	2019	Flood	Cross River, Kogi, Niger,Taraba States
2019-0435-NGA	2019	Flood	Borno, Jigawa, Kano, Yobe states
2020-0257-NGA	2020	Flood	Akwa Ibom (southern part of the country) and Kwara (west-central Nigeria)
2020-0321-NGA	2020	Flood	Suleja City, Gwagwalada area, Abuja
2020-0455-NGA	2020	Flood	Jigawa, Kebbi, Kwara, Sokoto, Zamfara
2021-0521-NGA	2021	Flood	Jigawa,Bauchi, Adamawa and Borno states; Jalingo, Taraba, and the city of Lagos
2021-0589-NGA	2021	Flood	Trademoore, Light Gold, Wisdom Estates and Lugbe (Abuja)



Figure 2: Map of Nigeria showing areas at risk of coastal flooding. Source: NEMA, Nigeria.

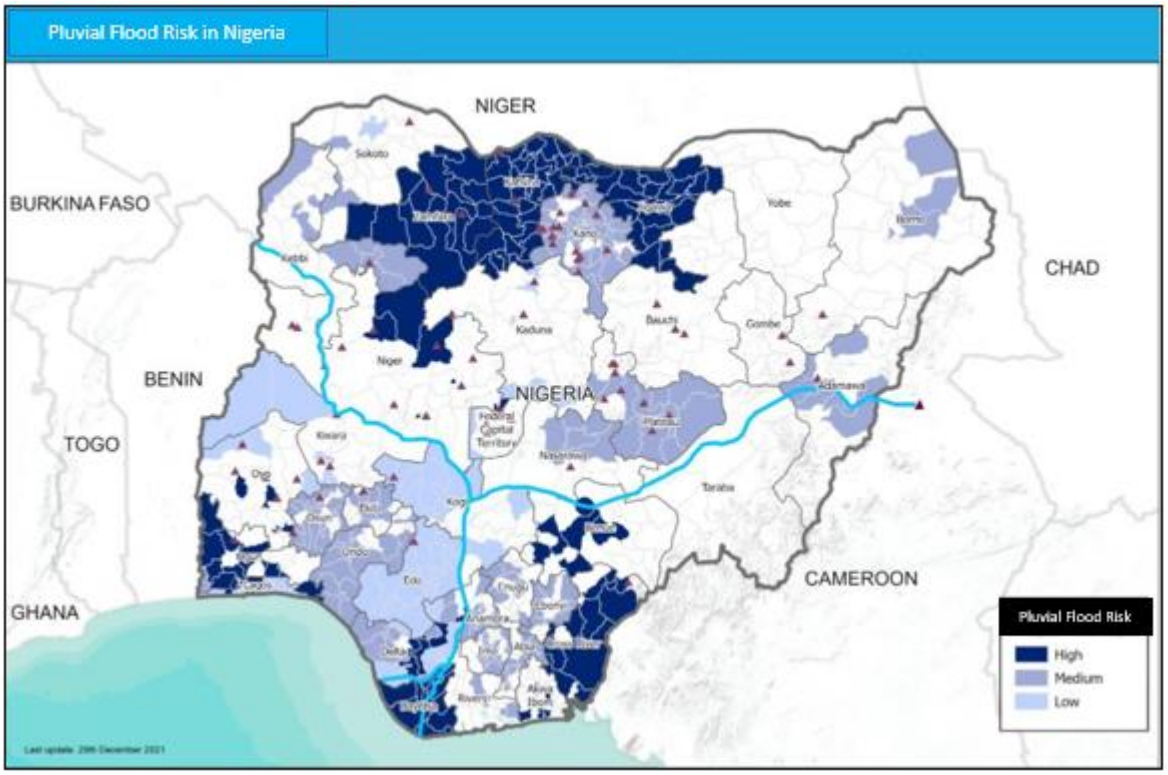


Figure 3: Map of Nigeria showing areas at risk of pluvial floods. Source: NEMA, Nigeria.

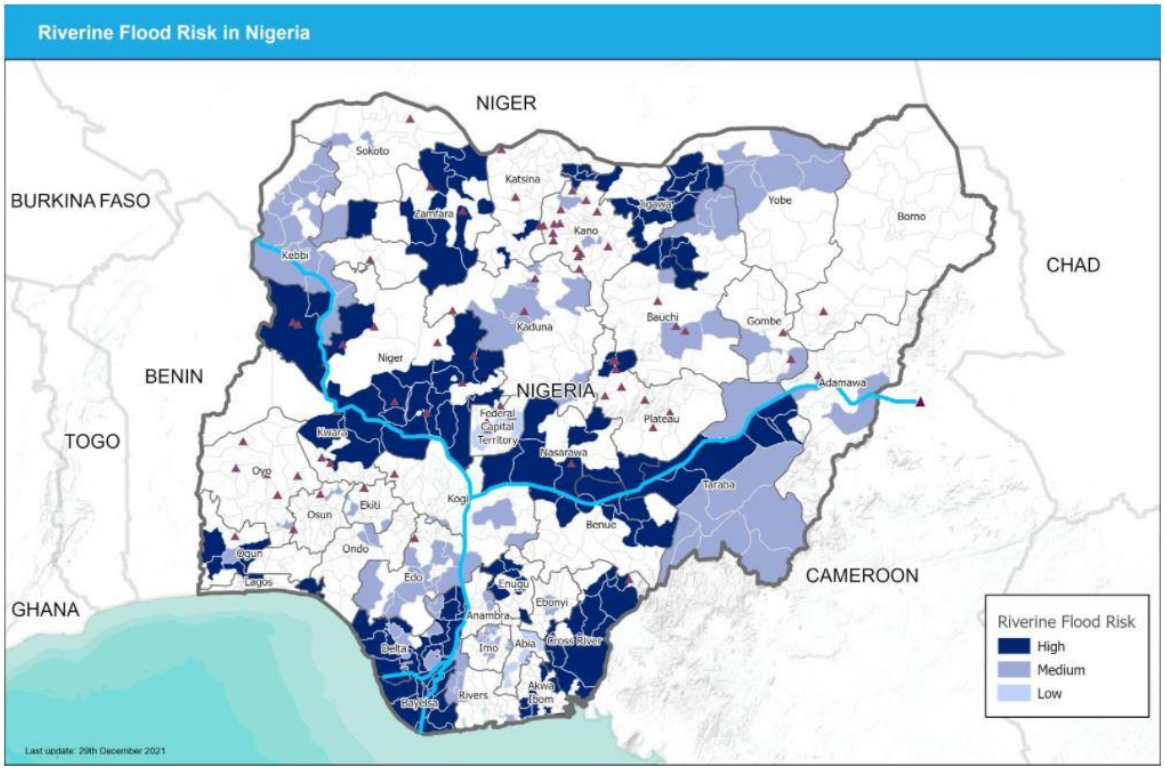


Figure 4: Map of Nigeria showing areas at risk of riverine flooding. Source: NEMA, Nigeria.

3.2 Study area and flood risk management

The study area consists of 3 sub-catchments in Lagos State and are from parts of Lagos Island, Ikoyi and Victoria Island. Average rainfall is about 1506.6mm annually in Lagos with the wettest and driest months being June and January having 315.5mm and 13.2mm of rainfall respectively. The study area is one of the most densely populated Islands in the world with a population density of 6,871 per square kilometre. It shares boundaries with the Atlantic Ocean to the south, and Lagos Lagoon to the north, east and west. It is characterized by low relief, has a large population vulnerable to floods due to high levels of poverty, is affected by data sparsity and is beleaguered by floods annually, especially during the rainy season. Lagos used to be the capital of Nigeria until it was changed to Abuja on 12th December 1991. Most countries still maintain their diplomatic offices in Lagos because the state is the commercial nerve centre of Nigeria. The Ports of Lagos are responsible for 80% of Nigeria's imports and exports. The 3 selected sub-catchment areas serve as major links between Lagos and the mainland, but these areas are flooded almost on a yearly basis. The areas are strategically important to the functioning of the state and a disruption of normal activities in the areas by flood, greatly affects its dense population and economic activities. The need to be able to forecast flooding in this area would serve as a springboard to fostering plausible flood risk management (FRM) strategies. This would be invaluable in curbing losses resulting from floods and then greatly assist in the sustenance of economic and business activities in Lagos.

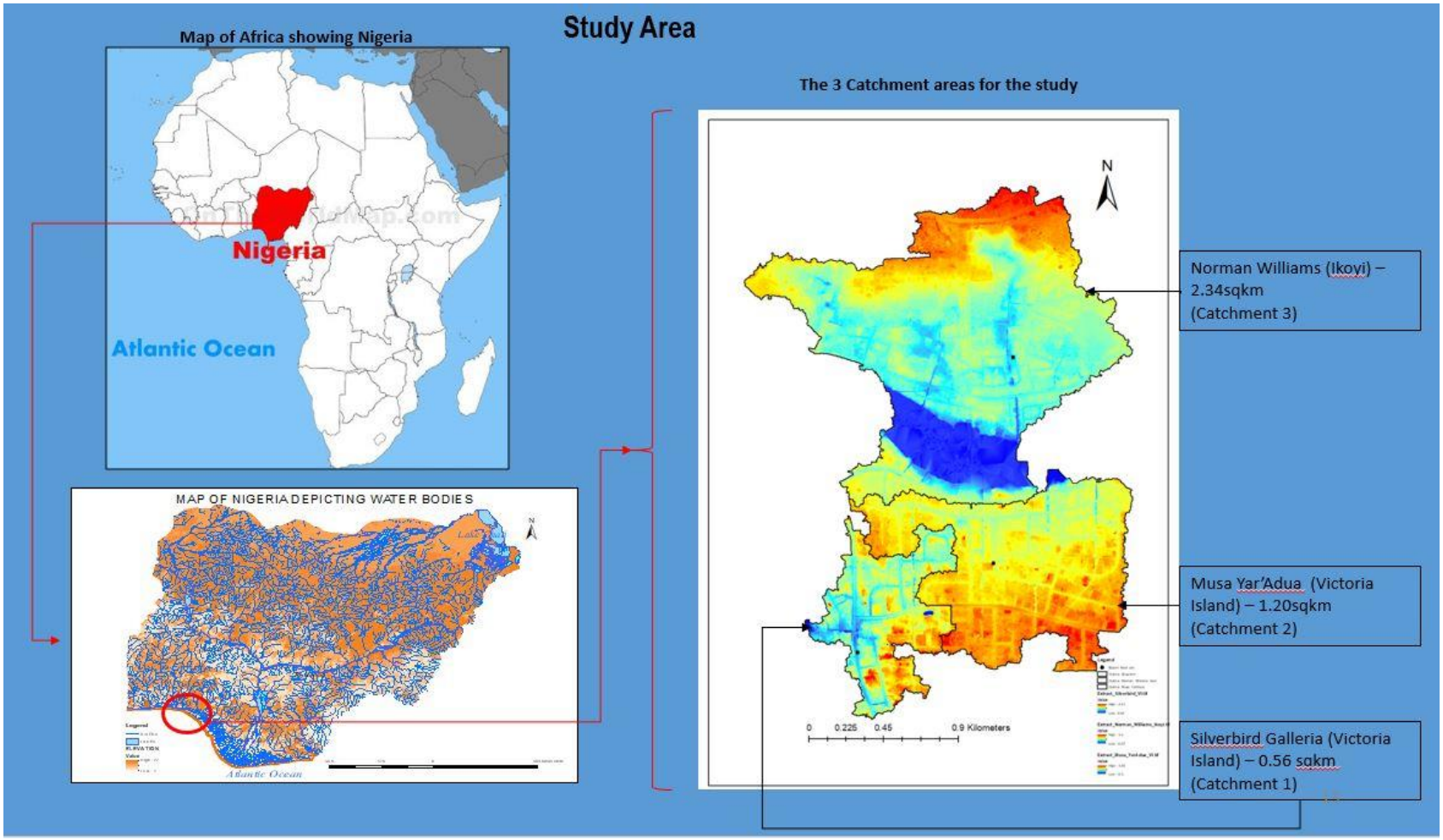


Figure 5: The study area top left-map of Africa showing the location of Nigeria; Bottom left- map of Nigeria showing the location of Lagos State; Right- The 3 sub-catchments under study in Lagos.

Table 10: Some flooding events that have occurred in Lagos.

Serial	Date	Affected Area	Duration (Days)	Cause	Displaced people
1	Jun-68	Lagos Island and Ijora	N/A	Heavy storm	No Info
2	Jun-69	Surulere and Yaba	10	High intensity rainfall	No Info
3	Jul-70	Lagos Island	N/A	rainfall and high winds	No Info
4	Jul-71	Lagos Island	5	Heavy rainfall	No Info
5	Jun-72	Lagos Island	N/A	Heavy rainfall	No Info
6	Jun-74	Areas in Lagos	Some days	Heavy rainfall	Thousands
7	Jul-90	Lagos City	2	Heavy rainfall	500
8	Jul-90	Lagos City	2	Heavy rainfall	3000
9	May-99	Mushin and Idiaraba	N/A	Heavy rainfall	N/A
10	Jun-99	Mushin and Idiaraba	N/A	Heavy rainfall	N/A
11	Jul-99	Mushin and Idiaraba	N/A	Heavy rainfall	N/A
12	Jun-00	VI and Ikoyi	2	Heavy rainfall	500
13	Jul-00	VI and Ikoyi	2	Heavy rainfall	*
14	Sep-00	VI and Ikoyi	2	Heavy rainfall	*
15	Jul_02	Lagos City	3	Heavy rainfall	200
16	Jun_04	Lagos City	2	Heavy rainfall	1000
17	Jul-05	Lagos City	5	Heavy storm	3000
18	Aug-07	Ikorodu	15	Heavy rainfall	5000
19	Oct-08	Lagos City	N/A	Heavy rainfall	N/A
20	Jul-09	Lagos City	Some days	Heavy rainfall	N/A
21	Jul_10	Ikoyi	N/A	Heavy rainfall	N/A
22	Oct-10	Lagos Island, Apapa, Kosefe	Some days	Heavy rainfall	Thousands
23	Jul-11	Lagos Island, Mainland, Mushin	2	Heavy rainfall	10000
24	Jun-12	Oshodi, Arowojobe	Some days	Heavy rainfall	N/A
25	Oct-12	Lagos City	Some days	Heavy rainfall	Thousands
26	Jul-17	Lagos Island	Some days	Heavy rainfall	500
27	08-Jul-17	Victoria Island, Lekki, Victoria Garden City and Ajah		Heavy rainfall	N/A
28	25-May-18	Ketu, Ojota, Bariga	Overnight rainfall	Heavy rainfall	N/A
28	13-Aug-18	Lekki		Heavy rainfall	N/A
29	07-Sep-18	Lagos roads	Overnight rainfall	Heavy rainfall	N/A
30	25 Jun 19	Lagos	Some days	Heavy rainfall	N/A
31	06 Jul 20	Ige road, Aboru lagos	Overnight rainfall	Heavy rainfall	N/A
32	16 Jul 21	Lekki, Lagos Island	Rainfall during the day	Heavy rainfall	N/A

3.3 Nexus of the geography of Lagos and flooding

The nexus of the geography of Lagos and flooding underscores the profound influence of the city's physical characteristics on its susceptibility to flooding. The interplay between geographical elements and flood occurrences is a crucial determinant of the city's resilience to these events. Lagos, characterized by its topography, urbanization, and proximity to the coast, experiences a complex relationship between geography and flooding. The city is characterized by low lying topography with 37% of its area lying between 0.5m and 3m while 63% is between 3m and 5m above mean sea level (Obiefuna et al., 2021) which amplifies flood risk with parts of the city at an elevation close to sea level where moderate rainfall events result in flood inundation due to the lack of a natural drainage. The proximity of the city to the coastline amplifies its flood vulnerability as storm surges and high tides lead to coastal flooding (Helderop & Grubesic, 2019). This is exacerbated by the city's urbanization which is rapid and somewhat unplanned resulting in concrete jungles without adequate drainage infrastructure despite the network of water bodies such as lagoons, rivers and canals. The undefined land use of Lagos comprising mixed patterns of urban areas and sparse green areas impart the flood dynamics of the area as runoff is faster in the concrete regions and sometimes result in ponding due to the infrastructure bottlenecks. The city is susceptible to

heavy rainfall, flash floods and tidal surges during extreme weather events (Aliyu et al., 2023) which is made worse by the lax building codes where flood plain are converted to urban areas without adequate plans for FRM in these areas. The flooding experienced in Lagos is worsened by the densely populated coastal regions of the city which strains existing infrastructure (Atufu & Holt, 2018) and this increases the vulnerability of communities living in flood-prone zones. The geography-flood nexus also showcases efforts to enhance resilience to flooding in Lagos. Initiatives like improved drainage systems, elevation of critical infrastructure, and the implementation of blue-green infrastructure aim to counteract flooding impacts. Unfortunately, the unavailability of precision data to evaluate the extent of the impact these initiatives have had is also a challenge. An understanding of the interwoven relationship between geography and flooding is paramount for sustainable FRM in Lagos. Integrated strategies that consider topography, hydrology, urban planning, and community engagement are vital. Investing in resilient infrastructure, incorporating nature-based solutions, and fostering community participation are ways to leverage the geography-flood nexus positively. However, these flood resilience building measures are vital in determining how best to embark these FRM and flood models form a vital part of achieving this with some certainty considering data may be a setback in this drive. Hence, novel approaches need to be evolved for generating data and obtaining validation data in data sparse regions to drive plausible FRM strategies.

3.4 Flood risk management in Nigeria

The National Emergency Management Authority (NEMA) is responsible for FDM in Nigeria and their activities fall under the purview of the Office of the Vice President of Nigeria who has oversight function over the Organisation. For funding, one percent of the Nigeria's annual budget is voted for the ecological fund while 20 percent of this ecological fund is given to NEMA for disaster management. The remaining 80 percent is given to affiliated disaster response stakeholders like hospitals, the armed forces amongst other agencies. The budget of Nigeria for 2021 was ₦ 13.588 Trillion Naira (Budget Office of Nigeria) which is about £23.88 Billion Pounds. NEMA subsequently receives about £46 Million pounds annually for disaster management where FRM falls under. Most times, the entire budget is not received by the organisation due to insufficient funding for the budget. For example, for the 2016 NEMA budget, only 10% of their funding which amounted to ₦ 1.3 Billion Naira (£2.28 Million Pounds) Naira was approved in 2016 as against ₦ 15 Billion Naira (£26.35 Million Pounds) due to paucity of funds which is largely insufficient for effective disaster management by NEMA (Krishi & Sule, 2016). In Nigeria, besides flood incidents, the country is also plagued with disaster related events such as internally displaced persons (IDP's) resulting from terrorism in the North-East of the country, desertification and deforestation in the North, landslides in the East amongst other disasters. NEMA is meant to coordinate DM down to the lower levels via technical expertise, funding, training and other roles but it is yet to be fully entrenched at the lower levels especially at the Local Government levels. The composition of NEMA at national

and state levels show that NEMA and State Emergency Management Agency are quite established, though there are still problems with funding especially at the State and Local Government levels where floods ravage the most. This is one of the reasons why there is a reactive approach to FRM in Nigeria because there is usually the need to justify resources for flood related problems and this justification is usually evident after there is some form of devastation following a flood event. Furthermore, there is almost a non-existent check-back mechanism from the communities to appraise the effect of FRM strategies at these lower levels who are meant to be the main beneficiaries of such mitigation strategies.

3.5 Flood risk management in regions with varying data availabilities

The data required for generating a flood model depends largely on the required detail and accuracy while is driven by the purpose of the flood model (Milanesi et al., 2018). The use of precision flood models which are required for enacting plausible FRM strategies largely require a detailed terrain and meteorological data at finer spatial and temporal resolutions. Despite international approaches to curb the impact of flooding globally such as the Sendai Framework for Disaster Risk reduction and regional approaches such as the EU Flood Directive 2007, countries have different exposures to flooding and have diverse approaches to curb flooding. The data available for FRM also differs amongst countries and this in conjunction with the available technical know-how, limits the level of FRM strategy that can be embarked upon especially in terms of flood forecasting, which is currently an approach to enhance FRM in countries. From the WFI Report for 2017, it shows that an inverse relationship exists between standard of living and risk of flooding. The UN Human Development Index for 2021 which ranks countries based on their health, education and income as a measure of human development will be used to appraise the FRM strategies of select countries based on their HDI ranking. The Netherlands has a very high HDI of 10 and is a country that is meant to be at high risk of flooding (WRI of 50) had evolved one of the most articulated FRM strategies to reduce its susceptibility to flooding. Furthermore, the UK has a very high HDI of 18 and a WRI of 153 despite the high exposure to flooding. This is where this research is being conducted will also be analysed as it is driven by the EU Flood Directive 2007 which has greatly shaped the country's approach to FRM. A country that has a low HDI 129 and a high WRI of 5 has evolved strategies to flooding it has been exposed to is Bangladesh. Finally, Mozambique which has a HDI of 185 and a WRI of 44 will also be analysed. The approaches adopted by 2 developed countries having high HDI rankings and 2 developing countries having low HDI rankings would help compare their approaches to FRM and also identify FRM possibilities that can be adopted by countries plagued by data sparsity.

3.5.1 FRM in the Netherlands

The Netherlands, being a low-lying country is at risk of flooding resulting from its geography and high population density. In the Netherlands, FRM has been a major challenge especially after the 1953 flooding in Europe. Over time, the Netherlands has one of the most elaborate

FRM measures in the work. The country adopts a combination of engineering solutions, land-use planning, and policies. One vital FRM approach in the Netherlands is the Delta Works project which consists of a system of dams, dikes, and barriers that protect the country's coastline from storm surges and sea-level rise (Van Slobbe et al., 2013). The Oosterscheldekering and Maeslantkering storm surge barriers are part of this project, which can be operated during high tides to prevent flooding. Besides the Delta Works, the Netherlands has diverse FRM policies and regulations. One of such programs is the Room for the River program which consists of measures such as dike relocation, construction of flood channels and widening of river floodplains which gives rivers more space to prevent flooding (Roth et al., 2021). The Netherlands Government also encourages nature-based solutions, such as green roofs and rain gardens, to manage urban runoff and prevent flooding (Davis & Naumann, 2017). Overall, the Netherlands' approach to FRM is characterized by a combination of engineering solutions, innovative policies, and stakeholder involvement. These measures have made the country one of the world leaders in FRM and can serve as a model for other countries facing similar challenges. Nigeria can emulate the Netherlands in the area of having robust engineering solutions like establishing dams as water retentions facilities and nature-based solution such as green roofs and rain gardens. Though the impact of green roofs on FRM in the study area was not investigated, it forms part of FRM approaches for Nigeria that can be further researched into.

3.5.2 FRM in the United Kingdom

The UK FRM has been identified to have flood resilience capacity to “transform and adapt” when compared to the other two capacities which are “to resist” and the capacity “to absorb and recover” (Hegger et al, 2016). FRM in the United Kingdom adopts diverse measures to reduce the risk of flooding and its impact on people and their property and build flood resilience. The key FRM agencies in the UK are the Environment Agency (EA) in England, Natural Resources Wales (NRW), the Scottish Environment Protection Agency (SEPA), and the Rivers Agency in Northern Ireland. The UK's approach to FRM is derived from the EU Flood Directive 2007 and is based on a combination of measures to enhance flood prevention, protection, and preparedness. Due to the coastal nature of the UK, the country has elaborate FRM infrastructure such as river and coastal flood defences, sustainable drainage systems, sea walls, tidal barriers, and flood storage areas. For example, the Thames Barrier which has been in operation since 1982, protects central London from tidal flooding. The UK also invests in natural FRM measures, such as restoring floodplains and planting trees, to help slow down runoff and as storage for floodwater (Broadmeadow & Nisbet, 2010). Despite these efforts, flooding still remains a major challenge in the UK, particularly in areas with high population density and at flood vulnerability areas especially at the coast. The UK has unfortunately experienced a number of major flood events in recent years, including the 2007 floods in Europe including England and Wales, the 2013/2014 winter floods, and the 2019/2020 winter floods. These events have spurred the UK Government to embark on investments in FRM measures and increased public awareness of the risks and impacts of flooding. One area the

UK has excelled in is the area of early warning systems. The UK has invested in flood warning systems that enable early response and flood mitigation (D. Green et al., 2017; Roberts et al., 2009). This is one area where Nigeria could garner lessons from UK's early warning systems approach to FRM as there are areas that are plagued with perennial flooding in the country. Another area is Blue-green cities, often referred to as sustainable urban drainage systems (SUDS) or nature-based solutions (NBS), which focus on integrating natural elements like green spaces, wetlands, permeable surfaces, and water bodies into urban planning to manage stormwater and reduce the risk of flooding. These strategies aim to mimic natural hydrological processes, enhance urban resilience, and create more liveable and sustainable environments. Manchester's Water Resilient Cities initiative focuses on managing stormwater using sustainable approaches. Projects like "GrowGreen" aim to create green spaces and retrofit urban areas with sustainable drainage systems to mitigate flooding and enhance biodiversity (Anderson et al., 2020). London also embraced blue-green infrastructure to manage its complex water challenges. The "Sponge Cities" project in Barking Riverside demonstrates the integration of sustainable drainage systems into large-scale urban developments (Williams et al., 2019). The integration of Blue-Green Cities in Nigeria could be a nature-based solution to FRM.

3.5.3 FRM in Bangladesh

Dhaka, the capital city of Bangladesh, is one of the most flood-prone cities in the world due the combination of natural and human factors. The city, which is characterized by low elevation, is located in the delta of the Ganges, Brahmaputra and Meghna rivers makes it vulnerable to flooding especially during the monsoon season from June to September which is exacerbated by poor drainage management. The heavy rainfall coupled with rapid urbanization has resulted in increased vulnerability to flooding in Dhaka. To address this challenge, various FRM efforts have been embarked upon in Dhaka. Some FRM efforts include the development of flood shelters and embankments in the region for the protection of people and properties during floods, and also serve as evacuation centres for affected communities (Rahman & Salehin, 2013). Dhaka has also evolved a flood warning system in collaboration with the Asian Development Bank to facilitate flood response and to drive FRM strategies called Bangladesh Flood Forecasting and Warning Centre (FFWC) (Forecasting, 2020). The FFWC consists of a network of rainfall and river gauges, water level sensors, and automated weather stations, which are distributed throughout the city and its surrounding areas. The data collected by these sensors is transmitted in real-time to a central command centre, where it is analyzed and used to generate flood forecasts and warnings. Another major effort in Dhaka is the improvement of drainage infrastructure that results in 'ponding' within the city. To address this, the city employs water retention facilities in addition to its newly constructed drainage systems and better management of the existing ones. Dhaka has also implemented FRM policies such as land-use planning policies to regulate development in flood-prone areas. The city has also designated low-lying areas as open spaces or parks to ensure flood resilience (Parvin et al., 2022). The city has enforced building codes and standards to ensure that new

constructions are flood-resistant (Fatemi et al., 2020). FRM efforts in Dhaka have involved a combination of blue-green approaches, including the construction of flood shelters and embankments, improvement of drainage infrastructure, FFWC, land-use planning policies, and building codes and standards. These approaches have built the resilience of the city to flooding and also reduced its vulnerability, however, the city is still at high risk of flooding due to its low elevation. Nigeria can build its resilience to flooding by adopting a building codes and standards by constructing flood resistant infrastructure. Flood shelters are also areas that Nigeria could investigate to reduce the impact of flooding amongst residents in flood prone areas.

3.5.4 FRM in Beira, Mozambique

Beira which is a coastal city in Mozambique which is just above sea level, is vulnerable to flooding due to its proximity to the sea and the impact of sea level rise due to climate change. The city has experienced several devastating floods, including the one caused by Cyclone Idai in 2019 (R. Emerton et al., 2020). The Mozambique Government and other NGOs in Beira have integrated approaches to manage flood risk in the area such as the construction of dams, developing early warning systems and community based initiatives. There are also exploiting Green Infrastructure as a way of managing flooding. An example is the Chiveve River rehabilitation which was blocked by rains and floods. Efforts have been to restore the drainage function of the river, construct a tidal outlet and dredge sediments to ensure tide-dependent port access (Soz et al., 2016), which has built the areas resilience to flooding. Another project is the Corumana Dam, located 90 km west of Beira and is one such project that is helps build resilience to flooding in the city. The Dam has a reservoir capacity of 979 million cubic meters and is equipped with a spillway and outlet works that is being used to control the release of water downstream, which helps to reduce the risk of flooding in Beira and other downstream areas (Knight & Evans, 2017). Another approach to manage floods in Beira is through early warning systems that use meteorological data for flood prediction (Engelbrecht & Vogel, 2021; Toté et al., 2015). The government has invested in several weather monitoring stations and has collaborated with international organizations to improve the effectiveness of these systems such as the Global Flood Awareness System (GloFAS) used in Mozambique to predict Tropical Cyclone Idai in 2019 (Harrigan et al., 2020). The Mozambique government has also instituted several community-based initiatives have been implemented to improve flood preparedness and response in Beira (Macamo, 2021). These include the formation of community disaster committees and training programs on flood response and evacuation. Despite all these efforts, Beira is still vulnerable to flooding due to inadequate funding for FRM, obstruction of drainages by buildings and the location of the city which makes it at risk of flooding. However, the integrated approach to flood risk management by the Mozambique Government has resulted in a whole-of-society approach to manage floods especially in the city of Beira and this has built resilience of the city to flooding. Nigeria can learn from Biera in the area of using water retention facilities as approaches to store excess runoff after a storm

event. The ability to also predict flooding by establishing early warning systems with a high degree of precision is another aspect of FRM that Nigeria could build upon.

3.6 Challenges of flood risk management in the study area

A comparison of FRM in countries with different data availabilities highlights the setbacks to FRM in developing countries such as Nigeria. The challenges of FRM in Nigeria and the institution NEMA include the lack of a policy on FRM, insufficient funding for FRM and insufficient skilled personnel for flood risk analysis including lack of data. Others include inability to entrench FDM frameworks at the lower levels and poor urban development/lax regulation. These are subsequently discussed to determine how best they could be overcome to evolve a proactive FRM strategy for Nigeria.

3.6.1 Lack of a Policy on flood risk management.

A thorough review of Nigeria's approach to FRM revealed that there is no National Policy on FRM or a flood management policy for the country. The guide used by NEMA for FRM is the overall approach used for disasters which flooding forms part of it. The policies closest to a flood management policy was the Nigeria Water Management Act which deals with the provision and optimal utilization of water and also the National Disaster Response Plan (NDRP) by NEMA. In Nigeria, the Government at all levels need to show better commitment towards providing an enabling environment for the professional working and functioning of DM agencies including favourable legislations to guide the activities of these agencies (Adefisoye, 2015). A policy on FRM would involve specific funding for FRM which would greatly affect technology, structures, data collection, analysis of data, planning direction and other requirements for an efficient FRM Plan for Nigeria. For example, the UK National Audit Office in 2014 conducted a strategic FRM of DEFRA and produced a report which assessed if current engagements for the strategic management of flood risk in England, delivered value for money. This kind of audit on FRM can be achieved when there are specific funds allocated for FRM. This check back mechanism is vital to ensure the judicious use of scarce funds for the right purposes in order to prevent exploiting loopholes for personal gains.

3.6.2 Insufficient Budget Allocation for Disaster Management.

In Nigeria, one percent of the country's annual budget is voted for the ecological fund while 20 percent of this ecological fund is given to NEMA. The remaining 80 percent is given to affiliated disaster response stakeholders like hospitals, the armed forces etc. This fund is insufficient for the disaster response needs of the Country as equipment, relief materials, funds for research amongst other requirements need to be met. Adequate funding is required for the DM agencies at federal, state and local government levels to build the professional competences and foster effective service-delivery (Adefisoye, 2015). A more favourable government policy relating to funding of FRM in Nigeria would increase the budgetary allocation to NEMA and ensure a transparent process of funds disbursement is in place. This

transparency can be improved upon when there exists specific funding for FRM which can be achieved when there is a policy on flooding.

3.6.3 Insufficient Skilled Personnel for FRM and Unavailable Data for Analysis.

The availability of skilled personnel and also data available for FRM is vital in all phases of the DM cycle. Current efforts of obtaining data is through remote means of satellites and similar platforms. These data need to be analysed, trends established, and projections made on flood risk including suggested mitigation strategies. Unfortunately, Nigeria currently has no DM satellite in space. The satellites that were initially launched for DM have been decommissioned without suitable replacements and the country relies on external sources for monitoring disasters in the country. These problems are further exacerbated by a gap that exists between NEMA, DM stakeholders and the educational/DM institutions in the country. There is the need for a nexus between NEMA and these institutions where research on flood risk is conducted by these institutions and plausible solutions are forwarded for implementation. NEMA also needs to make deliberate efforts to ensure they recruit DM specialists and train them to perform their DM tasks professionally.

3.6.4 Flood disaster management minimal at the local level.

The poor perception of flooding should be a concern for NEMA with the peculiar attitude of Nigerians towards issues they have no solution to, is to find a natural way of adapting which may lead to loss of lives and properties during disasters (Nkwunonwo et al, 2015). The EPR DRR Capacity Assessment Report 2014 report observed that FRM is absent at the Local level. These areas are worst hit whenever there is a flooding event and there is the need for NEMA to ensure it has offices at these levels. The bottom-top approach to DM fosters a participatory approach to FRM and also supports a proactive rather than a reactive approach to flood related issues. The problems associated with entrenching DM capabilities up to the lower levels are exacerbated by the lack of funding and technical expertise. It was observed that a lot of African countries were in the bottom places in the UN Human Development Index (Abdi et al., 2015), which evaluated the development of nations based on 3 indices which are life expectancy, education and per capita income. Nigeria, which is located in West Africa is rated 152 on the UN HDI as compared to a country like the UK being a developed nation and ranked 16th on the UN HDI. Current research on FRM posits the bottom-top approach to this continuous challenge with a proactive rather than a reactive stance to the subject. Citizens who fall within the poverty index may prefer government intervention funds for survival rather than an elaborate FRM plan that would be require huge financial obligations. Funding that could be utilized for entrenching FRM down to the local levels may look more appealing to the policy makers for tackling other competing demands for funding in the country. They fail to realize that more funds would be required for recovery whenever there is a flood disaster which will most likely surpass the mitigation effort that was rejected.

3.6.5 Poor urban development regulations and lax regulations

The land available for development is affected by uncontrolled expansion of impermeable surfaces, building on floodplains, lacks stormwater drainages and the available ones aren't well maintained including the weak capacity of institutions on urban administration (Adelekan, 2010). This results in increased runoff following a storm event and subsequently flooding. The lax regulations on urbanization have resulted in the conversion of dwellings into concrete-jungles which serves as flood enablers, instead of building sustainable and flood resilient societies that will better manage extreme rainfall events. This challenge is exacerbated with the current climate change induced hazards which are predicted to increase in the near future. For already existing concretized jungles, it may be challenging to embrace the building of flood resilient societies due to the legal implications and cost of reconstructions that will be required (Nkwunonwo et al., 2016). For developing satellite towns, the adoption of the blue-green infrastructure concept which focuses on the building of flood resilience societies by integrating urban flood risk management with green infrastructure (Thorne, 2020) will minimize the disruption of the original hydrological nature of catchments and evolve sustainable ways of optimally managing run-off when it occurs. A summary of the challenges of FRM in Nigeria is at Table 11.

Table 11: Challenges of FRM in Nigeria

Serial	Agency	Date	Role/Mandate/Mission/Goal	Achievements related to FRM	Challenges	Recommendations	Source
1.	National Emergency management Agency (NEMA)	1999	To coordinate resource towards efficient and effective disaster prevention, preparation, mitigation and response	- Awareness generation - Training and capacity building - provision of a National Disaster Response Plan - Contingency stockpiling - Establishment of a GIS Lab	- Insufficient Funding - Difficulty in Coordinating DM stakeholders -Coordination of FRM at lower levels - North East humanitarian crisis	1. Expand the functions of NEMA 2. Improved funding 3. Entrenching SEMA and LEMA at the local levels	1.DG NEMA- Sani Sidi, 2016. 2. Nkwunonwo et al,2015. 3. Nkwunonwo et al,2015.
2.	Federal Ministry of Environment (FME)	1999	Ensure environmental protection and the conservation of natural resources for sustainable development	Creation of department of flood, erosion and coastal management (shore protection)	-Insufficient experts on climate change - Need to develop increased technology on climate change	1. Need to intensify training on climate change 2. Increased funding	1. UNCCC, 2016 2. UNCCC, 2016
3.	Nigerian Agency for Space Research and Development (NASRDA)	2001	Pursue the development and application of space science application and technology for the socio-economic benefits of the nation	All earth observation satellites operating in space have been decommissioned	- Satellites may be decommissioned 2018	1. Need to replace or liaise with other agencies	1. Own analysis
4.	Nigerian Institute for Oceanography and Marine Research (NIOMR)	1975	Conduct Research into the resources and physical characteristics of the Nigerian territorial waters and the high seas	- Compilation of sea level rise data - Coastal erosion and ocean dynamics monitoring at Seme, Yovoyan, Olomometa, Lekki and Orimedu	- Inadequate human capacity and equipment, poor funding - Minimal data to support fluvial flooding	1. Improved funding and capacity building	1. (Awosika & Folorunsho, 2005)
5.	National Environmental Standards And Regulations Enforcement Agency (NESREA)	2007	Enforcement of environmental standards	- Creating awareness on the need for respect of ecosystems - Increase public awareness on environmental literacy	- Low poverty levels leading to ecosystem abuse - Lack of public awareness on respect of ecosystem and enabling legislation	1. Passing enabling laws for green growth 2. Encouraging better governance for sustainable ecosystems	1. Ladan, T.M (2017) 2. Ladan, T.M (2017)
6.	National Orientation Agency (NOA)	2005	To consistently raise awareness on environmental issues	- Disseminate flood threat to public	Insufficient orientation on flooding in Nigeria	1. Increase orientation on flood risk to the populace 2. Greater synergy between Nigerian Mass Media and NOA	1. Nkwunonwo et al,2015. 2. Atari, G (2016)
7.	Nigerian Meteorological Agency (NIMET)	2003	Provide Meteorological, Hydrological and Oceanographic Services	- Provide data on temperature, wind, ocean change and precipitation - Make monthly 2-Page drought and flood monitoring report	- Having 54 Stations instead of 9000 Stations (0.6% efficient)	1. Needs more Monotoring stations 2. Weak enabling laws	1. Mashi, A (2017) 2. Mashi, A (2017)
8.	Nigeria Hydrological Services Agency (NIHSA)	2010	To create a dynamic and advanced hydrological service	- Give warning of possible flooding - Inform public of effect of flooding	- No capacity for evacuation procedures for vulnerable persons - Reports on floods that affected communities almost has no effect	1. Work with NEMA for early planning for FRM and response 2. Early warning and possible rehearsed drills for FRM	1. Own Analysis 2. Ikpefan and Chinedu (2016)

3.7 Summary of Chapter 3

This chapter gave an overview of the study area and highlights the impact of flooding on the geography of the area. The area being generally low lying, urbanized and densely populated is an enabler to flooding and this is exacerbated by its proximity to the coast. An insight was given into the flood modelling approaches engaged by countries with varying data availabilities and how these countries were able to overcome the challenges posed by sparse data. A comparison of Nigeria's FRM was made with these countries and areas that could help strengthen Nigeria's FRM capabilities were outlined.

Chapter 4: Methodology for data processing, model parameterization and pluvial modelling in data sparse regions

4.1 Overview of Chapter 4

This chapter focuses on the processing of pointclouds to generate a DTM and the manipulation of rainfall data to conduct to replicate a historical flood event that occurred on 8th July 2017 in the study area that had a rainfall depth of 176.5mm for that day. From the generated DTM, 3 sub-catchments were identified that were flooded during the historical rainfall event and were selected for the calibration of parameter values for the FloodMap and CityCAT hydrological models. The overarching aim of this chapter was to use these sub-catchments to calibrate parameter values for both models and determine if these calibrated parameter values optimally represented the inundation extent for the entire catchment in order to save computation/processing time. The research of this chapter investigates Objective 3 and lays the foundation to achieving the aim of the entire research. The Chapter gives a description of the FloodMap and CityCAT models and then outlines the parameters that drive the FloodMap model (Mannings, hydraulic conductivity, and drainage capacity) and those that drive the CityCAT model (Mannings building, Mannings vegetation and hydraulic conductivity), including the approaches used in configuring each model to suit a data sparse region. The methodology adopted for the simulation of the historical flood event by both models was also explained here. The methodology involved the process of manipulating the terrain data to generate a DTM, assessing the DTMs suitability for hydrological modelling and conducting hydrological analysis of the DTM to delineate the sub-catchments that were used for the model calibration process. The justification of the selection of parameter values for each model was also showcased in this chapter with emphasis on the replication of the historical flood event that occurred on 8th July 2017.

4.2 Methodology for processing data and flood modelling

The methodology for this chapter consists of data processing of point clouds to DTM and conversion of rainfall data into rainfall intensity, model parameterizing and the conduct of the hydrological model simulations. The entire methodology consists of 4 stages as shown in Figure 6. Data required for hydrological modelling include dependent variables (DTM and rainfall) and independent variables (which are the parameters that drive the modelling process like the hydraulic conductivity, roughness coefficient and losses via drainages). The DTM represents topography and is the first-order control of hydrological response of a catchment to rainfall (Brasington & Richards, 1998) while the model parameters affect flow over the surface. In hydrological modelling, adequate representation of the DTM is vital especially when routing flow in catchments at high spatial resolution. Errors or imperfections of the DTM increase the uncertainty in the modelled flood output and affect the accuracy of flood predictions.

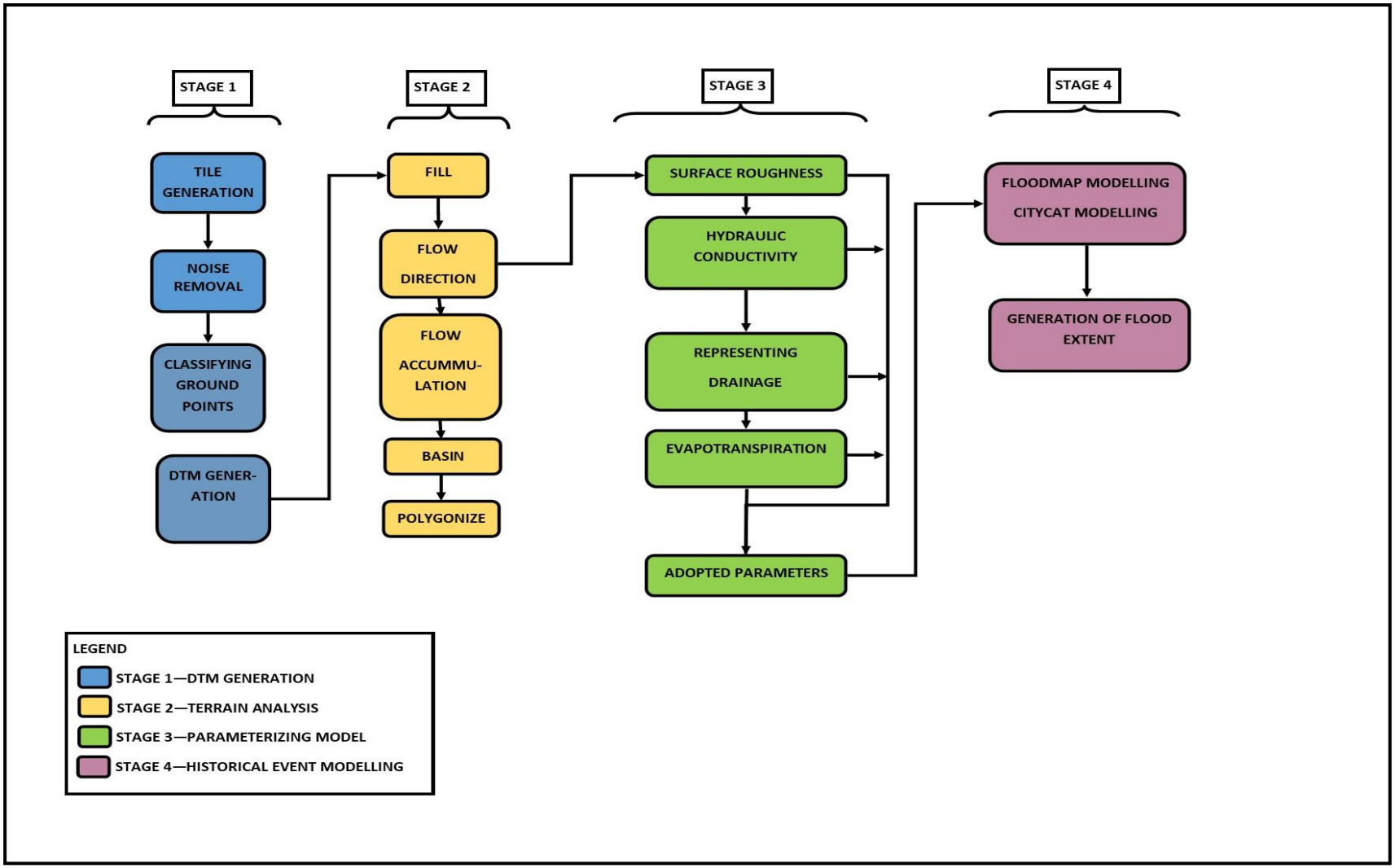


Figure 6: Methodology for data processing, parameterization and flood simulation using the FloodMap Model

The representation of rainfall during rainfall-runoff modelling depends on the hydrological model being used, but models usually capture the intensity of rainfall over the catchment area at predefined intervals. In hydrological modelling, the independent variables are usually not readily available in the desired format for direct inclusion in these models. This is worse for data sparse regions as the independent variables may need to be manipulated to suit the hydrological model which further relies on the purpose for conducting the flow routing process. This is the case for the study being conducted. The DTM is in point clouds at 1m resolution while the rainfall is represented as point depth at a measuring station.

4.2.1 Terrain Data and Analysis

The DTM for this study, a total of 34 tiles of point cloud data were purchased from the Lagos State Government GIS database. The LiDAR data had a resolution of 1m with each tile covering an area of $1km^2$. The LiDAR data was captured by Gemini 167 ALTM Equipment in March 2009. One tile had a total of 1,199,270 points with 1,188,904 first returns and 1,146,613 last returns. It also had 275,710 ground returns which shows that the low number of ground returns is consistent with a built-up area as shown in the depiction of how LiDAR works at Figure 7. The point clouds needed to be converted to a DTM for flood modelling.

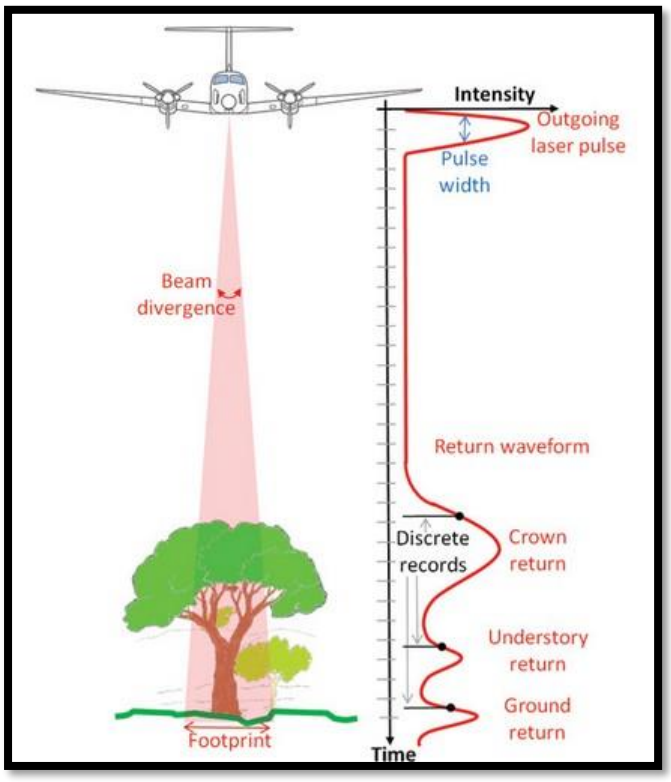


Figure 7: Path of a LASER pulse illustrating how LiDAR works (Fernandez-Diaz et al., 2014).

4.2.2 DTM Generation and Validation

The process for the generation of the DTM from point clouds was adapted from (Zhang et al., 2018) where various algorithms in LAStools were applied for the generation of the DTM in a built-up area. Additional processing was adapted from (N. Polat & Uysal, 2015) where different algorithms were used for the generation of a DTM in a rural and built-up area; the focus was

on the built-up area. The classified dense cloud of the study area was imported into lastools and the workflow at Figure 8 was adopted which was based on a modified version of (Zhang et al., 2018). The overall process adopted was that the image was tiled into smaller units (Jochem et al., 2012) so that the process of triangulation can work better over smaller areas. Noise was removed with a set bulge and offset (Wang et al., 2013) in order to preserve sharp features.

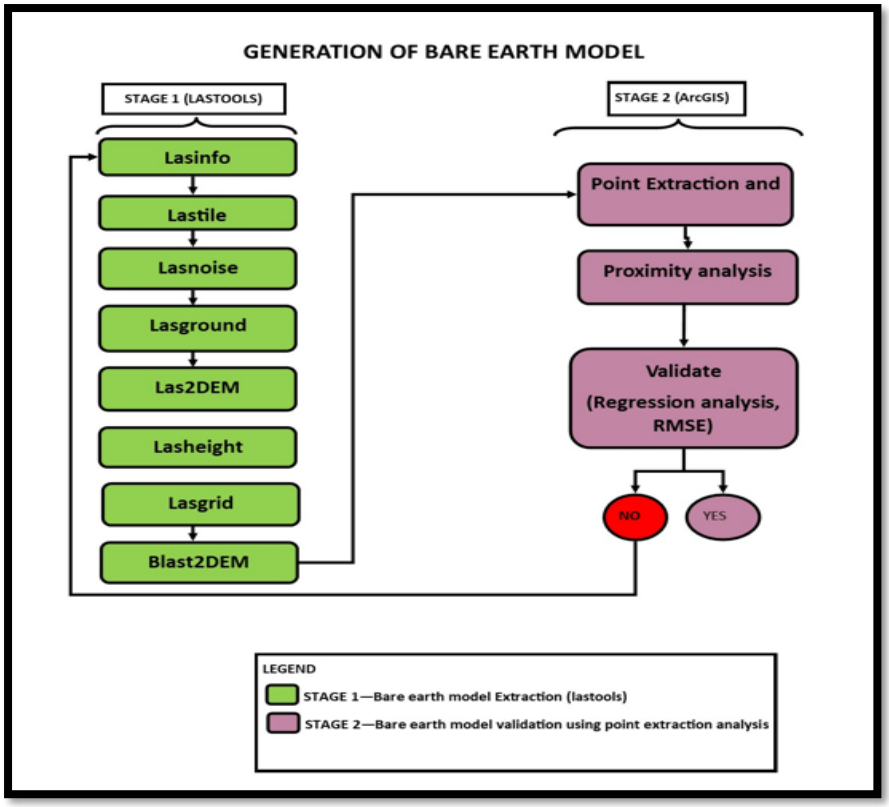


Figure 8: Process for DTM generation and validation

Ground points represent the points that strike the bare earth surface. Classifying ground points is vital in order to ensure that a DTM can be extracted from these points labelled as ground (Rizaldy et al., 2018), while other non-ground points can be extracted. The method of setting an appropriate threshold as embarked by (Vosselman, 2013) was modified to suit working in the study area. The ground points were subsequently classified using lasground before being rasterised into a 2m resolution bare earth model as shown in Figure 9.

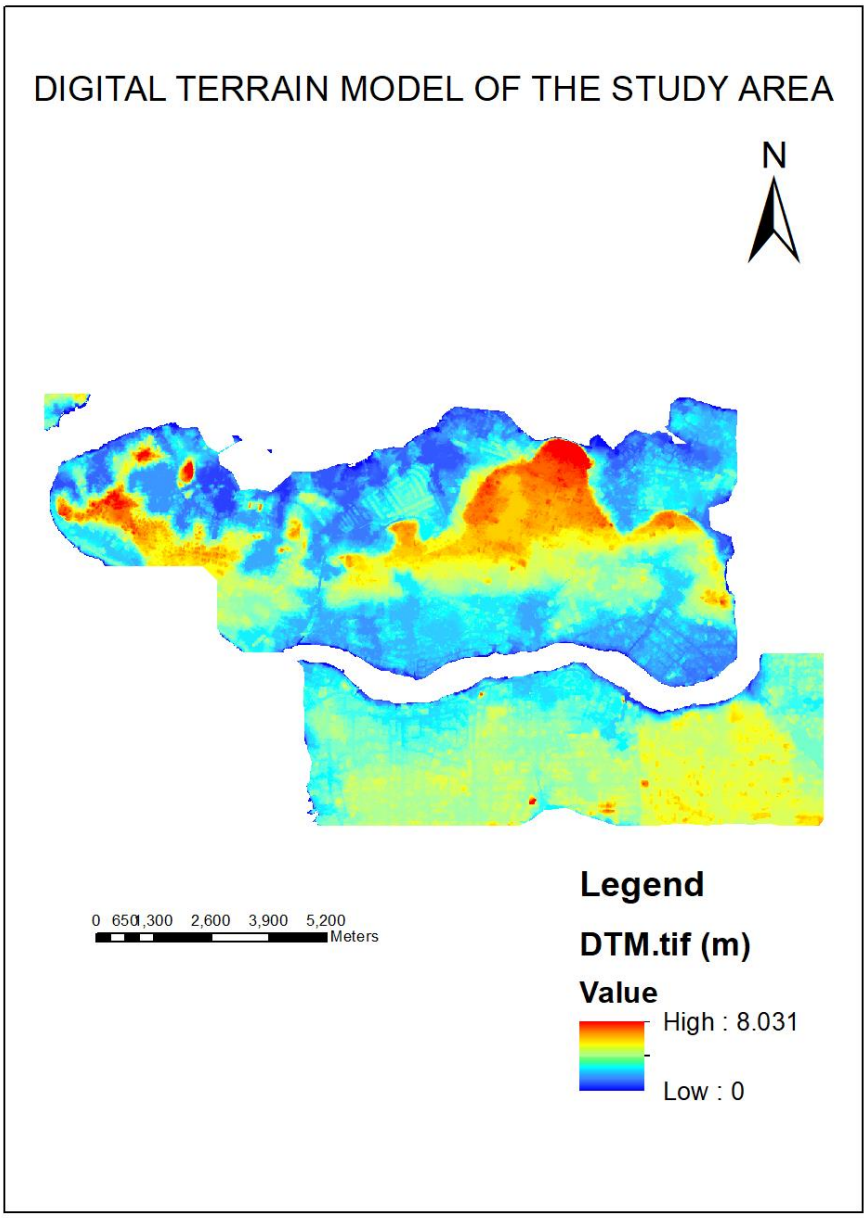


Figure 9: Generated DTM of the study area from LiDAR point clouds

4.2.3 Accuracy assessment of Generated DTM for Hydrological Modelling

Certain factors determine the local accuracy of DTMs such as proximity to nearest GCP, terrain, topography, image contrast, overlap of images amongst other factors (Gindraux et al, 2017), hence the need to ensure generated DTMs are suitably validated. The accuracy of a DTM is vital for diverse applications which determines its reliability and is centred around statistical measurements for particular applications (Pakoksung and Takagi, 2016). Accuracy assessments are carried out using check points which serve as reference data when validating DTMs and these check points need to be distributed randomly and need to be in sufficient quantity (Hohle and Hohle, 2009) in order to generate accurate reference data.

DTM validation for this study utilized hybrid methods derived from Leitao et al (2016) where quantitative/ qualitative procedures were used and Hohle and Hohle (2009) which concentrated on robust statistical methods. It also used approaches by Arungwa et al, (2018) which in addition to statistical methods, computed elevation differences between the DEMs for validation and reference GPS points which were subsequently compared using statistical means. The methodology adopted for the validation of the generated bare earth model is at Figure 8. The DTM validation for this study utilized established ground control points to compare against the generated DTM. The creation of a DTM especially in highly urban areas results in over-extraction and under-extraction of large objects like buildings during triangulation of ground points which could result in errors. Comparing the DGPS points to the same points extracted from the DTM, the linear regression value (R^2) was 0.9362 as shown in Figure 10 while the RMSE was 0.32. It also has a National Standard for Spatial Data Accuracy (NSSDA, 1998) of 0.63 (RMSE x 1.96) where accuracy reported at 95% confidence depicts that 95% of the positions in the dataset will have errors less than or equal to the reported accuracy value with respect to the ground position. The DGPS locations used for the validation is at Figure 11.

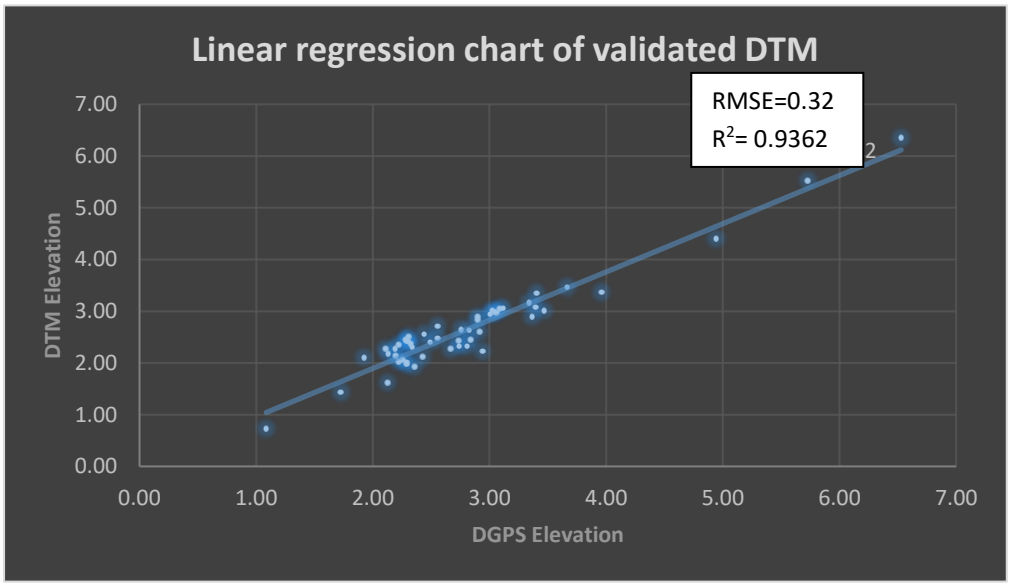


Figure 10: Linear regression chart validating the generated DTM

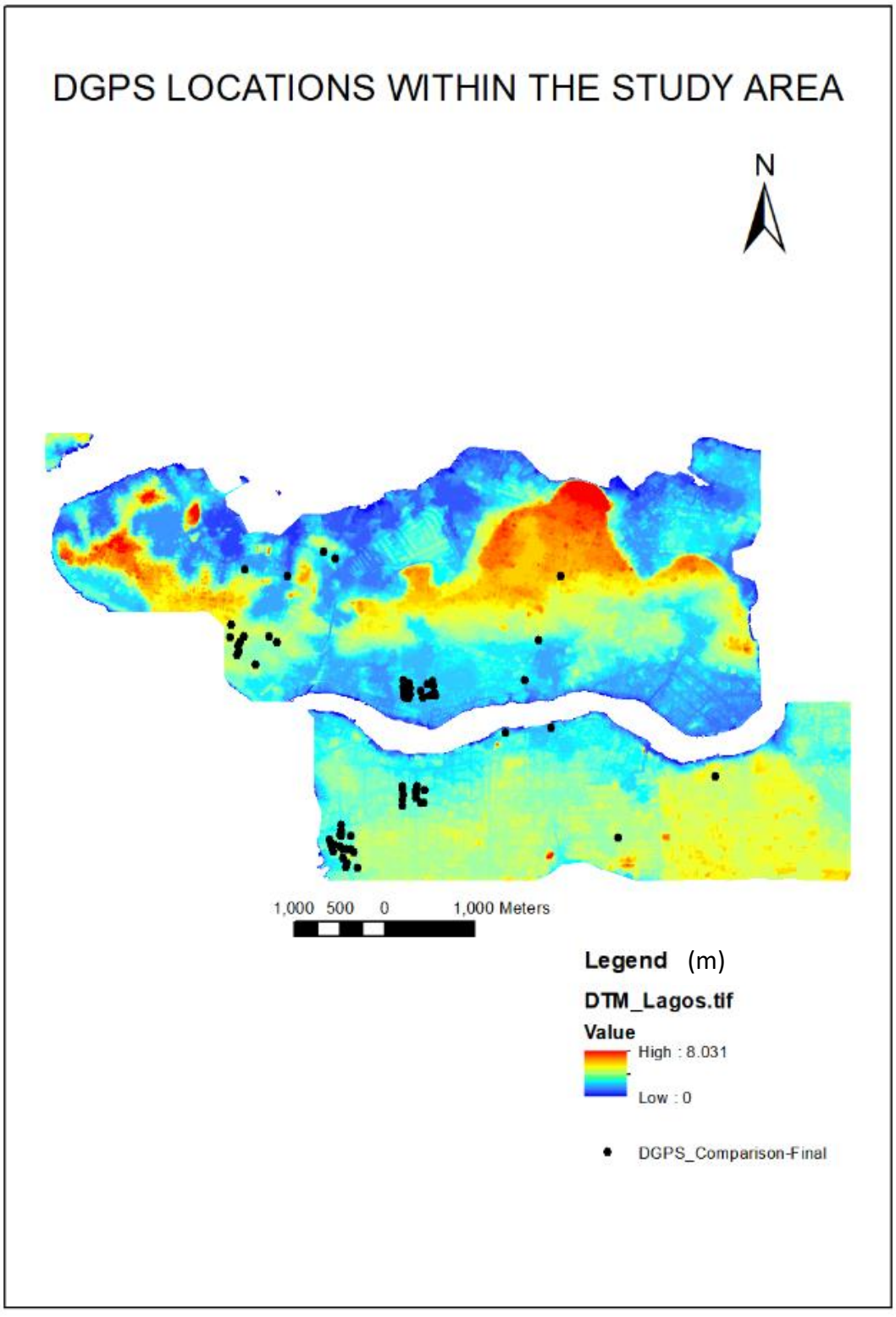
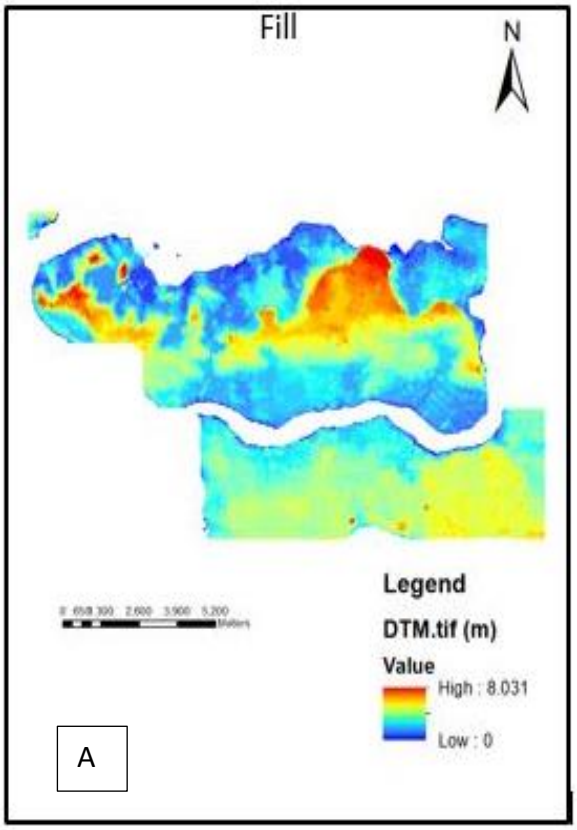
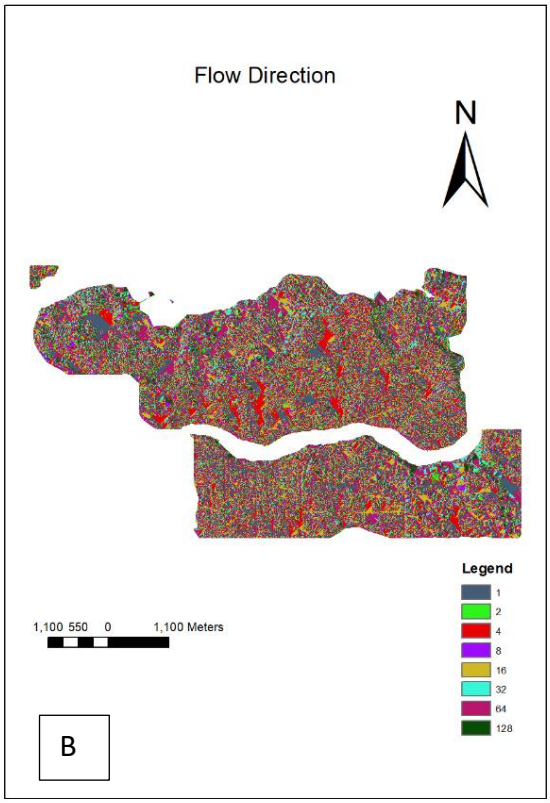


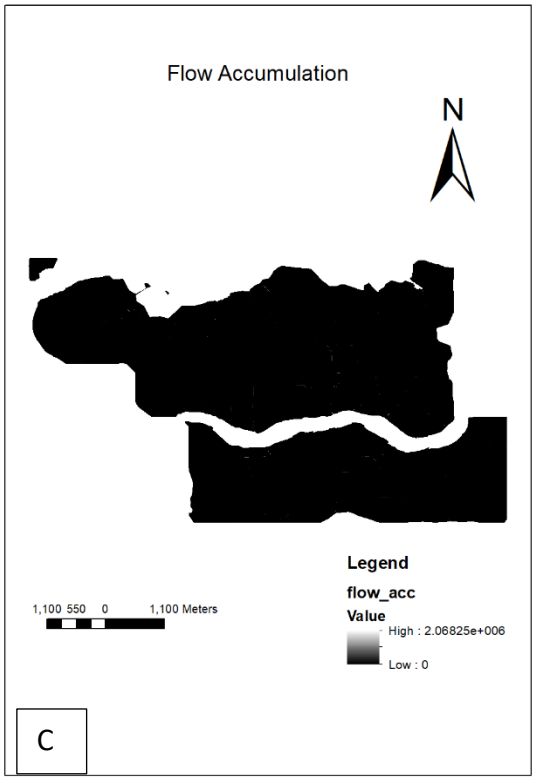
Figure 11: DGPS Locations within the study area

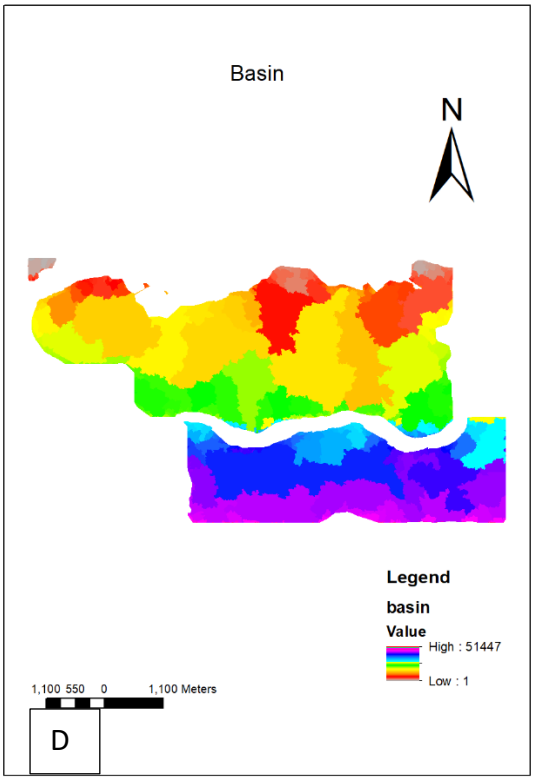
4.3 Terrain analysis

Drainage basins, catchment areas or sub-catchments represent the fundamental unit for the management of land and water resources (Moore et al., 1991). Hydrological analysis is vital in determining the natural drainage pattern of the earth's surface and this was achieved using the ArcHyro Toolbox on ArcMap. The procedure outlined in (Jimme et al., 2016) was adopted for the hydro-processing of the study area which involves pre-processing works on the DTM and thereafter, extracting channel networks and subsequently delineating watersheds. Small imperfections are sometimes present on DTMs which are caused by dips in elevation, and this makes ascertaining the flow direction of water difficult or impossible. A sink is a cell or more than one that has a lower elevation than its surrounding cells (Martz & Garbrecht, 1993, 1999) and these need to be removed from a DTM. The "*fill*" tool was used to remove such imperfections in the bare earth model as shown in Figure 12 (A). Flow on the surface raster was then determined using the "*flow direction*" tool in ArcGIS which identifies and routes flow down the lowest outer cell with respect to the central cell (Theobald et al., 2006). Further analysis of flow over a surface depends on the flow direction as depicted in Figure 12 (B). Establishing how flow accumulates into each cell via the established flow direction (Jenson & Domingue, 1988; Wallace et al., 2018) was achieved using "*flow accumulation*" tool and the product is at Figure 12 (C). Watersheds were subsequently delineated Figure 12 (D) using the "*basin*" tool and the flow direction raster output was used as the input. This basically creates watersheds for the entire bare earth model and converting the watersheds to a shapefile using basins as the individual watershed by using the "*raster to polygon*" tool under conversion tools and this produces a polygon of the entire watershed with the individual basins making up the entire watershed. The drainage network for the study was defined Figure 12 (E) by connecting points to the next lower pixel while the delineated sub-catchment drainage networks were identified Figure 12 (F). Sub-catchment 1 had one stream order, while sub-catchment 2 had three stream orders and sub-catchment 3 had 2 stream orders. The stream orders classify drainage basins based on their branching or bifurcation (Horton, 1945), which helps understand flow in the sub-catchment. The stream order is important in guiding hydrologists on the drainage capacity of the sub-catchment and the likely areas that could get flooded including the areas where gauges can be established when the need arises.


Fill
N
Legend
DTM.tif (m)
Value
High : 8.031
Low : 0
A


Flow Direction
N
1,100 550 0 1,100 Meters
Legend
1
2
4
8
16
32
64
128
B


Flow Accumulation
N
1,100 550 0 1,100 Meters
Legend
flow_acc
Value
High : 2.06825e+006
Low : 0
C


Basin
N
1,100 550 0 1,100 Meters
Legend
basin
Value
High : 51447
Low : 1
D

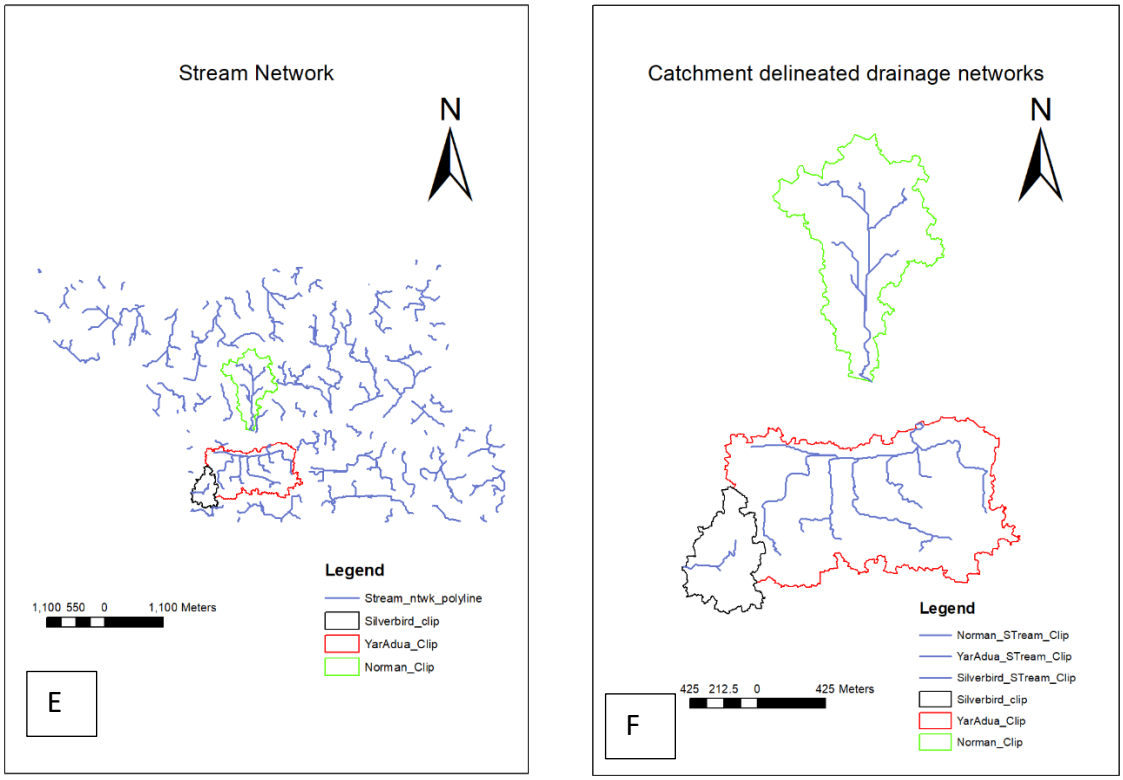


Figure 12: A- Fill, B-Flow direction, C- Flow accumulation, D-Basins, E-Drainage network, F-Delineated drainage network for sub-catchments under study

4.4 Rainfall Data Manipulation

The rainfall for this study was purchased from Nigeria Meteorological Agency (NiMET) which is the government agency in Nigeria charged with the responsibility of advising the Government of Nigeria on all aspects of meteorology including the collecting of meteorological data and the making of forecasts. The rainfall data was in daily rainfall depth measurements obtained from the weather monitoring station. This data is interpolated across areas where there are no weather monitoring stations. Considering that coastal areas are peculiar in that they are more exposed to diverse coastal dynamics which resulting in varying meteorological and sometimes unpredictable conditions, the use of satellite rainfall data could result in error. The variation in rainfall intensity experienced by coastal regions which this study area falls necessitates the adoption of observed rainfall depth for hydrological modelling in the catchment which will be better suited to generate the rainfall hyetographs for the model and represent the catchment under study. In order to simulate the rainfall-runoff using a physically based hydrological model, the rainfall intensity needs to be obtained. The rainfall depth for 8th July 2017 was 176.5mm and the rainfall lasted for about 5 hours. The Chicago rainfall hydrograph model which is a rainfall process based on rainstorm intensity equation (Xie et al., 2017; Zhang et al., 2008), was used to generate a rainfall hydrograph for the rainfall event. An early peak was simulated as obtained from citizen science of an initial high intensity rainfall and the rainfall intensity for the flood event is at Figure 14. Though a

point depth was used for the rainfall intensity generation, it still fell within acceptable distances though it may result in slight variations in the rainfall intensity at different parts of the catchment. The distance of the weather monitoring station in relation to the sub-catchment areas is at Figure 13.

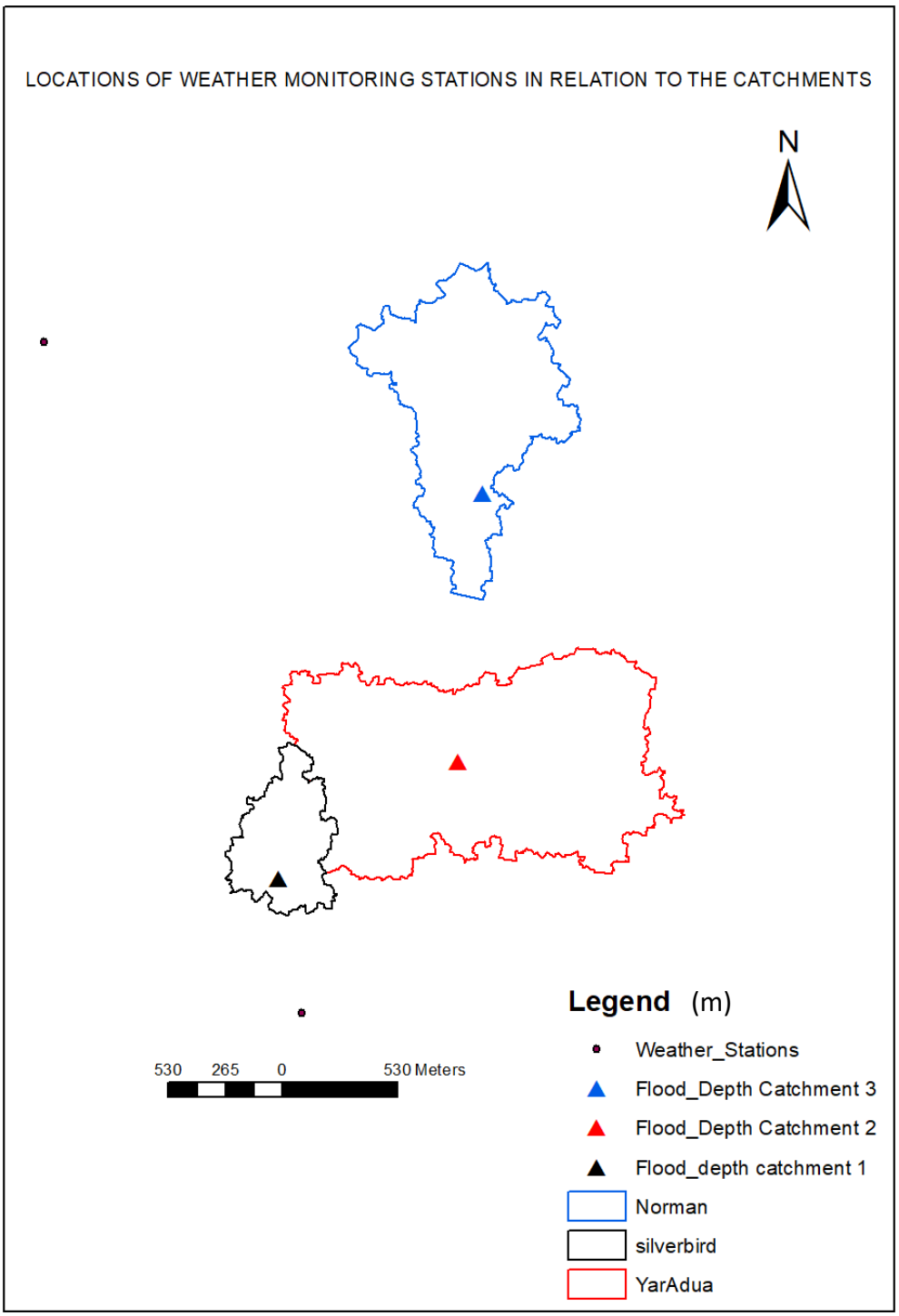


Figure 13: Locations of weather monitoring stations in relation to the sub-catchments

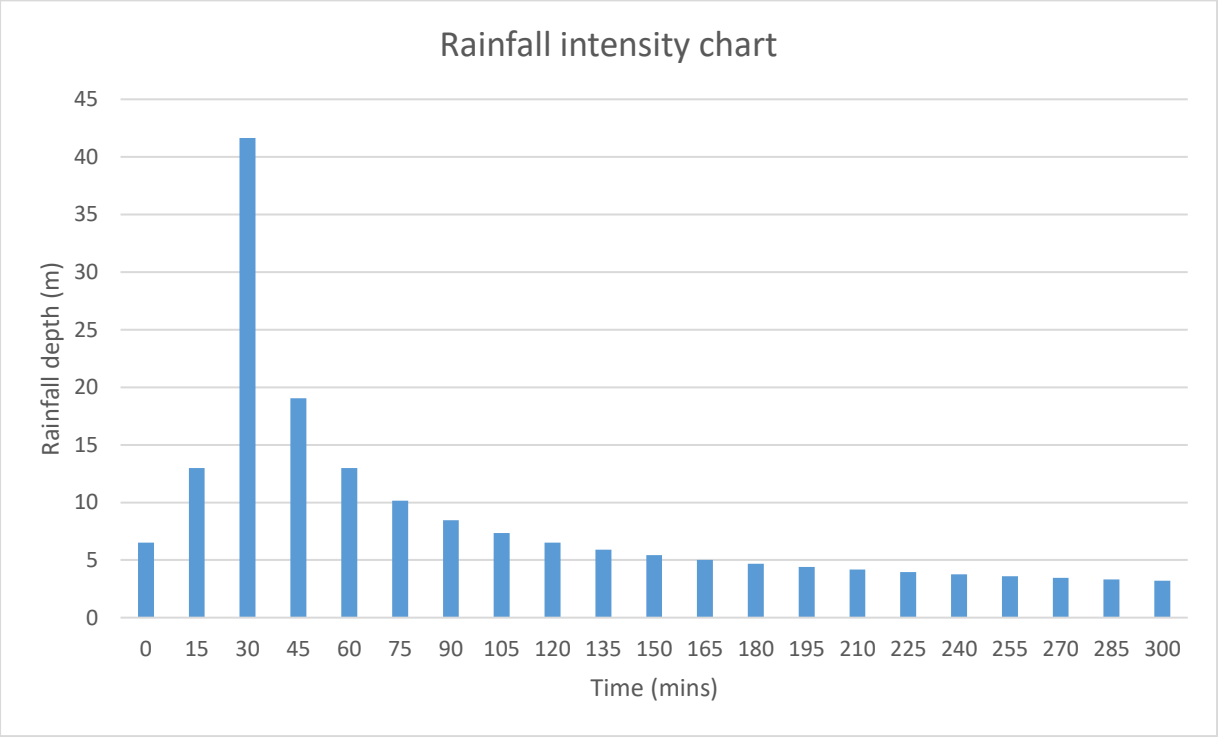


Figure 14: Rainfall intensity chart

4.5 Description of FloodMap-Hydro Inundation 2D

FloodMap is a 2D flood inundation model based on the partial inertia flow equation with a local adaptive time step (Courty et al., 2018). It was initially developed as an inertial-based model (Yu & Lane, 2006) and later modified into a 2D flood model with the capability to model flow over complex catchment areas by simulating important hydraulic and hydrological processes during an urban storm event, determining flood losses and subsequently routing surface flow over the terrain (Yu & Coulthard, 2015). The model employs a 2-D lattice of regular cells to maintain consistency with DEM in space which it later integrates with GIS software. The model has the capability of simulating vital processes such as surface flow, infiltration, representing drainage and evapotranspiration. Results are user friendly as the output is in both graphical and excel format which can be easily integrated with other software for interpretation. FloodMap is driven by the dependent variable (DTM and rainfall) and its independent variables (Mannings, hydraulic conductivity, drainage capacity and evapotranspiration). The model uses various equations to simulate these independent variables as it models flow over the DTM. A basic understanding of the way these parameters are represented by the model will give an understanding of how the output inundation extent was simulated and also help understand how each parameter contributed towards the output flood extent.

4.5.1 Modelling surface flow

FloodMap is a slightly modified version of the inertia model (Bates et al., 2010) where the approach to calculate time step neglects the convective acceleration in the Saint-Vernant equation taking the form:

$$\frac{\partial q}{\partial t} + \frac{\mathrm{gh}\,\partial(\mathrm{h+z})}{\partial x} + \frac{gn^2q^2}{R^{4/3}h} = 0$$

Where:

q is flow per unit width

g is acceleration due to gravity

R is hydraulic radius

z is bed elevation

n is Mannings roughness coefficient

The equation is further modified by factoring time resulting in

$$\frac{q_{t+\Delta t} - qt}{\Delta t} + \frac{\mathrm{g}h_t\,\partial(\mathrm{h+z})}{\partial x} + \frac{gn^2{q^2}_t}{ht^{7/3}} = 0$$

The above equation is then enhanced by replacing one of the q_t in the friction term to $q_{t+\Delta t}$ to give the detailed equation of the next time step

$$q_{t+\Delta t} = \frac{qt - \mathrm{g}h_t\Delta t\,(\frac{\Delta(\mathrm{ht+z})}{\Delta t})c}{1+\mathrm{g}h_t\Delta t n^2 q_t/ht^{10/3}}$$

The equation for the friction term is improved and flow in the x and y directions being decoupled to take the same form and subsequently elevated at the cell edges and depth at the centre. Net inflow is calculated on a pixel by pixel basis with each iteration based on the total inflow and outflow where water depth is updated for the time step.

$$\Delta t \leq \frac{w \times n \times (S_i^2 + S_j^2)^{1/4}}{d^{0.67}(S_i + S_j) + \sqrt{g \times D \times n} \times (S_i^2 + S_j^2)^{1/4}}$$

The subsequent iteration is based on the maximum water depth and velocity from the preceding step using the Forward Courant-Friederich-Levy Condition (FCFL) described in (Yu & Lane, 2011).

4.5.2 Modelling infiltration

Infiltration over saturation is represented using the Green-Ampt infiltration equation which has been extensively applied for calculating infiltration rates in uniform soils as it represents a number of processes that affect infiltration. Green-Ampt equation is a function of capillary potential, porosity, hydraulic conductivity and time (Yu et al., 2016).

$$f(t) = K_s \left(\frac{\varphi_t + h_o}{Z_f} + 1 \right)$$

Where:

K_s Represents the hydraulic conductivity of the soil at field saturation.

φ_t Is the capillary potential across the wetting front.

h_o Depicts the ponding water on the soil surface.

Z_f Accounts for the cumulative depth of infiltration.

The model uses hydraulic conductivity values in m/hr to determine infiltration rates during simulations.

4.5.3 Representing drainage

Drainage capacity is used to calculate mass losses to the storm water system which is determined by a rainfall event or return period where the runoff loss is calculated by scaling the drainage capacity for the time step (Yu & Coulthard, 2015). A uniform and distributed drainage capacity can be represented but manholes and drains are not explicitly represented by the model. Drainage is represented as a lump value (mm/hr) over the specific area based on its design capacity which captures mass loss to the storm system (Yu et al., 2016). Calibration of parameters would help identify the optimal drainage capacity to capture the mass loss via drainages for the rainfall event and the study area.

4.5.4 Flood loss from evapotranspiration

Evaporation is approximated using a seasonal sine curve for daily potential evapotranspiration (Calder et al., 1983) which the model recognises in mm/day. This is accounted for using the equation below:

$$E_p = E_p \left[1 + \sin \left(\frac{360i}{365} - 90 \right) \right]$$

Where:

$\overline{E_p}$ is the mean daily potential evapotranspiration

i is the day of the year.

Though flood loss via evapotranspiration may be minimal, accurate representation of all the flood loss processes will help reduce errors in the final predicted inundation extent. The observed evapotranspiration value of 2.5mm/day was used for this simulation.

4.6 Parameter Representation in FloodMap-HydroInundation 2D

The historical flood modelling of the 8th July 2017 flood event was modelled using the FloodMap model. The parameter representation and manipulation was made before the simulation of the flood event. Hydro-inundation models are driven by the hydraulic and hydrological processes that are used to simulate the actual flood event that occurs over the terrain and the allocation of the adequate parameters to the model to a large extent would greatly improve the accuracy of the simulations. There are a number of parameterization techniques applied for hydrological models but for distributed models which are spatially complex with a large number of unknown parameters, two widely used techniques are adopted which are; the hydrological response unit (Fakhruddin et al., 2015) and the regionalization technique (Kumar et al., 2013). These techniques rely on some form of proximity of a similar sub-catchment area that had been previously parameterized to assign parameter values to the area under study. Unfortunately, the current study area is a data sparse region with no previously known parameterization conducted in a similar catchment of close proximity. Subsequently parameterization of the models was achieved using an allocation technique based on LULC maps and soil profile analysis to define the possible range of parameters to be allocated for subsequent calibration (Yu & Coulthard, 2015).

4.6.1 Representing buildings in FloodMap

Representing resistance caused by buildings and other obstructions to flow is the most important parameter in modelling floods in urban areas (Bellos & Tsakiris, 2015). Buildings can be represented as block out or voids using the building block method, elevation rise or by increasing the roughness value. The applicability of increasing roughness value in areas where there is lack of dense topographical data or low computational cost (Bellos & Tsakiris, 2015) is also being researched into. The reflection boundary condition proved to be the best representation of buildings among the 3 methods under the same modelling conditions using FLOW-R2D flood model (Bellos & Tsakiris, 2015). This block out approach to representing buildings was adopted for this research using the FloodMap since a 2m resolution DTM was used as the terrain over which the flood was be modelled. FloodMap recognises buildings in raster format, but the building shapefiles were generated from Agisoft Photoscan in las format. The buildings were converted from las format into shapefiles retaining the same resolution as the terrain in order to minimize errors and then clipped to the terrain. The building shapefiles were then be reclassified in ArcGIS into buildings and non-buildings before raster calculator was used to define a uniform height of 40m for all buildings. The concept is for buildings to be treated as obstructions and flow is modelled around them.

4.6.2 Mannings roughness coefficient

The study area is an urban area with built-up areas (Buildings, roads, concrete surfaces) making up about 67% of the area, water (creeks or channels) cover 11%, short grass forms 11% while trees represent 10% as shown in the Land cover classification map at Figure 15.

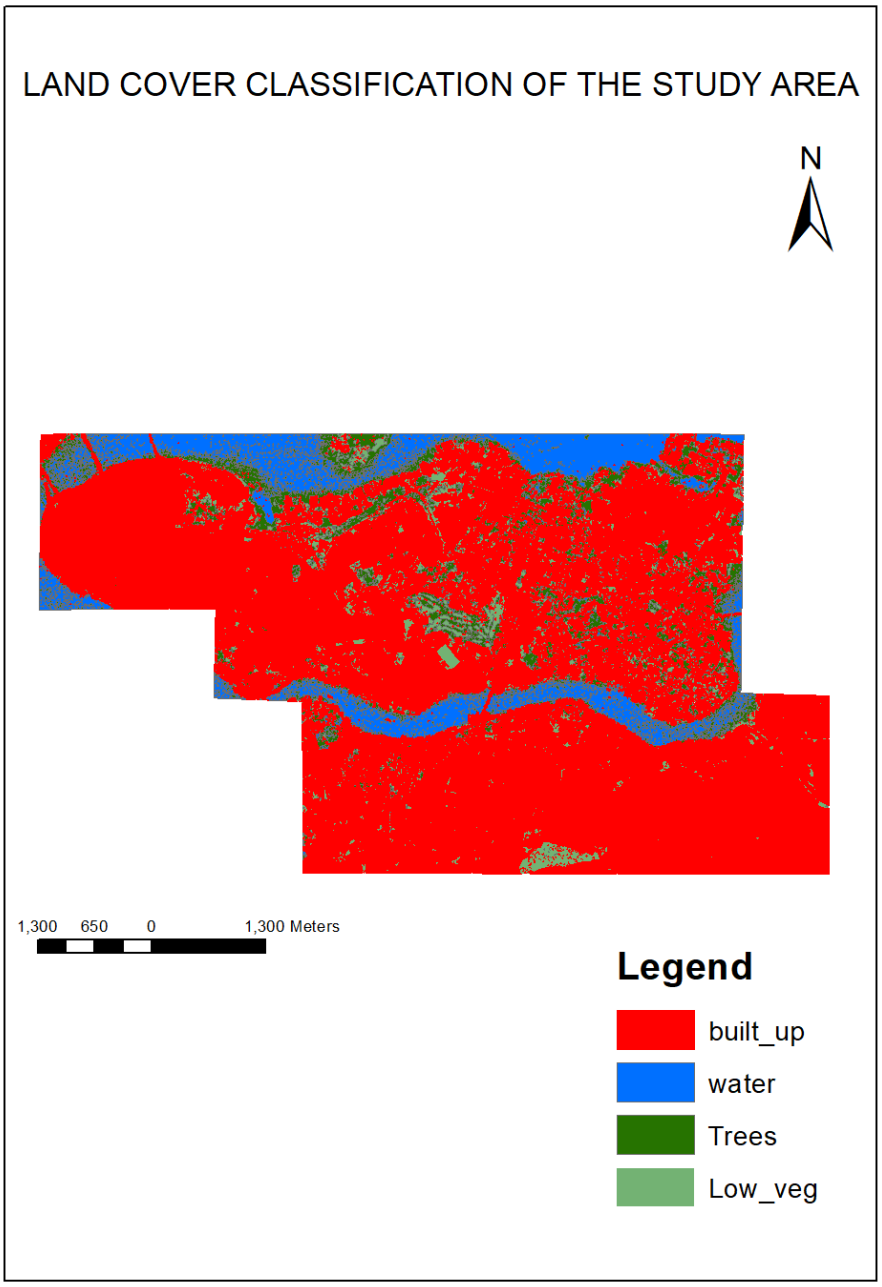


Figure 15: Land cover classification of the study area

Values of Manning's n were allocated to the various constituents of the study area derived from (Chow, 1959) as shown in Figure 16. The short grass and trees were merged to avoid model ambiguity (Unduche et al., 2018). The area occupied by buildings were treated as obstructions to flow. A distributed roughness was allocated based on the constituents of the land cover using the Manning's value as shown in Table 12.

Table 12: Selected range of Mannings values for the study area

Surface	Manning's value	Remarks
Roads (Alphalt)	0.013	Most of the roads are tarred
Short grass	0.25-0.35	
Channel (natural bottom)	0.03-0.04	

4.6.3 Hydraulic conductivity

Values for the hydraulic conductivity (HC) were assigned using the soil profile of the study area. The study area was made up of sand, silt and clay within 0-30cm of the top soil with sand being the predominant soil type ranging from 92-100% and silt comprising 0-8% while the least is clay 0-2.94% of the sampled areas (Rose et al., 2017). Sandy soil being the predominant soil type in the area was used for the study area and were assigned HC values (1 to 10^{-4} cm/s corresponding to 36, 3.6, 0.36, 0.036, 0.0036m/hr) based on the HC values obtained from (Freeze & Cherry, 1979). The pervious layers derived from the land use land cover (LULC) map generated for the study area were then allocated the above HC values.

4.6.4 Drainage loss

In flood modelling, representing floodwater losses through drainage systems involves accounting for the outflow of water from the flooded area through natural and man-made drainage pathways (Mark et al., 2004). This is typically done by incorporating hydraulic calculations and drainage infrastructure parameters into the model and its accuracy is dependent on a high level of data available on the drainage and sewer systems within the catchment area. The model considers factors such as the capacity of drainage channels, pipes, culverts, and other conveyance structures, as well as their locations and connectivity (Yazdi, 2018). By simulating the flow of water through these systems, the model can estimate how much water is drained away from the flooded area, thereby reducing the flood volume. This representation allows for a more accurate assessment of flood extent and depth within the affected region, aiding in FRM and emergency response planning. Validation and calibration of the model using observed flood events and drainage performance data are essential to ensure the accurate representation of floodwater losses through drainages. The calibration of the urban drainage model can be carried out by adjustment of the surface runoff model until subsequently the pipe flow model is calibrated towards measured flow and water level at the specific locations (Mark et al., 2004). In areas that do not have sufficient data on the drainages within the catchment under study, varying flood extractions can be applied, and the model calibrated to suit the flood losses from drainage systems. Obtaining values that can be assigned to simulate drainage losses in hydrological modelling can be achieved using either experimental or empirical methods. The difficulties and errors associated with the experimental approach, coupled with the data sparsity the study area is characterized by, resulted in the choice of obtaining drainage values using the empirical approach. For FloodMap, varying drainage rates from the range of drainage simulations of 10, 20, 30, 40, 50 and 60mm/hr corresponding to 0.24, 0.48, 0.72, 0.96, 1.20 and 1.44 m/day were used for

sensitivity analysis to calibrate the model for the best representation of flood loss via drainages.

4.6.5 Evapotranspiration

Nigerian Meteorological Agency (NiMET) used the water balance method to determine evapotranspiration in the study area and a value of 2.5mm/day was the observed value. This value was adopted for the study considering evapotranspiration has minimal effect on flood losses.

4.7 Parameters adopted for the FloodMap model

The range of values for parameterization of the FloodMap model is at Table 13 while the exact parameters used for the FloodMap models is at Table 14. The minimum, median and maximum parameter values were used to calibrate the FloodMap model.

Table 13: Range of values for parameterization of the FloodMap model

Serial	Parameter	Values
1.	Manning's roughness	
	a. Roads	0.013
	b. Vegetation (0.25-0.35)	0.25, 0.30, 0.35
	c. Channel with dense weeds and aquatic plants (0.03-0.04)	0.030, 0.035, 0.040
2.	Hydraulic conductivity (m/hr)	0.001, 0.002, 0.003, 0.004, 0.005
3.	Drainage loss (mm/hr)	10, 20, 30, 40, 50, 60
4.	Evapotranspiration (mm/day)	2.5

Table 14: Parameters adopted for FloodMap model

Simulation	Manning	DC (m/day)	HC (m/hr)
S01of27	0.01	0.24	0.001
S02of27	0.01	0.24	0.003
S03of27	0.01	0.24	0.005
S04of27	0.01	0.84	0.001
S05of27	0.01	0.84	0.003
S06of27	0.01	0.84	0.005
S07of27	0.01	1.44	0.001
S08of27	0.01	1.44	0.003
S09of27	0.01	1.44	0.005
S10of27	0.03	0.24	0.001
S11of27	0.03	0.24	0.003
S12of27	0.03	0.24	0.005
S13of27	0.03	0.84	0.001
S14of27	0.03	0.84	0.003
S15of27	0.03	0.84	0.005
S16of27	0.03	1.44	0.001

S17of27	0.03	1.44	0.003
S18of27	0.03	1.44	0.005
S19of27	0.05	0.24	0.001
S20of27	0.05	0.24	0.003
S21of27	0.05	0.24	0.005
S22of27	0.05	0.84	0.001
S23of27	0.05	0.84	0.003
S24of27	0.05	0.84	0.005
S25of27	0.05	1.44	0.001
S26of27	0.05	1.44	0.003
S27of27	0.05	1.44	0.005

4.8 Pluvial Flood Modelling using FloodMap

The modelling using FloodMap was simulated on the 3 sub-catchments. The purpose was to be able to calibrate the model effectively to suit the entire catchment area. FloodMap is run using a GUI where the model configuration GUI gives options to be run as a 1D River, 2Dfloodplain or a coupled model. Based on the study, a 2D model best represented the study being conducted. The model was then configured by adding the DSM under the Elevation Grid option. Other means of configuration were done by defining the Mannings roughness coefficient, the time the model was to run for which in this case was 18,000 seconds to correspond to the 5-hour rainfall being simulated. In defining the rainfall-runoff parameters, a uniform rainfall input was simulated and the values for the hydraulic conductivity, evapotranspiration and drainage capacity were inputted. The output hydrometrics were set to be exported every 300 seconds as well as the on-screen imagery. The modelling was conducted using 3 computers each with a 32GB RAM. The output for FloodMap is in an easily visualized ascii format that can be opened in ArcGIS, QGIS or other GIS softwares that can read data in ascii format. Modelling using the 3 sub-catchments used a DSM of the respective sub-catchments where the buildings were clipped to the DTM as shown in Figure 16, Figure 17 and Figure 18 then the parameters in Table 14 were used as the various parameter values. The flood depth for the flooding event that occurred on 8th July 2017 was the simulated. A total of 27 runs with the simulations were made in order to determine the optimal parameters that simulate the observed flood event.

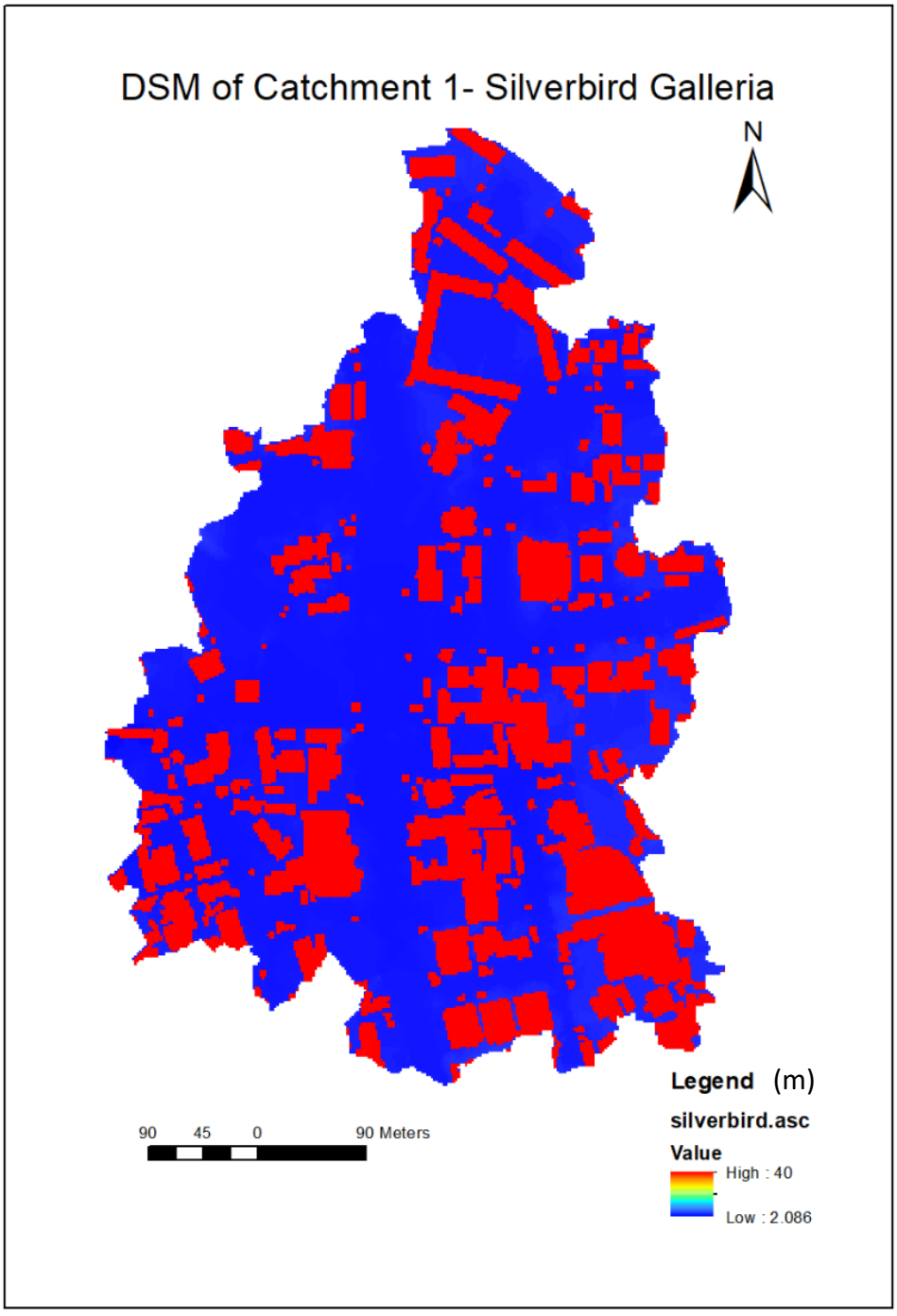


Figure 16: DSM of Sub-catchment 1 used for the FloodMap modelling.

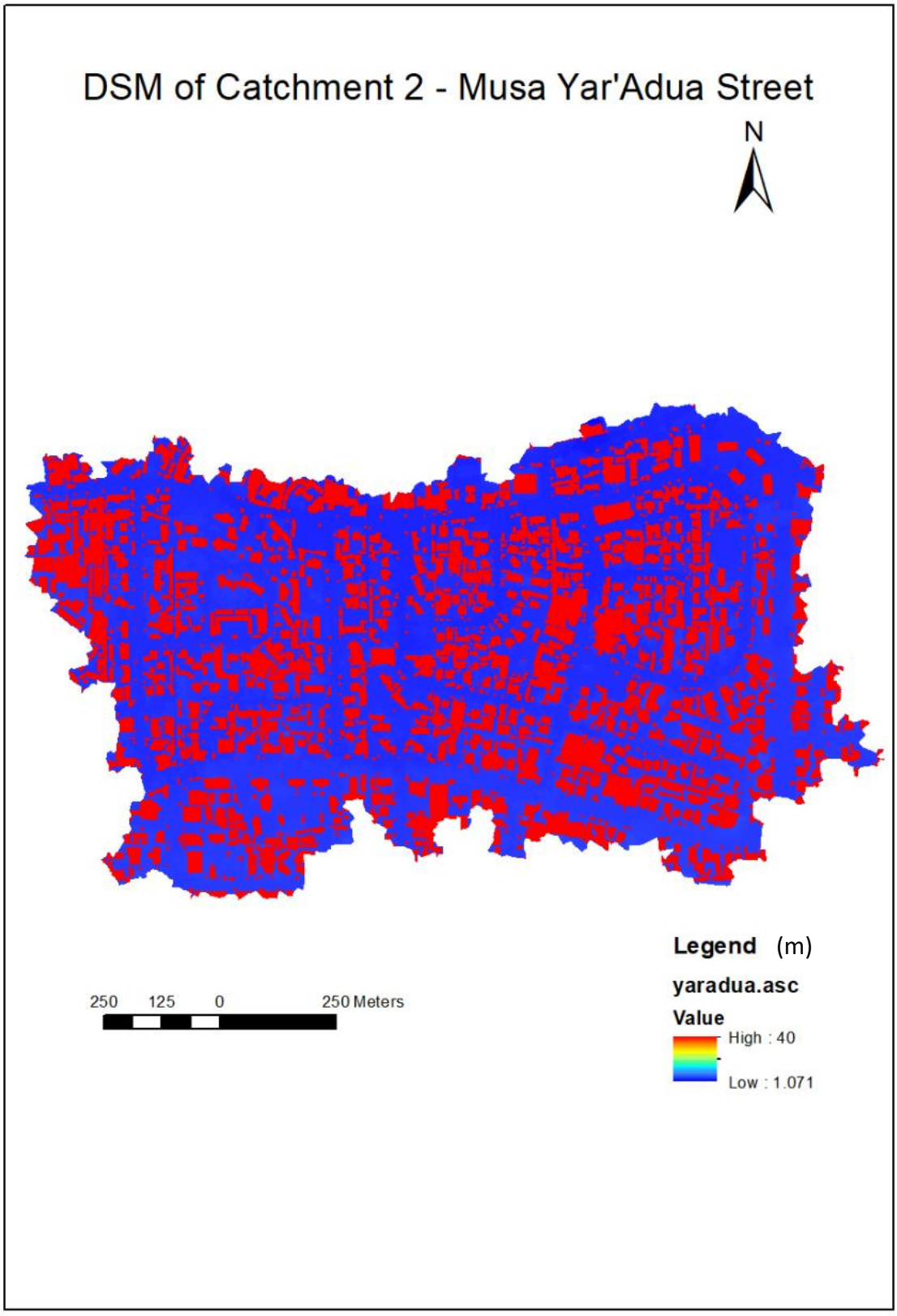


Figure 17: DSM of Sub-catchment 2 used for the FloodMap modelling.

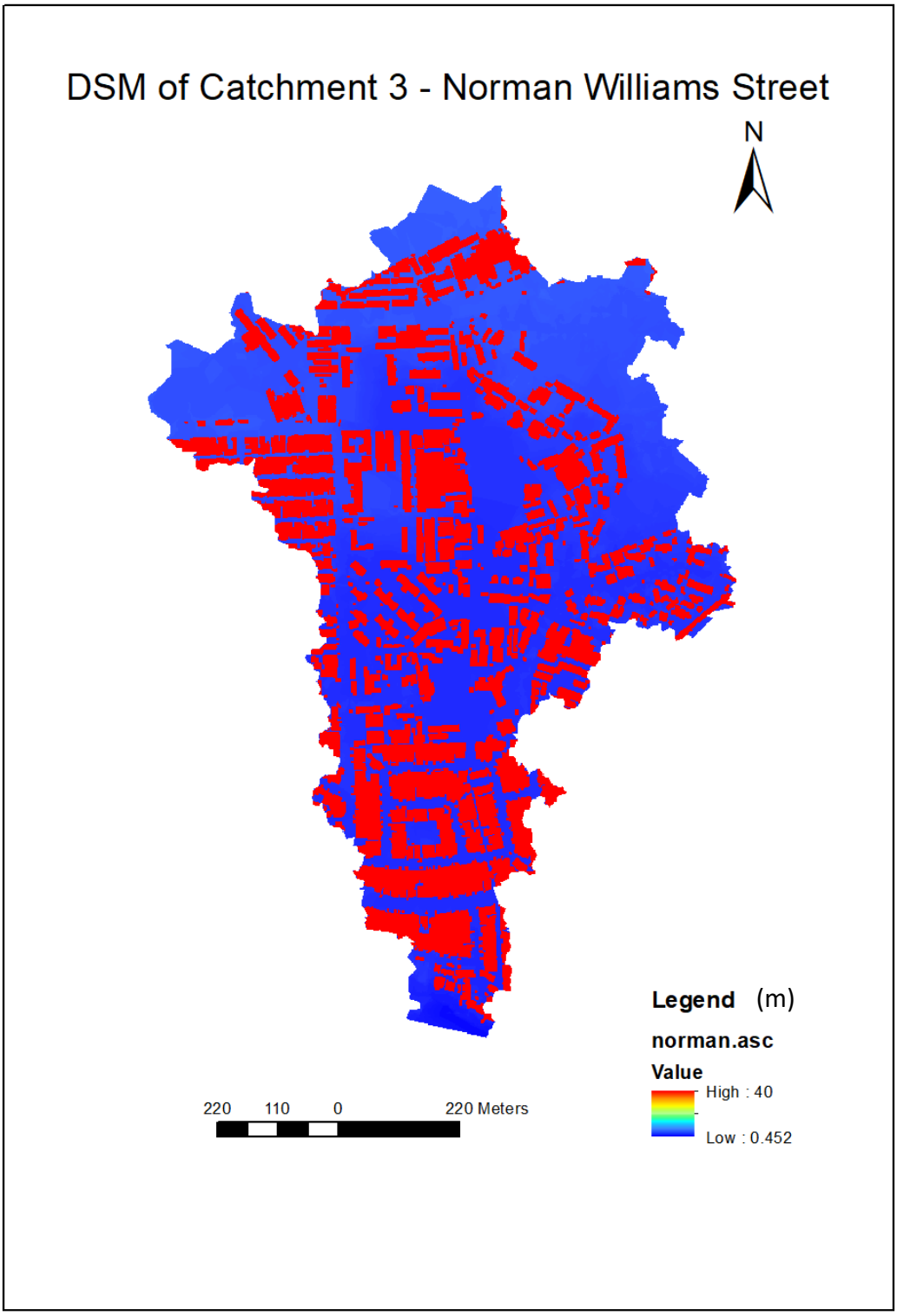


Figure 18: DSM of Sub-catchment 3 used for the FloodMap modelling.

4.9 Description of CityCAT

CityCAT is a 2D flow routing model that facilitates the speedy assessment of combined pluvial and fluvial flood risk in urban areas including the effectiveness of measures taken to reduce flooding (Vassilis Glenis et al., 2018). It is an urban flood modelling analysis and visualization tool that utilizes precise computer algorithms for the representation of flow over the terrain. The architecture of CityCAT is based on the object-oriented approach which provides great flexibility in development and allows rapid extension of functionality (Kutija et al., 2014) and this facilitates the processes and data to better represent the real-world objects the entire system interacts with. The model is written in Delphi (Embarcadero) which facilitates interoperability with other programs, is uniquely amongst hydrodynamic models for flood risk assessment, and is completely object-oriented (V Glenis et al., 2018). CityCAT has been tested in a variety of environments with the capability of testing flood intervention approaches in urban areas such as the use of roof storages for water retention. CityCAT uses a standard DTM for topography and subsequently delineates urban features such as roads, building and permeable surfaces from UK Ordnance Survey MasterMap. For other countries, varying GIS datasets can be integrated into CityCAT for modelling which was adopted for this modelling task. A detailed breakdown of the parameter representations by CityCAT is given below.

4.9.1 Modelling Surface Flow

The 2D shallow water equations are used to model surface flow in CityCAT. These equations are also known as the Saint-Venant equations and they are a set of partial differential equations that govern the conservation of mass and momentum in open channels (V Glenis et al., 2018). The equations are solved using numerical methods in CityCAT to simulate the flow of water over the ground surface during a flood event.

4.9.2 Depicting Buildings in CityCAT

The CityCAT flood model uses a 1D numerical solver based on the Shallow Water Equations (SWE) to model the interaction of water with buildings (V Glenis et al., 2018). The SWE are a set of partial differential equations that describe the flow of water in shallow depths, which are appropriate for modelling urban flood events. In addition to the SWE, the CityCAT model incorporates building drag equations to simulate the effect of buildings on the flow of water. These equations account for the momentum transfer between the flow and the buildings and help to accurately model the flow patterns around and through the buildings. The building drag equations are based on the work of Chaudhry et al. (1993) and are incorporated into the numerical solver used by the CityCAT model.

4.9.3 Modelling Infiltration in CityCAT

CityCAT uses the Green-Ampt equation to model infiltration, which is a widely used empirical model that describes the infiltration process in soil (V Glenis et al., 2018). The Green-Ampt equation relates the cumulative infiltration to time and the soil's hydraulic properties, including the hydraulic conductivity, water content, and suction head. In CityCAT, the Green-

Ampt equation is solved numerically along with the other governing equations to simulate the infiltration process during a flood event.

4.9.4 Modelling roof Drainage in CityCAT

The CityCAT model has a simple roof drainage algorithm that calculates the runoff from roofs and transfers it to the surface flow. The algorithm considers the roof area, rainfall intensity, and a roof runoff coefficient to estimate the amount of runoff. The runoff coefficient takes into account the type of roof material, slope, and the presence of gutters and downpipes (V Glenis et al., 2018). Once the runoff is estimated, it is routed to the nearest surface flow node, where it is added to the total surface flow discharge.

4.10 Parameter representations in CityCAT

Flood modelling in CityCAT involves the process of manipulating the rainfall data into rainfall intensity for CityCAT, representing buildings, modelling surface flow, evapotranspiration and infiltration as shown below.

4.10.1 Representing Rainfall in CityCAT

For pluvial flood modelling in urban areas, CityCAT recognises rainfall data as intensity (depth over time) in mm/s as shown in Figure 19. The format which is represented as a time-step value relative to depth is the format recognised by CityCAT. This rainfall data was introduced into the command prompt along with all the parameters specifying the directory as in line with the CityCAT recognisable format.

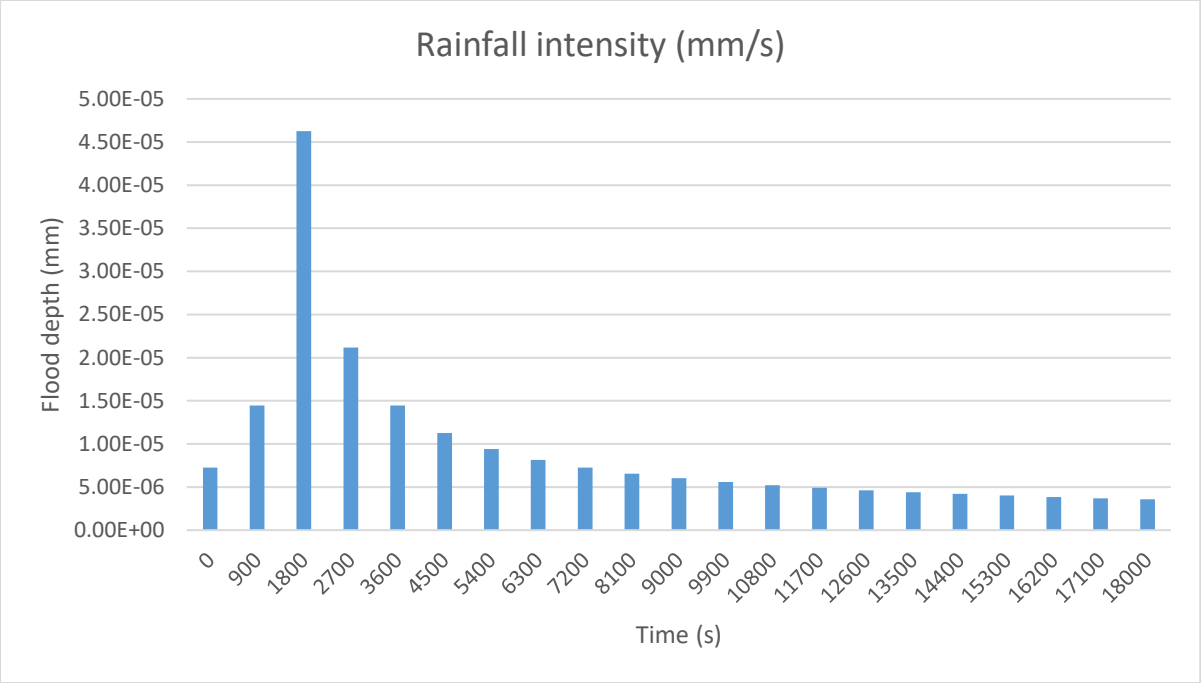


Figure 19: Rainfall intensity chart for the CityCAT model

4.10.2 Representing buildings in CityCAT

In CityCAT, buildings are treated as solid features from the buildings folder where flow is routed around them (V Glenis et al., 2018). Ideally, the buildings required for flood modelling using CityCAT are extracted from OS MasterMaps and incorporated into the model. Unfortunately, the OS Master Map does not have buildings for the study area, hence, buildings were converted into a format that will be recognised in CityCAT. The method for transforming buildings into CityCAT recognisable format is at Figure 20. Buildings in CityCAT are taken into account as solid boundaries by default and as such their footprint needs to be removed from the computational domain for the overland flow which improves the models ability to genuinely represent the flow path of urban areas whilst reducing computational time (Vassilis Glenis et al., 2018). The object-oriented architecture of CityCAT coupled with the polygon representation of buildings permits the alteration of attributes like elevation, flow permeability and modifying roof permeability in order to model diverse flood disaster management options.

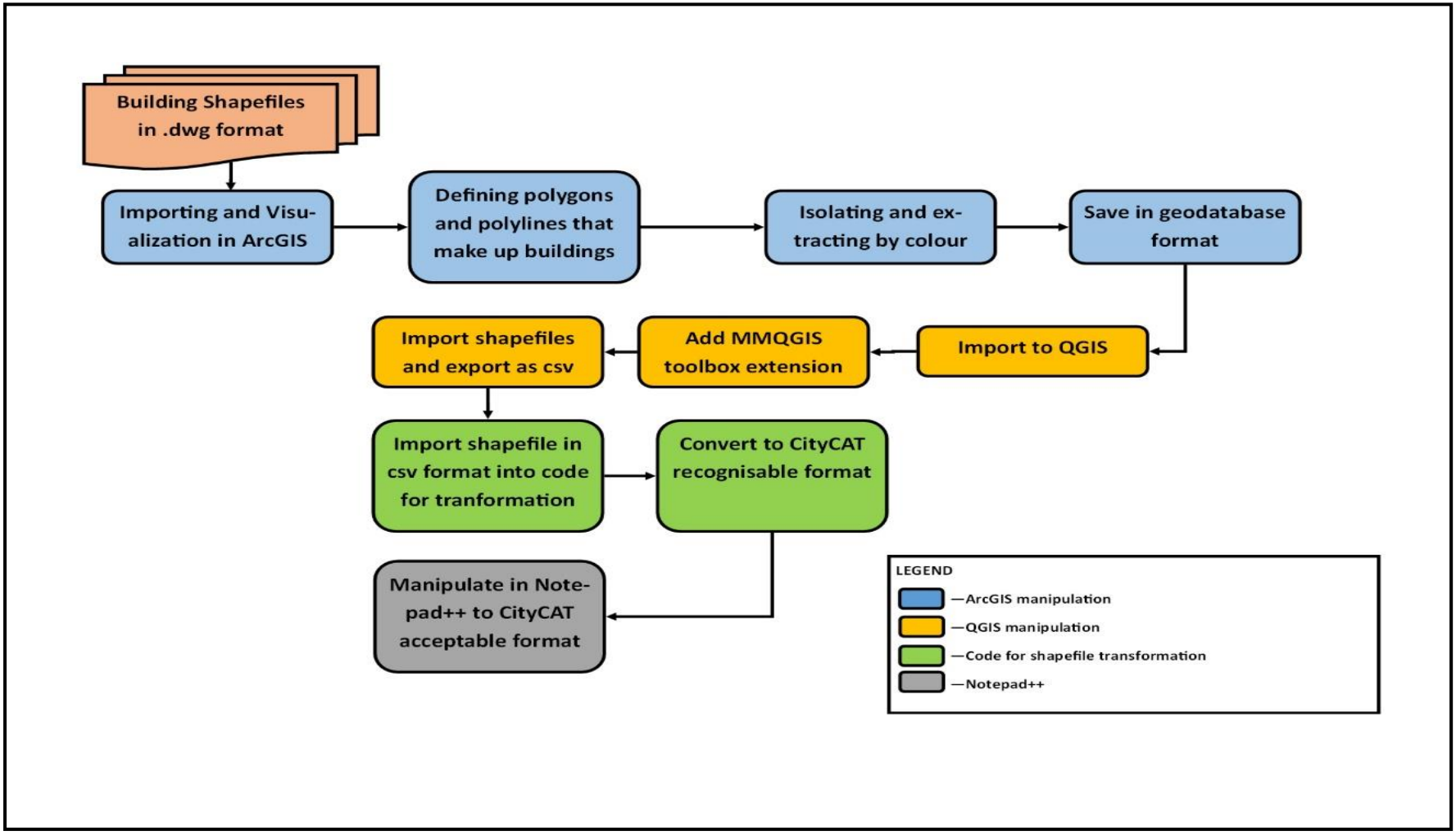


Figure 20: Procedure for converting shapefiles in .dwg to CityCAT recognisable format

4.10.3 Modelling surface flow

The overland flow component of CityCAT is based on the full shallow water equations where the procedure is obtained using the method of finite volumes with shock-capturing schemes (Vassilis Glenis et al., 2018). The Osher-Solomon solver is adopted which is one of the most accurate solvers that is complete as it solves all waves, differentiable with respect to arguments, is entropy satisfying and captures slow moving shocks (Vassilis Glenis et al., 2018). Despite the attractive features of the Osher-Solomon solver (robust, satisfies entropy, good behaviours for slowly moving shocks and smoothness), the solver is very complex and computationally expensive (Dumbser & Toro, 2011). The numerical methods of CityCAT in modelling flow have been validated against analytical solutions and experimental data (Vassilis Glenis et al., 2018) which posits that the largest sources of uncertainty originate from the input data and not from the approximations of numerical methods (McClean et al., 2020). This low uncertainty in numerical approximations favoured the use of CityCAT for this study.

4.10.4 Modelling infiltration

Infiltration in CityCAT is evaluated using the Green-Ampt method which is introduced into the model in the form of hydraulic conductivity (Vassilis Glenis et al., 2018) and this value is dependent on the soil type. CityCAT adopts the Green-Ampt infiltration equation using the iterative method specifically the Newton-Raphson's method which is a root-finding algorithm and this produces better approximations to the roots or zeroes of a real-valued function (Soram et al., 2013).

4.10.5 Flood loss from evapotranspiration

CityCAT is an urban flood modelling, analysis and visualization tool (V Glenis et al., 2013) where focus on flood losses is from the intervening terrain and the effect of flood upon this terrain. Evapotranspiration contributes a limited amount to flood losses in urban areas due to the short duration of urban pluvial floods (Yin et al., 2016). Therefore, CityCAT being a model intended for flood modelling in urban areas, does not simulate evapotranspiration processes (Krivtsov et al., 2020).

4.10.6 Representing green areas in CityCAT

CityCAT extracts green surface polygons from OS MasterMaps layers and also reads green surfaces generated by other softwares. These green areas are classified as permeable and are allotted appropriate infiltration rates and roughness values which CityCAT adopts for the modelling process. For this modelling task, a shapefile of the green areas was converted to ascii format and subsequently modified to CityCAT recognisable format just like the buildings in Figure 20 above. These green areas were allotted appropriate hydraulic conductivity and Mannings values representing infiltration and roughness respectively.

4.11 Parameters adopted for CityCAT

The parameters adopted for optimizing the CityCAT hydrological model to adequately represent the historical flood event was the minimum, median and maximum values for the

Mannings and hydraulic conductivity values as shown in Table 15 while the adopted parameters are at Table 16.

Table 15: Range of values for parameterization of the CityCAT model

Serial	Parameter	Values
1.	Manning's roughness	
	a. Buildings	0.5, 0.6, 0.7,0.8,0.9,1
	b. Vegetation (0.25-0.35)	0.25, 0.27, 0.29, 0.31, 0.33, 0.35
2.	Hydraulic conductivity (m/hr)	0.001, 0.002, 0.003, 0.004, 0.005
3.	Evapotranspiration (mm/day)	2.5

Table 16: Parameters adopted for CityCAT simulations

Simulation	Manning - Buildings	Manning - Vegetation	HC (m/hr)
1	0.5	0.25	0.001
2	0.5	0.25	0.003
3	0.5	0.25	0.005
4	0.5	0.3	0.001
5	0.5	0.3	0.003
6	0.5	0.3	0.005
7	0.5	0.35	0.001
8	0.5	0.35	0.003
9	0.5	0.35	0.005
10	0.75	0.25	0.001
11	0.75	0.25	0.003
12	0.75	0.25	0.005
13	0.75	0.3	0.001
14	0.75	0.3	0.003
15	0.75	0.3	0.005
16	0.75	0.35	0.001
17	0.75	0.35	0.003
18	0.75	0.35	0.005
19	1	0.25	0.001
20	1	0.25	0.003
21	1	0.25	0.005
22	1	0.3	0.001
23	1	0.3	0.003
24	1	0.3	0.005
25	1	0.35	0.001
26	1	0.35	0.003
27	1	0.35	0.005

4.12 Pluvial Flood Simulation using CityCAT

Two graphical outputs are generated by CityCAT which is the time series of water depths and flow velocities for the entire simulation and snapshots of water depths and velocities at predetermined intervals during the simulations. The outputs can be integrated with various softwares for analysis. A total of 27 simulations were made using the parameter values in Table 2. The CityCAT is a robust flood model which requires data in a specific format for flood inundation modelling. The simulation adopted was a modified version of (Vassilis Glenis et al., 2018). CityCAT modelling is achieved using a command prompt and the modelling parameters are stored in a folder with each file representing the various parameters. Launching the run command prompt, the model paths are established, and the simulation commences. Just like the FloodMap simulation, 3 computers were used with a 32GB RAM. The DTM used was in ascii format and stored in the folder as shown in Figure 21. The resulting output was in .rsl format where additional softwares were used for converting them into a .tif format where the outputs were visualized. Modelling for the 3 sub-catchments used their respective DTMs at shown in Figure 21, Figure 22 and Figure 23 as the input terrain and the parameter values outlined in Table 16. A total of 27 simulations were run using these different parameter values to simulate the flood event that occurred on 8th July 2017.

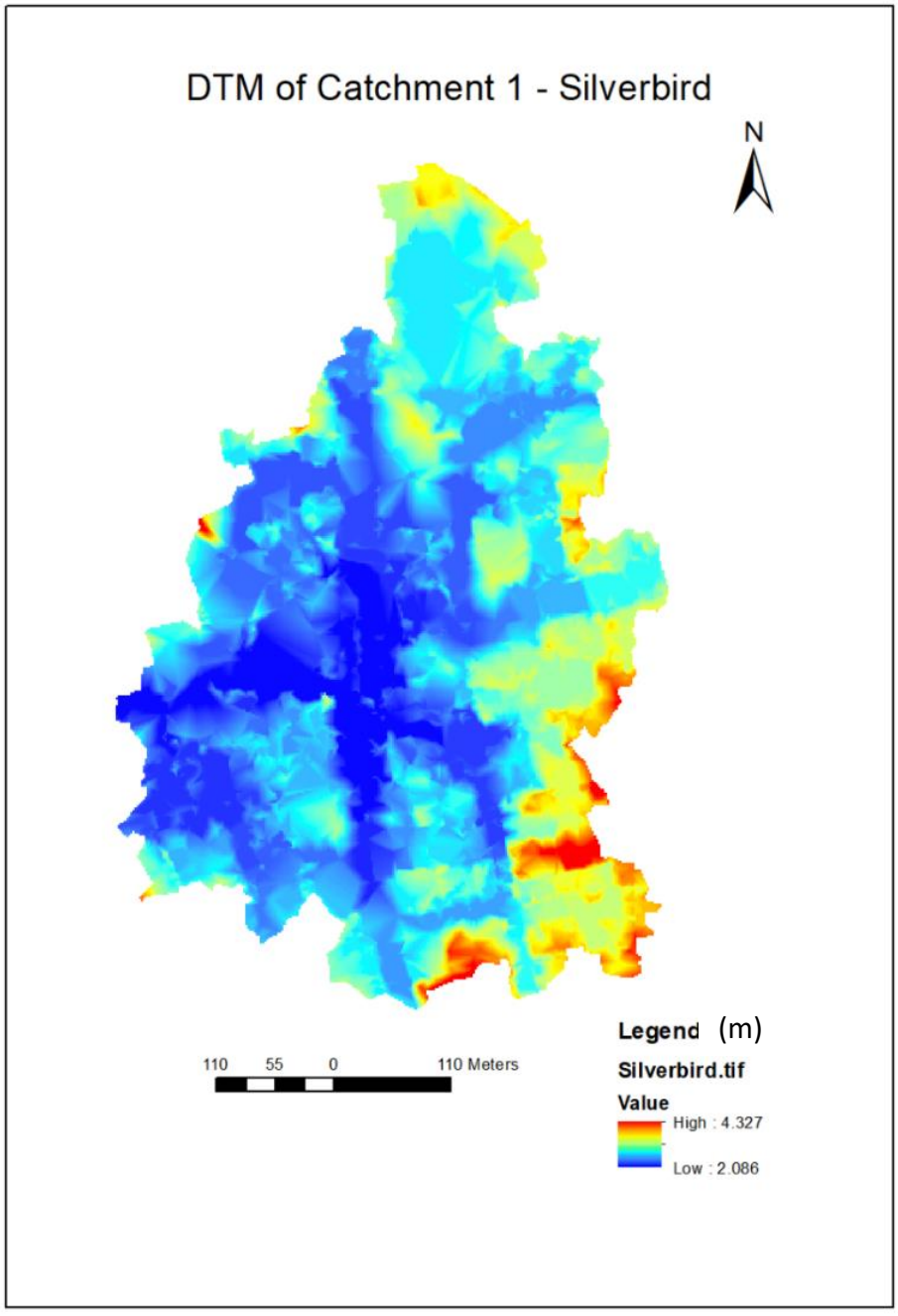


Figure 21: DTM of sub-catchment 1 used for the CityCAT modelling

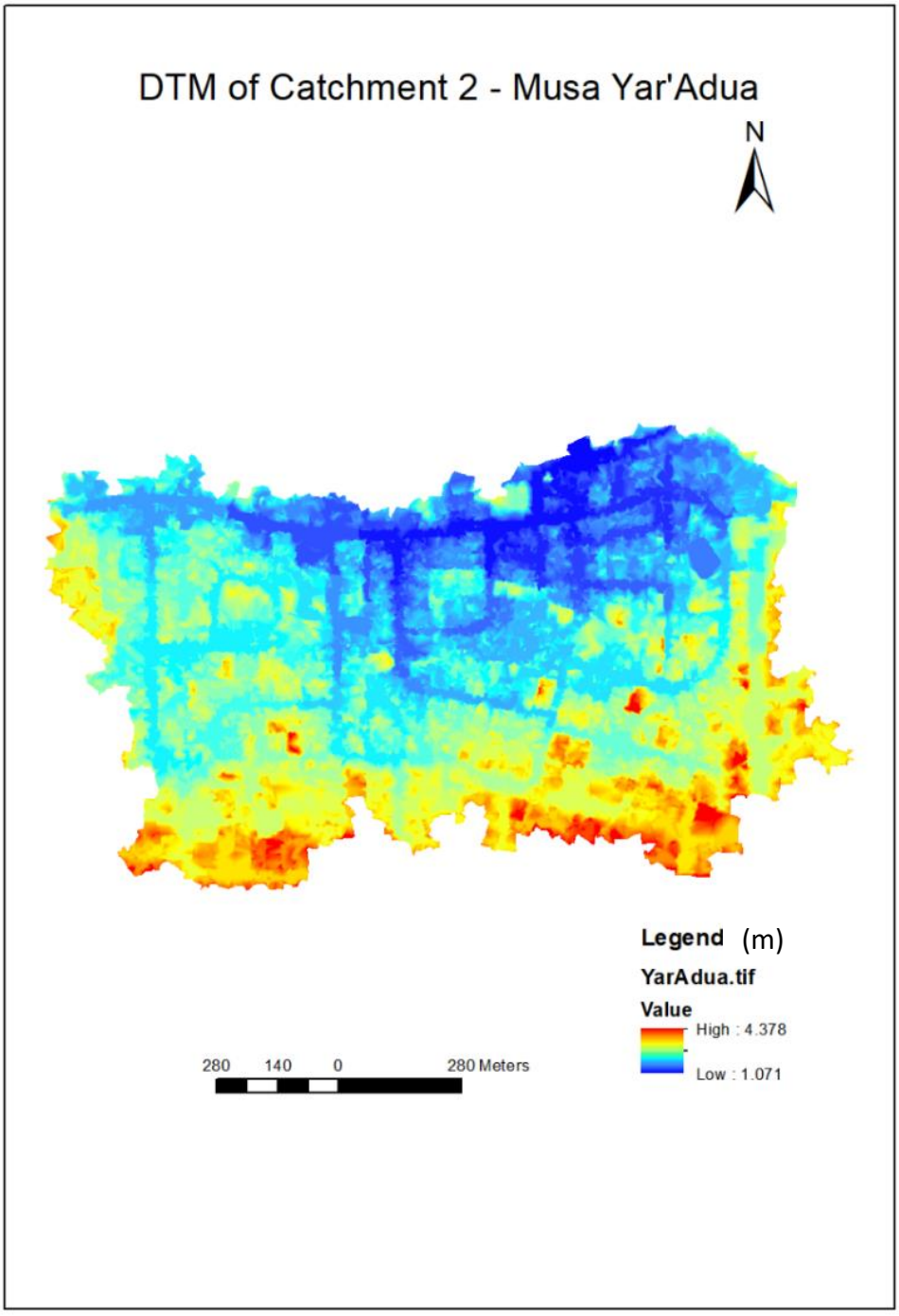


Figure 22: DTM of sub-catchment 2 used for the CityCAT modelling

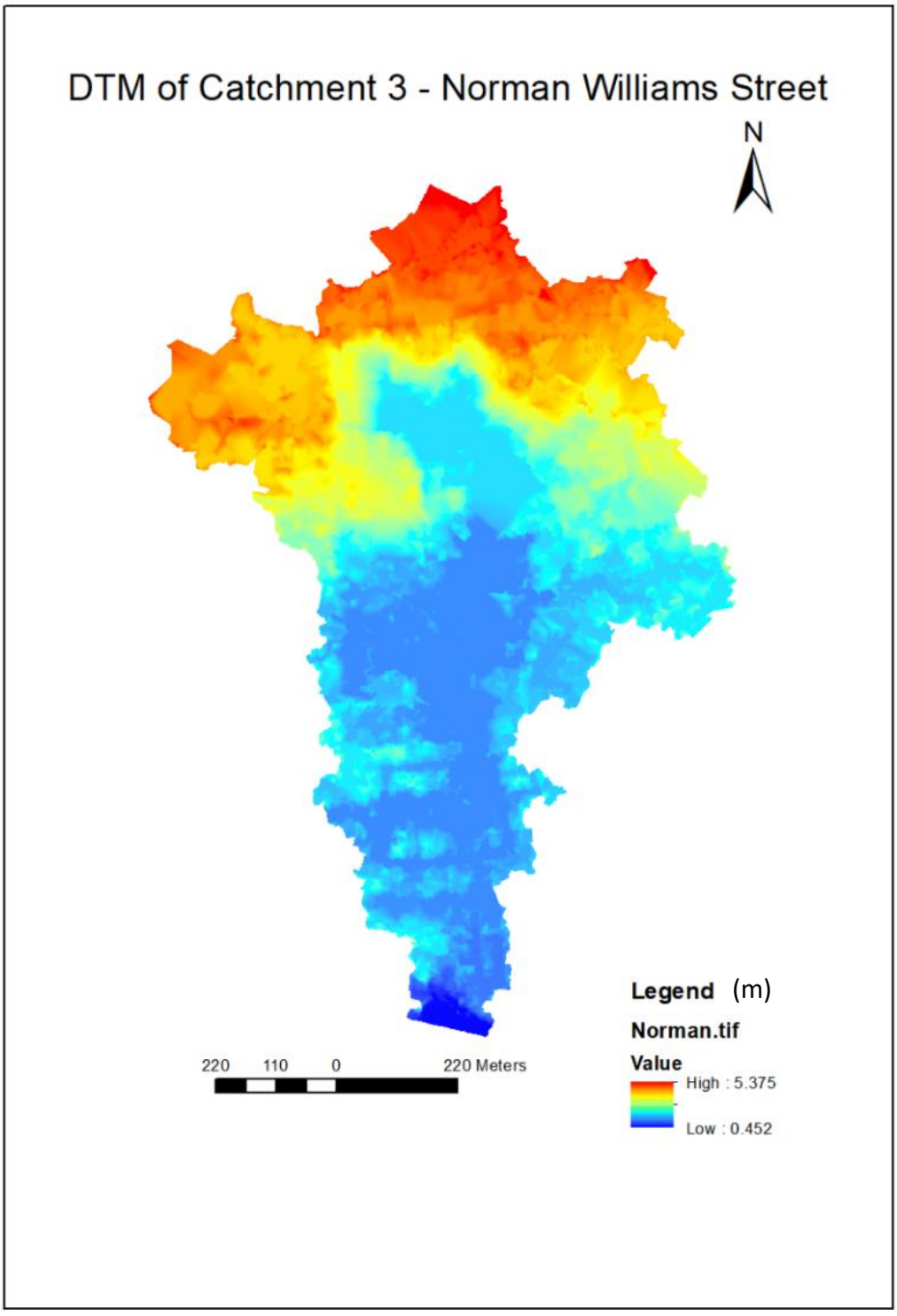


Figure 23: DTM of sub-catchment 3 used for the CityCAT modelling.

4.13 Summary of Chapter 4

This chapter presented the data used for the modelling, the methods adopted for the processing of these data to suit the needs of both the FloodMap and CityCAT models, including the procedure adopted for replicating the historical flood event that occurred on 8th July 2017. The LiDAR point clouds were used to generate a DTM and the accuracy of the output was tested using the linear regression value (R^2) which was 0.93 while the RMSE was 0.32. The range of parameter values for both models were generated and used for parameterizing the models. FloodMap was used to replicate the flood event in its low-complexity state where uniform values of Mannings, hydraulic conductivity and drainage capacity are allotted throughout the sub-catchment. CityCAT flood model was used in its high-complexity state where the distinct representation of the impact buildings and vegetation will have on modelled flood output was simulated.

Chapter 5: Generation of validation data for flood models in data sparse regions

5.1 Overview of Chapter 5

This Chapter outlines the approach adopted for generating validation data in data sparse regions. The emphasis of this chapter is on low-cost approaches to generate validation data to replicate a historical flood event and how the validation data could be used for flood model calibration and subsequently validation. The importance of citizens' science in generating low-cost validation data was showcased in this chapter.

5.2 Generating low-cost flood model validation data in regions affected by data sparcity

One of the flood modelling protocols in the validation of a hydrological model involves establishing the models capability of making accurate predications outside a calibration period; with a model being validated when its predictive capability falls within acceptable errors (Refsgaard, 1997). Validation is also a means to ascertain that the model on which the simulation is based, represents reality with an acceptable level of accuracy (Giannasi et al., 2001). The underlying approach to validation involves error identification and quantification including uncertainty with emphasis on the comparison between the computational results and the actual data (Martins, 2006). One vital requirement for the successful validation of a flood model is the availability of accurate observed data to authenticate the simulated data. In other words, validation data serves as a baseline for the entire modelling process and any errors contained in the validation data, will ultimately affect the accuracy of modelled results. In hydrological modelling, many researchers have employed diverse ways of obtaining validation and calibration data such as; daily stream flow time series (Wijayarathne & Coulibaly, 2020), remotely from satellite data (Bernhofen et al., 2018; Notti et al., 2018; Revilla-Romero et al., 2015) etc. However, the uncertainty in satellite images of floods needs more attention to enable more precise model validation (Stephens et al., 2012). In areas that do not have reliable ways of determining flood extent, validation data have been obtained with point measurements of flood depth and via crowd sourced means (Yu et al, 2016). Crowdsourced methods are becoming increasingly popular and serve as a cost effective means of generating validation data (V Glenis et al., 2013) especially with diverse online platforms being available for uploading events and sharing information. This study is focused on modelling a flood event that occurred on 8th July 2017 at Lagos, Nigeria. Satellite imagery from Sentinel 1 SAR could not capture the flood event even though there was an image available shortly after the event. This was either due to the study area being urbanized which could have caused obstructions to the side looking incident angle range of 18.3^{o} - 46.8^{o} of Sentinel 1 (ESA, 2020) or the resolution of the satellite could not capture the flood event. A hybrid approach to generate validation data was thus employed. The approach involved generating validation data from a combination of crowdsourced videos/still images of the flood event and further authenticating the flood depth generated.

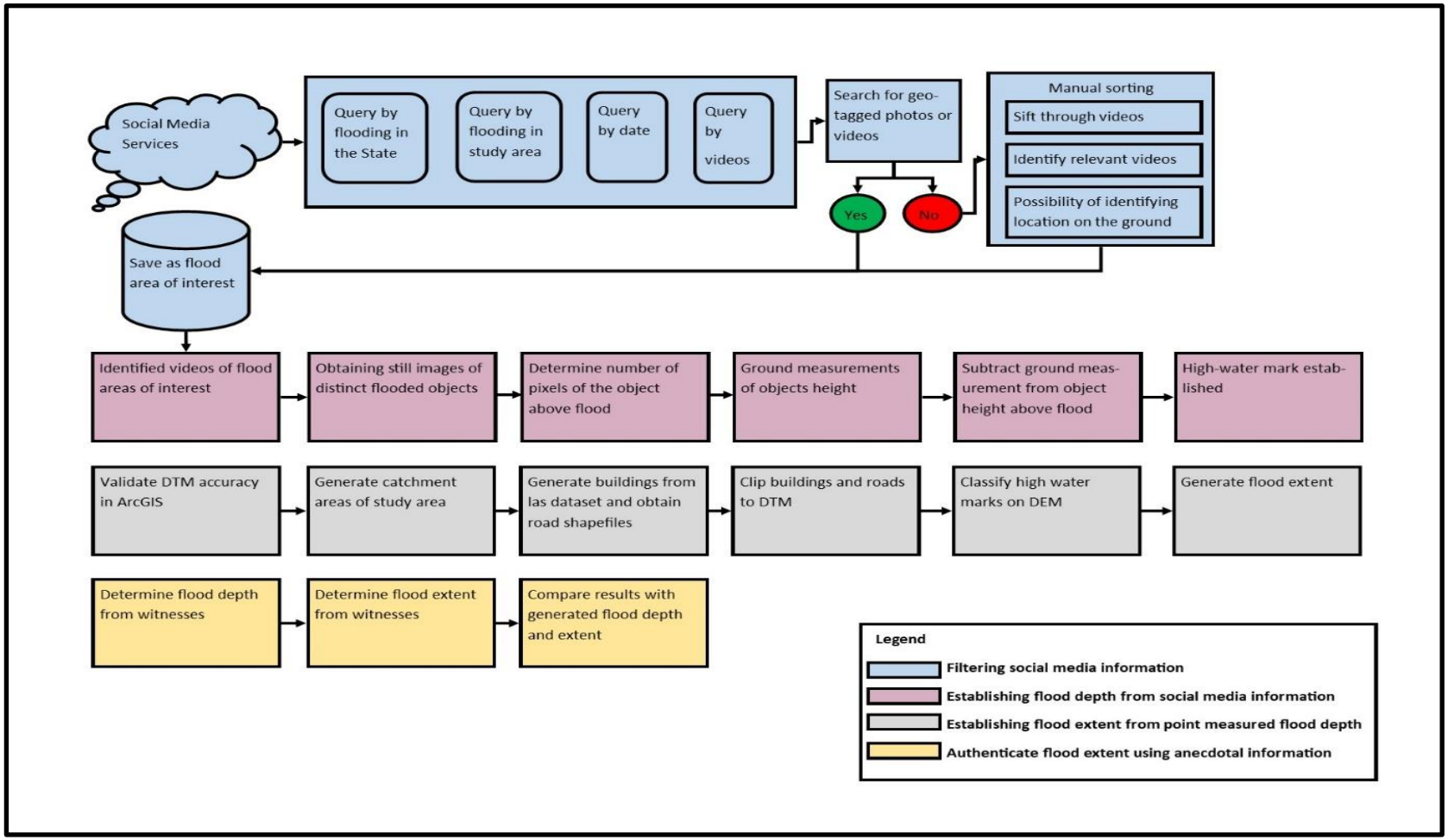


Figure 24: Generating flood depth and extent from social media information.

The methodology adopted for generating validation data from crowdsourced imagery, modified from (Bhola et al., 2019; Fohringer et al., 2015; Kutija et al., 2014; Yu et al., 2016) is at Figure 24.

5.2.1 Filtering crowdsourced information

The crowdsourced approach employed to sift relevant videos and photos was in line with (Fohringer et al., 2015) and (Bhola et al., 2019) where catch phrases related to the flood event; in this case was 'flooding in Lagos, Nigeria' was searched for online using google search engine which generated 1,960,000 results. In order to narrow down the search, further queries involving the specific study areas were included in the search which was 'Flooding in Lagos Island, Ikoyi and Victoria Island' and this resulted in 125,000 results. The date of the flood was subsequently included in the search 'Flooding in Lagos Island, Ikoyi and Victoria Island on 8th July 2017' and this generated 59,300 results. The option to view only videos of the flood was selected as this would give a better idea of the flood extent with the ability to also generate still images from a specific area of interest and 470 results were generated which spanned Twitter, YouTube and Instagram. After sifting through the videos, a total of 5 videos were obtained which covered 3 different sub-catchments within the study area.

5.2.2 Extracting flood depth from crowd sourced information

The approach to employing high-water marks usually immediately after a flood event to determine the flood depth and extent (Fritz et al., 2010) in order to drive flood inundation mapping efforts is being adopted especially when there is no real-time monitoring equipment. This involves identifying stage marks resulting from high water levels which are evident in marks left when turbid water comes in contact with tree trunks and branches, buildings and other natural or man-made objects (Koenig et al., 2016). Since the flood occurred in 2017 and the fieldwork was done in 2018 and 2019, this research employed crowdsourced means to obtain valuable information about the flood. This information was used to generate point depth flood measurements which corresponded to high-water marks and thereafter GIS techniques were employed to generate the flood extent. A field trip was made to the 3 flooded areas of interest in the 3 sub-catchments and objects that were visible during the flood event that were previously identified from the crowdsources images were located on the ground as shown in Figure 25. Subsequently, measurements were taken of those objects in order to generate the high-water marks during the flood which fall into the drainage basins in Figure 26. The procedure outlined in Figure 27, Figure 28 and Figure 29 was used to generate the flood depth at these locations.

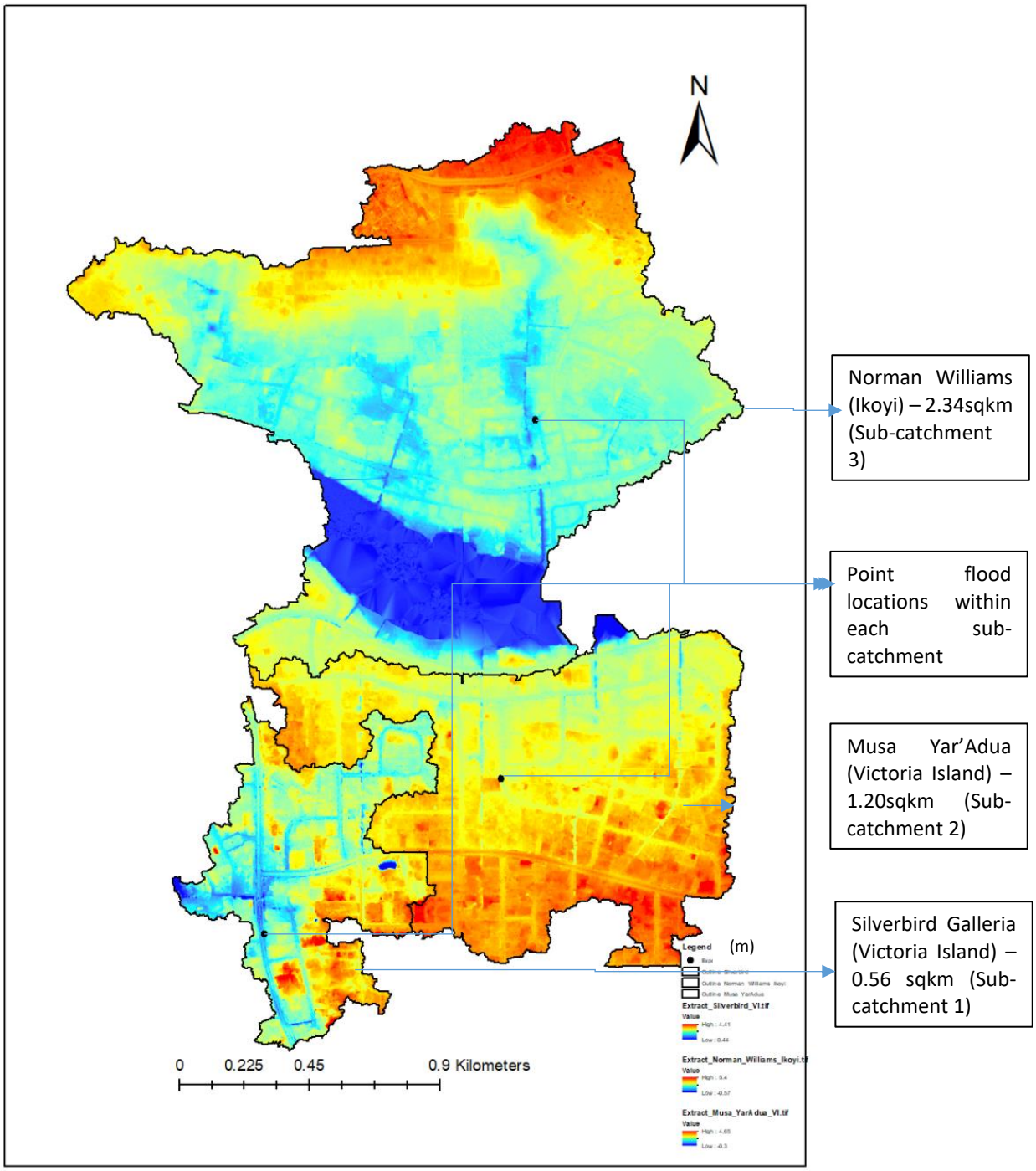


Figure 25: The 3 sub-catchment areas for the study showing their point flood locations

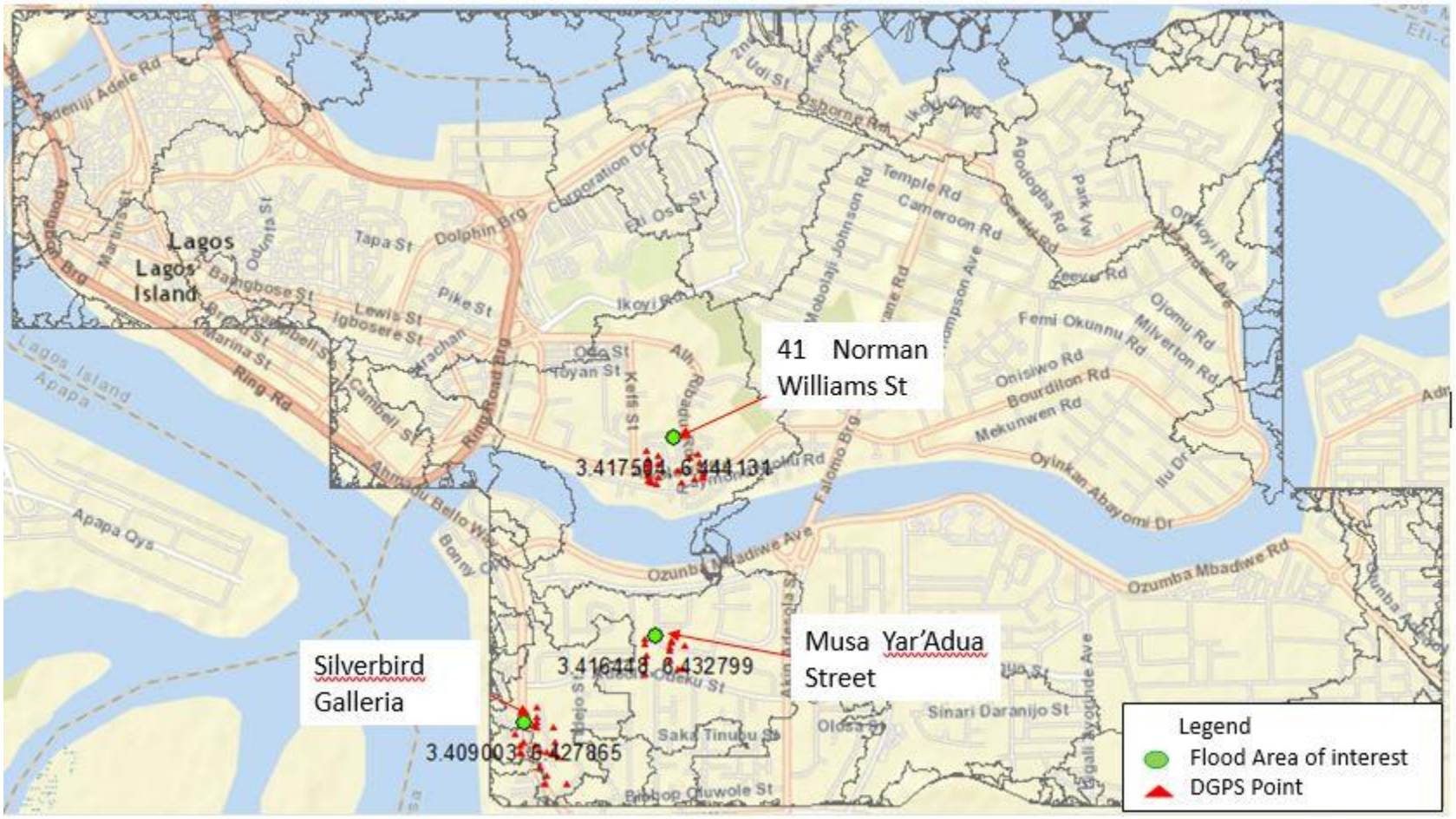


Figure 26: The 3 crowd sourced flooded areas of interest within their drainage basins and the DGPS locations



Figure 27: left: Pole identified during flood for validation: Right- Object used to generate flood depth

Sub-catchment 1 stage point recreation

1. Pole length- 235cm
2. Circumference – 54cm
3. Diameter = 54/pi(3.14)= 17.20cm
4. Diameter of pole- 7 pixels
5. Length of 1 pixel = 17.20/7=2.46cm per pixel
6. Number of pixels visible = 67 pixels
7. Visible pole extent = 67 x2.46cm = 164.82
8. Flooded depth = length of pole – visible extent
9. = 235-164.82= 70.18cm = 0.7m

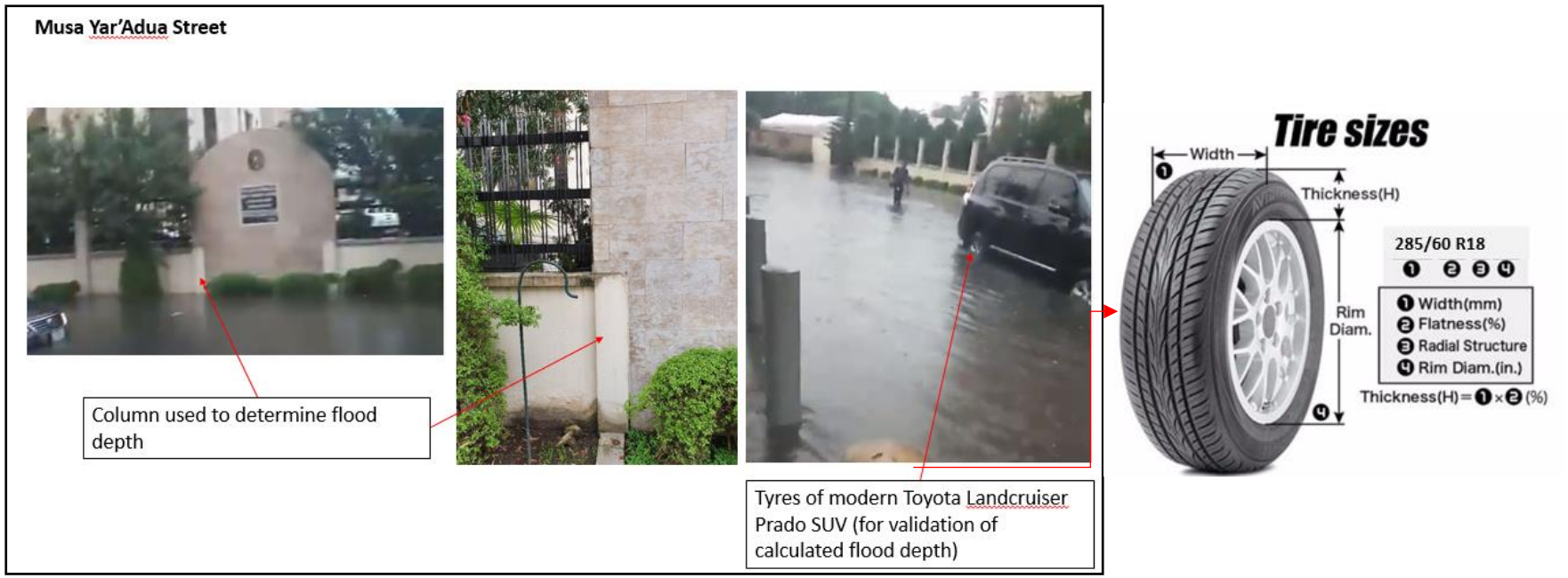


Figure 28: A: Fence identified during flood for validation, B- Fence used to generate flood depth, C-Car tyre used to validate flood depth, D-Configuration of car tyre.

Sub-catchment 2 stage point recreation

1. Fence column height- 140cm
2. Number of pixels – 41
3. Width of fence = 27.5cm
4. Pixels that form width of fence - 12 pixels
5. Length of 1 pixel = 27.5/12 = 2.29cm per pixel
6. Pixels on fence = 140cm/2.29cm = 61.13 pixels
7. Depth of flood = Pixels on fence-number of visible pixels = 61.13 – 41 = 20.13 pixels.
8. Flood depth = 20.13 x 2.29cm = 46.10cm=0.46m

Confirmation using tyres of Toyota Landcruiser Prado SUV with 285/60 R18 (https://tiresize.com/tires/Toyota/Land-Cruiser/)
Rim= 18 inches = 45.72cm.
Thickness = 285mm x 60 (1/100)=171mm= 17.1cm
For both sides = 17.1cm x 2= 34.2
Tyre height = 45.72 + 34.2 = 79.92
Slightly above half of the tyre is visible from the image of the Toyota in the flooded area of interest.

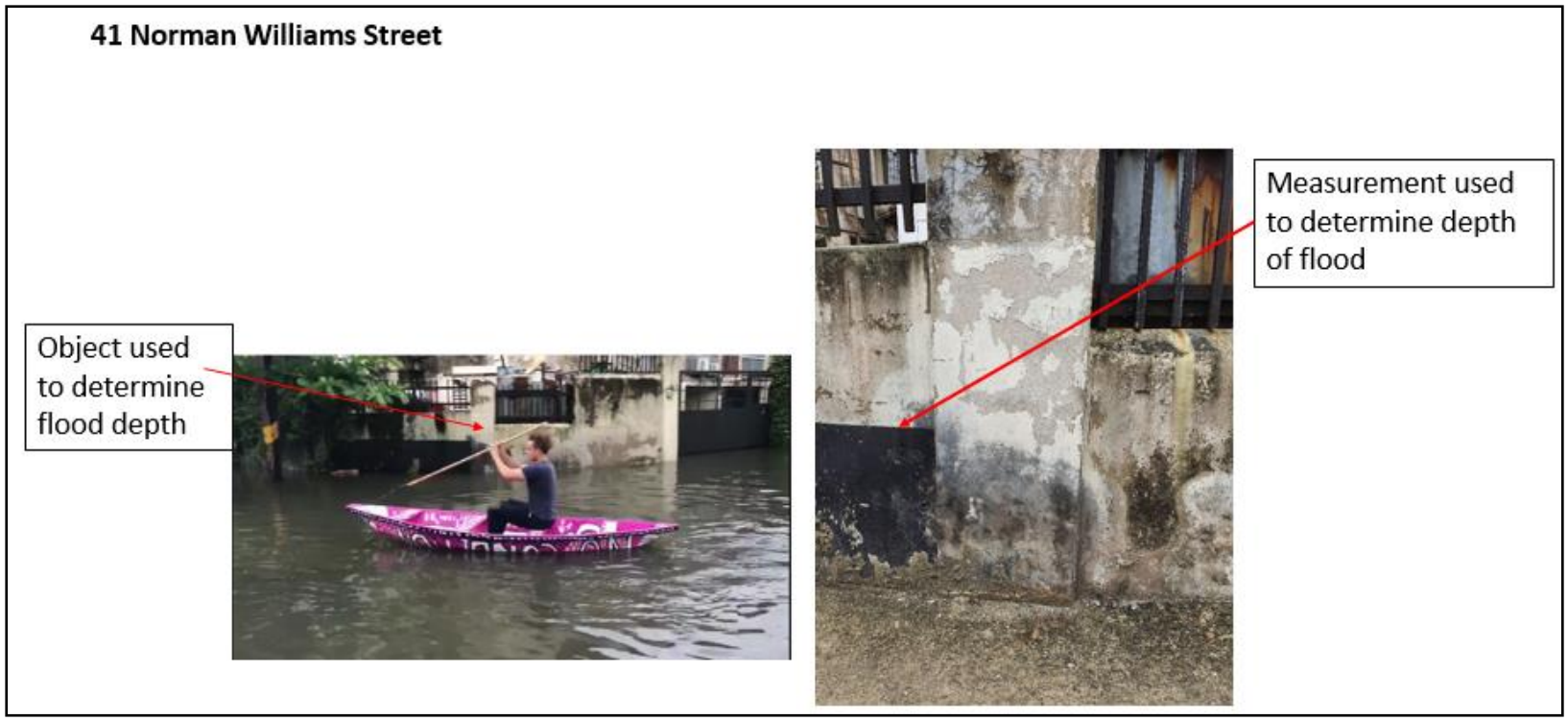


Figure 29: Left: Fence identified during flood for validation: Right- Same fence used to generate flood depth

Sub-catchment 3 stage point recreation

1. Fence column – 47.5cm = 475mm
2. Number of pixels on fence - 30
3. Length of 1 pixel (mm) = 475/30= 15.83
4. Number of pixels from blackline to water surface – 33 pixels
5. Height of blackline above water in picture = 33x15.83 = 522.39mm = 52.239mm
6. Depth of water = 59.5-52.239= 7.21cm (to fence).
7. Height of flood = (base of fence + depth of water) = 25cm+7.261= 32.261cm = 0.32m

5.3 Application of crowd sources in generating flood validation data

The challenges that occur in obtaining data from crowd sources include quality control (G. Li et al., 2017; Meek et al., 2014) and bias resulting from the demographics of the contributors (Chakraborty et al., 2017; Hettiachchi et al., 2021) or collection manner. Other challenges are volume of data resulting in difficulty to manage (Mavandadi et al., 2012), maintaining privacy of the contributors (Hensen et al., 2021), motivation of contributors (Aitamurto & Saldivar, 2017; Budhathoki & Haythornthwaite, 2013) and technical challenges (Minh et al., 2019) such as the need for data at the appropriate scales and with appropriate data storages. In the generation of flood validation data for the historical flood event that occurred on 8th July 2017 within the study area, crowd sources were employed who had witnessed the flooding event. The methodology adopted for this aspect of generating validation data took into cognisance these challenges and the methodology is as shown in Figure 30.

5.3.1 Defining the Strata

The purpose of defining the strata was to ensure that the sample population can be split into subgroups to ensure each stratum was homogenous with respect to the information required about the flooding event. The study was conducted within the 3 sub-catchments in the study area. From the point flood of interest obtained as shown Figure 26, the flood affected the population around that location and a proximity analysis was found suitable for the generation of the flood extents. Subsequently, the sample size was dependent on the affected population who were in close proximity to the flooded points of interest.

5.3.2 Determining the Sample Size

The sample size was dependent on the scope of the study, nature of the research and the quality of the data to be obtained (Morse, 2000). The sample size for this research was dependent on the availability of respondents within the 3 sub-catchments. Sub-catchment 1 was a business district on a busy street and the flooding affected businesses. A lot of people were available to volunteer information on the flooding. Sub-catchment 2 was mostly residential, not a busy street and flooding affected social services and homes. Fewer people were available for volunteer information. Sub-Catchment 3 is mostly residential and not a busy street and flooding affected mostly residents. There were limited number of volunteers available.

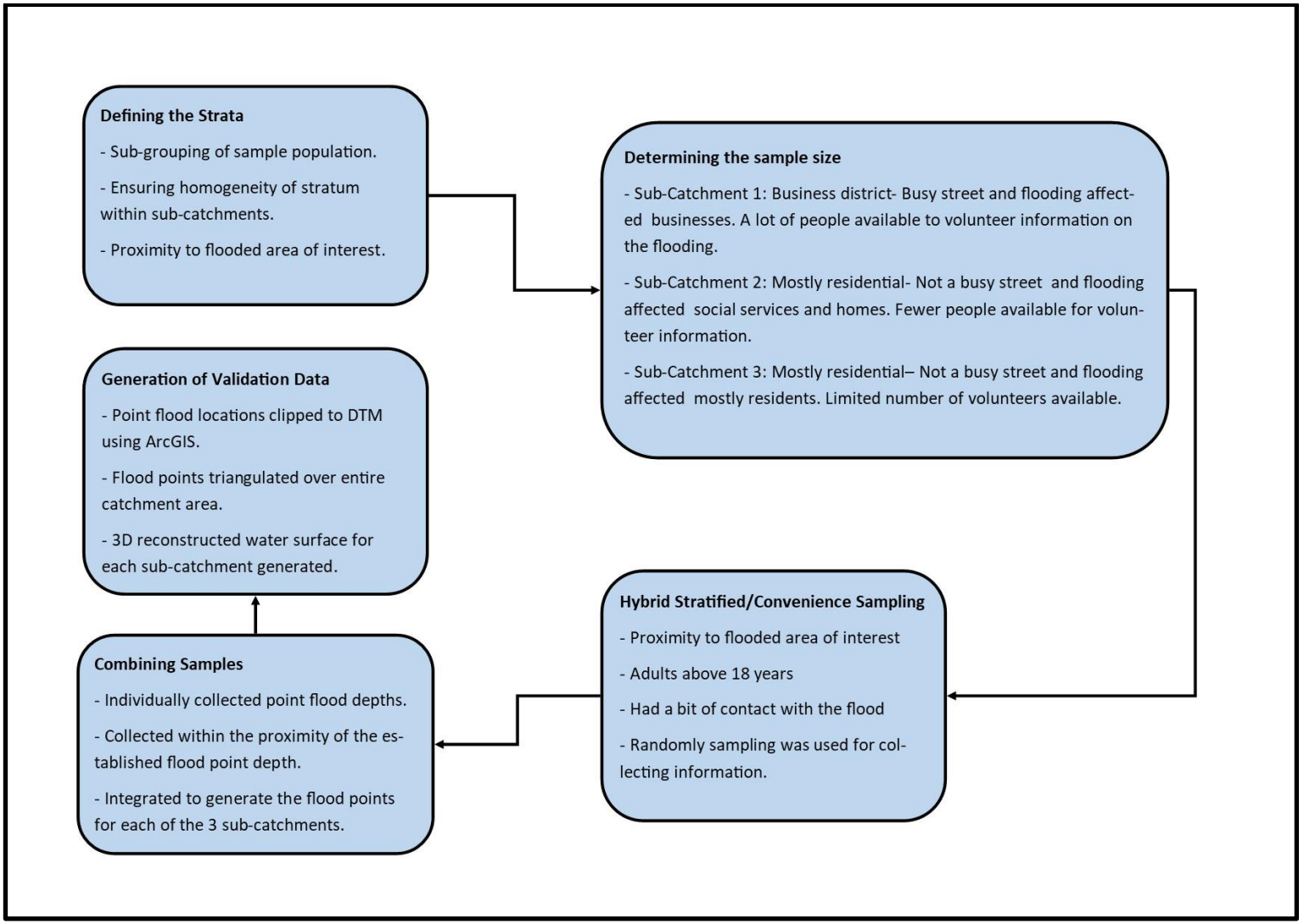


Figure 30: Methodology for the generation of 3D reconstructed flood extents from respondents for the 3 sub-catchments.

5.3.3 Hybrid Stratified Random/Convenience Sampling

A hybrid stratified random and convenience sampling method was adopted to generate flood depths from respondents. For the stratified random sampling, data is divided into sub-groups that share similar characteristics (Acharya et al., 2013). The stratified method used the age of respondents which focused on those above 18 years of age, as interactions with individuals below 18 years require parental consent as they legally fall in a protected class of people and by law cannot give consent. The second stratification was location based with those in close proximity to the flooded point of interest and also who witnessed the flood. Convenience sampling was further adopted on the already stratified sample population. The convenience sampling was adopted to obtain data from respondents who were at the right place at the right time (Acharya et al., 2013). The approach is less expensive and relies on respondents who meet the selection criteria. Consequently, data on flood point depth were obtained from respondents based on these criteria of age and proximity to identified flood point within the 3 sub-catchments.

5.3.4 Combining the Samples

The flood point depths collected from the 3 sub-catchments were collected from individual respondents. These points were obtained on sub-catchment basis and subsequently integrated to form the flood points for the various sub-catchments. These flood points generated represented the flood depths at various locations within the various sub-catchments. All that was required was to be able to integrate these points in order to generate the flood extent for each sub-catchment.

5.3.5 Generation of Validation Data

The triangulation of points can be adopted for the generation of a layer. The approach to generate the flooded extent was adopted from (Gebrehiwot & Hashemi-Beni, 2021), where a water depth map was generated using a 3D reconstructed water surface and a pre-flood DEM. The flood points generated from the respondents were clipped to the generated DTM using ArcGIS. Subsequently, these points were triangulated to form a uniform layer over the surface, and this formed the 3D reconstructed water surfaces for the 3 sub-catchments. This triangulated surface represented the DTM with flooded areas. The original DTM was then subtracted from this newly generated 3D reconstructed water surfaces for each of the sub-catchments and the flood extent was reconstructed for the various sub-catchments as shown in Figures 13, 14 and 15.

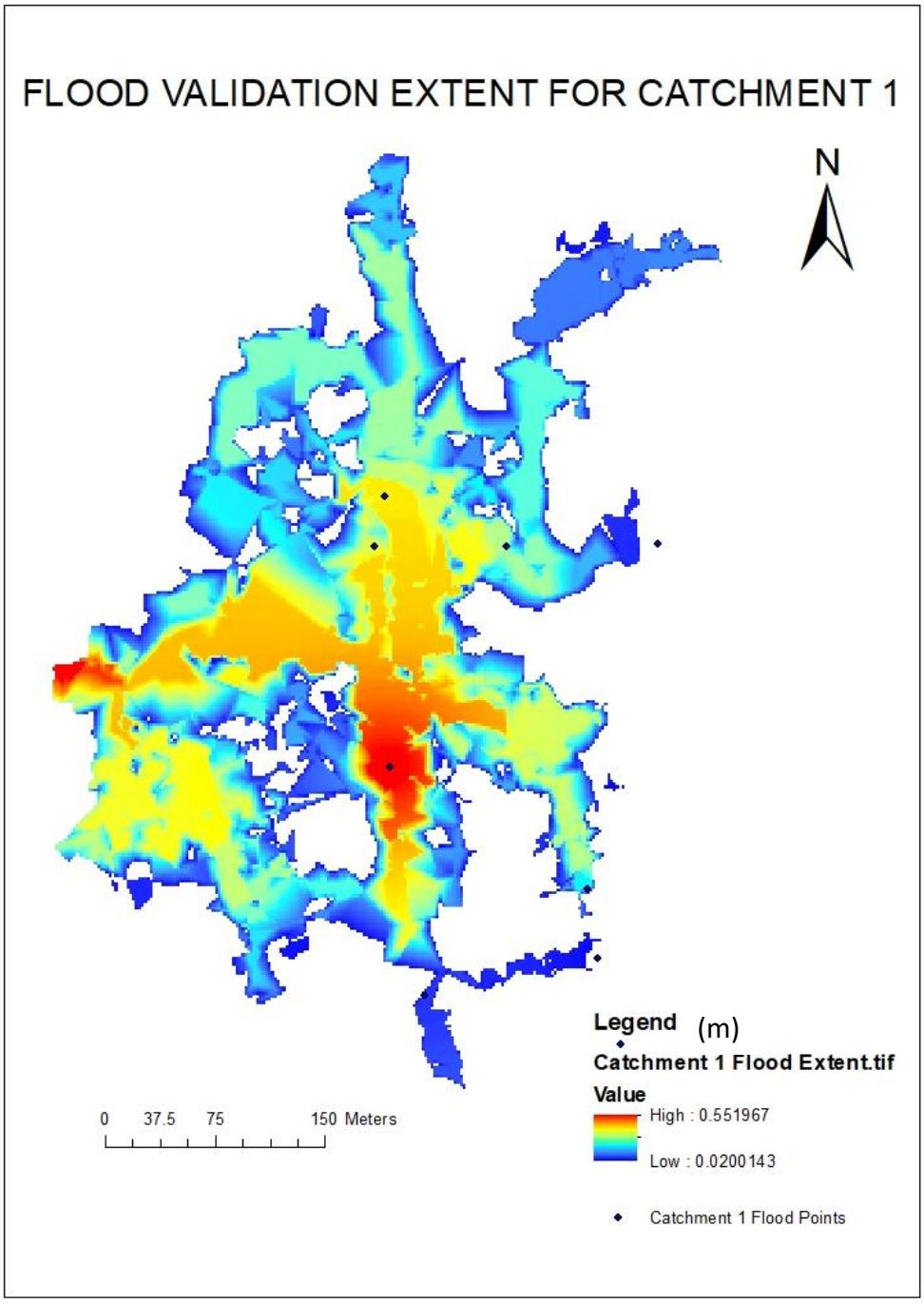


Figure 31: Catchment 1 validation flood extent

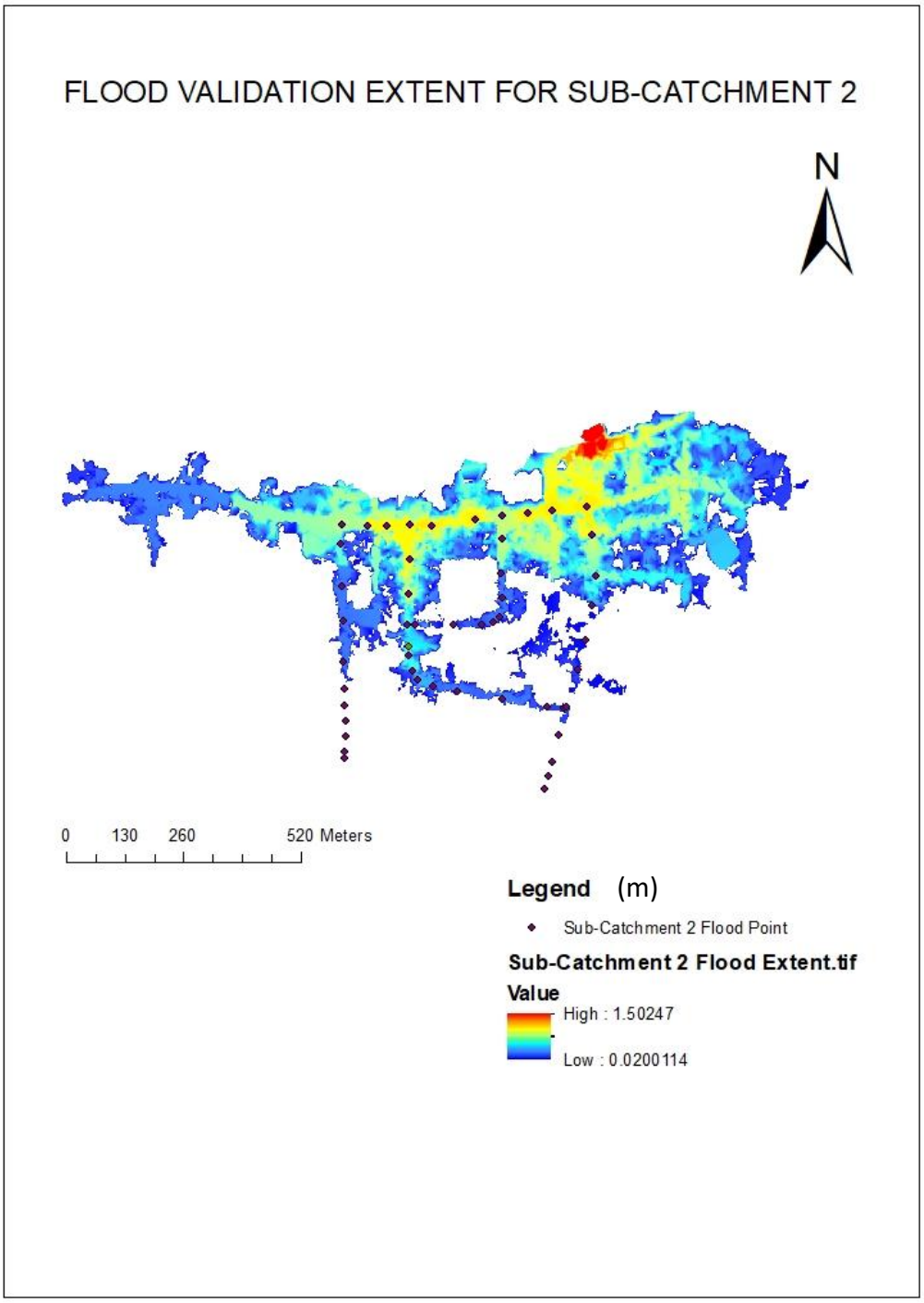


Figure 32: Sub-catchment 2 flood validation extent

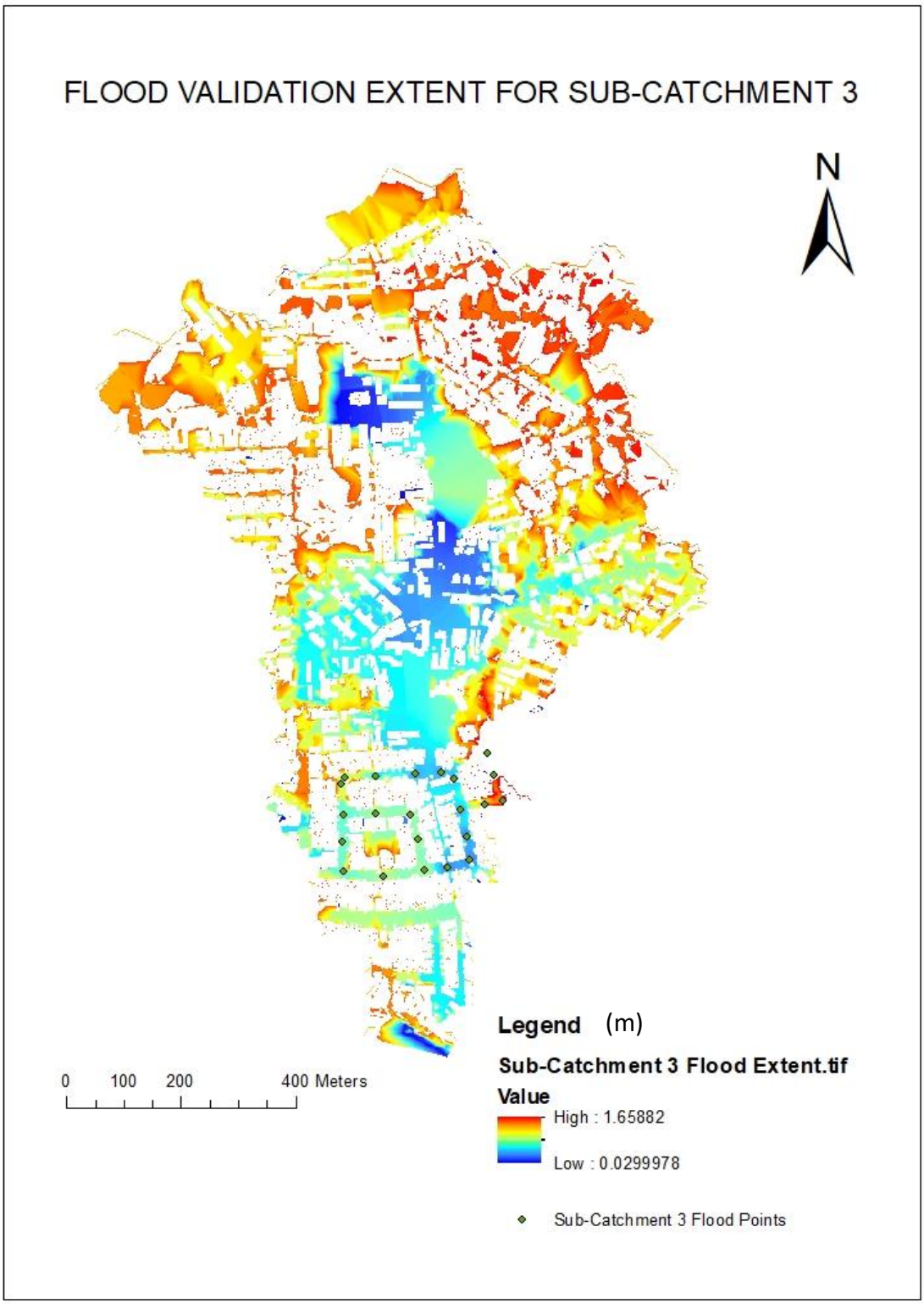


Figure 33: Sub-catchment 3 validation flood Extent

5.4 Summary of Chapter 5

This chapter gives the methodology adopted for the generation of flood validation data for the study. Flooded locations were identified in the 3 sub-catchments and the point flood depth for selected areas were generated. Thereafter, a proximity criterion was used to map the areas for the sampling technique to generate the entire flood validation extent that would serve as the validation data for the historical flood that was simulated for this research. Subsequently, citizens science was used with a sampling technique to generate the flood validation extent for the 3 sub-catchment areas, and these served as the validation data for the simulated flood in all the sub-catchments.

Chapter 6: Flood modelling results and model validation

This Chapter presents the results of the historical flood modelling conducted using the FloodMap and the CityCAT models. The point depth and area extent of the flood event were presented for the 3 sub-catchments that was generated for this study. The sensitivities of the driving parameters for each model were assessed and the models were subsequently calibrated. The calibrated parameter values were then used to model the historical flood for the entire catchment area using both flood models and the point flood depths and extents were compared with that of the observed flood.

6.1 Methodology

The methodology for this chapter adopted a modified version of (Leandro et al., 2009) where the outputs from two models used for urban flood mapping were compared using their profile shapes and their point depths. The methodology for the presentation of the results was executed in 3 stages as shown in Figure 34. Stage 1 was the presentation of results for the FloodMap model and subsequent analysis of the point depth and flood extent for the 27 simulations conducted. The second stage was the presentation of results for the FloodMap model and analysis of the point depth and flood extent for the 27 simulations conducted. The final stage was the comparison of the historical flood extent from the modelling conducted over the entire study area using the calibrated parameters from the sub-catchments using both the FloodMap and CityCAT hydrological models. The comparison of flood model output using the criteria outlined in Table 8 will be done in the analysis and discussion in Chapter 8.

6.2 Modelling Results for FloodMap

The modelling results for the 27 simulations were analysed for the 3 sub-catchments at their point depth and flood extent.

6.2.1 Validation Point Flood Depth for Sub-catchments

The point depth was obtained from the location where the flood stages were recreated, and this served as the validation data. The observed point depths for sub-catchments 1, 2 and 3 were 0.7m, 0.46m and 0.32m respectively. Additional flood points were obtained from the crowd sourced validation data, and these were used for comparing the observed flood depth from the flood modelling conducted.

6.2.2 Validation Flood Extent for Sub-Catchments

The flood extents for sub-catchments 1, 2 and 3 were also recreated and served as the validation data. The flood extents for sub-catchments 1, 2 and 3 were 109,269 m^2, 367,202 m^2 and 369,857 m^2 respectively. The results of the comparison of the flood extents from the validation data and the modelled flood extent is at Appendix E1-3.

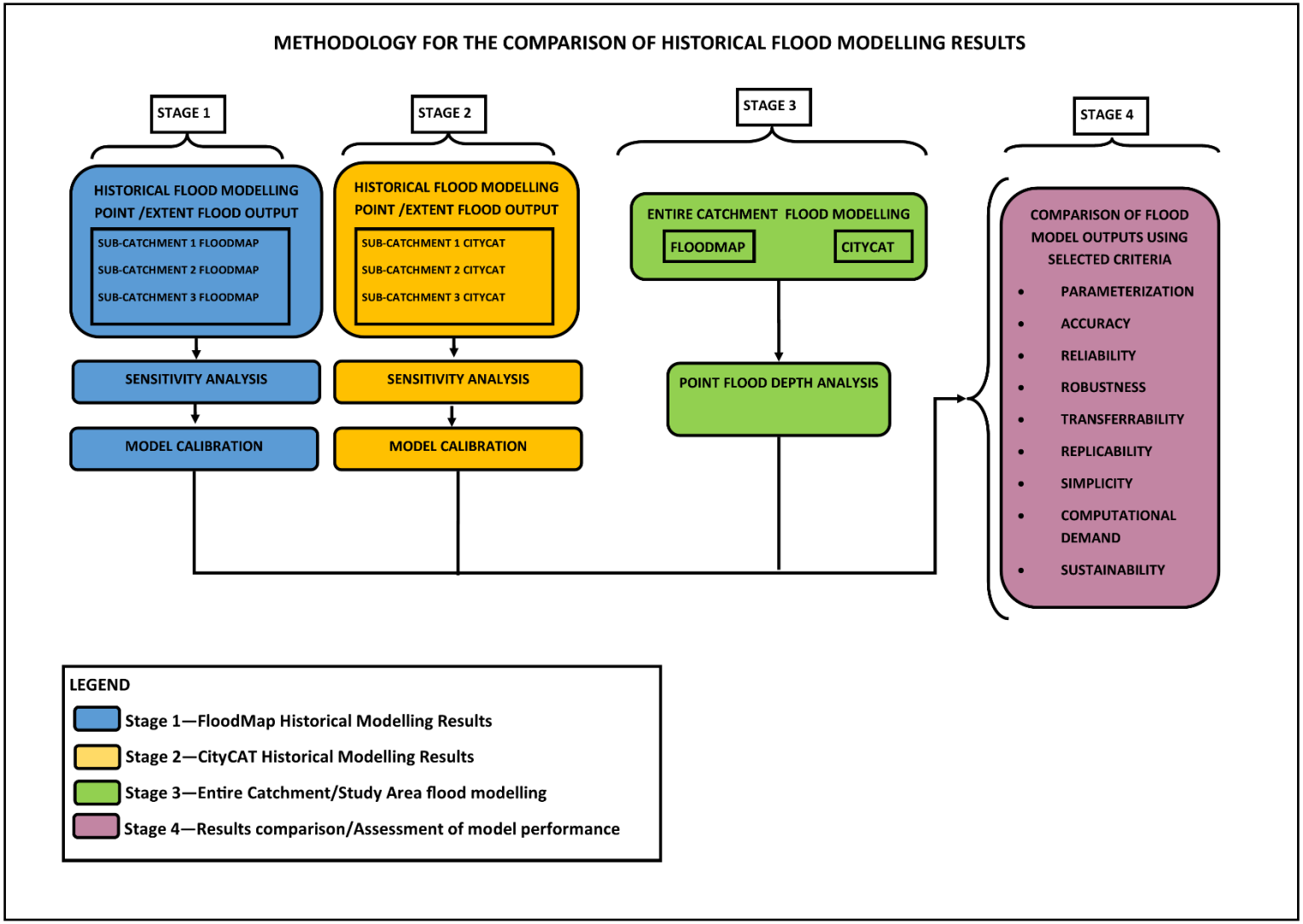


Figure 34: Methodology for the comparison of historical flood modelling results

6.2.3 Sensitivity Analysis

Random Forest (RF) was used for the assessment of the sensitivities of the parameters used in all the 3 sub-catchments. RF was used to identify the most significant variables for the model (Variable importance) in estimating depth from Manning, hydraulic conductivity and drainage capacity. Depth was estimated using the 3 independent variables and from this, their contribution towards flood depth was determined. The correlation plots for sub-catchment 1, 2 and 3 is at Figure 35.

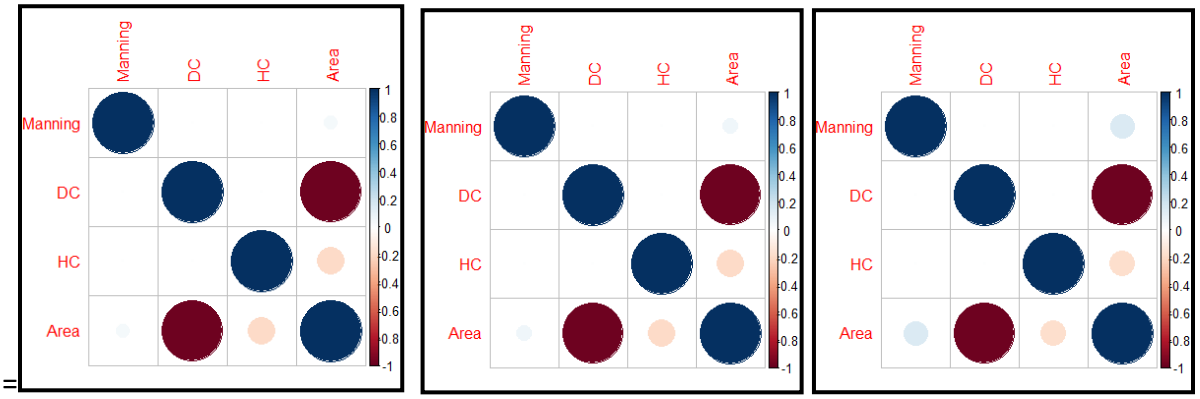


Figure 35: Correlation plots of Depth and model parameters for sub-catchments 1-3 (L-R)

6.2.4 Calibration using ROC Curve

Calibration of a hydrological model involves systematic tweaking model parameters in order to increase the predictive accuracy of a model (Unduche et al., 2018). For this research, model calibration was aimed at determining the best combination of model parameters that best represents the historical flood event that occurred on 8th July 2017 using ROC Curve. Due to the calibration data being just flood extent and the progression of the flooding wasn't documented, the comparison of flooded and non-flooded extent was embarked. The ROC Curve for the calibration of sub-catchments 1, 2 and 3 are at Figure 36, Figure 37 and Figure 38 respectively while the tables depicting the Boolean classification and the ROC Area under the Curve for the 3 sub-catchments is at Appendix F. From the ROC results, the optimal parameter was the first simulation parameter with values of Mannings, drainage capacity and hydraulic conductivity of 0.01, 0.24m/day and 0.001m/hr for the 3 sub-catchments.

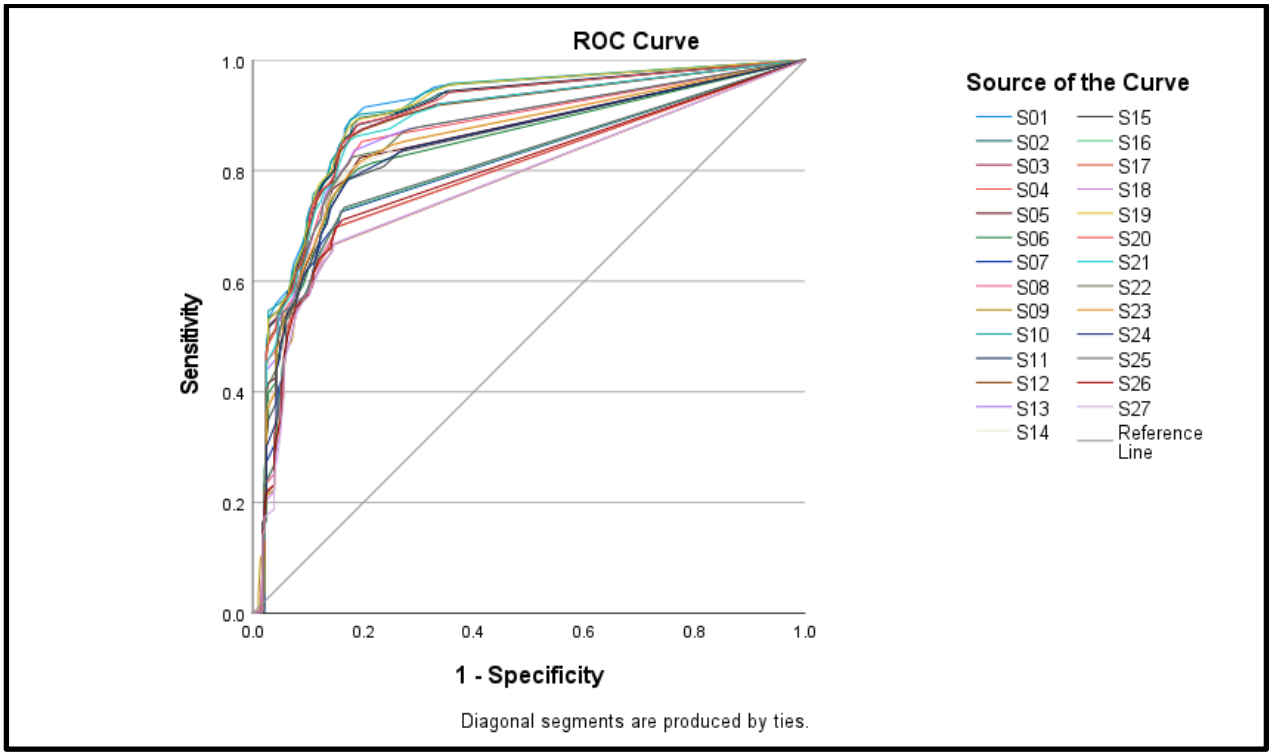


Figure 36: ROC Curve for sub-catchment 1

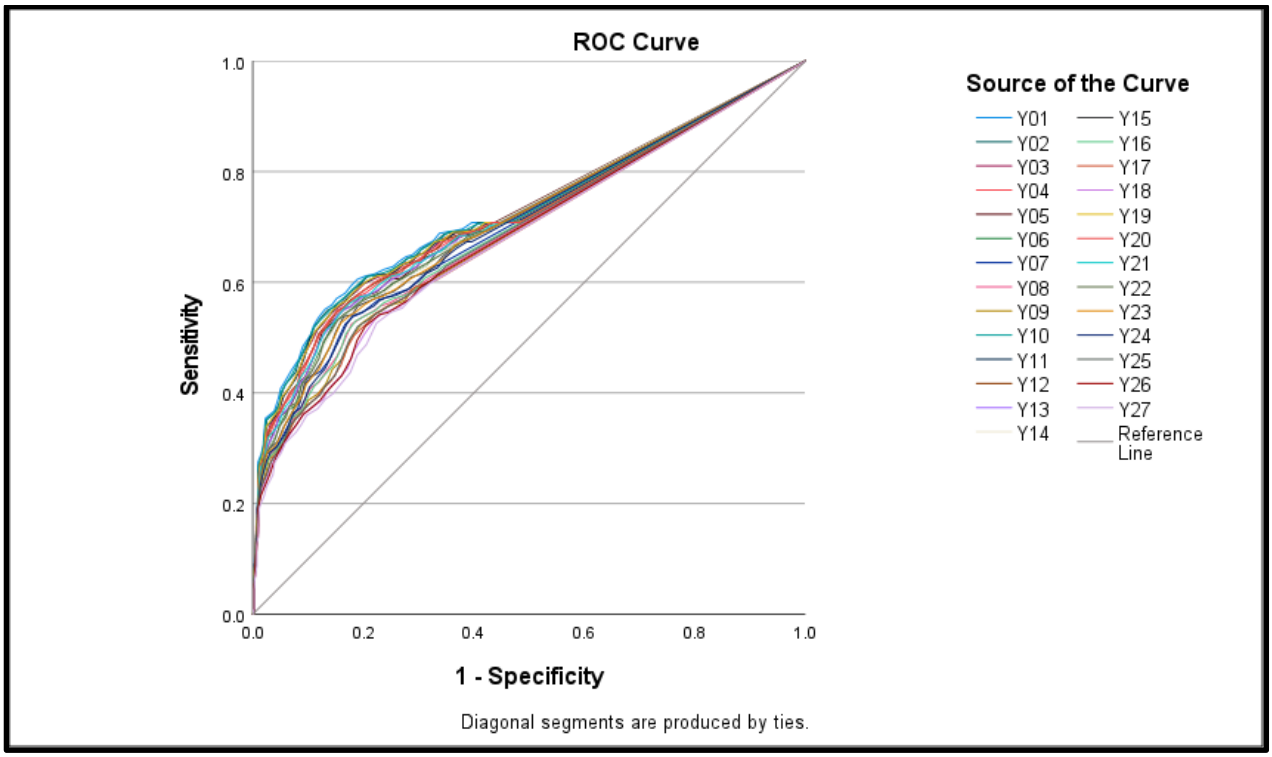


Figure 37: ROC Curve for sub-catchment 2.

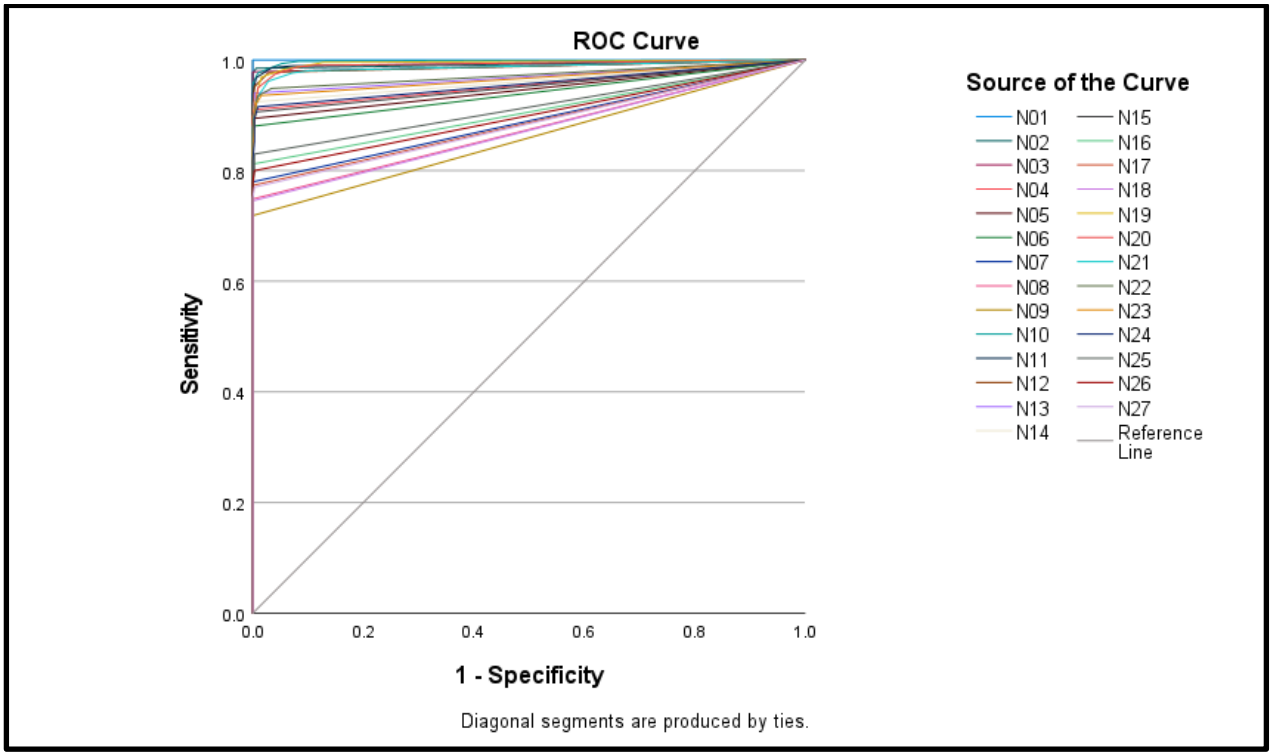


Figure 38: ROC Curve for sub-catchment 3.

6.2.5 Catchment area flood modelling using FloodMap.

The aim of calibrating a model is to be able to use defined parameter values to simulate a real-world process. Optimal parameter values were identified for both the FloodMap and CityCAT models at sub-catchment levels were used to replicate the historical flood event that occurred on 8th July 2017 at the entire catchment area. This was to save computational time and ensure the optimal parameter values were used to represent the catchment area. From the calibration of FloodMap parameter values as show in Table 14, the optimal parameter was the first simulation parameter with values of Mannings, drainage capacity and hydraulic conductivity of 0.01, 0.24m/day and 0.001m/hr. These parameters were used to simulate the historical flood event over the entire catchment area and the flood extent is at Figure 39. At the recreated flood stage point depths, the flood depth in relation to the observed flood depth is at Table 17.

Table 17: FloodMap simulated flood depth from the entire catchment area compared to the observed flood depth

Sub-Catchment	Observed flood (m)	Flood depth from entire catchment area (m)	Residual (m)
1.	0.7	0.64	0.06
2.	0.46	0.49	-0.03
3.	0.32	0.44	-0.12

Comparing the flood depth obtained using FloodMap to simulate the historical flood event and the flood depth obtained when trying to calibrate the parameter values at sub-catchment levels (Table 18) depicts a very interesting phenomenon which highlights the differences in modelling flood events at sub-catchment and catchment level.

Table 18: Comparison of FloodMap simulated flood depth from the 3 sub-catchment areas and the observed flood depth.

Sub-Catchment	Observed flood (m)	Flood depth from sub-catchment simulations (m)	Flood depth from entire catchment area (m)	Residual between sub-catchment and entire catchment(m)
1.	0.7	0.47	0.64	-0.17
2.	0.46	0.52	0.49	0.03
3.	0.32	0.47	0.44	0.03

Comparing the flood depths at the catchment and sub-catchment level using FloodMap as depicted in Table 18 shows that simulating the historical flood event at the catchment level gives a much better representation of the historical flood event when compared to the observed flood depth. This would be further explained in the comparison of the flood output in subsequent paragraphs.

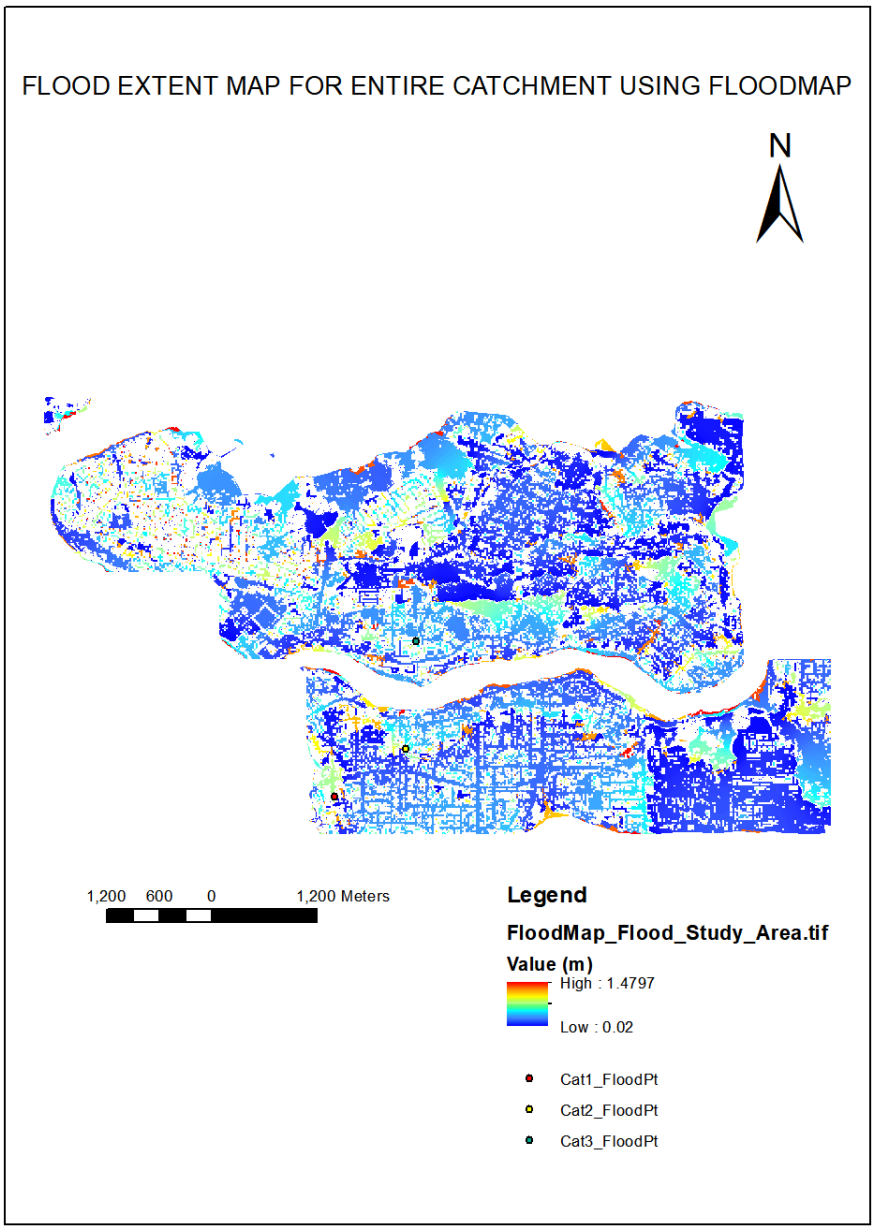


Figure 39: Flood depth for the entire catchment area using FloodMap.

6.3 Replicating historical flood event

Replicability of a flood model is its ability to produce consistent results over either different catchments or of different flood events. The ability of being able to replicate a flood event is vital in flood forecasting as it eliminates the need to undergo the process of certifying the modelling approach suitable for its application. For this research, the ability of FloodMap and CityCAT to replicate a second flood event that occurred on 19th October 2019 at sub-catchment 1 was embarked. The calibrated parameters were used for both models.

6.3.1 Replicating historical flood event using FloodMap

Another flood event which occurred on 19 October 2019 at sub-catchment 1, had an observed rainfall depth for that day of 89.3mm. The rainfall intensity for the period was obtained using the method outlined in section 3.3.3 and the rainfall intensity for the flood event is at Figure 40.

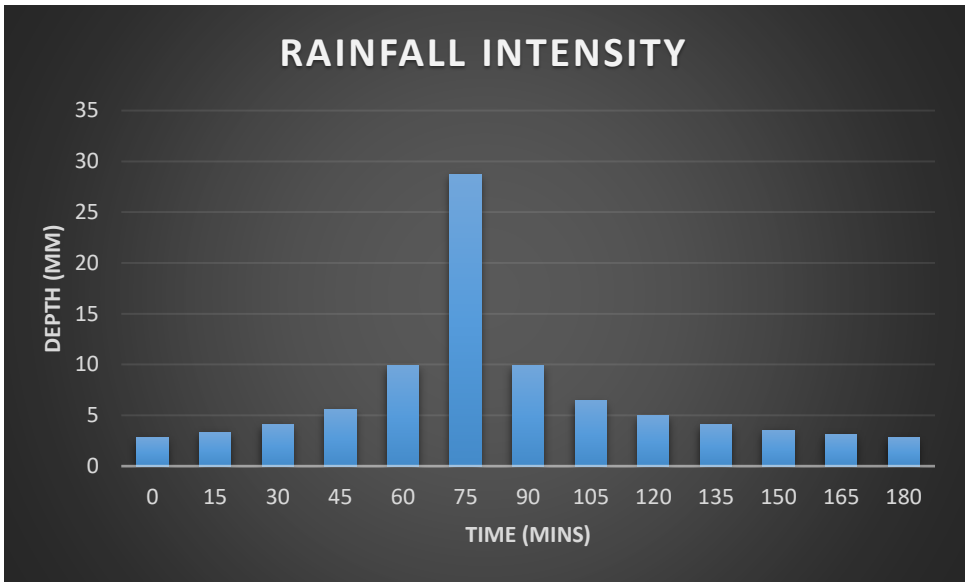


Figure 40: Rainfall intensity for 19th October 2019 for FloodMap

The rainfall depth was used to simulate inundation using the FloodMap model to determine if a different flood event could be replicated using the calibrated parameters for sub-catchment 1 as the flood event occurred within the same sub-catchment that we had calibrated parameter values for it.



Figure 41: Picture showing the tyres of a Toyota Highlander 2006 used to determine the depth of the flood

- Standard Toyota Highlander 2001-2006 model tyre configuration 225 70 R16
- From the picture, tyre diameter= 14 pixels; visible = 9 pixels; flood depth = 5cm)
- Tyre width = 225mm=25.5cm
-16 inch rim=40.64cm+25.5cm=66.14cm
- Width of one pixel = width of tyre/no of pixels=66.14/14 pixels= 4.7cm/pixel
- 5 Pixels = 4.7x5=23.5cm.

Flood depth was approximately = 0.24m

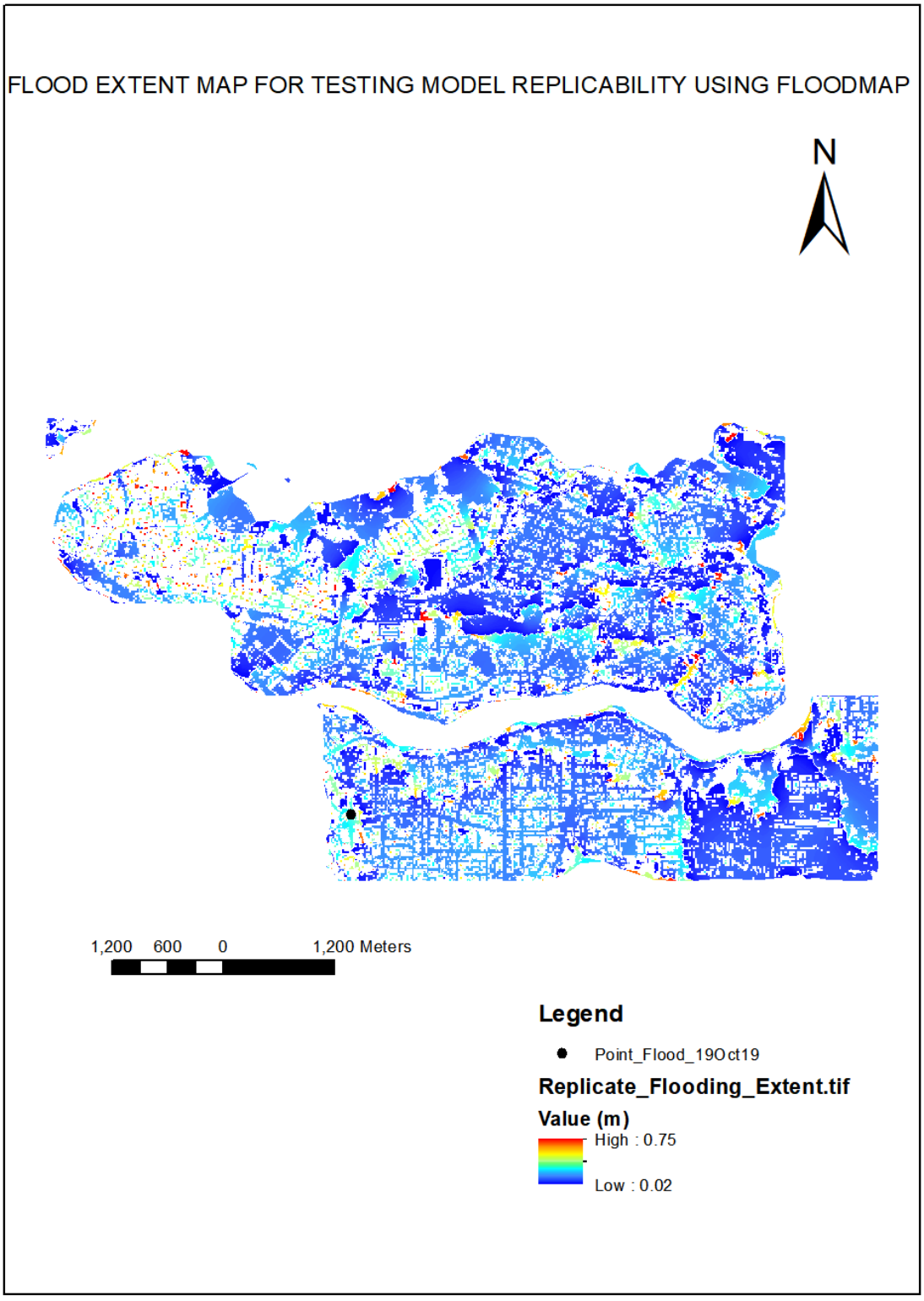


Figure 42: Map showing the flood depth for the 19th October 2019 flood simulation using FloodMap

The flood depth was 0.24m for the rainfall depth of 89.3mm for the flood stage point in sub-catchment 1 while the observed flood depth is 0.24m. The flood depth was able to accurately replicate the flood stage point that was recreated which shows the possibility of replicating the flood events using FloodMap within the study area.

6.4 Modelling Results for CityCAT

The modelling results for the 27 simulations using CityCAT were analysed for the 3 sub-catchments at their point depth and flood extent.

6.4.1 Validation Point Flood Depth for Sub-catchments

The point depth was obtained from the location where the flood stages were recreated, and this served as the validation data. The observed point depths for sub-catchments 1, 2 and 3 were 0.7m, 0.46m and 0.32m respectively. The results of the comparison of the flood depths from the validation data and the modelled flood extent is at Appendix F.

6.4.2 Validation Flood Extent for Sub-Catchments

The flood extents for sub-catchments 1, 2 and 3 were also recreated and served as the validation data. The flood extents for sub-catchments 1, 2 and 3 were 109,269 m^2, 367,202 m^2 and 369,857 m^2 respectively. The results of the comparison of the flood extents from the validation data and the modelled flood extent is at Appendix F.

6.4.3 Sensitivity Analysis

Determining the impact that alterations of parameter values will have on modelled flood output is vital in determining which parameters to use for modelling and the importance of each parameter value. Just like the FloodMap model, Random Forest was used to ascertain the sensitivity of the parameters used in the 3 sub-catchments in order to rank them in order of variable importance. The output here was the flood depth while the parameter values were Mannings-buildings, Mannings-vegetation and hydraulic conductivity. The outputs were then tested to determine their parameter value sensitivities in the three sub-catchments.

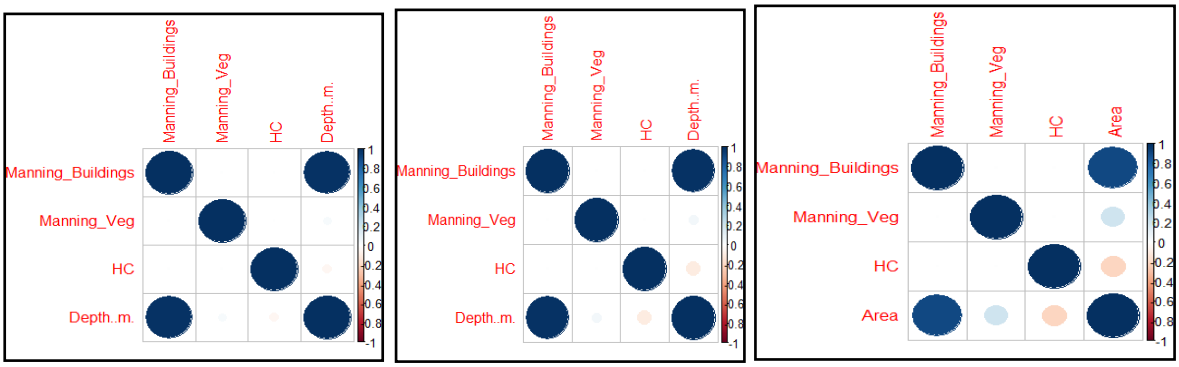


Figure 43: CityCAT Correlation plots of Depth and model parameters for sub-catchments 1-3 (L-R)

6.4.4 CityCAT Calibration using ROC Curve

CityCAT was also used for modelling the historical flood event that occurred on 8th July 2017 using ROC Curve and was also calibrated using ROC Curve. The ROC Curve for the calibration of sub-catchments 1, 2 and 3 are at Figures Figure 44, Figure 45 and Figure 46 respectively while the tables depicting the Boolean classification and the ROC Area under the Curve for the 3 sub-catchments is at Appendix F. From the ROC results, the optimal parameter was the third simulation parameters for the 3 sub-catchments with values of Mannings-buildings, Mannings-vegetation and hydraulic conductivity of 0.5, 0.25 and 0.001m/hr for the 3 sub-catchments.

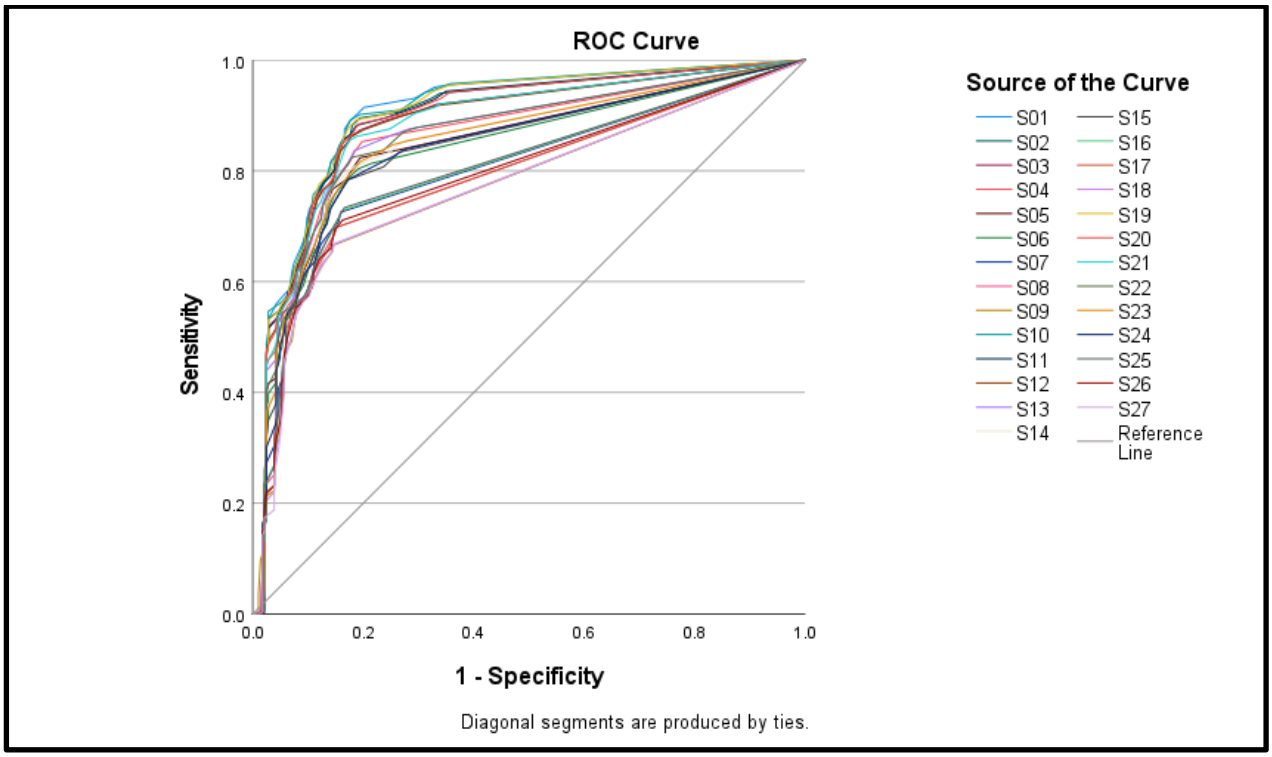


Figure 44: ROC Curve for sub-catchment 1.

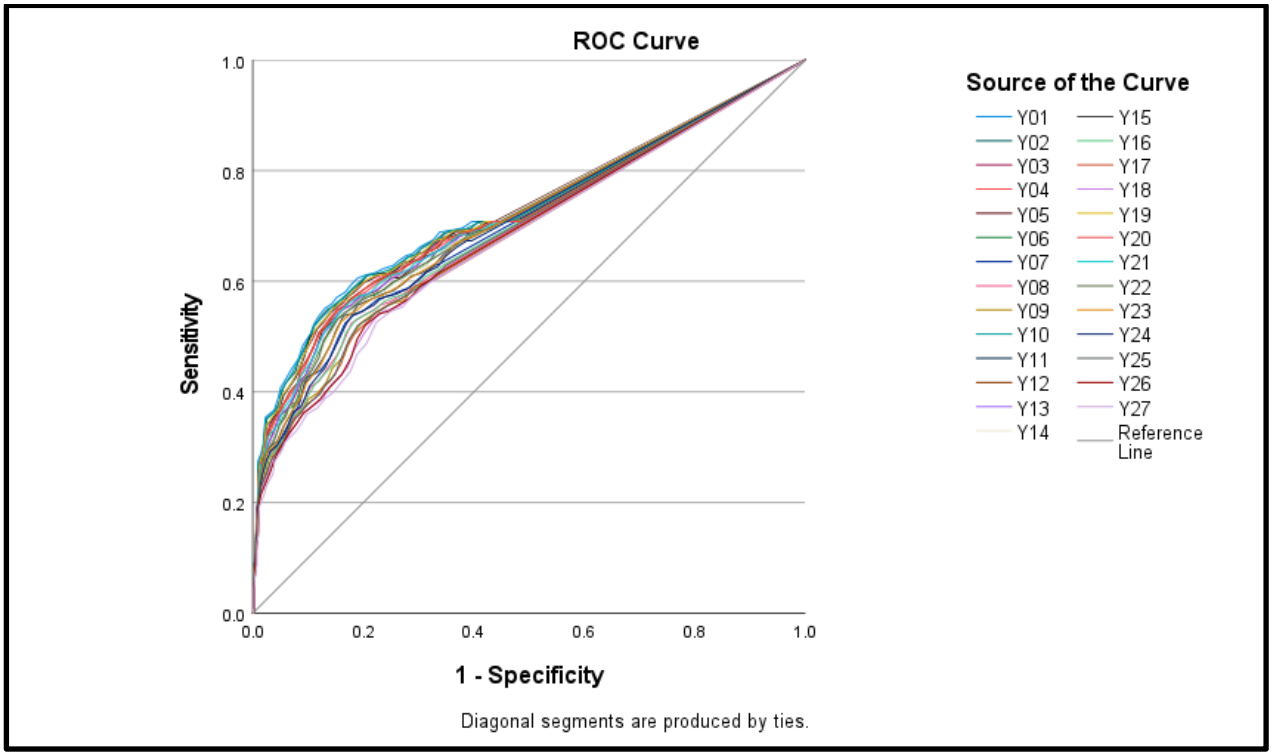


Figure 45: ROC Curve for sub-catchment 2.

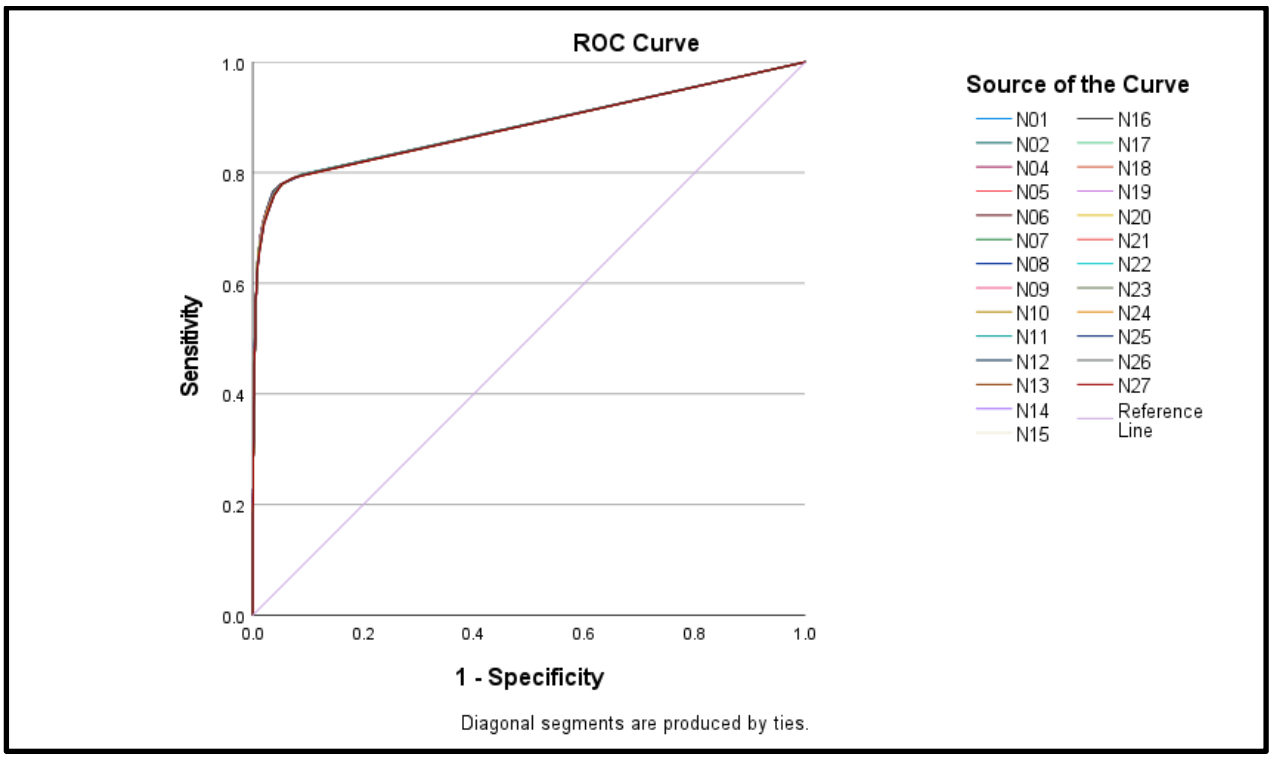


Figure 46: ROC Curve for sub-catchment 3.

6.4.5 Catchment area flood modelling using CityCAT

From the calibration of FloodMap parameter values as show in Table 18, the optimal parameter was the third simulation parameters for the 3 sub-catchments with values of Mannings-buildings, Mannings-vegetation and hydraulic conductivity of 0.5, 0.24 and 0.001m/hr. These were the parameters that were used to simulate the historical flood event over the entire catchment area using CityCAT and the flood extent is at Figure 47. The flood depth in relation to the observed flood depth is at Table 19.

Table 19: CityCAT simulated flood depth from the entire catchment area compared to the observed flood depth

Sub-Catchment	Observed flood (m)	Flood depth from entire catchment area (m)	Residual (m)
1.	0.7	0.27	0.43
2.	0.46	0.31	0.15
3.	0.32	0.19	0.13

Comparing the flood depth obtained using the CityCAT flood model to simulate the historical flood event and the flood depth obtained when trying to calibrate the parameter values at sub-catchment levels at Table 20, shows that the flood depths from both approaches was closely replicated less sub-catchment 1. A huge difference of 0.27m shows the uncertainty that may arise when using sub-catchments to represent flood forecasts and is further discussed in section 8.8.4.

Table 20: Comparison of CityCAT simulated flood depth from the 3 sub-catchment areas and the observed flood depth.

Sub-Catchment	Observed flood (m)	Flood depth from sub-catchment simulations (m)	Flood depth from entire catchment area (m)	Residual between sub-catchment and entire catchment(m)
1.	0.7	0.54	0.27	0.27
2.	0.46	0.3	0.31	-0.01
3.	0.32	0.21	0.19	0.02

The difference in the catchment and sub-catchment flood depth using the CityCAT model did not result in a significant difference compared to the results obtained from its FloodMap counterpart. Further assessment of the results was done in the comparison of results chapter in subsequent paragraphs.

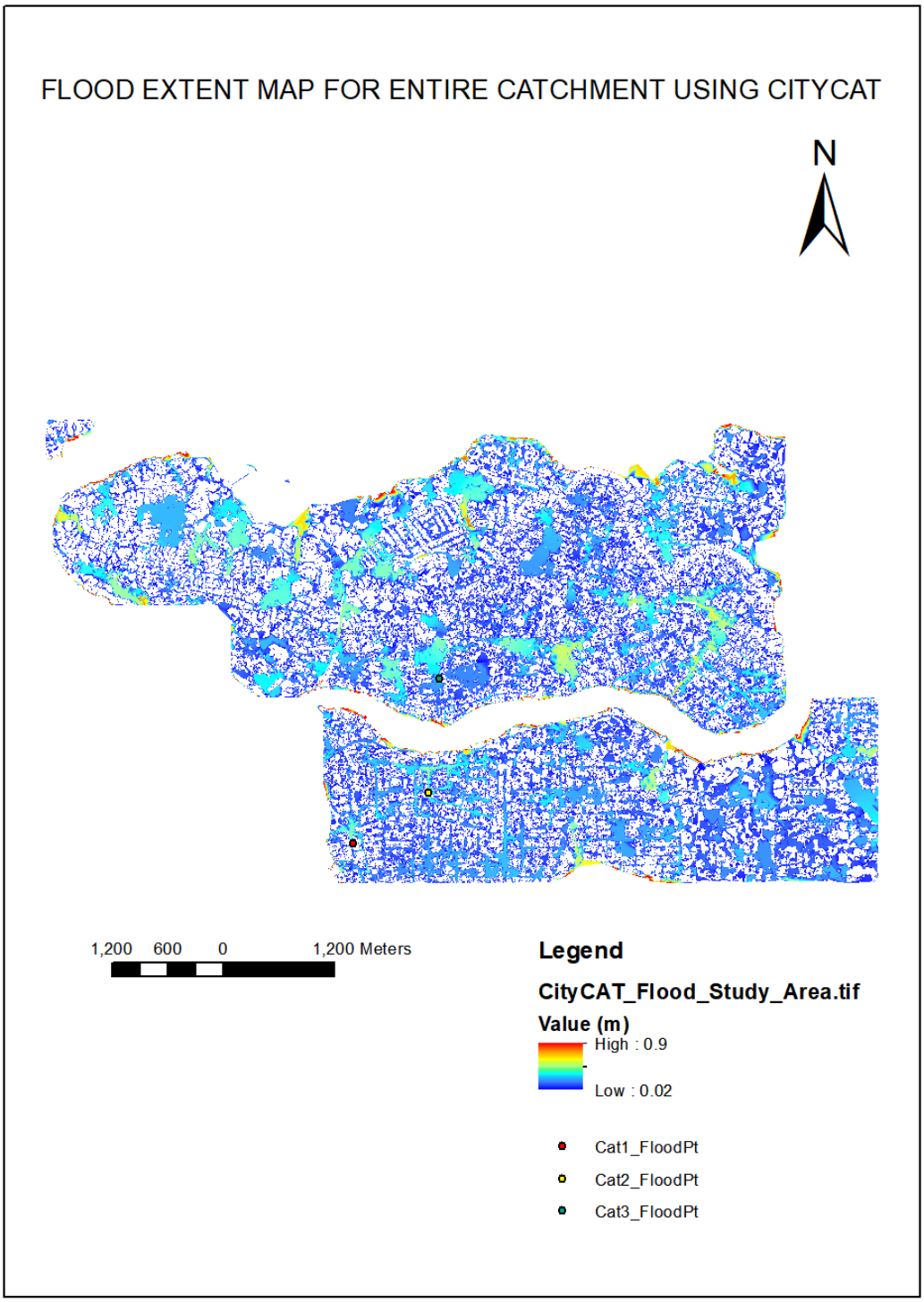


Figure 47: Flood depth for the entire catchment area using CityCAT

6.4.6 Replicating historical flood event

The CityCAT model was used to replicate the same flood event that occurred on 19th October 2019 using the rainfall intensity at Figure 48 and the flood extent simulated is at Figure 49.

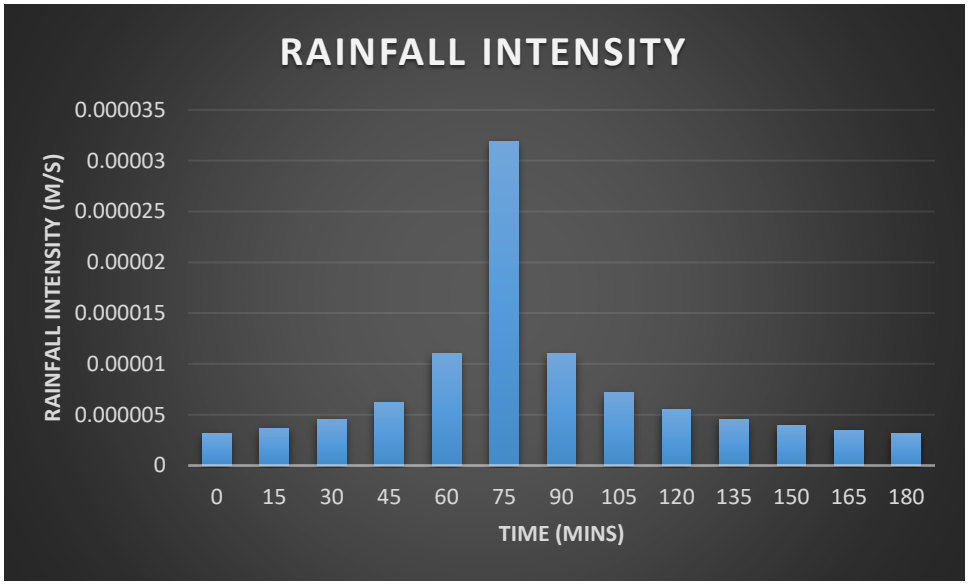


Figure 48: Rainfall intensity for 19th October 2019 for CityCAT

The flood depth was 0.22m for the rainfall depth of 89.3mm for the flood stage point in sub-catchment 1 while the observed flood depth is 0.24m. The flood depth was slightly under-predicted by 0.02m using CityCAT.

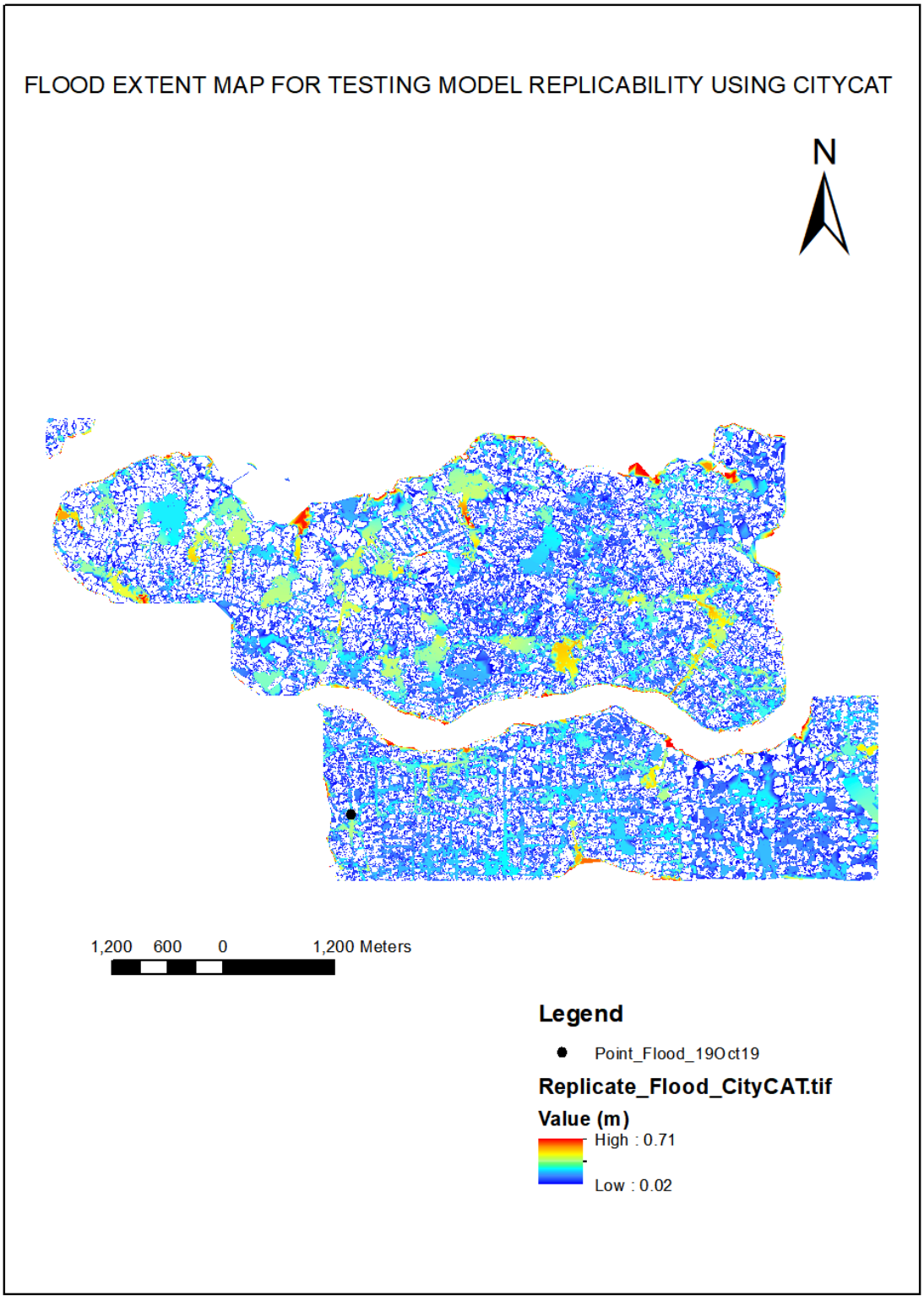


Figure 49: Map showing the flood depth for the 19th October 2019 flood simulation using CityCAT

6.5 Comparison of FloodMap and CityCAT modelling outputs

The modelling process plays a vital role in the driving flow routing process of a hydrological model. A comparison of some of the modelling processes of FloodMap and CityCAT are at Table 21.

Table 21: FloodMap and CityCAT modelling processes

Serial	Modelling process	FloodMap Hydro-Inundation 2D	CityCAT
1.	Code	Java/Python scripts	Delphi (Embarcadero)
2.	Computational power requirement	Computational power depends on catchment size and resolution	Programmable size of ~5mb with a hardware of 32 or 64bit CPU.
3.	Flow routing	Modified version of the inertia model of where the approach to calculate time step neglects the convective acceleration in the Saint-Vernant equation	Based on the shallow water equations where solution is obtained using the method of the finite volumes with shock-capturing schemes
4.	Infiltration	Flood losses via infiltration introduced using the Green-Ampt equation by allotting hydraulic conductivity values	Infiltration is also determined using the Green-Ampt equation where allotted hydraulic conductivity values are used to calculate flood loss
5.	Drainage	Drainage loss is accounted for by determining losses via drainage channels from total flood	Drainage loss accounted for by simulating losses from sewers and rainwater harvesting initiatives
6.	Evapotranspiration	Accounted for in mm/day	Not accounted for
7.	Buildings	Treated as either voids, elevated areas or allotted roughness values. Introduced into model as a DEM where building shapefiles are added to the DTM.	Treated as solid (no flow) boundaries. Can be extracted easily from OS MasterMaps or introduced from other softwares as shapefiles.
8.	Green areas	Introduced into model and allotted infiltration/ roughness values. Introduced as a layer with allotted infiltration and roughness values	Can be extracted from OS MasterMaps like buildings and allotted infiltration and roughness values as permeable surfaces.
9.	Rainfall	Inputted into model as rainfall intensity as uniform or distributed rainfall	Inputted into model as uniform rainfall
10.	Roughness	Roughness values introduced as Mannings coefficient which can either be as a distributed or uniform values	Roughness value introduced as Mannings coefficient for permeable or impermeable surfaces

The criteria generated in Chapter 2 section **Error! Reference source not found.** was used as the yardstick for the comparison of both models. The comparison of the two models focused on the resulting outputs from the simulations conducted and their ability to replicate the flood event that occurred on 8th July 2017.

6.5.1 Model parameterization

The ability to parameterize a flood model using available data to represent a historical flood event is a necessary requirement for flood forecasting (R. E. Emerton et al., 2016). In using parameters to test the validity of flood forecasts, an assessment of the parameterization process of FloodMap and CityCAT was embarked upon. The optimal parameters from the individual sub-catchments for both models were used to simulate the historical flood event for the entire study area in order to test how well the parameters from the sub-catchments represent the entire catchment area. As shown in Table 17 and Table 19 representing the adoption of parameter values for FloodMap and CityCAT respectively, it shows that FloodMap gave a good representation of sub-catchments 1 and 2 but slightly under-predicted Catchment 3 by 0.12m. CityCAT on the other hand under-predicted the flood depth in all the 3-stage points flood depth recreated for this study. The reason for the slight under-prediction of the flood depth by FloodMap in the third sub-catchment could be due to the use of a point flood depth to uniformly simulate precipitation over the study area. A variable rainfall intensity may have resulted in a better simulation of the rainfall event and over the entire catchment area.

6.5.2 Accuracy

The ability to replicate historical flood events with a high level of accuracy is vital as this will determine the reliability of the flood models to forecast flooding. From the calibration of both models using the ROC curve, the FloodMap model was able to better reproduce the historical flood event compared to CityCAT as shown in Table 22.

Table 22: Accuracy of simulated historical event of FloodMap and CityCAT

Sub-catchment	ROC Curve	Standard error	Asymptotic 95% confidence interval	Model
1	0.903	0.014	0.881-0.926	FloodMap
	0.765	0.014	0.738-0.792	CityCAT
2	0.872	0.01	0.853-0.891	FloodMap
	0.751	0.014	0.723-0.778	CityCAT
3	0.845	0.013	0.821-0.870	FloodMap
	0.675	0.017	0.641-0.709	CityCAT

The accuracy of the predictions was also evident when trying to replicate the entire catchment area using both models. FloodMap gave a better representation of the recreated stage points compared to CityCAT as shown in Table 17 and Table 19.

6.5.3 Reliability

The reliability of a flood forecast represents the lead period of a flood forecast and the certainty at which the forecast was made. Some vital things drive the reliability of a forecast which are the lead time at which a precipitation is made, the accuracy of such predictions and the time taken for a forecast to be generated by the appropriate FFWS and disseminated. A

FFWS loses it reliability if there is no sufficient lead period to reduce the impact of the flood hazard by responders and the population affected. As the FloodMap gave a more accurate representation of the historical flood event, it serves as a more reliable representation for flood forecasting for the catchment area.

6.5.4 Robustness

A robust FFWS refers to its ability to generate accurate results when the inputs are uncertain and how well the parameters interact including the parameters that influence the flood extent the most. The sensitivity analysis of FloodMap showed that Mannings had a weak direct relationship with flood depths in all the 3 sub-catchments. Furthermore, drainage capacity was the most significant driver of the model outputs in all the sub-catchments and displayed a very strong indirect relationship with flood depth. Hydraulic conductivity displayed a weak indirect relationship with flood depth in all the 3 sub-catchments. The consistency in the response of the parameter values to flood depth in the FloodMap model is encouraging and shows that the model can produce near consistent results from the parameter values when used in the catchment area. The sensitivity of CityCAT showed that Mannings buildings had a strong direct relationship with flood depth in all the 3 sub-catchments. Mannings vegetation showed a weak direct relationship with flood depth in all the 3 sub-catchments. Hydraulic conductivity on the other hand, had a weak indirect relationship with flood depth in all the 3 sub-catchments. Comparing the sensitivity analysis of the response of both models to Mannings, both models displayed a direct relationship with flood depth. This is significant as an increase in the opposition to flow posed by buildings results in an increase in flood depth and subsequently leads to flooding. The response to hydraulic conductivity of both models shows that they both exhibit an indirect relationship to flood depth. This is also significant as FDM approaches can be focused on increasing hydraulic conductivity in the catchment area by the use of green infrastructure and green roofs in order to reduce flooding within such catchments.

6.5.5 Replicability

Replicability of a flood model is its ability to produce consistent results over either different catchments or of different flood events. The ability of being able to replicate a flood event is vital in flood forecasting as it eliminates the need to undergo the process of certifying the modelling approach suitable for its application. For this research, the ability of FloodMap and CityCAT to replicate a second flood event that occurred on 19th October 2019 at sub-catchment 1 was embarked. The calibrated parameters were used for both models. The rainfall depth was used to simulate inundation using the FloodMap model to determine if a different flood event could be replicated using the calibrated parameters for sub-catchment 1 as the flood event occurred within the same sub-catchment that we had calibrated parameter values for it. The flood depth was 0.24m for the rainfall depth of 89.3mm for the flood stage point in sub-catchment 1 while the observed flood depth is 0.24m. The flood depth was able to accurately replicate the flood stage point that was recreated which shows the possibility of

replicating the flood events using FloodMap within the study area. The flood depth was 0.22m for the rainfall depth of 89.3mm for the flood stage point in sub-catchment 1 while the observed flood depth is 0.24m. The flood depth was slightly under-predicted by 0.02m using CityCAT.

6.5.6 Transferability

Transferability refers to the versatility of the FFWS and its interoperability across diverse temporal and spatial contexts for which its calibration was done. The calibration of the models was to determine if the parameter values from the sub-catchments can be calibrated and then these values are used to model the flood event for the entire catchment area. Transferring the calibrated parameter values to both the FloodMap and CityCAT models showed that the calibrated parameter for FloodMap could be easily transferred to the entire catchment area compared to the CityCAT calibrated parameters. Transferability can be observed between catchments and also the ability to replicate different flood events. Both models were able to replicate the flood event that was used for testing the replicability of a model. However, more research needs to be done to see how well the modelled parameters behaved in other catchments.

6.5.7 Simplicity

The simplicity of a model refers to the relative ease at of its operation and the ease of replicating it especially with uncertain data. From Table 21, in terms of the input data, FloodMap can be applied in its simplified form, and it was able to simulate the historical flood event with a degree of accuracy. The output generated by FloodMap is a flood extent map in ascii format that can be easily interoperable without the need to modify the results. The version of CityCAT used was the 'command prompt' where the input data needed to be in a specific format as the easily adoptable format that CityCAT recognises from OS Master Maps was not available for the study area. The input data had to be converted manually to CityCAT recognisable format using additional programs. The results were also in .rsl format and had to be converted to .tif using additional software programs. Overall, both models were simple to apply to a data sparse region, but FloodMap required no additional programs to modify input data neither did it require any software to modify its output.

6.5.8 Computational demand

The computational demand of a 2D model is overall high especially when working representing terrain at very high resolution and also when working on a large catchment area. Computational requirements of both models were similar. Both models successful ran using an 8GB RAM computer and also ran using a 32GB RAM computer. As with all 2D flood models, the smaller sub-catchments modelled the historical flood event faster than the larger sub-catchments. Both models had a similar run time and were able to generate results using an 8GB RAM. However, a system with a higher computational time will be better when a FFWS is going to be setup using any of the flood models.

6.6 Summary of Chapter 6

This chapter presented the results from the simulations conducted using the FloodMap and CityCAT models and the results were analysed using the criteria developed for testing the meaningfulness of flood forecasts in Chapter 2. The chapter also investigated how well calibrated model parameters from sub-catchments could be applied to the entire catchment areas. For FloodMap, the simulation parameter values (0.01, 0.24, 0.001) representing Mannings roughness, drainage capacity and hydraulic conductivity values respectively was the best predictor amongst the simulations for all the 3 sub-catchments. A sensitivity analysis of the parameter values revealed that drainage capacity had by far the greatest influence over modelled flood depth with an inverse relationship to flood depth. This shows that lower drainage capacity values would result in high flood depth and vice versa. Hydraulic conductivity was the next parameter that influenced the model where it had a weak inverse relationship with flood depth. This translates to lower hydraulic conductivity values resulting in more flooding. Mannings roughness had the lowest influence over the model, and it had a very weak direct relationship with flood depth, meaning an increase in manning resulting in an increase in flood depth. In comparing the FloodMap and CityCAT modelling results, both models displayed a direct relationship between Mannings values and flood depth except in Sub-catchment 1 using the CityCAT model. Hydraulic conductivity displayed an inverse relationship with flooding in both models. Both models responded adequately to parameter values showing that the models were working properly. The importance of the results shows that societies can plan FDM strategies and be able to test the impact these strategies can have on building their resilience to flooding. In testing the ability to utilize calibrated parameters at sub-catchment level to represent entire catchment areas, it was observed that some calibrated parameters gave a good representation of the flood event when used in modelling the entire catchment area. In the FloodMap model, sub-catchments 2 and 3 gave a good representation of the entire catchment area, however, sub-catchment 1 greatly under-predicted the flood event at the sub-catchment but gave a better representation at the catchment level. The CityCAT showed a similar response like FloodMap with sub-catchment 1 largely under-predicting the flood depth when modelled over the entire catchment using the calibrated parameters. The results showed that errors could emanate from the representation of flood extents using events modelled at sub-catchment level to represent the entire catchment area.

Chapter 7: Suitability of photogrammetric data from UAV for generating terrain data for flood modelling

7.1 Overview of Chapter 7

This chapter investigates the plausibility of generating a DTM from photogrammetry point clouds obtained from Unoccupied Aerial Vehicles (UAVs) to assess the suitability of the DTM generated for flood forecasting. The importance of UAV DTMs are due to the much cheaper alternatives of generating terrain data at high spatial resolutions compared to LiDAR DTMs. These UAV DTMs would also fill vital gaps created by unavailable terrain data especially in data sparse regions where the unavailability of resources hinders the generation of DTMs at high spatial resolutions. The methodology for this Chapter is in 4 stages. The first stage is the process of acquiring photogrammetry point clouds using a (Vertical take-off and landing) VTOL UAV including the generation of a DTM from the point cloud. The second stage is the comparison between the DTM generated using a UAV and the DTM that was initially generated from LiDAR data. The third stage is the conduct of hydrological modelling using the UAV DTM which was achieved by the FloodMap model as it gave a better representation of the historical flood event. A further comparison was made after using the DTM from the UAV to model the historical flood event that occurred on 8th July 2017 and the flood extent was compared with the flood extent generated using the DTM from the LiDAR data to simulate the same historical event which formed the fourth stage.

7.2 Introduction

The process of forecasting flood requires diverse data about the terrain, prediction of various atmospheric conditions as well as the use of suitably parameterized hydrological models (Solaimani, 2009). In driving effective FDM policies, the ability to forecast floods will serve as a vital tool in decision making regarding the adoption of favourable FRM policies. The inclusion of local communities in the process of enacting plausible FRM policies suffers setbacks as the funding for the implementation of these FRM originate from the national or state level (Mees et al., 2016) as is the case of Lagos State (study area focus of this thesis). The local community in flood prone areas have a lot of knowledge about the peculiarity of floods that occur in their communities including the perceived intensity and duration of the rainfall likely to cause flooding and their coping strategies. The availability of data is a major factor that prevents the inclusion of local communities in FDM policy generation, and this problem is exacerbated in areas plagued by data sparsity. In flood forecasting, terrain data is one of the most important datasets required and its accuracy will determine errors that could result from input data. Terrain data for the world can be obtained from databases such as Space Radar Topography Mission (SRTM) 30m resolution, Advanced Space-borne Thermal and Reflection Radiometer (Reduction) Global DEM of 90m resolution and Advanced Land Observing Satellite (ALOS) PALSAR DEM at 12.5m and 30m resolutions, amongst others. One characteristic of these freely available DTMs is their low spatial resolution which would be

useful in hydrology for global flood forecasting over large areas. However, for precision of flood simulation during point flood forecasting, DTMs of higher resolution are required as they can factor the effect buildings, roads, vegetation have on modelled flood output. In data sparse regions, DTMs pose a major problem when they have not been generated by the State. The freely available DTMs are usually of low spatial resolution which may not suit the high precision inundation flood simulation required for point flood inundation modelling as shown in Table 23. One approach to generate high resolution DTMs involves the use of LiDAR data (Chen et al., 2017; Pfeifer & Mandlburger, 2017) which is expensive to acquire. Other approaches to generate high resolution DTMs involve the use of high resolution imagery stacking (Dai et al., 2019; Shean et al., 2016; Takaku et al., 2014) which involves the use of imagery over the same location multiple times (usually from different passes) to generate DTMs. The constraint of this approach is that the images are usually not freely available and need to be purchased. UAVs pose an emerging field for data acquisition for diverse applications. The rising application of UAVs for diverse uses have seen their application extend to generating DTMs from overlapped imagery using methods such as structure-from-motion (SfM) for generating point clouds (Hashemi-Beni et al., 2018). The absence of data has prevented the justification of plausible FRM and also limited the participation of the local communities in driving FRM policies. This chapter therefore seeks to highlight the opportunities and fundamental constraints of embarking on plausible and sustainable means of acquiring data required to run precision hydrological models, specifically the use of UAVs for the generation of DTMs. The study intends to advance data acquisition methods to drive hydrological analysis for more effective FRM strategies for data sparse regions and encourage the participation of local communities in these FRM policy making. It is based on this premise that this chapter was undertaken.

Table 23: List of some freely available global DEMs

Serial	Dataset	Resolution (m)
1	ASTER GDEM	30
2	SRTM 1 arc-second	30
3	ALOS World 3D	30
4	EU-DEM	25
5	GMTED2010	30
6	MERIT DEM	90
7	Copernicus DEM	30
8	TanDEM-X	12
9	SRTM 3 arc-second	90
10	AW3D30	30
11	SRTMGL1	30
12	TDX90m	90
13	TDX30m	30
14	TDX12m	12
15	EarthEnv-DEM90	90
16	EarthEnv-DEM30	30
17	ALOS PALSAR	12.5

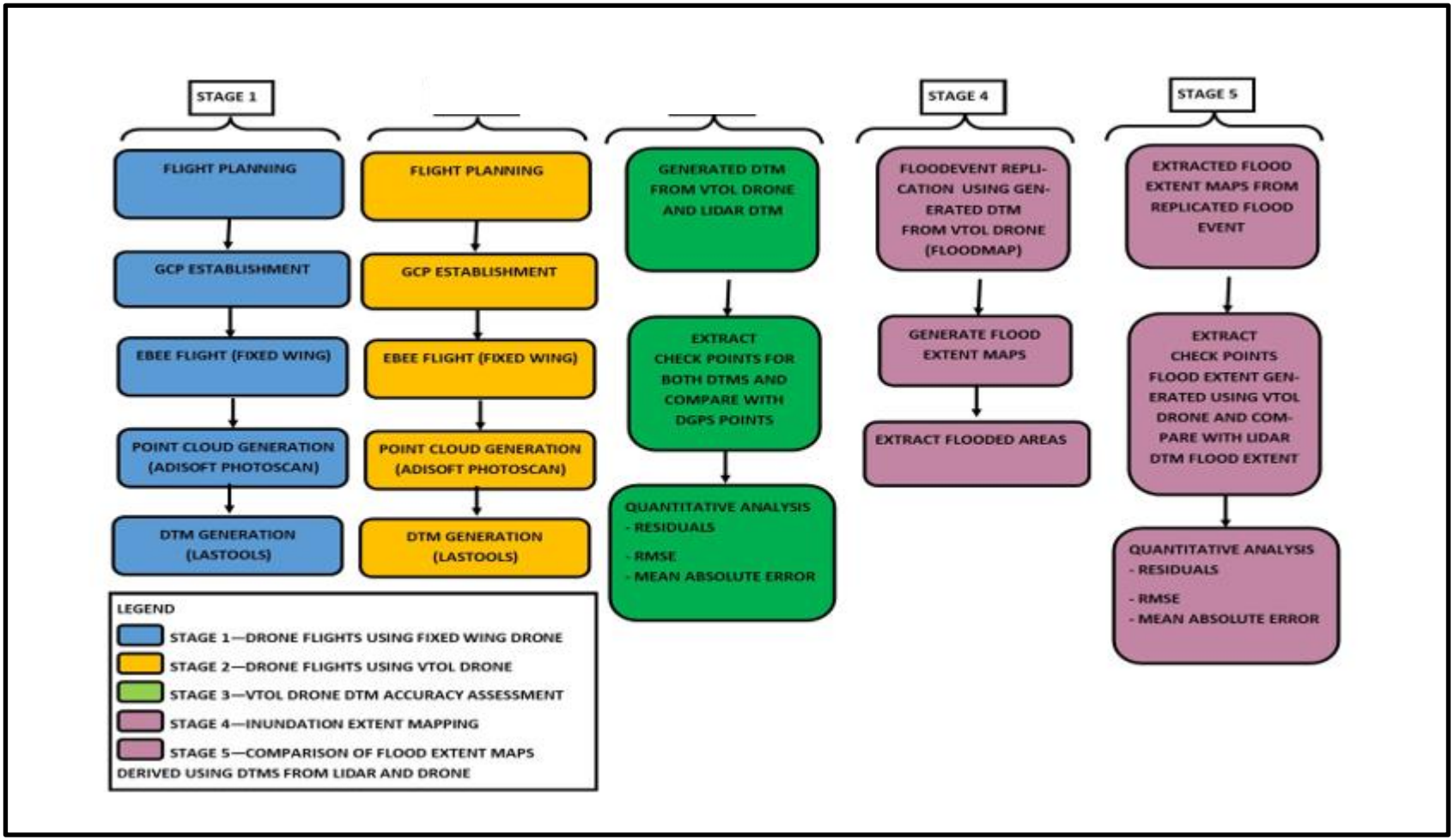


Figure 50: photogrammetric data from UAV for generating terrain data for flood modelling.

7.3 Photogrammetry point cloud acquisition using a vertical take-off and landing UAV

The procedure used for the acquisition of photogrammetry point clouds and the subsequent processing into a DTM for the 3 sub-catchment areas is at Figure 50.

7.3.1 Pre-flight assessment

The use of a quadcopter with the capability of taking off vertically and landing vertically was easier to engage in conducting photogrammetric studies in the built-up area. The take-off and landing sites could be almost anywhere within the sub-catchment areas. The selection of the day and time varied for the 3 locations in order to select a time that avoided adverse weather like rains and extreme winds.

7.3.2 Obtaining DGPS Points

DGPS positions were obtained for each of the sub-catchments that were used for check and control points when generating the DTM just like the fixed-wing UAV. Due to the area being built-up, DGPS points were marked on road and culverts. The distribution of the DGPS locations within the sub-catchments is at Figure 51.

7.3.3 UAV flights

The best time for UAV flights over an area is at noon (Keyvanfar et al., 2021) with air temperature, speed of the wind, rainfall amongst other atmospheric conditions that affect the UAV performance (Gao et al., 2021). However, other prevailing atmospheric conditions may prompt UAV flight to be conducted during other times that guarantee better weather conditions (Metzakis, 2019). The UAV flight was conducted at sub-catchment 1 at around noon on 21st September 2019 and consisted of 437 images. The flight over the sub-catchment 2 was conducted at around 9am on 29th December 2019 with 112 images while the flight over sub-catchment 3 was conducted on 9th December 2019 and had 516 images. The flights for the other sub-catchments 2 and 3 were conducted at times devoid of precipitation and at wind speeds that permitted the use of the VTOL Quadcopter.

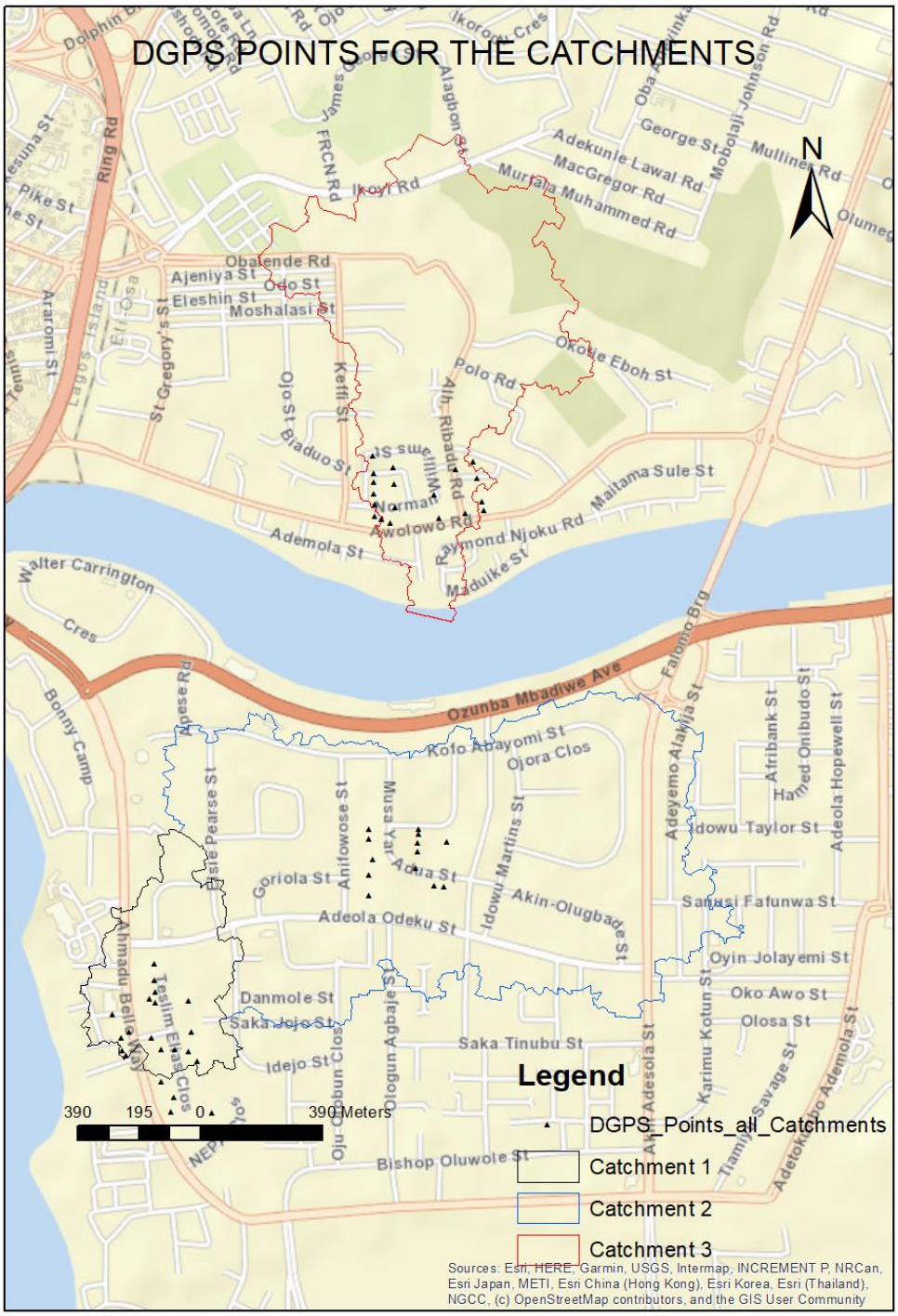


Figure 51: Location of DGPS in the various Sub-catchments

7.4 Processing UAV imagery using Pix 4D

7.4.1 Alignment of photos and quality assessment

Alignment of images is part of structure-from-motion (SfM) imaging technique where overlapping photos taken digitally from different positions relative to a location have their common points in the photos matched (Meijer, 2015). The alignment phase plays a large role in determining the final accuracy of the product and ensures that the quality of the images suit further processing. The quality of a photograph depends on photos that are sharp, well exposed, well distributed over the target and at right angles to the target location (Meijer, 2015). The alignment and quality assessment of the image quality for the 3 sub-catchments was done using Pix4D. Alignment of photos was performed on all 3 sub-catchments where sub-catchments 1, 2 and 3 had 412, 112 and 534 images respectively. All the images had picture qualities greater than 0.5 and they were all used for the point cloud generation. Picture quality < 0.5 would have been deleted as these pictures affects alignment and reduce the overall quality of the mosaicked image.

7.4.2 Building photogrammetry point cloud

The process of generating photogrammetry point clouds involves the generation of a sparse point cloud which is then used to generate the dense point cloud. The GCP's were used to enhance the geolocation of the DTM being generated and was applied to the 3 sub-catchments. Sparse point clouds are applied to determine which image pairs overlap by possessing sufficient number of common tie points (Xu et al., 2014). The sparse point cloud was then used to generate a high-quality dense cloud which was then exported for

7.4.3 DTM Extraction from photogrammetry point cloud data using LAStools

The procedure outlined in (Polat & Uysal, 2017) was used for the DTM generation where the ground-points were first identified and then triangulated across the entire area covered by the UAV. The process of generating the point clouds was achieved using LAStools which is a software that uses robust algorithms to perform diverse functions on point clouds. The advantage of using LAStools is that in generating the final DTM, the software uses Delaunay triangulation which has been shown to give the best description of surface morphology in relation to the generation of triangulated irregular networks (Tsai, 1993). The LASinfo report for the point clouds confirmed that sub-catchments 1, 2 and 3 had a total of 52,711,038, 17,753,704 and 44,694,060 points respectively. The process of generating a suitable DTM involves creating buffers to split the points into smaller segments for ease of manipulation, then the points are classified, noise removed and finally the triangulation of the ground points across extraneous surfaces to generate the DTM.

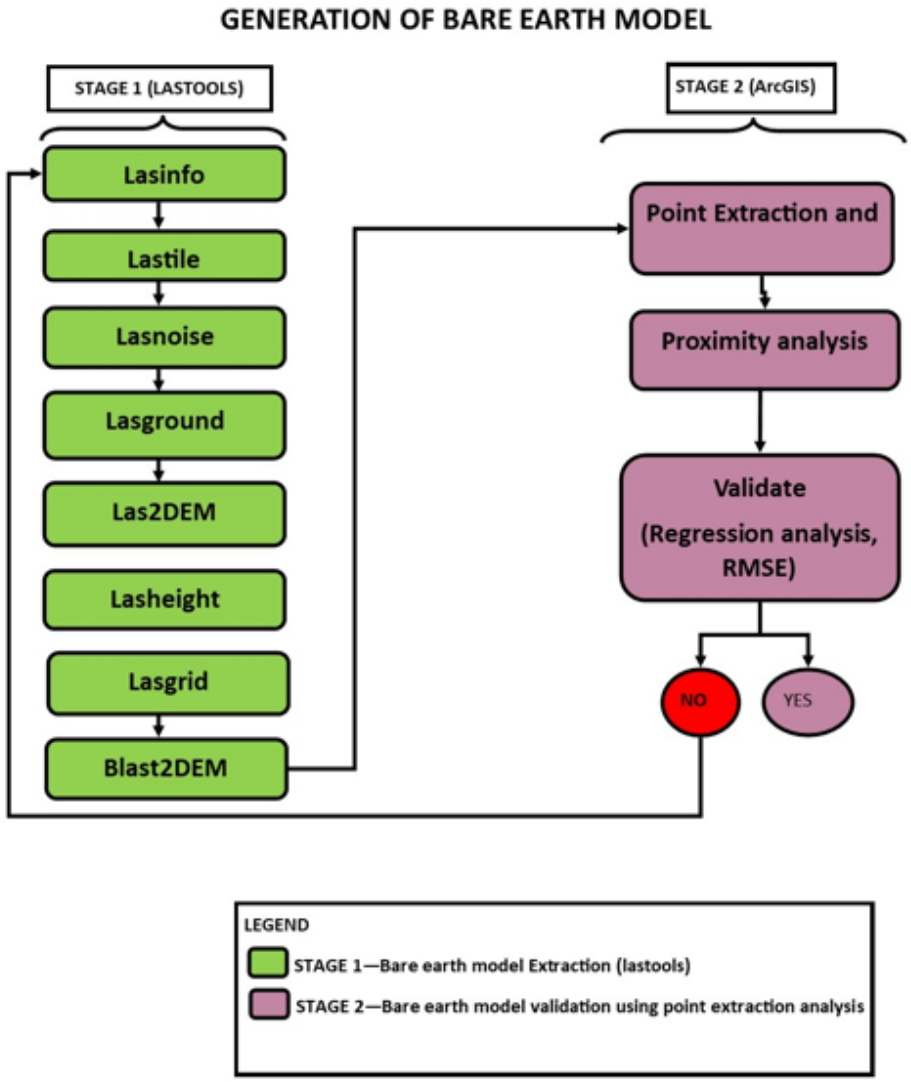


Figure 52: Process for DTM extraction and validation

7.4.4 Tiling of point clouds.

The point clouds were tiled using LAStile into smaller splines of 200x200m for ease of the algorithms processing them (Sithole & Vosselman, 2004) to ensure the interpolations between points effectively extracted buildings and other artefacts. A buffer of 50 metres was introduced around the tiles and the buffer points were flagged as withheld so that they can be easily merged together when generating the DTM.

7.4.5 Classifying noise.

Noise is usually generated during the generation of point clouds which results in errors during classification of the point cloud. A good cleanup algorithm should be able to denoise and preserve the features of the terrain (Rakotosaona et al., 2020). Lasthin was used to classify all points as code 8 that lie closest to the 50^{th} percentile in elevation within every 50cm-by-50cm cell provided the cells contained at least 20 points. This was to ensure outliers and artefacts were classified as noise.

7.4.6 Classifying ground and non-ground points.

Lasground is a lastool algorithm used to classify ground points into class 2 and non-ground points into class 1 which is vital for bare earth extraction. The ground points were subsequently triangulated to eliminate extraneous objects and generate a bare earth model using Delaunay Triangulation. The classification code 8 was ignored, and a custom classification was used with a step size of 50m since the area is an urban area to interpolate across buildings. A bulge parameter of 0.5 was used to eliminate extraneous objects like buildings, cars, low walls etc. A low threshold was set for incident and reflected pulse to ensure only ground points were classified by setting a spike of 0.5.

7.4.7 Ground point extracting.

Las2dem creates a DEM from las data. The command “keep classification 2” was used to ensure only ground points were used generate a bare earth model. A step size of 1 for a 1m resolution and an interpolation across large buildings set by a kill triangle command of 200 to ensure triangles with edges longer than 100m are not rasterized. A tile bounding box was used to ensure that the entire scene can be successfully mosaicked. Lasheight was used to further smoothen the bare earth model to be generated by classifying as ground points, all points that fall within a certain distance of the triangulated surface. A 5cm distance vertically below and a 15 cm distance vertically above was used to further classify these points as classification 2 (ground).

7.4.8 DTM generation.

Blast2dem triangulates points into a TIN using the Delaunay triangulation. A step size of 2 representing the resolution was used and the entire dataset was merged to produce a tif output as shown in Figure 53, Figure 54 and Figure 55 representing the DTMs for sub-catchments 1, 2 and 3 respectively.

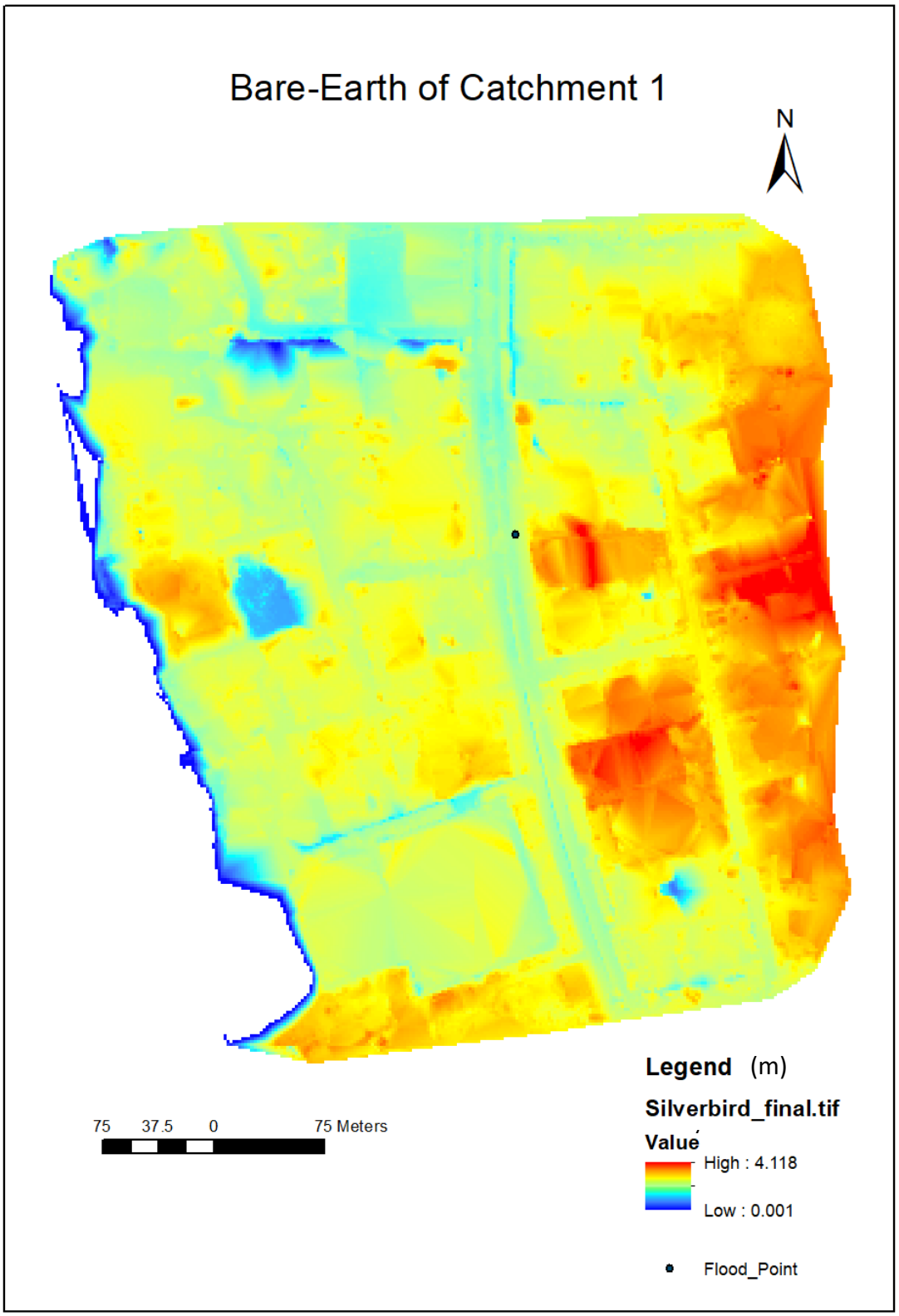


Figure 53: DTM of sub-catchment 1

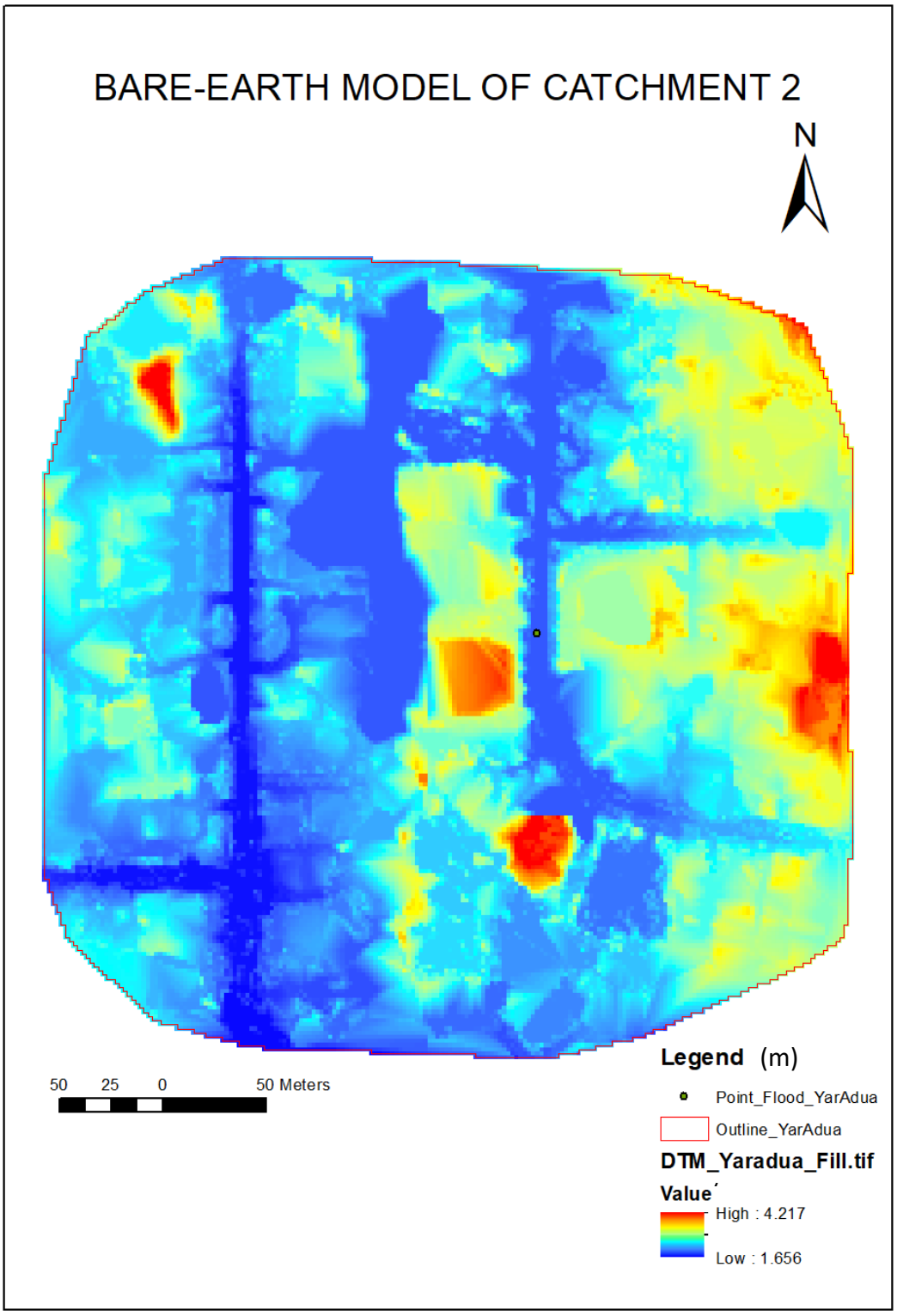


Figure 54: DTM of sub-catchment 2

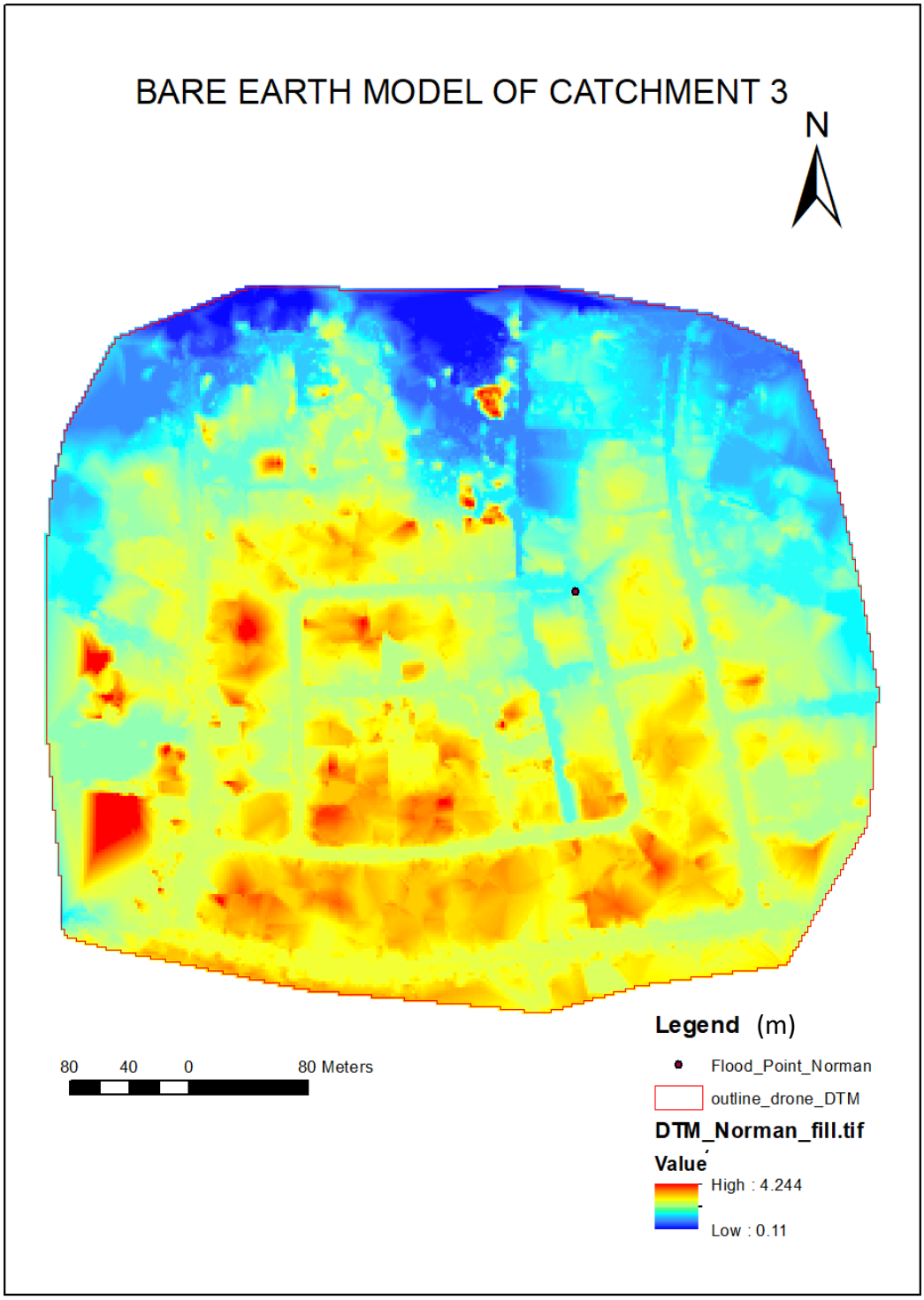


Figure 55: DTM of sub-catchment 3

7.4.9 Accuracy assessment of DTMs generated using UAV imagery

The accuracy assessment of the DTMs generated using imagery from UAVs was done by determining their horizontal accuracy, specifically by comparing the DGPS heights with the elevation from the generated DTMs. The horizontal accuracy of the bare earth model was subsequently obtained using the extraction point method in Figure 52 and compared against the DGPS control points. For sub-catchment 1, the RMSE and MAE was 0.098 and 0.077 as shown in Figure 56. The RMSE and MAE for sub-catchment 2 was 0.212 and 0.17 see Figure 57. For sub-catchment 3, the RMSE are MAE was 0.203 and 0.17 as shown in Figure 58. The low RMSE and MAE values for the 3 sub-catchments indicates that the UAV derived DTM is a good measure of fit compared to the DGPS points and appropriately represents the terrain.

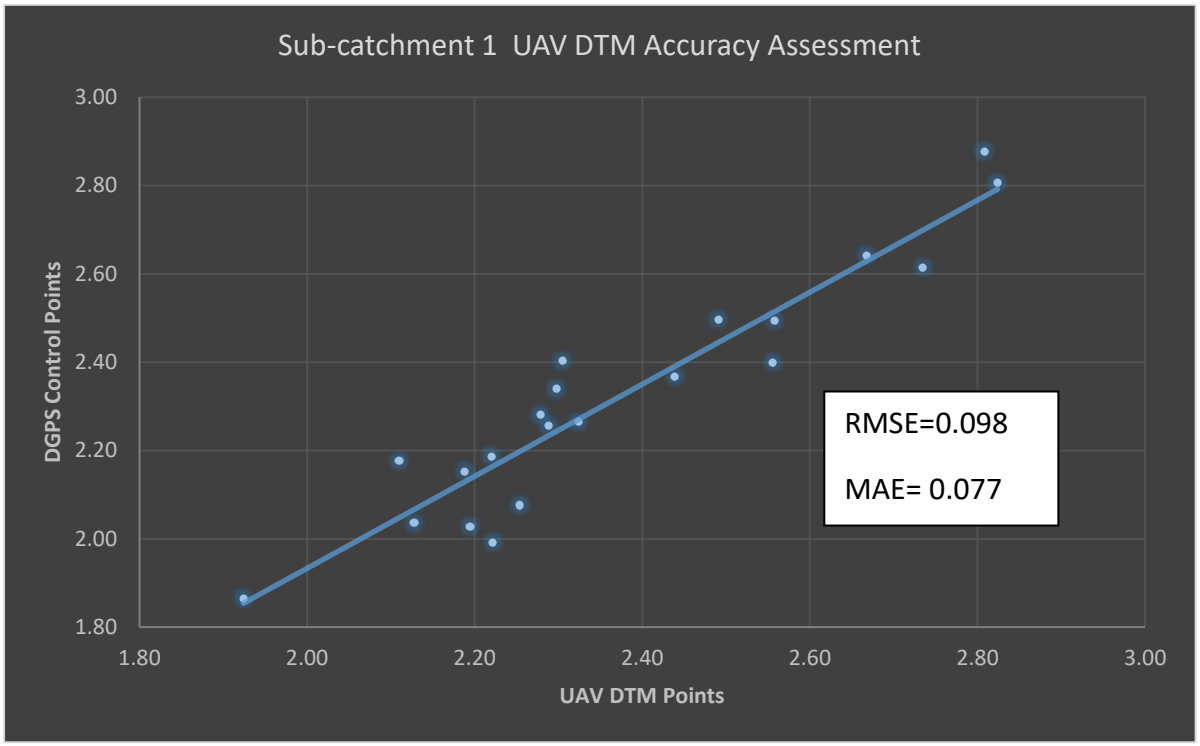


Figure 56: RMSE and MAE for the assessment of the accuracy of the DTM for sub-catchment 1

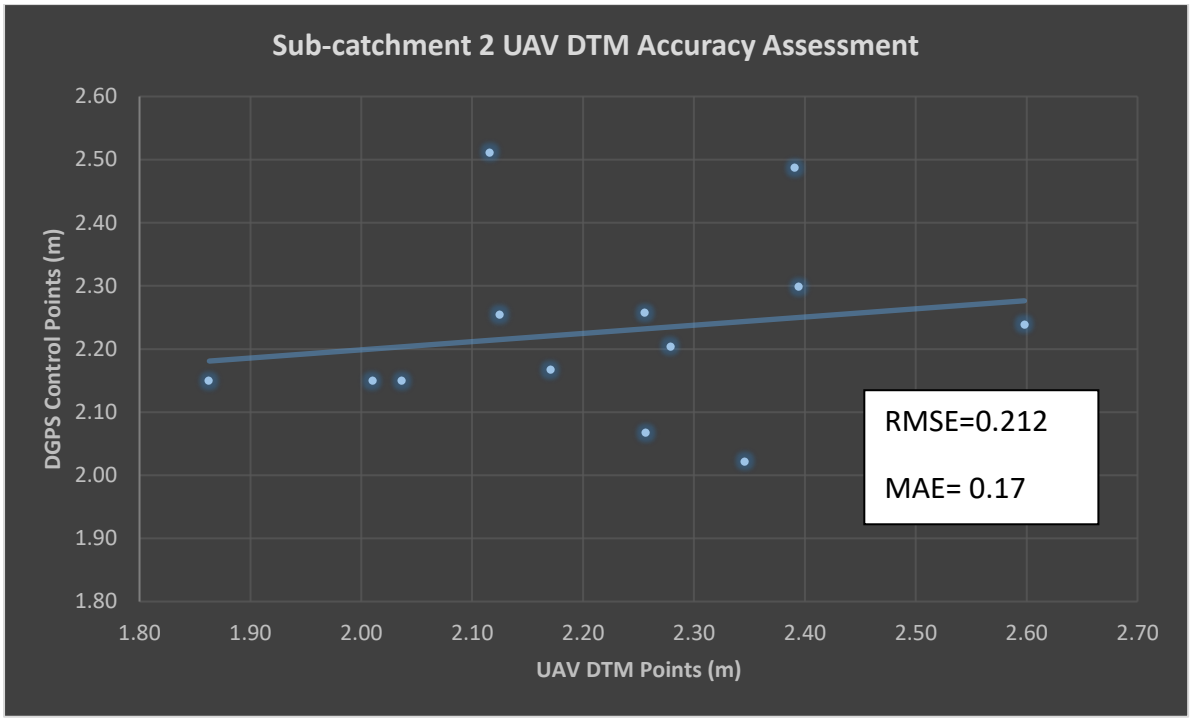


Figure 57: RMSE and MAE for the assessment of the accuracy of the DTM for sub-catchment 2.

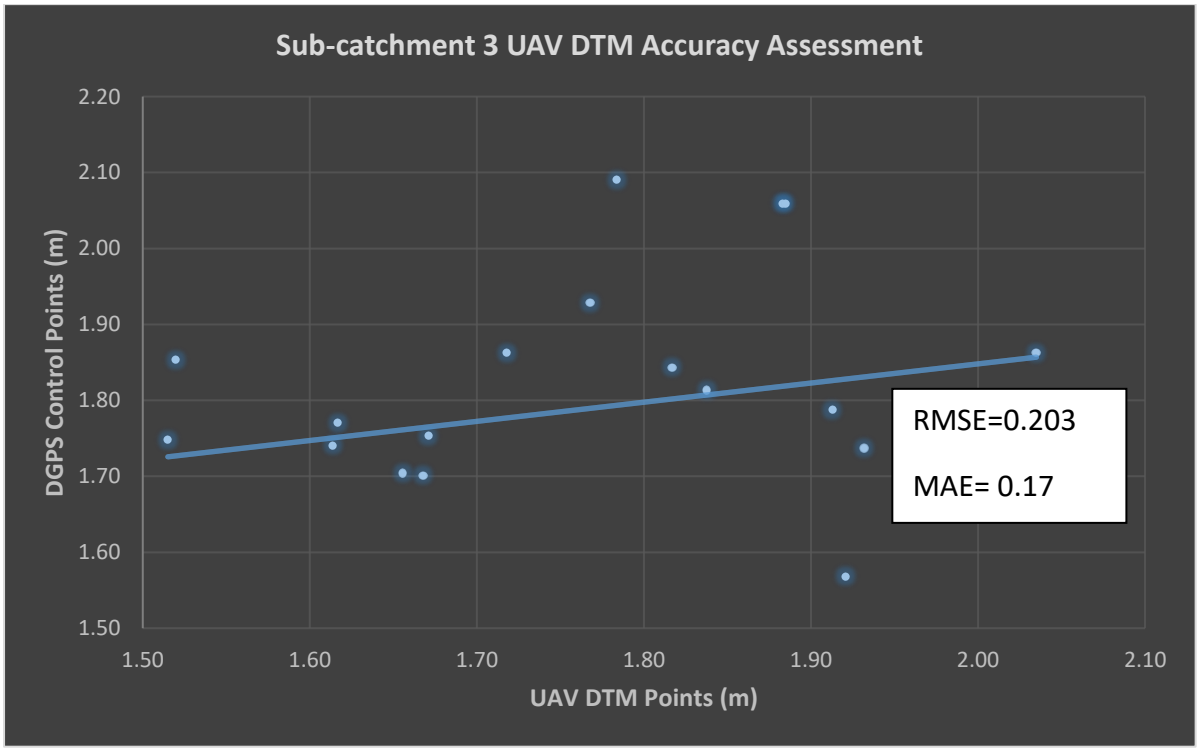


Figure 58: RMSE and MAE for the assessment of the accuracy of the DTM for sub-catchment 3.



Figure 59: Map of catchments showing areas the UAV DTMs intersect in the 3 catchments.

7.5 Comparison of DTMs generated using UAV photogrammetry and LiDAR

The acquisition of LiDAR data is still quite expensive compared to data from UAVs which are more available, cheaper and easier to use (Serifoglu Yilmaz & Gungor, 2018). Comparing the output of the DTM generated using LiDAR and UAVs was used to confirm the reliability of generating DTM from UAVs in an urbanized, densely populated data sparse region. The approach from Figure 52 was used for the comparison where the elevation of extracted points from the LiDAR DTM was compared against the same points extracted from the UAV DTM. The RMSE and mean absolute error (MAE) were computed and used for the comparison of both DTMs. The MAE was computed using the DTM from LiDAR as the true value and the UAV DTM as the observed value. For sub-catchment 1, the RMSE and MAE was generated and was 0.319 and 0.233 respectively as shown in Figure 60. This means that on average, the UAV derived DTM's elevation difference from that of the LiDAR DTM was 0.233m. The RMSE of the UAV derived DTM and that of the LiDAR DTM was 0.319. The RMSE tells us the average difference between the observed and the predicted values. For Sub-catchment 2, the RMSE and MAE was 0.354 and 0.287 respectively as shown in the line chart at Figure 61. The RMSE and MAE for Sub-catchment 3 was 0.336 and 0.271 as shown in Figure 62. From the RMSE and MAE for the sub-catchments, the DTMs gave a good representation when compared to the LiDAR DTM.

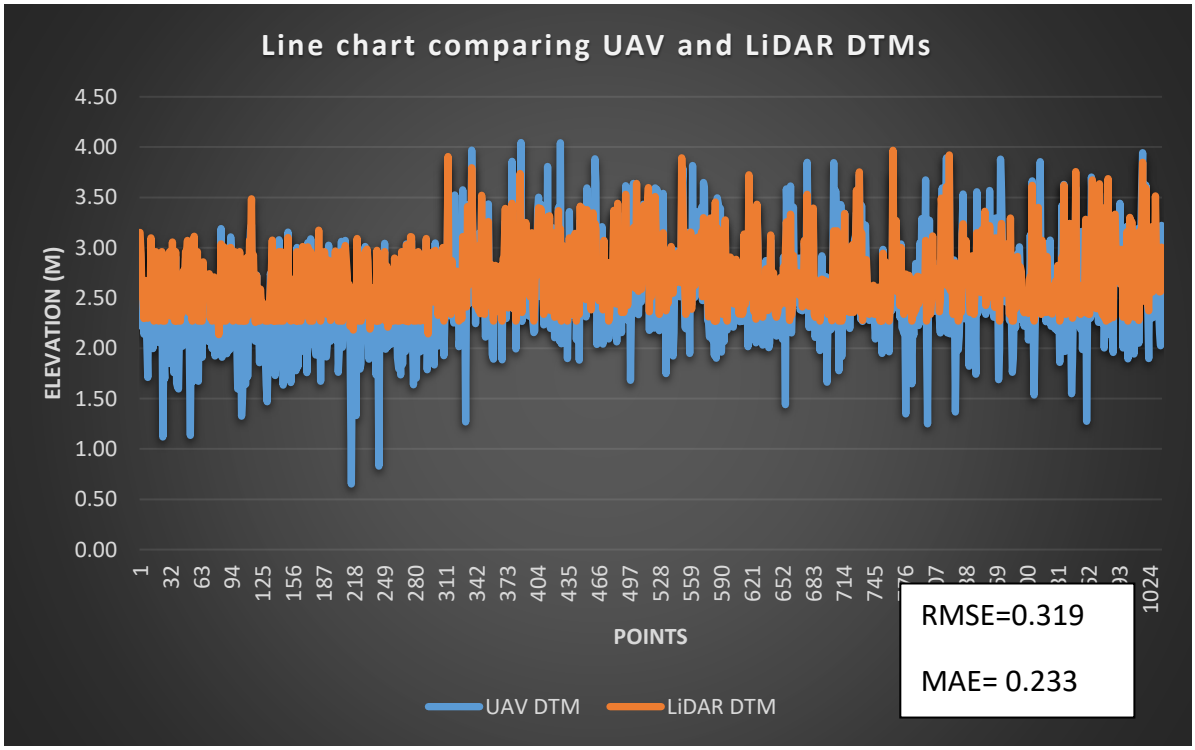


Figure 60: Line chart for the comparison of UAV and LiDAR DTMs for sub-catchment 1 depicting their RMSE and MAE

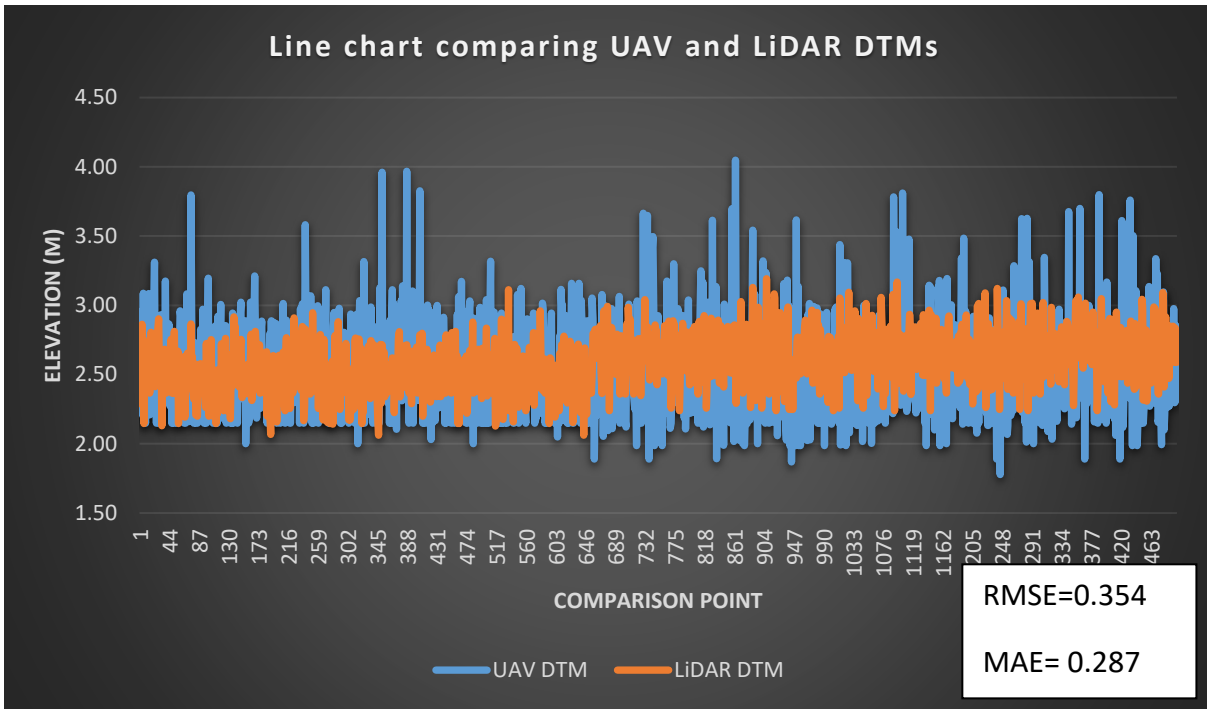


Figure 61: Line chart for the comparison of UAV and LiDAR DTMs for sub-catchment 2 depicting their RMSE and MAE

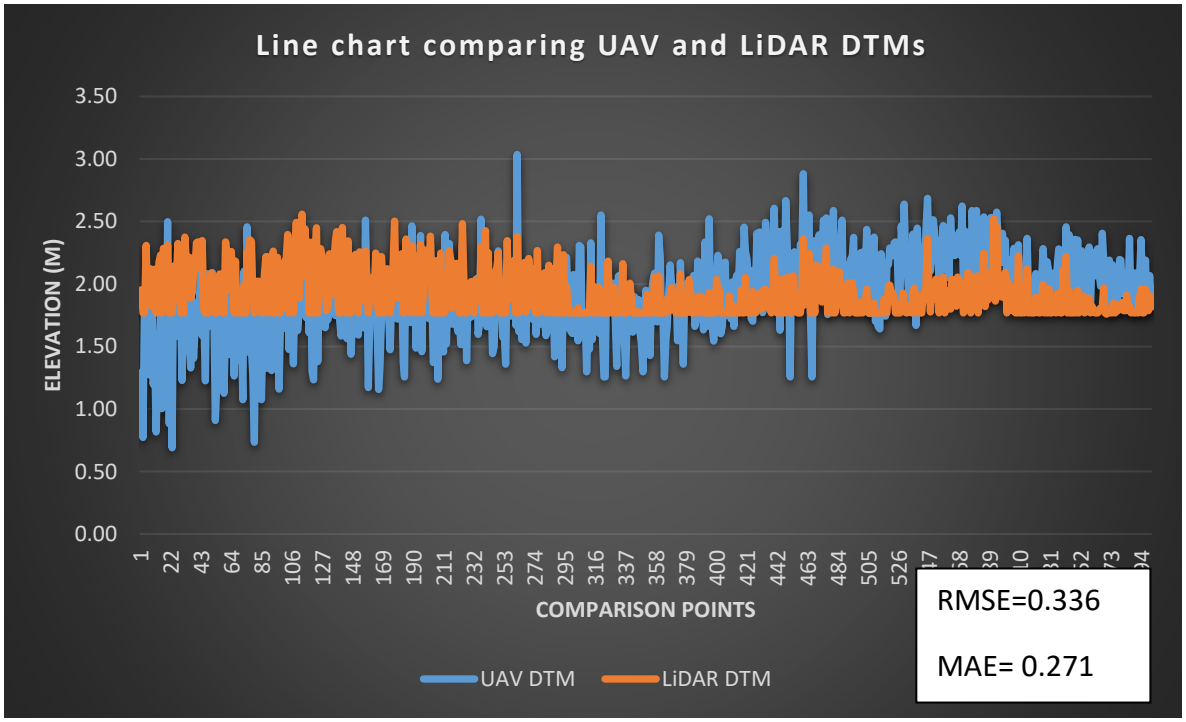


Figure 62: Line chart for the comparison of UAV and LiDAR DTMs for sub-catchment 3 depicting their RMSE and MAE

7.6 Flood Modelling using UAV generated DTMs

FloodMap was used to replicate the flood event that occurred on 8th July 2017 using the UAV DTM because the model gave a better representation of the flood event that occurred on 8th July 2017 when compared to CityCAT. This was done using the calibrated parameter values of (0.01, 0.24, 0.001) representing Mannings, drainage capacity and hydraulic conductivity values respectively for all the sub-catchments. The DTM used was the one generated using the UAV DTM and the rainfall intensity previously used. The flood extent of the simulation of the 8th July 2017 flood events for sub-catchments 1, 2 and 3 are at Figure 64, Figure 65 and Figure 66 respectively. The point flood depth for sub-catchment 1 was 0.45m while the point flood depth obtained by simulating using the LiDAR DTM and the same parameter values as this one was 0.47m. The difference in the point flood depth was 0.02m or 2cm. This shows that the DTM generated using the UAV is a good representation of the terrain represented by the LiDAR generated DTM. For sub-catchment 2, the point flood depth for the LiDAR generated DTM was 0.47m while the point flood depth for our UAV generated DTM was 0.52m. The UAV derived DTM over-predicted the flood depth predicted by the LiDAR DTM by 0.05m or 5cm. For Sub-catchment 3, the point flood depth for the LiDAR generated DTM was 0.60m while the point flood depth for our UAV generated DTM was 0.52m. The UAV derived DTM under-predicted the flood depth simulated by the LiDAR DTM by 0.08m or 8cm. The graph showing the comparison is at Figure 63.

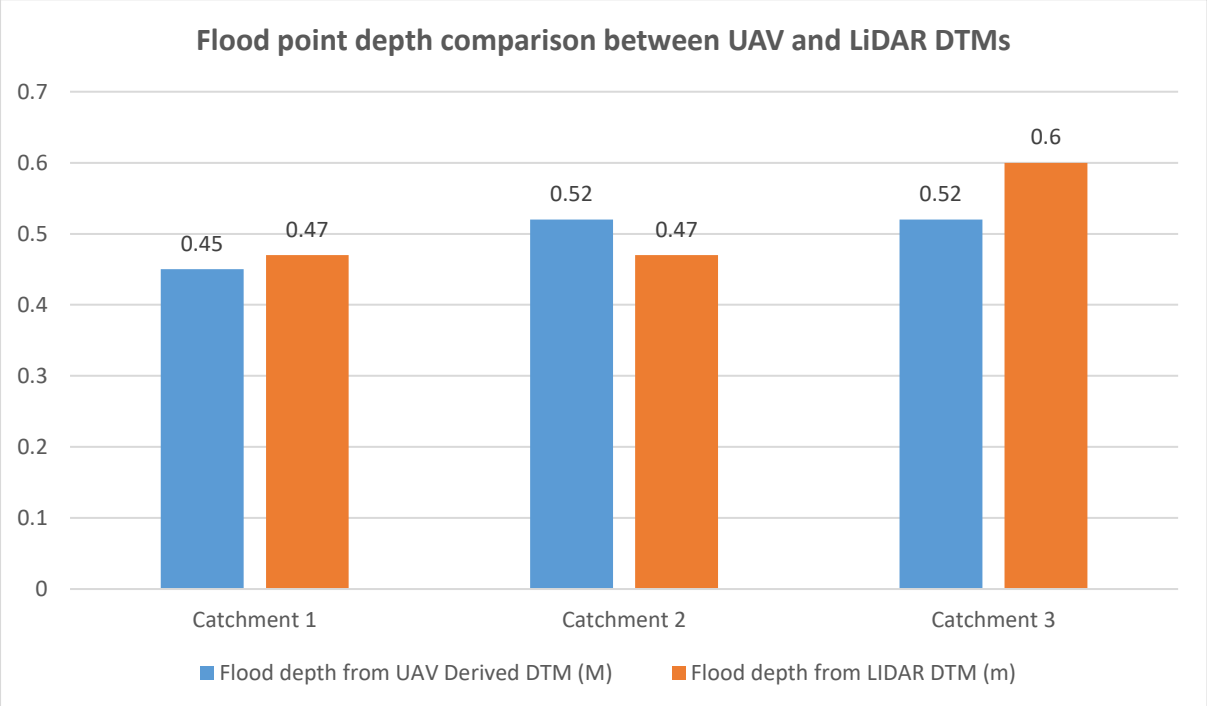


Figure 63: Flood point depth comparison between UAV and LiDAR DTMs

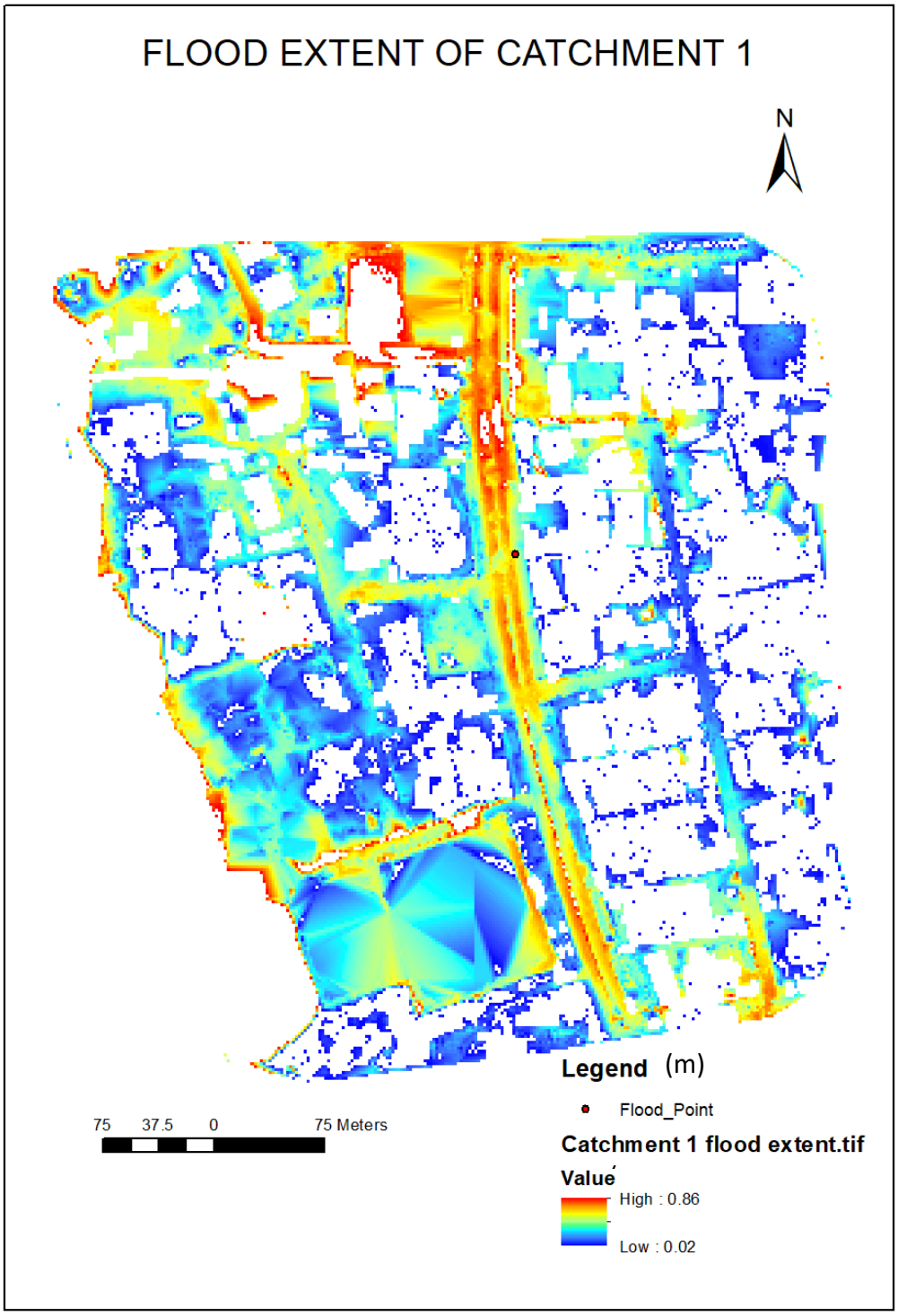


Figure 64: Flood extent for sub-catchment 1 using the UAV DTM

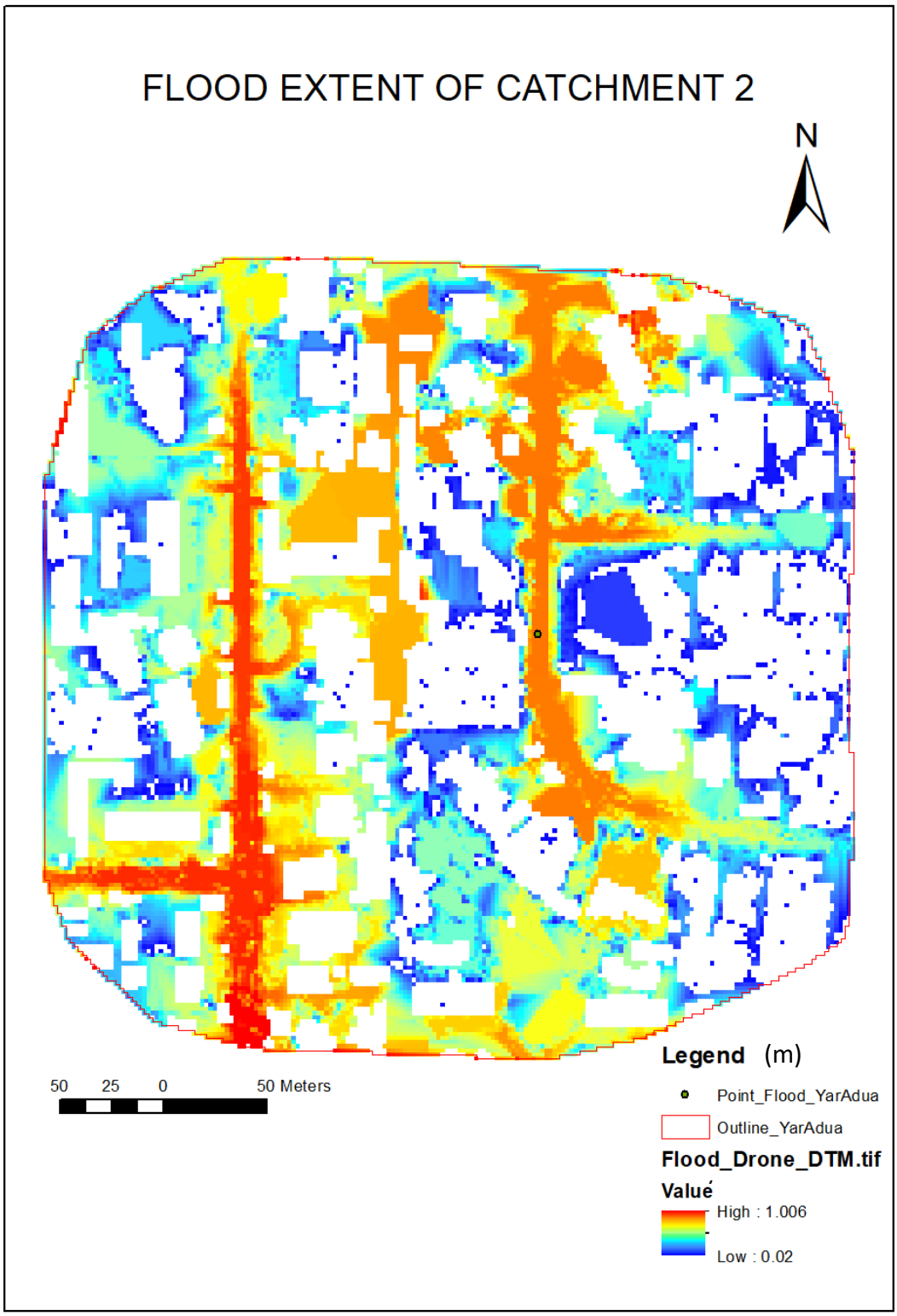


Figure 65: Flood extent for sub-catchment 2 using the UAV DTM

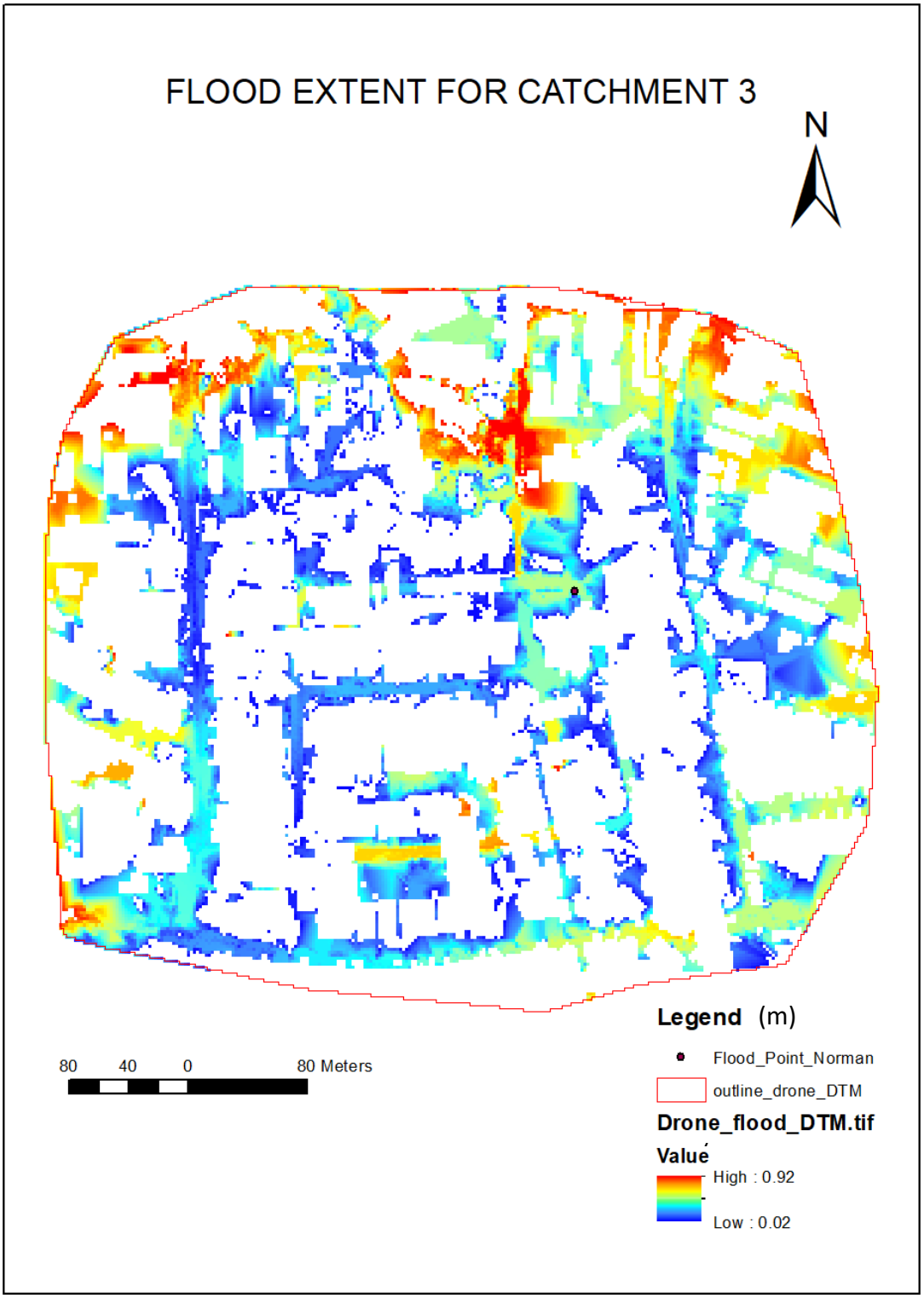


Figure 66: Flood extent for sub-catchment 3 using the UAV DTM

7.6.1 Comparison of flood simulations between the DTMs generated from UAV photogrammetry and LiDAR DTMs

The DTMs generated from the UAV derived imagery was smaller than the sub-catchments that were generated from the LiDAR DTM. This evaluation therefore compared the FloodMap simulation outputs that overlapped between the 2 DTMs in each of the sub-catchments.

7.6.2 Sub-catchment 1 flood simulation comparison

For sub-catchment 1, the point flood depth for the UAV derived DTM was 0.63m while the point flood depth for the LiDAR derived DTM was 0.65m. In comparing the simulated inundation extent of the 8th July 2017 flood, random points were obtained from the intersection of the inundation extent from the LiDAR DTM and UAV DTM as shown in Figure 67. These points were subjected to further statistical analysis and the RMSE was 0.21 while the mean absolute error (MAE) was 0.126 as shown in Figure 68. The low values of both the RMSE and the MAE show that there is a good agreement between the UAV DTM and the LiDAR DTM.

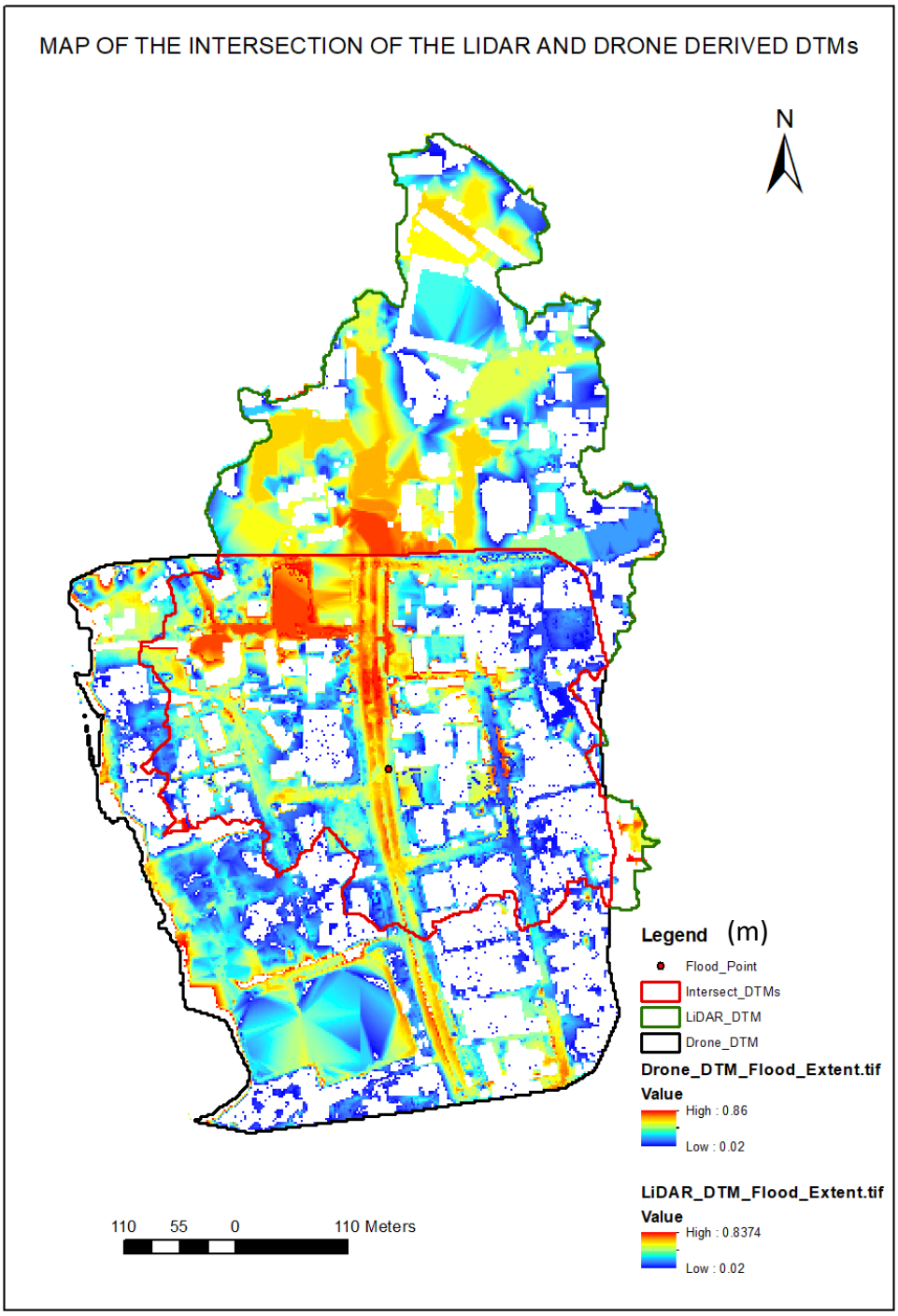


Figure 67: Map showing the intersection (red polygon) of the LiDAR and UAV derived DTMs' flood extent for sub-catchment 1.

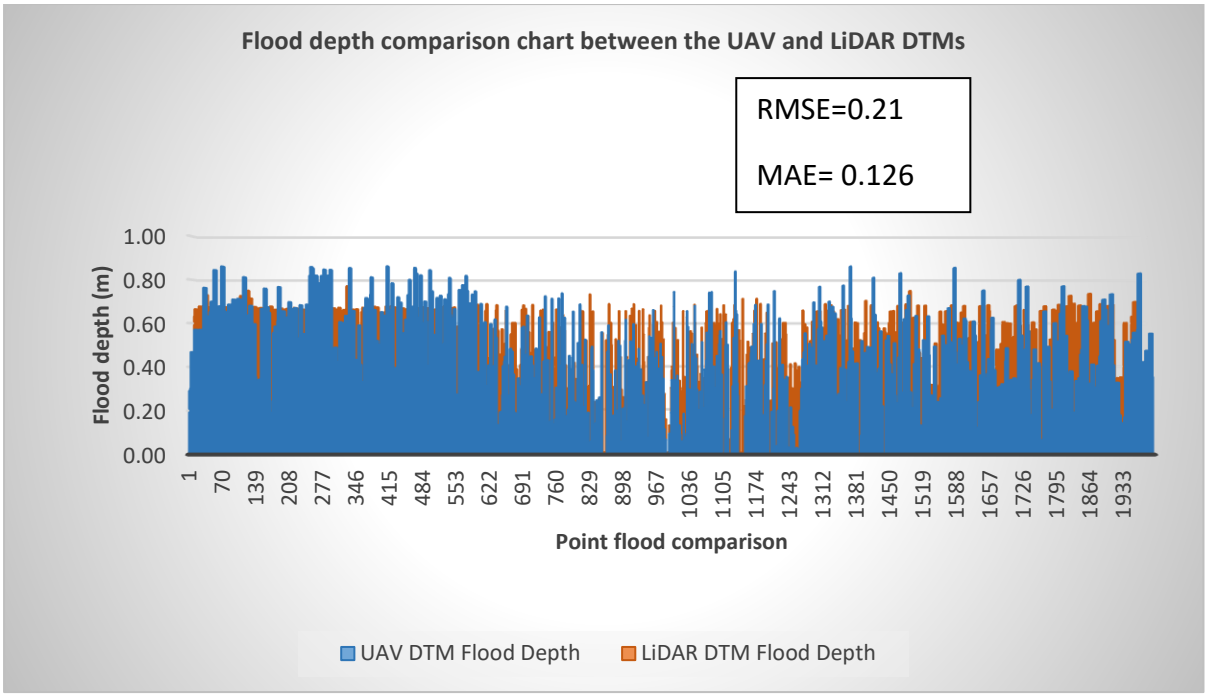


Figure 68: Chart comparing the flood extent obtained using the UAV DTM and the LiDAR DTMs for sub-catchment 1 with the RMSE and MAE values

7.6.3 Sub-catchment 2 flood simulation comparison

From the comparison of the flood extents from both sources as shown in Figure 69, the point flood depth for the UAV derived DTM was 0.70m while the point flood depth for the LiDAR derived DTM was 0.73m. The RMSE was 0.209 while the mean absolute error was 0.126 as shown in Figure 70. The low values of both the RMSE and the MAE shows that just like the previous sub-catchment, there is a good agreement between the UAV DTM and the LiDAR DTM for sub-catchment 2.

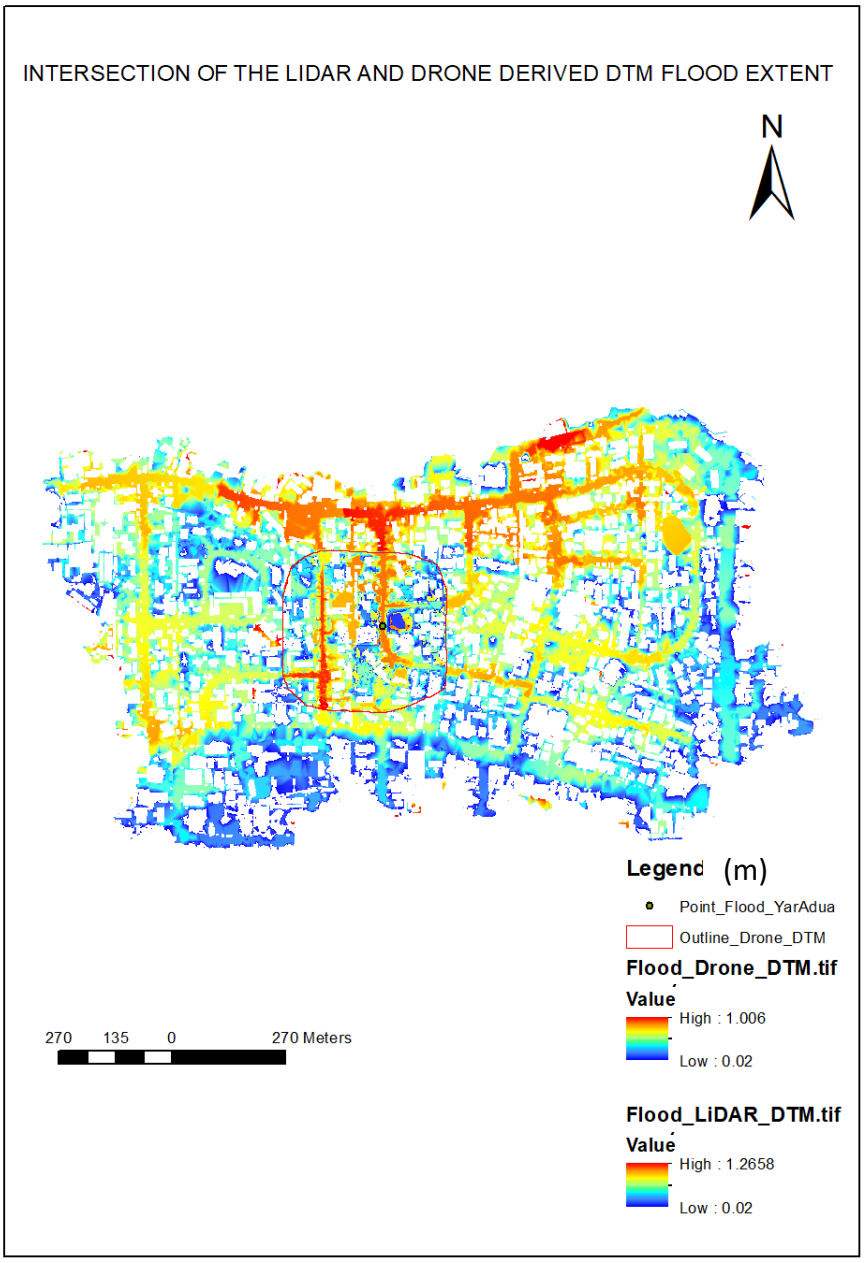


Figure 69: Map showing the intersection (red polygon) of the LiDAR and UAV derived DTMs' flood extent for sub-catchment 2.

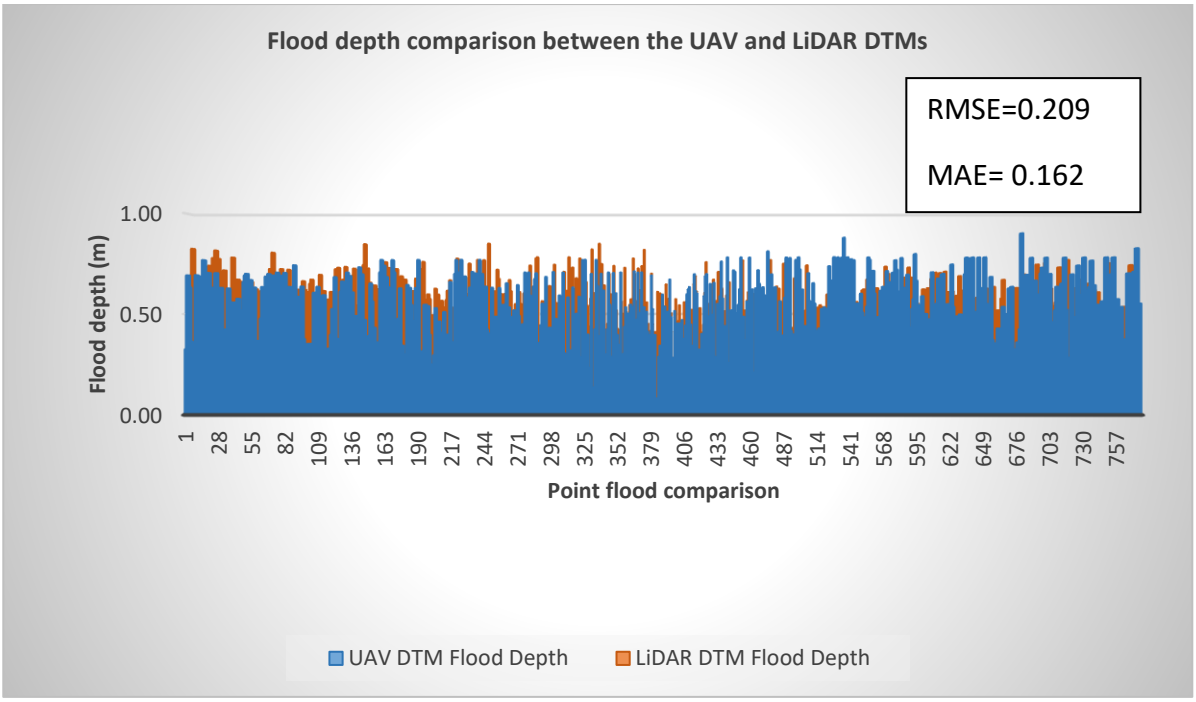


Figure 70: Chart comparing the flood extent obtained using the UAV DTM and the LiDAR DTMs for sub-catchment 2 with the RMSE and MAE values.

7.6.4 Sub-catchment 3 flood simulation comparison

For sub-catchment 3, the comparison of the flood extents from both sources is as shown in Figure 71, the point flood depth for the UAV derived DTM was 0.50m while the point flood depth for the LiDAR derived DTM was 0.45m. The RMSE was 0.291 while the mean absolute error was 0.228 as shown in Figure 72. The low values of both the RMSE and the MAE show that there is a good agreement between the UAV DTM and the LiDAR DTM for sub-catchment 3, just like the other sub-catchments.

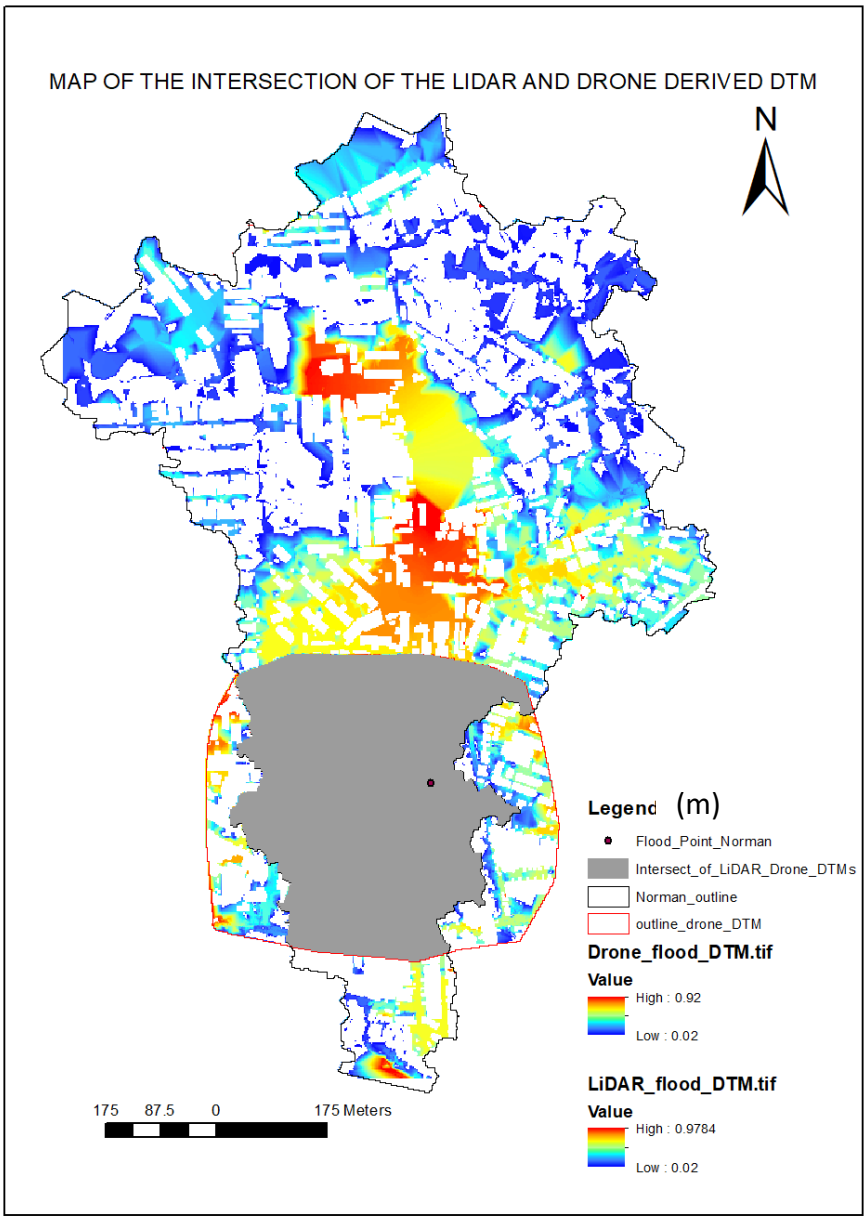


Figure 71: Map showing the intersection (red polygon) of the LiDAR and UAV derived DTMs' flood extent for sub-catchment 3.

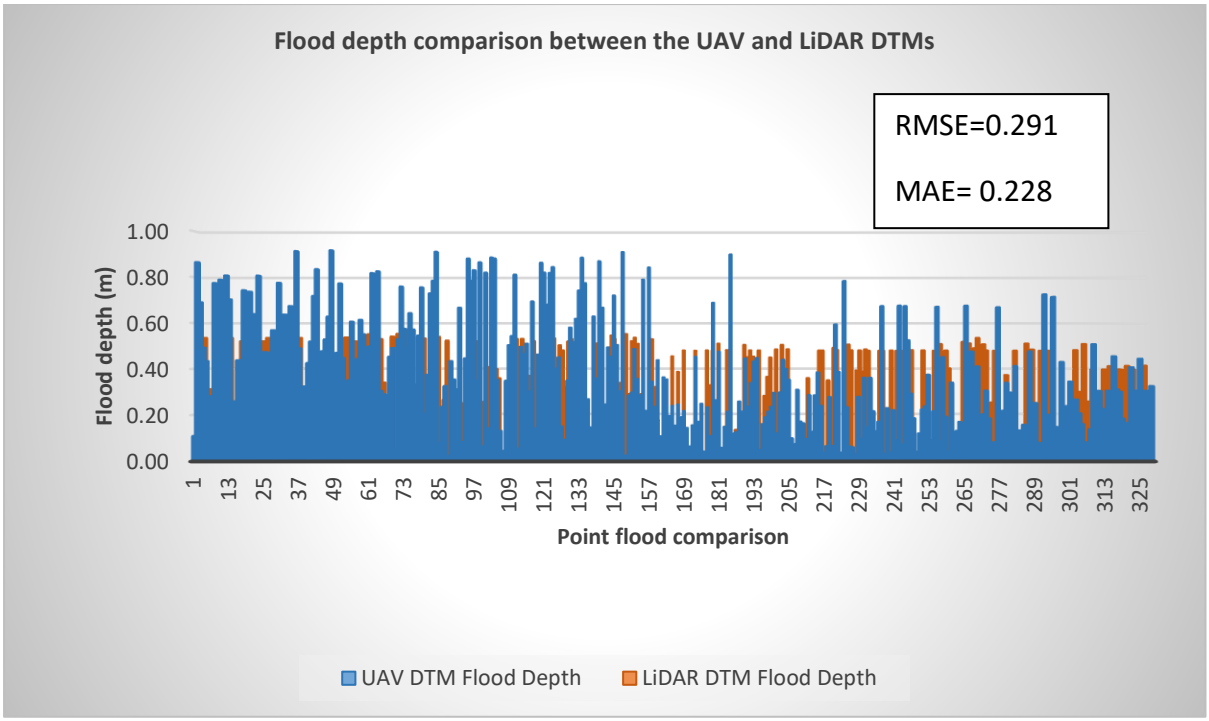


Figure 72: Chart comparing the flood extent obtained using the UAV DTM and the LiDAR DTMs for sub-catchment 3 with the RMSE and MAE values.

7.7 Summary of Chapter 7

This chapter presents the outcome of a flood simulation using a DTM generated using aerial photogrammetry obtained with a vertical take-off and landing (VTOL) UAV. The focus of this chapter was to confirm how cost effective and replicable means of generating a DTM using a UAV could compare with high-end DTM from high-tech sources like LiDAR; including how feasible it would be to use such UAV DTMs for hydrological modelling. The accuracy assessment conducted on the UAV DTM, when compared to DGPS points, confirmed that the RMSE and MAE values obtained in the 3 sub-catchments was a 'good fit'. Sub-catchment 1 had RMSE and MAE values of 0.098 and 0.077 respectively. Sub-catchment 2 had RMSE and MAE values of 0.212 and 0.17; while sub-catchment 3 had RMSE and MAE values of 0.203 and 0.17. The above result of the assessment shows that the UAV DTM is a 'good fit' for the terrain representation. When comparing the UAV DTM to the LiDAR DTM, all 3 sub-catchments showed a fair representation with the LiDAR DTM, catchments 1, 2 and 3 had (RMSE 0.319, MAE 0.233; RMSE 0.354, MAE 0.287 and RMSE 0.336, MAE 0.271 respectively). Though there was some variation in the flood modelling between the UAV and LiDAR DTMs, the results show good promise in the application of UAVs for DTM generation. A comparison of the FloodMap simulation for both DTMs displayed similar outputs. The point flood depth for the UAV DTM for sub-catchments 1, 2 and 3 were 0.45m, 0.52m and 0.52m respectively when compared to the same point depth for the LiDAR DTM which was 0.47m, 0.47m and 0.60m respectively; with residuals of 0.02m, 0.05m and 0.08m respectively. Though the UAV DTM slightly under-predicted the simulated flood depth in sub-catchments 1 and 3; and over-predicted flood

depth in sub-catchment 2, the result showed a 'good fit' when compared to the high-tech LiDAR DTM. Comparing the flood extent of the UAV DTM vs the LiDAR DTM, sub-catchment 1 had a RMSE and MAE of 0.21 and 0.126 while sub-catchment 2 had RMSE and MAE of 0.209 and 0.126 respectively. Sub-catchment 3 had RMSE and MAE of 0.291 and 0.228 respectively. The flood modelling results using the UAV DTM showed it was a good representation of the LiDAR DTM from the RMSE and MAE results comparison of the 3 sub-catchments. The overall results from the use of the UAV DTM shows that there exists great potential in using UAVs for generating vital terrain data that can drive flood forecasting in data sparse regions.

Chapter 8: Analysis and discussion

8.1 Overview of Chapter 8

This Chapter analyses the results of the flood modelling conducted using FloodMap and CityCAT by conducting an assessment of the extent to which the research objectives were achieved was made. It also analyses the results obtained from using UAVs for the generation of terrain data and assessing the suitability of this data for modelling flow in data sparse regions and other areas where terrain data suitable for conducting hydrological studies may not be readily available. The Chapter compares how the findings obtained from this research compares with similar research conducted at the international scene. It also compared FRM amongst countries with varying data availability and a brief comparison was made between the FRM in some developed countries and other developing countries in order to see if there were positive FRM approaches that could be adopted to build flood resilience capabilities in developing countries.

8.2 Outcome of Research Objective 1.

To determine if pluvial flood modelling can be meaningfully conducted in data-sparse regions of the developing world.

The aim of this objective was to investigate the feasibility of conducting pluvial flood modelling in data-sparse regions of the developing world and to propose criteria for validating flood models in such challenging contexts. The study successfully conducted pluvial flood modelling using available data; however, it was evident that the limited data availability significantly affected the accuracy and reliability of the results. Therefore, there is a clear need for additional data generation, particularly for meteorological and terrain modelling, to improve the robustness of the flood models. Despite the data limitations, the pluvial flood modelling was able to capture the general patterns and potential flood-prone areas in the study region. The models highlighted areas with high vulnerability and provided valuable insights into potential flood extents and depths. However, it is important to acknowledge that the accuracy of the modelling results is constrained by the scarcity of data inputs. To enhance the reliability and applicability of pluvial flood models in data-sparse regions, several criteria for validating the models should be considered. First, efforts should be made to collect additional meteorological data, such as rainfall intensity and duration, to improve the accuracy of precipitation inputs. Local weather stations or ground-based rain gauge networks can be established, or existing stations upgraded to gather relevant meteorological data. Second, terrain modelling can be enhanced by generating high-resolution elevation data through remote sensing techniques, such as LiDAR or satellite imagery. These data sources can provide detailed information about the topography and surface characteristics, enabling more accurate representation of flow paths and potential flood-prone areas. Furthermore, validation of the flood models should involve field observations and local knowledge. Engaging with local communities and stakeholders can provide valuable insights into historical flood

events, flood-prone areas, and local drainage systems. This participatory approach can help validate the model results and identify areas where the models may need refinement.

8.2.1 Sensitivity analysis of modelling results

For FloodMap, the sensitivity analysis of the model parameters for the 3 sub-catchments exhibited a similar correlation. Drainage capacity influenced the model the most in all 3 sub-catchments as shown in the correlation plots. Hydraulic conductivity next influenced flood depth while Mannings least influenced flood depth. The results of the parameters that drove flood output depicts the importance drainage plays in curbing flooding in an urbanised sub-catchment area. For the SA of CityCAT modelling parameters, the output was the flood depth while the parameter values were Mannings-buildings, Mannings-vegetation and hydraulic conductivity. The analysis of the results for FloodMap and CityCAT are outlined below.

8.2.2 Drainage Capacity

Drainage capacity was found to be the most significant parameter in hydrological response in urban areas compared to vegetal cover and impervious surfaces. This finding is consistent by research by (Meierdiercks et al., 2010) which suggest that drainage density and presence of stormwater ponds impact peak discharge more significantly compared to percent impervious or land cover of sub-basins. This finding is all important as emphasis when enacting FRM policies for these regions could focus on building overall resilience by the introduction of appropriate building practices like blue-green cities and the impact these initiatives could have on FRM in such regions. Their research by Meierdiercks et al., 2010 further analysed 5 basins and the most impervious basin was the most controlled by stormwater management ponds which coincidentally had the smallest drainage density. Research is mostly focused on the impact of urbanization of flooding but more effective approaches to build resilient societies need to be further investigated such as the introduction of blue-green cities. The FRM for the study area would involve improving the ability of flow to drain off the catchment area or introduce water retention facilities which excess flow drains into.

8.2.3 Roughness

For FloodMap, Mannings had a strong direct relationship on flood depth with increased Mannings values resulting in an increase in flood depth. This finding was consistent with research on increased impervious areas resulting in increased runoff (Oudin et al., 2018) but the introduction of stormwater treatment facilities greatly compensated for the impact of imperviousness. This interesting development is seeing a shift from traditional condemnation of increased imperviousness to more efficient ways of managing stormwater, which further buttresses the importance of sustainable approaches to managing flooding in societies such as the introduction of blue-green cities. For CityCAT, in sub-catchment 1, the Mannings roughness for buildings had the highest impact on flood depth displaying a strong direct relationship with flood depth as shown in Figure 36. This means increases in the roughness values for buildings, result in increased flooding. This relationship is in line with researches that posit that buildings result in increased runoff and increases the risk of flooding (Devi et al., 2019). The Mannings vegetation parameter values displayed a weak direct relationship

with flood depth, with an increase in roughness values for vegetation resulting in an increase in flood depth and vice-versa. For sub-catchment 2, Mannings roughness for buildings displayed the same relationship to flood depth as the previous sub-catchment as it had the strongest influence on flood depth exhibiting a strong direct relationship with flood depth as shown in Figure 37. This means that increases in Mannings building values result in a corresponding increase in flood depth. Mannings vegetation displayed a very weak direct relationship with flood depth in as the previous sub-catchment. In sub-catchment 3, the relationship between Mannings building and Mannings vegetation has the same relationship as the previous catchments as shown in Figure 38. However, the relationship between Mannings vegetation and flood depth in (Ebrahimi et al., 2008) revealed that the Manning roughness coefficient increases as vegetation density increases, while it decreases when the flow depth and velocity increase. The research further posited that significant variation of the Manning's value with flow and vegetation conditions urges the consideration of the flow and vegetation conditions in estimation of the Manning roughness coefficient. For this research, the very weak direct relationship between Mannings vegetation and flood depth could be due to the sparsely vegetated urbanized study area and the interaction of flow with other opposition to flow such as buildings, roads and aspect/slope could have resulted in the interaction witnessed.

8.2.4 Hydraulic conductivity

For FloodMap, hydraulic conductivity also had an inverse relationship with flood depth, but a much weaker relationship existed compared to drainage capacity. The finding on HC is consistent with researches by (Pratomo, 2016) where their HC values were the greatest influencers of flash flooding in Vegetal cover had a weak inverse relationship with flood depth which is consistent with research by (Hu et al., 2021) where decreases in vegetal cover resulted in increased runoff in urbanized sub-catchments. For CityCAT, in sub-catchment 1, hydraulic conductivity had a small impact on modelled flood output as it exhibited a very weak inverse relationship with flood depth as shown in Figure 44. An increase in hydraulic conductivity values resulted in a decrease in flood depth and vice-versa. This relationship is in line with researches conducted on the impact on vegetation on flooding where vegetal cover increases infiltration and mitigates runoff (Bai et al., 2018). In sub-catchment 2, hydraulic conductivity had the same relationship as the previous sub-catchment with flood depth but still had a slighter stronger inverse relationship as depicted in Figure 45. This is possibly due to the increased vegetal cover in that sub-catchment compared to the previous one. Sub-catchment 3 also displayed a weak inverse relationship with flood depth just like the previous sub-catchments see Figure 46 but it had a stronger impact of flood depth due to it having the highest vegetal cover amongst all the sub-catchments. The inverse relationship displayed by hydraulic conductivity and flood depth is important in FRM as measures to increase the hydraulic conductivity values, like having more pervious layers including the adoption of green roofs (Cao et al., 2021) will reduce the flooding experienced by the sub-catchments. The introduction of emerging approaches like Blue-Green Cities could greatly maximize FRM in the study area and this could result in the adoption of the most efficient FRM policies.

8.2.5 Model Calibration

The model calibration was achieved using ROC curve for both models. For FloodMap, lower Manning values, lower drainage capacities and lower HC values best represented flow in all three catchment areas. From the low drainage capacities that characterized the catchments, it showed that plausible FRM approaches would have to increase the drainage capacity of the study area. Unfortunately, in a densely urbanized urban area, this poses challenges (Francisco et al., 2022; A. K. Gupta & Nair, 2011) with some suggestions to counter this to include the introduction of Blue-Green concepts (Miguez et al., 2015) such as green roofs, SUDs and water retention reservoirs amongst other emerging FRM approaches. For CityCAT, higher Mannings Buildings, lower Mannings Vegetation and low HC values characterised the sub-catchments and best represented them. For the higher Mannings Buildings corresponding to flood depth, this correlated research that posit building result in impervious layers and also restrict flow which results in flooding (Bruwier et al., 2018; Huang et al., 2014). The low Mannings Vegetation witnesses could be due to the sparse vegetal cover in the study area as earlier explained. The low HC could be attributed to the highly urbanized study area which results in lower permeability in the sub-catchments (Bricker & Bloomfield, 2014). In both models, the impact of urbanization has greatly affected the flow resulting in increased flood depth. The application of Blue-Green Approaches for enhanced FRM in such densely urbanized areas is necessary and favourable policies need to be enacted to drive such Blue-Green Concepts.

8.3 Outcome of Research Objective 2.

To determine how low-cost methods can be utilized for the generation of flood model validation data in data sparse regions.

The hindrance posed by data unavailability of data towards enacting plausible FRM policies in Nigeria was examined and means to overcome this challenge was tested by investigating the role UAVs could play in generating terrain data for inundation extent modelling. A UAV was flown over the identified 3 sub-catchments under study and the results were validated using DGPS points obtained within the sub-catchments. For sub-catchment 1, the RMSE and MAE was 0.098 and 0.077 as shown in Figure 56 while the RMSE and MAE for Sub-catchment 2 was 0.212 and 0.17 see Figure 57. For sub-catchment 3, the RMSE are MAE was 0.203 and 0.17 as shown in Figure 58. The validation showed a good measure of fit between the UAV derived DTM and the DGPS points. The UAV and LiDAR DTMs were then compared using random elevation points extracted from both DTMs. The RMSE and MAE for the 3 sub-catchments were 0.319 and 0.233, 0.354 and 0.287, 0.336 and 0.271 for sub catchments 1-3 respectively as shown in Figure 60, Figure 61 and Figure 62 respectively. Modelling of the inundation extent was tested between a high end DTM generated from LiDAR point clouds and the UAV DTM. The output of the flood extent of the UAV derived DTM vs the LiDAR derived DTM showed some similarity. Sub-catchment 1 had a RMSE and MAE of 0.21 and 0.126, Sub-catchment 2 had RMSE and MAE of 0.234 and 0.178 while Sub-catchment 3 had RMSE and MAE of 0.291 and 0.228. The ability to generate vital terrain data that is suitable for hydrological modelling

in data sparse regions will definitely bridge the gap created by the absence of high-resolution terrain data for hydrological modelling. A table showing the overall comparison of the UAV and LiDAR DTMs is at Table 24.

Table 24: Table showing the comparison of the UAV DTM and LiDAR DTM

Comparison	**Sub-catchment 1**		**Sub-catchment 2**		**Sub-catchment 3**	
	RMSE	**MAE**	**RMSE**	**MAE**	**RMSE**	**MAE**
DGPS Elevation	0.098	0.077	0.212	0.17	0.203	0.17
UAV and LiDAR DTM	0.319	0.233	0.354	0.287	0.336	0.271
Flood Extent from UAV and LiDAR DTMs	0.21	0.126	0.209	0.162	0.291	0.228

8.4 Outcome of Research Objective 3

To determine how well sub-catchments are able to represent the hydrological processes of entire catchment areas for pluvial flood modelling.

The lead-time given by a flood forecast plays a vital role in the reliability of that FFWS. Due to the size of catchment areas and the high computational requirement including the time needed to simulate a predicted flood event, sub-catchments are sometimes used to represent larger hydrological processes. This is further hinged on the assumption that catchments in close proximity usually have similar catchment characteristics. Modelling flood over a terrain is complex requiring the simulation of diverse flow processes. In extreme rainfall events, there is the possibility of flow from one sub-catchment into another. When a sub-catchment process is then used to represent the entire flow process of the catchment area, errors may then emanate, specifically in the computational process and result in inaccurate flood forecasts. This was evident in this research where the calibrated parameter values from the 3 sub-catchments were used to represent the historical flood event in the entire catchment area. There were differences in the simulated flood depth at sub-catchment and the entire catchment area which were (-0.17m, 0.03 and 0.03m) for the FloodMap model and when CityCAT was used, the differences were (0.27m, -0.01m and 0.02m respectively) as shown in Table 18 and Table 20. The differences show the likely errors that could emanate when flood forecasts are made at sub-catchment and catchment area levels and the uncertainty that could be associated with such forecasts.

8.5 Outcome of Research Objective 4.

To determine how well terrain data for pluvial flood modelling generated from UAV photogrammetry point clouds compares with terrain data generated from high-tech LiDAR point clouds.

Analysing the results from the modelled inundation extent and the ability to use UAV's for generating vital data for FRM purposes shows potential for flood forecasting especially in areas plagued with data sparsity. Using the FloodMap Model, increasing the drainage capacity of a sub-catchment has significant effect on flood extent, hence, identifying areas that are at risk of flooding and modelling potential efforts to build their resilience to flooding can be achieved. Furthermore, hydraulic conductivity has an inverse relationship with flood depth. Increasing the green areas of a sub-catchment including the adoption of sustainable green roofs can further build flood resilient cities. There can also be approaches to model the impact of water retention facilities within sub-catchments as part of building flood resilience cities. Traditional grey infrastructure results in a change in the local hydrological cycle, increases peak flows, results in downstream flooding risks, changes groundwater and surface water levels including increased climate change related flooding events (Brears, 2018). Modern approaches to restoring the hydrological function of the urban landscape including the management of stormwater involves the integration of natural and semi-natural areas (Brears, 2018). The impact these measures can have on policy and plans governing FRM could be in the areas of driving sustainable means of constructing buildings in order to ensure maximum drainage capacity within the sub-catchment such as the adoption of blue-green infrastructure approaches. Furthermore, the availability of data and the provision of adequate technology can enhance the participation of local communities in FRM and leverage on their local knowledge of the sub-catchment areas to foster a bottom-top approach to FRM.

8.5.1 Suitability of UAV's for generating data for FRM

The UAV-derived DTM exhibited a high level of detail, capturing fine-scale terrain features and variations. The accuracy of the UAV-derived DTM was assessed by comparing it with a reference DTM derived from LiDAR point clouds, which are considered fairly accurate. The vertical accuracy of the UAV derived DTM was within an acceptable range, though there were deviations observed especially in sub-catchments 2 and 3. The comparison between the UAV derived DTM and the LiDAR-derived DTM revealed a good level of agreement especially in sub-catchment 1. Visual inspection of the DTM surfaces showed similar patterns and variations in elevation. Quantitative analysis, including point-to-point comparisons and statistical metrics, demonstrated a reasonable level of consistency between the two datasets. The differences observed were attributed to the inherent limitations of the UAV-based approach, such as limited penetration and potential errors in image matching and georeferencing.

The accuracy assessment conducted on the UAV DTM, when compared to DGPS points, confirmed that the RMSE and MAE values obtained in the 3 sub-catchments was a 'good fit'.

Sub-catchment 1 had RMSE and MAE values of 0.098 and 0.077 respectively. Sub-catchment 2 had RMSE and MAE values of 0.212 and 0.17; while sub-catchment 3 had RMSE and MAE values of 0.203 and 0.17. The above result of the assessment shows that the UAV DTM is a 'good fit' for the terrain representation. When comparing the UAV DTM to the LiDAR DTM, all 3 sub-catchments showed a 'good fit' with the LiDAR DTM, catchments 1, 2 and 3 had (RMSE 0.319, MAE 0.233; RMSE 0.354, MAE 0.287 and RMSE 0.336, MAE 0.271 respectively). A comparison of the FloodMap simulation for both DTMs displayed similar outputs. The point flood depth for the UAV DTM for sub-catchments 1, 2 and 3 were 0.45m, 0.52m and 0.52m respectively when compared to the same point depth for the LiDAR DTM which was 0.47m, 0.47m and 0.60m respectively; with residuals of 0.02m, 0.05m and 0.08m respectively. Though the UAV DTM slightly under-predicted the simulated flood depth in sub-catchments 1 and 3; and over-predicted flood depth in sub-catchment 2, the result showed potential applications in the field of data generation for hydrological modelling when compared to the high-tech LiDAR DTM. Comparing the flood extent of the UAV DTM vs the LiDAR DTM, sub-catchment 1 had a RMSE and MAE of 0.21 and 0.126 while sub-catchment 2 had RMSE and MAE of 0.209 and 0.126 respectively. Sub-catchment 3 had RMSE and MAE of 0.291 and 0.228 respectively. The flood modelling results using the UAV DTM showed it was a good representation of the LiDAR DTM from the RMSE and MAE results comparison of the 3 sub-catchments.

The overall results from the use of the UAV DTM shows that there exists great potential in using UAVs for generating vital terrain data that can drive flood forecasting in data sparse regions just like researches by (Jeziorska, 2019) and also the mounting of LiDAR on-board UAV platforms like (Trepekli et al., 2022) due to miniaturized LiDAR sensors and higher UAV payloads. The UAV derived DTM showed acceptable accuracy and was able to capture detailed terrain features. The comparison with the LiDAR derived DTM indicated a good level of agreement, suggesting that the UAV-based approach can serve as a viable and cost-effective alternative for acquiring elevation data in hydrological modelling applications (Casado & Leinster, 2020; Hackl et al., 2018; Hashemi-Beni et al., 2018). The acceptable results obtained from the comparison between the UAV derived DTM and the LiDAR derived DTM further support the usability of the UAV-based approach for hydrological modelling. The generated DTM was then utilized in hydrological modelling simulations, where it demonstrated satisfactory performance. The UAV-derived DTM provided valuable input for flow routing and flood modelling, enabling effective analysis of flood patterns and water flow dynamics. Overall, the findings of this study highlight the potential of using UAVs for generating photogrammetric points and DTMs in hydrological modelling. The UAV-derived DTM, compared to a reference LiDAR-derived DTM, showed promising accuracy and was successfully employed in hydrological modelling with quite acceptable results. This establishes the UAV-based approach as a valuable tool for acquiring elevation data and supporting hydrological studies, offering benefits such as cost-effectiveness, accessibility, and flexibility in data acquisition for flood risk assessment and management.

8.6 Research outcomes and implications on FRM in data sparse regions

The conduct of this research brought out several salient issues that are vital in facilitating flood modelling in data sparse regions. Several insights also emerged from this work that could assist researchers especially those interested in conducting flood modelling in data sparse regions. These span the types of models best suited for flood simulations in data sparse regions, which investments countries bedevilled with sparse data could make that would enhance their approach to flood modelling and also the best ways to overcome the challenges militating against embarking on scientific FRM strategies and policies in data sparse regions. These are subsequently discussed below.

8.6.1 Plausibility of flood modelling in data sparse regions

This research showed how flood models could be adopted for driving plausible FRM policies in data sparse regions. In data sparse regions, where access to reliable flood data and information is poor, this poses unique challenges and has significant implications for FRM in these areas. The lack of comprehensive meteorological and terrain data, which play fundamental roles in accurate flood modelling are absent in such areas which could result in difficulties in producing precise predictions for such areas which is inimical to effective FRM and flood preparedness including the ability to forecast floods. Despite these challenges, this research was able to model a historical flood event, calibrate the event and thereafter validate the model parameters adopted using a totally different flood event with acceptable results, and this marks a shift in the way FRM could be embarked in data sparse regions. The study explored alternative sources of generating terrain data which is the use of UAVs. A comparison of the generated UAV terrain data and that of high-tech LiDAR showed some good promise in the area of generating terrain data. Furthermore, the comparative analysis of the FloodMap and CityCAT modelling approaches highlights the significance of model selection. It emphasizes the need for parsimonious models that can deliver acceptable inundation outputs despite limited data availability. This finding has great implications in modelling flood in data sparse regions where complex models may not be practical due to data constrains and the lack of the technical and cognitive abilities to embark on flood modelling in these regions. Overall, flood modelling is vital in all phases of the disaster management cycle in data sparse regions, but this is dependent on obtaining data from alternative sources to overcome data limitations and ensuring the accuracy of modelled flood inundation. While data sparcity still poses a significant challenge to FRM, innovative approaches to overcome this challenge offer promising avenues to engage in plausible flood modelling approaches to evolve effective FRM strategies for these vulnerable regions.

8.6.2 Outcome for researchers on flood modelling in data sparse regions

During this research, it was observed that the gap caused by lack of data and also the lack of technical knowledge on flood modelling in these regions, resulted in a lot of flood modelling conducted on data sparse regions devoid of validation data. The knowledge of the community of flood processes in these regions were also not being harnessed to drive plausible FRM

policies and strategies. This research on flood modelling in data sparse regions characterized by limited access to data and the manipulation of available data to suit flood models yields critical outcomes for researchers in the field of hydrology. Drawing from this detailed study of flood modelling in a data sparse region, two models were employed, attempts were made to generate validation data, UAVs were used for the generation of terrain data, the community was engaged, and a comparative analysis of the flood models was made, resulting in key implications and flood model needs. One primary outcome was the importance of the community in generating validation data. The aspect of also generating validation data from stage marks and also recreating such stage marks was also showcased. The research also showcased the importance of institutional collaboration and in general the importance of a Whole of Society Approach (WoSA) to FRM involving the government, institutions and the people. A critical need identified from this study is the generation of validation data using crowd sources and recreating flood stage marks in the field. This research shows that the conduct of flood modelling in data sparse regions requires the availability of validation data and the importance of selecting the appropriate flood model that will produce reasonable inundation extents is vital in such areas with limited data availability. Generally, researchers in flood modelling in data sparse regions are faced with both challenges and opportunities. These challenges are in the areas of the limited data available in such regions and the need to be innovative in addressing the unique demands of flood modelling in data sparse environments. The opportunities abound in the areas of community inclusiveness, institutional collaborations and the generation of vital flood modelling data through various means. With these opportunities to overcome these challenges on flood modelling in data sparse regions, the ability to evolve pragmatic approaches to FRM in this region are thereby feasible and could drive favourable FRM policies in such regions.

8.6.3 Types of flood models suitable for flood inundation modelling in **data sparse regions**

This research explored the suitability of the FloodMap and CityCAT flood models in simulating a historical flood event in Lagos, Nigeria. The process of manipulating available data to suit the models was painstaking and there was the need to generate validation data for the flood models. A key takeaway from this entire research is the need for simplicity in flood models when working in data sparse regions especially when dealing with regions with dense urban fabrics. In working with complex flood models, the extensive data inputs coupled with the computational resources they require, underscores the need for simplified modelling approaches. Parsimonious models thus emerge as a preferred choice when working in data sparse regions as they offer pragmatic solutions that align with the realities of limited data availabilities. Their ability to generate reasonable flood inundation extents in the absence of comprehensive data is pivotal in flood modelling success in data sparse regions. In the choice of models, the ability to generate validation data and diverse means of obtaining data such as the use of UAVs for terrain data, contributes immensely to enhancing the credibility of these flood models and making them invaluable in enacting FRM strategies. It is worthy to note that the research stresses that the suitability of adopting flood models in data sparse regions is linked to their simplicity and ability to replicate complex urban environments. A balance thus

needs to be struck between simplicity and accuracy coupled with the need to develop validation data through innovative means. By adopting these measures, researchers would thus contribute more to effective flood modelling and improve resilience to flooding in data sparse regions through proactive FRM strategies.

8.6.4 Investment to ensure greatest improvement in model performance

The outcome of this research identified numerous gaps in FRM in Nigeria and provided valuable insights into critical areas that should be prioritized to ensure substantial improvements in model performance for enhanced FRM studies. First of all, this research underscores the importance of investing in parsimonious models as the simplicity of these models including reducing their data requirements and improving their applicability in complex urban environments without significantly compromising their accuracy, is vital in FRM studies in data sparse regions. Furthermore, the need to invest in data collection technologies such as meteorological data and terrain data acquisition is vital. The importance of emerging technologies such as the miniaturizing of sensors like LiDAR that can be attached to UAV platforms is a great area where investments could be directed in to ensure improvements in model performance. Adequate training, manpower acquisition and capacity building in FRM in data sparse regions is also an area where investment is necessary to improve model performance. The investment in international collaboration to leverage on available databases on both meteorological and terrain that is currently available to ensure research on FRM could be conducted in data sparse regions and also by making these data available. For this research both meteorological and terrain data had to be bought and this could discourage researchers from engaging in such research works. Another area that investment is necessary in fostering community involvement is in data collection, validation and awareness of these communities. Investments in community outreaches, capacity building and collaborative decision making would foster a sense of ownership and responsibility which would strengthen the overall FRM approaches. For instance, on rainfall data, the rainfall monitoring stations are inadequate, hence, there could be inaccuracies in approximating rainfall intensities away from the meteorological point. The temporal measurement is another area that needs to be of an appropriate frequency to ensure the variations rainfall are adequately captured to facilitate understanding the rainfall pattern of the area. Adequate meteorological stations with the requisite temporal measurements are this necessary in Nigeria. Investment in institutional support at the international and local levels is also vital in aligning various stakeholders towards common objectives. This approach will foster interdisciplinary collaborations, data sharing and the exchange of knowledge on FRM. The investment in data is another crucial area that would ensure the improvement in model performance. A model result is highly dependent on the input data as models are meant to replicate a real-world event. Data in the areas of meteorological and terrain data including adequate updates of these data is vital in improving model performance. On the whole, investments in refining models to be simpler without necessarily compromising accuracy, adopting emerging technologies for generating terrain data, garnering the capabilities of communities and involving them in FRM strategies and policy enacting,

generating adequate meteorological data, developing measures to obtain validation data and adequate collaborations, would ensure an improvement in model performance that will drive FRM strategies and policies.

8.6.5 Establishment of a flood policy for Nigeria

In Section 3.5.2, this research presented the FRM strategy in the UK. The UK being a developed nation with the advantage of its regional alliance for FRM, encapsulates diverse methodologies, strategies and approaches to evolve a more resilient approach to a proactive FRM which is a departure from the hitherto reactive FDM. This is evident in the UK FRM policy which encapsulates guidelines down to the local levels to evolve an efficient FRM plan for the UK. Nigeria on the other hand, just has a National Disaster Response Plan (NDRP) with the National Emergency Management Agency (NEMA) entrusted to implement the plan and coordinate disaster management. The stance here is more of a reactive approach to FRM as against a proactive approach. The absence of a policy on FRM in Nigeria is a major source of the lax regulations and approach to FRM. Though some milestones have been achieved in the area of flood vulnerability assessment in Nigeria, a lot is still desired in order to meet up with modern FRM trends. Global (UN, NGO's etc), regional (EU Directive on Floods [Directive 2007/60/CE]) or a country's policy on flooding shape FRM in a region or country. The geostrategic location of Europe being bound to the North by the Artic Ocean, to the South by the Mediterranean Sea and the Atlantic Ocean to the West, makes Europe susceptible to extreme rainfall and subsequent flood events after heavy precipitation. After river flooding events that affected Danube and Elba in 2002, a Netherlands group proposed a European approach to flood protection (Bakker et al, 2013). This gave birth to the European Directive on Floods (Directive 2007/60/CE). The UK is a signatory to the EU Directive and this Directive fostered a regional and more coordinated approach to flooding. The Directive ensures concerted efforts are encouraged at the international level even if countries still have their own policies on flood prevention (Nones and Pescaroli, 2016). In the UK, FRM is aptly captured in the policy guidelines clearly spelt out in the FWMA 2010 (Flood and Water Management Act, 2010) including flood insurance guidelines for property owners circulated by DEFRA. Other parastatals draw their strength from the well-articulated document which caters for most exigencies and spells out guidelines down to the local level for actions to be taken during a flood event. DEFRA is expected to work in line with the national flood and coastal erosion risk management strategy outlined in FWMA 2010 and ensure that the FRM end state is achieved. DEFRA is expected to draw up transparent approaches to flood risk strategies and generate/update flood data which usually involves the local communities. The FWMA 2010 in conjunction with DEFRA produced the National Flood and Coastal Erosion Risk Management Strategy for England in 2011 with goals which include evolving strategic plans and preventing unauthorized development in areas that are at risk from flooding and coastal erosion (McLuckie et al., 2018). Other plans include building, maintaining and asset improvement, building flood resilience by raising awareness and improving the accuracy of FFWS. These strategies ensure that FRM is very objective and streamlined with various checks and balances for implementation, financing, technology review, research etc. Flood risk analysis by DEFRA

puts 1 in 6 homes in the UK at risk of flooding with 5 million properties at risk of flooding in UK as at December 2013 (DEFRA, 2014). Nigeria on the other hand has the NDRP which was articulated by NEMA to guide its activities during a disaster does not have a flood policy to guide its FRM drives. Taking a cue from the UK Planning Policy Statement 25 which takes flood risk into consideration in the planning process. The sequential approach used by this Policy statement is outlined below:

1. Consider flood risk in the planning process.

2. Assess flood risk based on site-specific challenges.

3. The sequential and exemption tests – The sequential approach is applied at the lower level and the exemption test is applied when necessary.

4. Managing surface water - Applying the blue-green approach.

5. Flood risk management – Based on site specific flood challenges at the lower levels.

6. Residual risk management – Caters for exigencies after FRM has been implemented.

The importance of a flood policy will be the inclusion of the local communities and the partnership with local institutions for its generation which will reflect the bottom-top approach to FRM. It will be easier for budgetary allocations and coordination will be easier. A well-articulated FRM policy for Nigeria would guide all FRM stakeholders and allot specific tasks for disaster managers including insurance policies and guidelines for property owners. Funding would also be easier to budget for and monitor since the emphasis for FRM has shifted from a reactive to a proactive approach. This approach will foster good cooperation between the local authorities and the national level. A similar involvement of the local population in Nigeria would foster cooperation amongst populace and the government of Nigeria. It would also depict a transparent process of FRM being planned and implemented.

8.7 Research challenges and Limitations

Quite a number of challenges hindered the scope of this research which are partly related to the dearth of data and the quality of data available. In other to overcome these limitations, alternative approaches were sought which were time consuming, but the objectives of the research were kept in focus. Some of the limitations are outlined below:

8.7.1 Dearth of observed validation data

One very important data required during inundation extent modelling is the availability of observed time-step validation data which is vital in assessing the accuracy of models. For pluvial flooding, this is a challenge and attempts to overcome this includes the use of flood sensors within the sub-catchment areas. For this research, crowd sourced validation data was used at the end of the storm event and the flood extent generated using a plane across the sub-catchment. This approach uses the bath-tub method and may not take into consideration artefacts that may exist on the topography. The inundation extent was modelled using a

different flood model and then compared with the results obtained using the models adopted for the research.

8.7.2 Distance to study area

This research was conducted at the University of Nottingham, but the study area is in Sub-Saharan Nigeria. A total of 2 trips were made to the study area to obtain data and for the field work. The distance to the study area including the associated costs hindered the ability to possibly conduct UAV flights immediately after a flood event to obtain validation data that would have been invaluable to the research. Furthermore, on-site obtaining of flood depths during a storm event would have been possible which would have been used as validation data. Despite these shortcomings, the importance of crowd sourced data was clearly displayed but this was obtained at the termination of the rainfall event.

8.7.3 Difficulty in obtaining data for flood inundation extent modelling

There were bureaucratic procedures that hindered the timely acquisition of data. This led to time being wasted trying to obtain data from government agencies that could be used to further the research. Furthermore, the LiDAR point clouds, and the rainfall data had to be purchased. The availability of such data especially for research purposes at no costs to the researcher will greatly encourage studies related to FRM.

8.7.4 Limitations on the use of UAV's in urban area

Limitations on the use of UAVs in urban areas were showcased in the country specific regulations/restrictions governing their use. The regulation of a height of 40m by the Federal Airports Authority of Nigeria (FAAN) restricts the area that can be covered by UAVs at a time due to altitude having a direct relationship with the instantaneous field of view of a sensor or the sensors swath width. Special procedures are required for UAV's to be flown at higher altitudes which are really difficult to meet. One limitation for the application of fixed-winged UAVs was aptly encountered in this research using the eBee UAV for capturing photogrammetry points over the study area. The fixed-winged UAVs had to be swapped for Vertical take-off and landing (VTOL) UAV's. Other limitations of UAV's are their endurance, especially the VTOL UAV's which could only cover limited areas within a sub-catchment especially when high percentage vertical and horizontal overlaps are required.

8.8 Recommendations for further research

This research was able to model a historical flood event and obtain parameter values that could be used for flood forecasting when there is predicted weather data available. Areas that need further research to enhance FRM with the study area are outlined below:

8.8.1 Flood Policy for Nigeria

The process of generating this flood policy will involve the adoption of multi-criteria analysis to identify areas at risk of flooding and use the peculiarities of the affected communities to draft a flood policy for the country. Validation of the flood risk map produced can be achieved using hotspots of historical flood events. This approach will help generate a flood policy that

is robust. At the lower levels, plans can be embarked to build the resilience of these communities to flood, and urban sprawl can be coordinated to ensure the hydrological response of these sub-catchment areas are preserved. Adequate funding can be sought for plausible FRM to be embarked at the lower levels which will be a more transparent approach to FRM in these areas.

8.8.2 Generating weather data at higher temporal resolution

One of the major requirements for flood forecasts is the availability of reliable precipitation data at sub-minute intervals. Rainfall data for the study area at this temporal resolution is not available. There is the need to set up weather monitoring stations particularly along the coast to enable accurate weather measurements are made. The study compared available rainfall data from Tropical Rainfall Measuring Mission Multi-satellite Precipitation analysis (TMPA) and the observed rainfall depth from the Nigerian Meteorological Agency (NiMET) and noticed that there was some discrepancy in the rainfall data. Accurate rainfall data is vital in flood forecasting and the establishment of weather monitoring stations especially along the coast of Lagos will greatly assist in flood forecasting within that region.

8.8.3 Application of UAVs for disaster management

The approach to generate terrain data using UAV photogrammetry and the close accuracy to DTMs generated from the purchased LiDAR point clouds shows that there are prospects in the applicability of UAVs for disaster management purposes and data gaps that can be filled using them. UAV's have played vital roles in all phases of the disaster management cycle from the pre-disaster planning phases (Erdelj & Natalizio, 2016) to the response/intervention phase (Restas, 2015) and also in the post-disaster phase of determining the extent of flood damages (Zwęgliński, 2020). The application of UAV's for FRM especially in data sparse regions has great potential and further research on this will be conducted.

8.8.4 Hydrological modelling at catchment and sub-catchment scales

One outcome of this research was the under-predicting of flood by both models in sub-catchment 1. The calibration of the flood models for this study was done using sub-catchments and the calibrated parameters were used to drive the entire catchment area. During extreme storm events, there is the possibility of flow into or out of a sub-catchment depending on the elevation of neighbouring sub-catchments and their flow process. There is the assertion that the assessment of flood risk management at sub-catchment scale enable the appraisal of different interventions at extreme rainfall events within the entire catchment (Hankin et al., 2017), but modelling at the sub-catchment scale may result in misrepresentation of the way in which water interacts with the complex landscape as shown in the residuals at Table 17 and Table 19. This issue is likely dependent on the catchment area and misrepresentations may occur if the response of sub-catchments is used to represent the flow process of the entire catchment area. This reinforces the need for FRM to be instituted down to the local levels including research which will help checkmate the misrepresentation of catchment and sub-catchment flow process representation at these scales.

8.8.5 Flood forecasting

The underlying focus of this research was to be able to calibrate parameters for a model in order to replicate a historical rainfall event. The reason was to be able to identify the optimal modelling parameter values for those sub-catchments that could be applied to Numerical Weather Predictors (NWP) to forecast flood. Further research will entail identifying suitable NWP that can be used with these calibrated parameters for flood forecasting within these sub-catchments. Subsequently, the process of parameter calibration can be applied to entire catchment areas and a flood forecasting and warning system (FFWS) can be generated for such data sparse regions. The lead time for a hydrological forecast refers to the period from the time of making the forecast to the time where the forecast applies (WMO, 2011) and a longer lead time is favoured to trigger an early response. After a rainfall forecast is made, the flood forecast is subsequently generated. The process of forecasting floods is thus hinged on the ability to predict the meteorology of the catchment and translate this into flood extent. Though the reliability of flood forecasts depend on the lead-time given by a forecast, the accuracy in terms of spatial extent and the uncertainty conveyed by a forecast (Jain et al., 2018); data still plays a major role in the reliability of such forecasts. One of the major outcomes of a flood forecast is to be able to constantly regenerate the process to disseminate information about an impending flood event with a degree of certainty and this process metamorphoses into a flood forecasting and warning system (FFWS). The most useful outputs of flood forecasting is the ability to generate a warning system which comprises river elevations, inundation extents, peak discharge occurrence times and lead times that will result in the appropriate response times by relevant flood response stakeholders and the affected population (Jain et al., 2018). Flood warnings allow the adverse effects of flooding to be reduced and increases the beneficial effects of flooding (Parker et al., 2005). A FFWS will be beneficial to Nigeria and will greatly assist in FRM strategies directed at building resilience and directing response to flooding events whenever they occur.

8.9 Summary of Chapter 8

This chapter presents the analysis and discussion of the entire research processes and links them to similar research that have been conducted on FRM. It examines the FRM process in Nigeria, where flooding is a critical issue due to the country's vulnerability to frequent flood events. It assesses the existing policies and approaches to flood risk management in Nigeria, highlighting the need for sustainable and proactive measures. The chapter focuses on FRM and hydrological modelling in the context of Nigeria, comparing it with the experiences in Mozambique, Bangladesh, Netherlands, and the UK. It investigates the FRM process in Nigeria, explores the outcomes of hydrological modelling, and evaluates the effectiveness of flood management strategies in different countries. Additionally, it examines the role of blue-green cities in flood mitigation, highlights the importance of local community involvement, and explores the potential contributions of UAVs in flood risk management in data-sparse regions. To evaluate the effectiveness of FRM strategies, the chapter explored the outcomes of hydrological modelling in Nigeria, analyzing the accuracy and reliability of the models in

capturing the dynamics and extent of flooding. The limitations imposed by data scarcity in Nigeria's flood modelling process are discussed, emphasizing the challenges faced due to the lack of meteorological and terrain data. The chapter compared the FRM approaches and experiences in Mozambique, Bangladesh, Netherlands, and the UK with those in Nigeria. It analyzes the strategies implemented by these countries in managing flood risks, considering factors such as data availability, infrastructure development, and community involvement. The research highlights lessons learned from these countries that can be applied to improve FRM in Nigeria. One promising approach explored in the study is the concept of blue-green cities. It discusses the importance of nature-based solutions, such as green infrastructure, in mitigating flood risks. The chapter emphasizes the potential of incorporating parks, wetlands, and permeable surfaces to absorb and store excess rainfall, reducing the reliance on detailed data inputs. The role of blue-green cities in enhancing flood resilience and creating sustainable urban environments is highlighted. Another crucial aspect addressed in the chapter is the importance of local community involvement in FRM. The chapter emphasizes the value of local knowledge in identifying flood-prone areas, understanding local drainage systems, and historical flood events. It advocates for community participation through awareness campaigns, workshops, and collaborative decision-making processes to enhance the accuracy and effectiveness of flood models and management strategies. Additionally, the chapter explores the potential contributions of UAVs in flood risk management in data-sparse regions. It discusses the use of UAVs for generating high-resolution terrain data, particularly in areas where data scarcity poses challenges. The limitations of UAV-based approaches, such as sensitivity to dense vegetation and image processing errors, are acknowledged, and the need for further research to address these limitations is emphasized. The findings contribute to the growing body of knowledge on effective flood management strategies and provide recommendations for enhancing flood resilience in data sparse regions.

Chapter 9: Conclusion

This research sheds light on the intricate dynamics of flooding, flood modelling, and the challenges faced in data sparse regions, while also presenting proactive strategies for effective FRM. The study underscores the pervasive threat that flooding poses to vulnerable regions worldwide and highlights the urgent need for advanced flood modelling techniques to mitigate its impacts. FRM in Lagos, Nigeria is a critical issue due to the vulnerability of the city to frequent flood events. The approach to manage flood risk in Lagos, Nigeria which is applicable in other data sparse regions presents significant challenges due to the lack of meteorological and terrain data in such regions. Flood modelling emerges as a pivotal tool in understanding flood behaviour and devising optimal FRM strategies. However, the efficacy of flood models heavily relies on the quality and quantity of data used for their calibration and validation. The essential data for flood modelling encompass a range of parameters, from topography and land cover to meteorological and hydrological data. In data sparse regions, the absence of comprehensive datasets poses significant challenges, limiting the precision and reliability of flood models. This study set out to examine the plausibility of conducting flood modelling in a data sparse region and test the validity of alternative means of generating terrain data that would be suitable for flood enacting effective flood risk management strategies in data sparse regions. The outcomes of the flood modelling of the historical flood event using FloodMap and CityCAT models for the study area clearly demonstrates the restrictions imposed by data scarcity in modelling flood events. While the flood models provide invaluable understanding of flood behaviour and potential inundation areas, the accuracy and reliability of the model output rely on the availability and quality of input data and validation data. For the study area, the lack of reliable meteorological and terrain data affected the precision and reliability of flood models and their ability to capture the full extent and dynamics of flooding, but it is a good step in the right direction in charting a plausible approach to FRM in Lagos state. These limitations highlight the need for innovative approaches to overcome data scarcity in flood modelling.

In the modelling approach for this research, a comparison of parameter value representation when working in data sparse regions using a simple approach compared to a complex one, showed that the simple approach can present acceptable flood inundation results. This is very important when representing complex terrain in determining inundation extent during storm events in data sparse regions. Emphasis could thus be on generating accurate precipitation predictions and obtaining good terrain representations. Furthermore, the challenge of obtaining high resolution terrain representation could be overcome with the application of UAV's for generating photogrammetric data for regions affected by data sparsity. However, it is important to consider the limitations of the UAV-based approach, including its sensitivity to dense vegetation and potential errors in image processing and georeferencing. Future research should focus on addressing these limitations and refining the drone-based methodology for improved accuracy and reliability. Overall, the findings of this study contribute to the growing body of knowledge on the application of UAVs in hydrological

modelling and highlight their potential in generating accurate DTMs for various environmental applications. Though the major limitations of this research include the study area not being in close proximity to the researcher and lack of validation data; the research has prospects in the areas of use of UAV's for data generation, encouraging the local community to take part in FRM, flood forecasting in data sparse regions and the growing importance of crowd sourced data in FRM. Being proactive in FRM within data sparse regions requires a multi-faceted approach. Implementing nature-based solutions, like blue-green infrastructure, can bolster resilience by using natural features to mitigate flood impacts. Equally crucial is community engagement, as local knowledge complements scientific data in understanding flood dynamics. The formation of localized flood policies, coupled with increased investment in data collection initiatives, can drive proactive FRM efforts.

This research demonstrated the need for sustainable policies on FRM especially in data sparse regions. It also observed that the approach by Lagos to flooding was rather reactive instead of being proactive. This could be due to an observation that there was no flood policy for Lagos to drive sustainable and proactive FRM in Lagos. An enabling policy on flooding for Lagos would ensure there are funds available for research for FRM especially in areas that are prone to flooding especially areas that their vulnerability is increased with data sparsity. Another potential solution to address the data scarcity challenge in flood modelling is the development of blue-green cities. Blue-green cities employ nature-based solutions to manage and mitigate flood risks, incorporating green infrastructure, such as parks, wetlands, and permeable surfaces, to absorb and store excess rainfall. These approaches can help reduce the reliance on detailed data inputs and provide effective flood management strategies in data sparse regions like Lagos. By implementing blue-green infrastructure, the city can enhance its resilience to flooding while creating more sustainable and liveable urban environments.

Furthermore, the involvement of the local community in flood risk management is crucial. Community participation can provide valuable insights into flood-prone areas, local drainage systems, and historical flood events. This local knowledge, combined with scientific modelling techniques, can enhance the accuracy and effectiveness of flood models. Engaging the community through awareness campaigns, workshops, and collaborative decision-making processes can foster a sense of ownership and responsibility in flood risk management efforts. Moving forward, it is essential to prioritize data collection efforts in data sparse regions like Lagos, focusing on meteorological and terrain data to enhance the accuracy of flood models. Collaborative efforts between government agencies, researchers, and the local community are crucial for collecting and sharing data, fostering community resilience, and developing effective flood risk management strategies. By integrating local knowledge, innovative modelling techniques, and nature-based solutions, cities like Lagos can strive towards a more sustainable and resilient future, mitigating the impacts of flooding and ensuring the safety and well-being of its residents.

The research on overland flood modelling in data sparse regions, with a focus on flood risk management in Lagos, Nigeria, has highlighted the challenges posed by data scarcity and

vulnerabilities to flooding. The outcomes of flood modelling using CityCAT and FloodMap models have underscored the limitations imposed by the lack of meteorological and terrain data. However, solutions such as community involvement in flood risk management and the implementation of blue-green cities offer promising avenues for addressing these challenges. This research underscores the interconnectedness of flooding, flood modelling, and proactive FRM strategies in data sparse regions. The challenges posed by data scarcity necessitate innovative approaches and collaborative efforts to bridge the gap between data availability and the exigencies of effective flood management. By integrating technological advancements, community participation, and forward-looking policies, regions prone to flooding can fortify their resilience, minimize risks, and pave the way for a more secure and sustainable future. Finally, the adoption of a flood policy in Nigeria will streamline FRM plans that will be local community driven, will ensure dedicated funding is budgeted for FRM and will result in a shift from Nigeria's flood response approach to FRM, to flood mitigation, with emphasis on being proactive to flood management rather than being reactive.

Appendix

A1. FloodMap Point flood depth for sub-catchment 1

Simulation	Manning	DC (m/day)	HC (m/hr)	Point flood depth (m)	Residual
S01of27	0.01	0.24	0.001	0.47	-0.23
S02of27	0.01	0.24	0.003	0.45	-0.25
S03of27	0.01	0.24	0.005	0.43	-0.27
S04of27	0.01	0.84	0.001	0.38	-0.32
S05of27	0.01	0.84	0.003	0.36	-0.34
S06of27	0.01	0.84	0.005	0.34	-0.36
S07of27	0.01	1.44	0.001	0.29	-0.41
S08of27	0.01	1.44	0.003	0.28	-0.42
S09of27	0.01	1.44	0.005	0.26	-0.44
S10of27	0.03	0.24	0.001	0.47	-0.23
S11of27	0.03	0.24	0.003	0.45	-0.25
S12of27	0.03	0.24	0.005	0.43	-0.27
S13of27	0.03	0.84	0.001	0.38	-0.32
S14of27	0.03	0.84	0.003	0.36	-0.34
S15of27	0.03	0.84	0.005	0.34	-0.36
S16of27	0.03	1.44	0.001	0.29	-0.41
S17of27	0.03	1.44	0.003	0.27	-0.43
S18of27	0.03	1.44	0.005	0.26	-0.44
S19of27	0.05	0.24	0.001	0.47	-0.23
S20of27	0.05	0.24	0.003	0.45	-0.25
S21of27	0.05	0.24	0.005	0.43	-0.27
S22of27	0.05	0.84	0.001	0.38	-0.32
S23of27	0.05	0.84	0.003	0.36	-0.34
S24of27	0.05	0.84	0.005	0.34	-0.36
S25of27	0.05	1.44	0.001	0.29	-0.41
S26of27	0.05	1.44	0.003	0.27	-0.43
S27of27	0.05	1.44	0.005	0.26	-0.44

Appendix

A2. FloodMap Point flood depth for sub-catchment 2

Simulation	Manning	DC (m/day)	HC (m/hr)	Depth (m)	Residual (m)
Y01of27	0.01	0.24	0.001	0.52	0.06
Y02of27	0.01	0.24	0.003	0.50	0.04
Y03of27	0.01	0.24	0.005	0.48	0.02
Y04of27	0.01	0.84	0.001	0.43	-0.03
Y05of27	0.01	0.84	0.003	0.41	-0.05
Y06of27	0.01	0.84	0.005	0.39	-0.07
Y07of27	0.01	1.44	0.001	0.34	-0.12
Y08of27	0.01	1.44	0.003	0.32	-0.14
Y09of27	0.01	1.44	0.005	0.30	-0.16
Y10of27	0.03	0.24	0.001	0.52	0.06
Y11of27	0.03	0.24	0.003	0.49	0.03
Y12of27	0.03	0.24	0.005	0.47	0.01
Y13of27	0.03	0.84	0.001	0.43	-0.03
Y14of27	0.03	0.84	0.003	0.41	-0.05
Y15of27	0.03	0.84	0.005	0.38	-0.08
Y16of27	0.03	1.44	0.001	0.33	-0.13
Y17of27	0.03	1.44	0.003	0.31	-0.15
Y18of27	0.03	1.44	0.005	0.29	-0.17
Y19of27	0.05	0.24	0.001	0.51	0.05
Y20of27	0.05	0.24	0.003	0.49	0.03
Y21of27	0.05	0.24	0.005	0.47	0.01
Y22of27	0.05	0.84	0.001	0.43	-0.03
Y23of27	0.05	0.84	0.003	0.40	-0.06
Y24of27	0.05	0.84	0.005	0.38	-0.08
Y25of27	0.05	1.44	0.001	0.33	-0.13
Y26of27	0.05	1.44	0.003	0.31	-0.15
Y27of27	0.05	1.44	0.005	0.28	-0.18

Appendix

A3 - FloodMap Point flood depth for sub-catchment 3

Simulation	Manning	DC (m/day)	HC (m/hr)	Depth (m)	Residual (m)
N01of27	0.01	0.24	0.001	0.47	0.15
N10of27	0.03	0.24	0.001	0.44	0.12
N19of27	0.05	0.24	0.001	0.41	0.09
N02of27	0.01	0.24	0.003	0.36	0.04
N11of27	0.03	0.24	0.003	0.33	0.01
N20of27	0.05	0.24	0.003	0.31	-0.01
N03of27	0.01	0.24	0.005	0.26	-0.06
N12of27	0.03	0.24	0.005	0.24	-0.08
N21of27	0.05	0.24	0.005	0.22	-0.10
N04of27	0.01	0.84	0.001	0.46	0.14
N13of27	0.03	0.84	0.001	0.44	0.12
N22of27	0.05	0.84	0.001	0.41	0.09
N05of27	0.01	0.84	0.003	0.35	0.03
N14of27	0.03	0.84	0.003	0.33	0.01
N23of27	0.05	0.84	0.003	0.30	-0.02
N06of27	0.01	0.84	0.005	0.25	-0.07
N15of27	0.03	0.84	0.005	0.24	-0.08
N24of27	0.05	0.84	0.005	0.21	-0.11
N07of27	0.01	1.44	0.001	0.46	0.14
N16of27	0.03	1.44	0.001	0.43	0.11
N25of27	0.05	1.44	0.001	0.41	0.09
N08of27	0.01	1.44	0.003	0.35	0.03
N17of27	0.03	1.44	0.003	0.32	0.00
N26of27	0.05	1.44	0.003	0.30	-0.02
N09of27	0.01	1.44	0.005	0.25	-0.07
N18of27	0.03	1.44	0.005	0.23	-0.09
N27of27	0.05	1.44	0.005	0.21	-0.11

Appendix

B1 - FloodMap Flood extent of the flood in sub-catchment 1

Simulation	Manning	DC (m/day)	HC (m/hr)	Flood extent (m^2)	Residual (m^2)
S01of27	0.01	0.24	0.001	140958	-27768
S02of27	0.01	0.24	0.003	138177	-30549
S03of27	0.01	0.24	0.005	135240	-33486
S04of27	0.01	0.84	0.001	124769	-43957
S05of27	0.01	0.84	0.003	119709	-49017
S06of27	0.01	0.84	0.005	113694	-55032
S07of27	0.01	1.44	0.001	101430	-67296
S08of27	0.01	1.44	0.003	96901	-71825
S09of27	0.01	1.44	0.005	92632	-76094
S10of27	0.03	0.24	0.001	141674	-27052
S11of27	0.03	0.24	0.003	138827	-29899
S12of27	0.03	0.24	0.005	135984	-32742
S13of27	0.03	0.84	0.001	125777	-42949
S14of27	0.03	0.84	0.003	121515	-47211
S15of27	0.03	0.84	0.005	117747	-50979
S16of27	0.03	1.44	0.001	102620	-66106
S17of27	0.03	1.44	0.003	97239	-71487
S18of27	0.03	1.44	0.005	92966	-75760
S19of27	0.05	0.24	0.001	142164	-26562
S20of27	0.05	0.24	0.003	139400	-29326
S21of27	0.05	0.24	0.005	136568	-32158
S22of27	0.05	0.84	0.001	126797	-41929
S23of27	0.05	0.84	0.003	122346	-46380
S24of27	0.05	0.84	0.005	118220	-50506
S25of27	0.05	1.44	0.001	103405	-65321
S26of27	0.05	1.44	0.003	98908	-69818
S27of27	0.05	1.44	0.005	94379	-74347

Appendix

B2- FloodMap Flood extent (Area) of the flood in Sub-catchment 2

Simulation	Manning	DC (m/day)	HC (m/hr)	Flood extent (m^2)	Residual
Y01of27	0.01	0.24	0.001	753058	316368
Y02of27	0.01	0.24	0.003	740073	303383
Y03of27	0.01	0.24	0.005	726956	290266
Y04of27	0.01	0.84	0.001	680682	243992
Y05of27	0.01	0.84	0.003	660943	224253
Y06of27	0.01	0.84	0.005	642358	205668
Y07of27	0.01	1.44	0.001	579839	143149
Y08of27	0.01	1.44	0.003	559310	122620
Y09of27	0.01	1.44	0.005	536372	99682
Y10of27	0.03	0.24	0.001	757037	320347
Y11of27	0.03	0.24	0.003	744479	307789
Y12of27	0.03	0.24	0.005	731690	295000
Y13of27	0.03	0.84	0.001	686055	249365
Y14of27	0.03	0.84	0.003	666457	229767
Y15of27	0.03	0.84	0.005	647878	211188
Y16of27	0.03	1.44	0.001	587576	150886
Y17of27	0.03	1.44	0.003	567350	130660
Y18of27	0.03	1.44	0.005	543445	106755
Y19of27	0.05	0.24	0.001	760649	323959
Y20of27	0.05	0.24	0.003	748660	311970
Y21of27	0.05	0.24	0.005	735868	299178
Y22of27	0.05	0.84	0.001	690258	253568
Y23of27	0.05	0.84	0.003	671152	234462
Y24of27	0.05	0.84	0.005	653514	216824
Y25of27	0.05	1.44	0.001	594399	157709
Y26of27	0.05	1.44	0.003	573975	137285
Y27of27	0.05	1.44	0.005	551644	114954

Appendix

B3- FloodMap Flood extent (Area) of the flood in sub-catchment 3

Simulation	Manning	DC (m/day)	HC (m/hr)	Flood extent (m^2)	Residual (m)
N01of27	0.01	0.24	0.001	370553	226369
N02of27	0.01	0.24	0.003	365291	221107
N03of27	0.01	0.24	0.005	359193	215009
N04of27	0.01	0.84	0.001	332705	188521
N05of27	0.01	0.84	0.003	324110	179926
N06of27	0.01	0.84	0.005	315055	170871
N07of27	0.01	1.44	0.001	282574	138390
N08of27	0.01	1.44	0.003	273664	129480
N09of27	0.01	1.44	0.005	264976	120792
N10of27	0.03	0.24	0.001	378707	234523
N11of27	0.03	0.24	0.003	373869	229685
N12of27	0.03	0.24	0.005	367383	223199
N13of27	0.03	0.84	0.001	341501	197317
N14of27	0.03	0.84	0.003	331705	187521
N15of27	0.03	0.84	0.005	322587	178403
N16of27	0.03	1.44	0.001	290833	146649
N17of27	0.03	1.44	0.003	280905	136721
N18of27	0.03	1.44	0.005	271547	127363
N19of27	0.05	0.24	0.001	385471	241287
N20of27	0.05	0.24	0.003	380005	235821
N21of27	0.05	0.24	0.005	373960	229776
N22of27	0.05	0.84	0.001	347837	203653
N23of27	0.05	0.84	0.003	338400	194216
N24of27	0.05	0.84	0.005	329302	185118
N25of27	0.05	1.44	0.001	297795	153611
N26of27	0.05	1.44	0.003	287989	143805
N27of27	0.05	1.44	0.005	277947	133763

Appendix

C1- CityCAT point flood depth for sub-catchment 1

Simulation	Manning - Buildings	Manning-vegetation	HC (m/hr)	Depth (m)	Residual
S01of27	0.5	0.25	0.001	0.54	-0.16
S02of27	0.5	0.25	0.003	0.54	-0.16
S03of27	0.5	0.25	0.005	0.54	-0.16
S04of27	0.5	0.3	0.001	0.54	-0.16
S05of27	0.5	0.3	0.003	0.54	-0.16
S06of27	0.5	0.3	0.005	0.54	-0.16
S07of27	0.5	0.35	0.001	0.54	-0.16
S08of27	0.5	0.35	0.003	0.54	-0.16
S09of27	0.5	0.35	0.005	0.54	-0.16
S10of27	0.75	0.25	0.001	0.54	-0.16
S11of27	0.75	0.25	0.003	0.54	-0.16
S12of27	0.75	0.25	0.005	0.54	-0.16
S13of27	0.75	0.3	0.001	0.54	-0.16
S14of27	0.75	0.3	0.003	0.54	-0.16
S15of27	0.75	0.3	0.005	0.54	-0.16
S16of27	0.75	0.35	0.001	0.54	-0.16
S17of27	0.75	0.35	0.003	0.54	-0.16
S18of27	0.75	0.35	0.005	0.54	-0.16
S27of27	1	0.35	0.005	0.53	-0.17
S19of27	1	0.25	0.001	0.53	-0.17
S20of27	1	0.25	0.003	0.53	-0.17
S21of27	1	0.25	0.005	0.53	-0.17
S22of27	1	0.3	0.001	0.53	-0.17
S23of27	1	0.3	0.003	0.53	-0.17
S24of27	1	0.3	0.005	0.53	-0.17
S25of27	1	0.35	0.001	0.53	-0.17
S26of27	1	0.35	0.003	0.53	-0.17

Appendix

C2- CityCAT point flood depth for sub-catchment 2

Simulation	Manning - Buildings	Manning-vegetation	HC (m/hr)	Depth (m)	Residual (m)
Y01of27	0.5	0.25	0.001	0.3	-0.16
Y02of27	0.5	0.25	0.003	0.3	-0.16
Y03of27	0.5	0.25	0.005	0.3	-0.16
Y04of27	0.5	0.3	0.001	0.3	-0.16
Y05of27	0.5	0.3	0.003	0.3	-0.16
Y06of27	0.5	0.3	0.005	0.3	-0.16
Y07of27	0.5	0.35	0.001	0.3	-0.16
Y08of27	0.5	0.35	0.003	0.29	-0.17
Y09of27	0.5	0.35	0.005	0.29	-0.17
Y10of27	0.75	0.25	0.001	0.29	-0.17
Y11of27	0.75	0.25	0.003	0.29	-0.17
Y12of27	0.75	0.25	0.005	0.29	-0.17
Y13of27	0.75	0.3	0.001	0.29	-0.17
Y14of27	0.75	0.3	0.003	0.29	-0.17
Y15of27	0.75	0.3	0.005	0.29	-0.17
Y16of27	0.75	0.35	0.001	0.29	-0.17
Y17of27	0.75	0.35	0.003	0.29	-0.17
Y18of27	0.75	0.35	0.005	0.29	-0.17
Y19of27	1	0.25	0.001	0.29	-0.17
Y20of27	1	0.25	0.003	0.29	-0.17
Y21of27	1	0.25	0.005	0.29	-0.17
Y22of27	1	0.3	0.001	0.29	-0.17
Y23of27	1	0.3	0.003	0.29	-0.17
Y24of27	1	0.3	0.005	0.29	-0.17
Y25of27	1	0.35	0.001	0.29	-0.17
Y26of27	1	0.35	0.003	0.29	-0.17
Y27of27	1	0.35	0.005	0.29	-0.17

Appendix

C3- CityCAT Point flood depth for sub-catchment 3

Simulation	Manning - Buildings	Manning-vegetation	HC (m/hr)	Depth (m)	Residual (m)
N01of27	0.5	0.25	0.001	0.21	-0.11
N02of27	0.5	0.25	0.003	0.21	-0.11
N03of27	0.5	0.25	0.005	0.21	-0.11
N04of27	0.5	0.3	0.001	0.21	-0.11
N05of27	0.5	0.3	0.003	0.21	-0.11
N06of27	0.5	0.3	0.005	0.21	-0.11
N07of27	0.5	0.35	0.001	0.20	-0.12
N08of27	0.5	0.35	0.003	0.20	-0.12
N09of27	0.5	0.35	0.005	0.20	-0.12
N10of27	0.75	0.25	0.001	0.19	-0.13
N11of27	0.75	0.25	0.003	0.19	-0.13
N12of27	0.75	0.25	0.005	0.19	-0.13
N13of27	0.75	0.3	0.001	0.19	-0.13
N14of27	0.75	0.3	0.003	0.19	-0.13
N15of27	0.75	0.3	0.005	0.19	-0.13
N16of27	0.75	0.35	0.001	0.19	-0.13
N17of27	0.75	0.35	0.003	0.19	-0.13
N18of27	0.75	0.35	0.005	0.19	-0.13
N19of27	1	0.25	0.001	0.19	-0.13
N20of27	1	0.25	0.003	0.18	-0.14
N21of27	1	0.25	0.005	0.18	-0.14
N22of27	1	0.3	0.001	0.18	-0.14
N23of27	1	0.3	0.003	0.18	-0.14
N24of27	1	0.3	0.005	0.18	-0.14
N25of27	1	0.35	0.001	0.18	-0.14
N26of27	1	0.35	0.003	0.18	-0.14
N27of27	1	0.35	0.005	0.18	-0.14

Appendix

D1- CityCAT Flood extent (Area) of the flood in sub-catchment 1

Simulation	Manning - Buildings	Manning-vegetation	HC (m/hr)	Area (m^2)	Residual (m^2)
S25of27	1	0.35	0.001	138184	-30542
S19of27	1	0.25	0.001	138165	-30561
S22of27	1	0.3	0.001	138164	-30562
S26of27	1	0.35	0.003	138155	-30571
S23of27	1	0.3	0.003	138154	-30572
S24of27	1	0.3	0.005	138147	-30579
S21of27	1	0.25	0.005	138140	-30586
S20of27	1	0.25	0.003	138140	-30586
S27of27	1	0.35	0.005	138136	-30590
S16of27	0.75	0.35	0.001	137993	-30733
S13of27	0.75	0.3	0.001	137981	-30745
S18of27	0.75	0.35	0.005	137975	-30751
S17of27	0.75	0.35	0.003	137975	-30751
S10of27	0.75	0.25	0.001	137972	-30754
S14of27	0.75	0.3	0.003	137954	-30772
S11of27	0.75	0.25	0.003	137954	-30772
S12of27	0.75	0.25	0.005	137945	-30781
S15of27	0.75	0.3	0.005	137944	-30782
S04of27	0.5	0.3	0.001	137615	-31111
S07of27	0.5	0.35	0.001	137610	-31116
S08of27	0.5	0.35	0.003	137602	-31124
S05of27	0.5	0.3	0.003	137602	-31124
S06of27	0.5	0.3	0.005	137599	-31127
S01of27	0.5	0.25	0.001	137597	-31129
S09of27	0.5	0.35	0.005	137588	-31138
S03of27	0.5	0.25	0.005	137569	-31157
S02of27	0.5	0.25	0.003	137569	-31157

D2- CityCAT Flood extent (Area) of the flood in sub-catchment 2

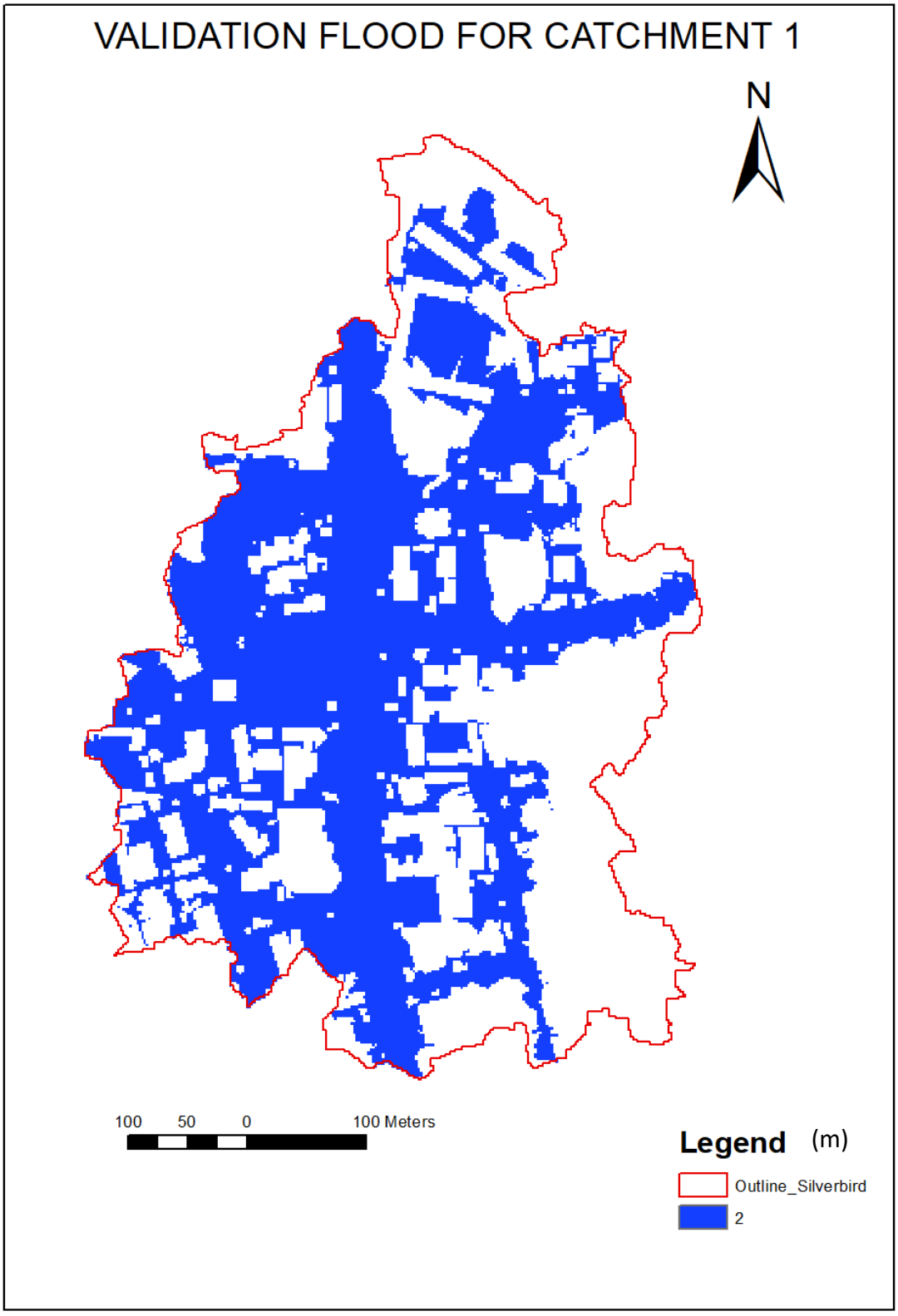
Simulation	Manning - Buildings	Manning-vegetation	HC (m/hr)	Area (m^2)	Residual (m^2)
Y25of27	1	0.35	0.001	588263	151573
Y22of27	1	0.3	0.001	588213	151523
Y26of27	1	0.35	0.003	588144	151454
Y23of27	1	0.3	0.003	588125	151435
Y19of27	1	0.25	0.001	588101	151411
Y27of27	1	0.35	0.005	588005	151315
Y24of27	1	0.3	0.005	587991	151301
Y20of27	1	0.25	0.003	587966	151276
Y21of27	1	0.25	0.005	587908	151218
Y16of27	0.75	0.35	0.001	587438	150748
Y13of27	0.75	0.3	0.001	587395	150705
Y10of27	0.75	0.25	0.001	587359	150669
Y17of27	0.75	0.35	0.003	587287	150597
Y14of27	0.75	0.3	0.003	587243	150553
Y18of27	0.75	0.35	0.005	587205	150515
Y11of27	0.75	0.25	0.003	587194	150504
Y15of27	0.75	0.3	0.005	587131	150441
Y12of27	0.75	0.25	0.005	587074	150384
Y07of27	0.5	0.35	0.001	586009	149319
Y04of27	0.5	0.3	0.001	586000	149310
Y01of27	0.5	0.25	0.001	585963	149273
Y08of27	0.5	0.35	0.003	585875	149185
Y05of27	0.5	0.3	0.003	585865	149175
Y09of27	0.5	0.35	0.005	585814	149124
Y06of27	0.5	0.3	0.005	585789	149099
Y02of27	0.5	0.25	0.003	585771	149081
Y03of27	0.5	0.25	0.005	585670	148980

D3- CityCAT Flood extent (Area) of the flood in sub-catchment 3

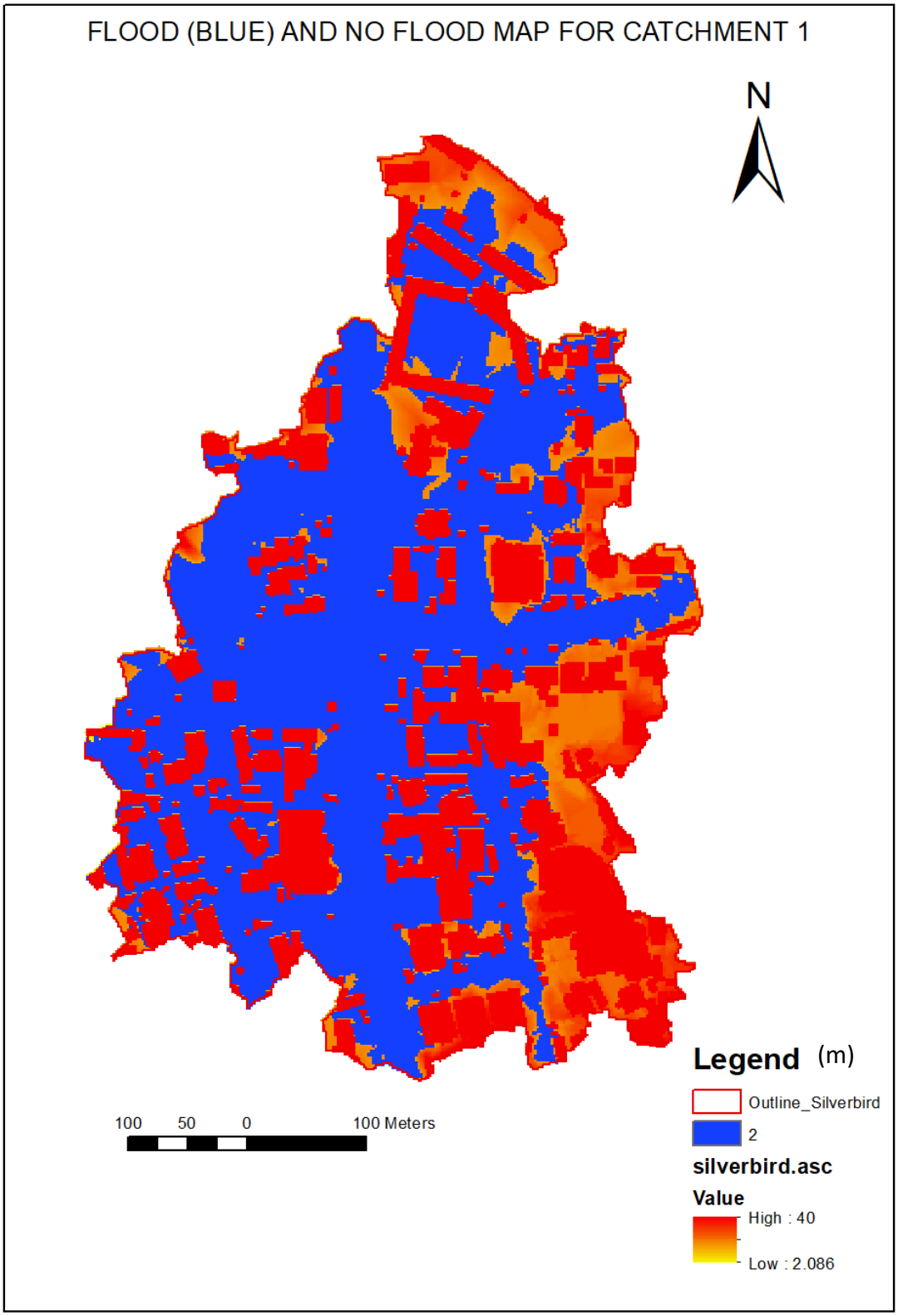
Simulation	Manning - Buildings	Manning- vegetation	HC (m/hr)	Area (m^2)	Residual (m^2)
N25of27	1	0.35	0.001	330416	-106274
N22of27	1	0.3	0.001	330320	-106370
N26of27	1	0.35	0.003	330229	-106461
N23of27	1	0.3	0.003	330141	-106549
N16of27	0.75	0.35	0.001	330138	-106552
N19of27	1	0.25	0.001	330134	-106556
N27of27	1	0.35	0.005	330112	-106578
N24of27	1	0.3	0.005	330039	-106651
N13of27	0.75	0.3	0.001	330037	-106653
N17of27	0.75	0.35	0.003	330023	-106667
N20of27	1	0.25	0.003	329997	-106693
N18of27	0.75	0.35	0.005	329938	-106752
N14of27	0.75	0.3	0.003	329900	-106790
N10of27	0.75	0.25	0.001	329886	-106804
N21of27	1	0.25	0.005	329849	-106841
N15of27	0.75	0.3	0.005	329798	-106892
N11of27	0.75	0.25	0.003	329712	-106978
N12of27	0.75	0.25	0.005	329536	-107154
N07of27	0.5	0.35	0.001	329226	-107464
N04of27	0.5	0.3	0.001	329115	-107575
N08of27	0.5	0.35	0.003	329056	-107634
N01of27	0.5	0.25	0.001	328922	-107768
N05of27	0.5	0.3	0.003	328884	-107806
N09of27	0.5	0.35	0.005	328859	-107831
N02of27	0.5	0.25	0.003	328800	-107890
N06of27	0.5	0.3	0.005	328773	-107917
N03of27	0.5	0.25	0.005	328653	-108037

Appendix

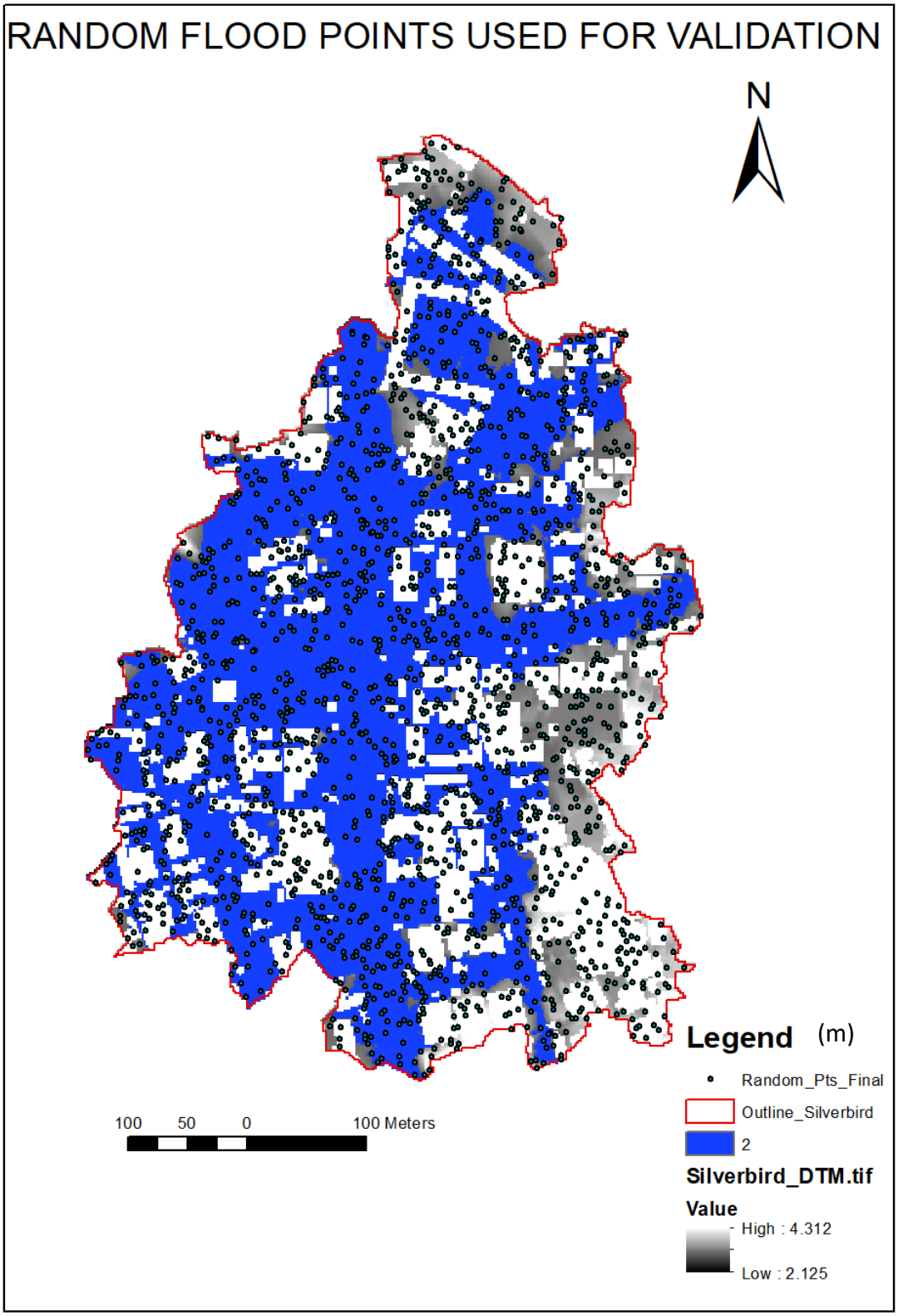
E1 - Validation flood map for sub-catchment 1



E2- Flood (blue) and no flood (red) Boolean classification of validation flood

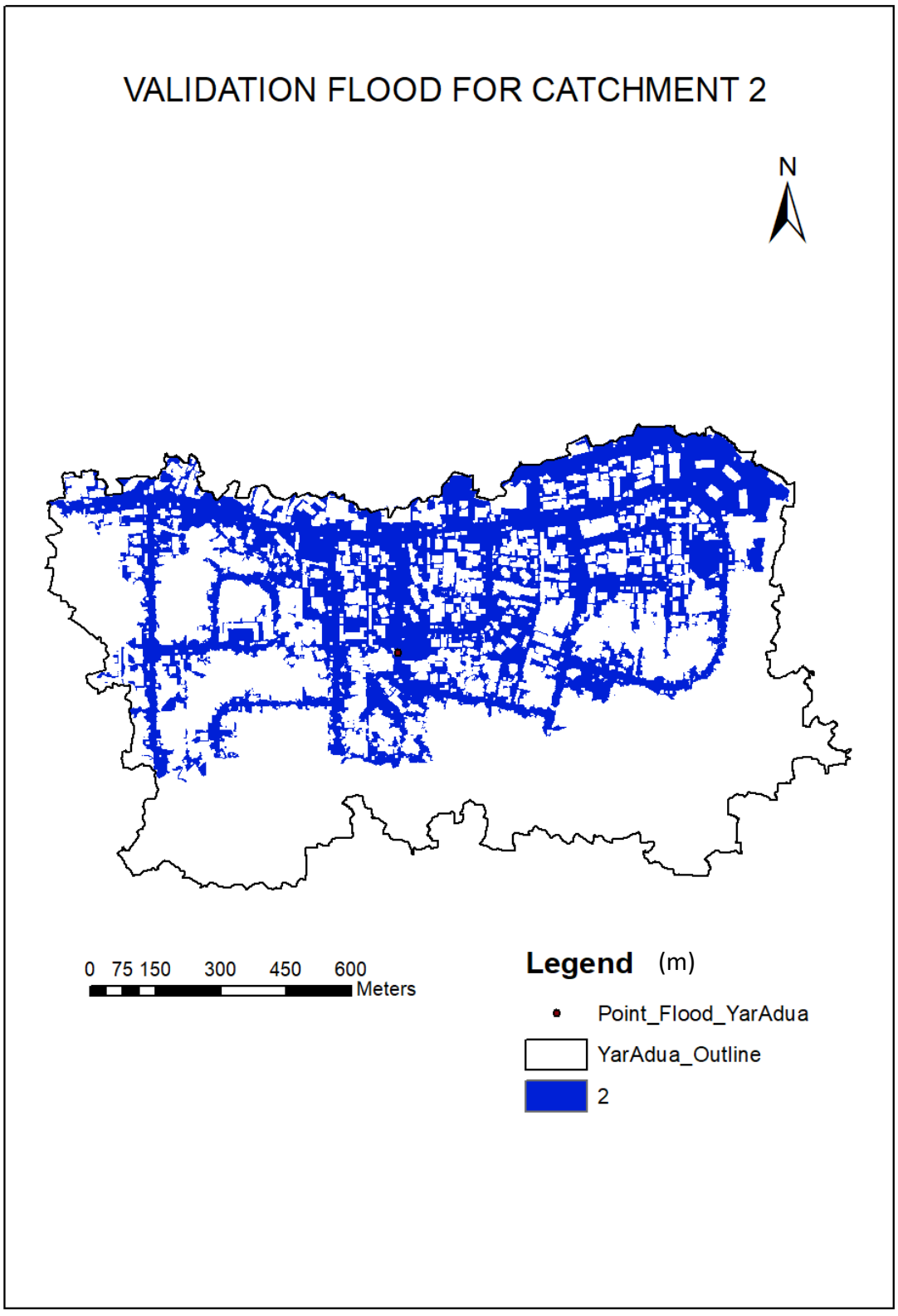


E3- Random points for analysis with predicted flood

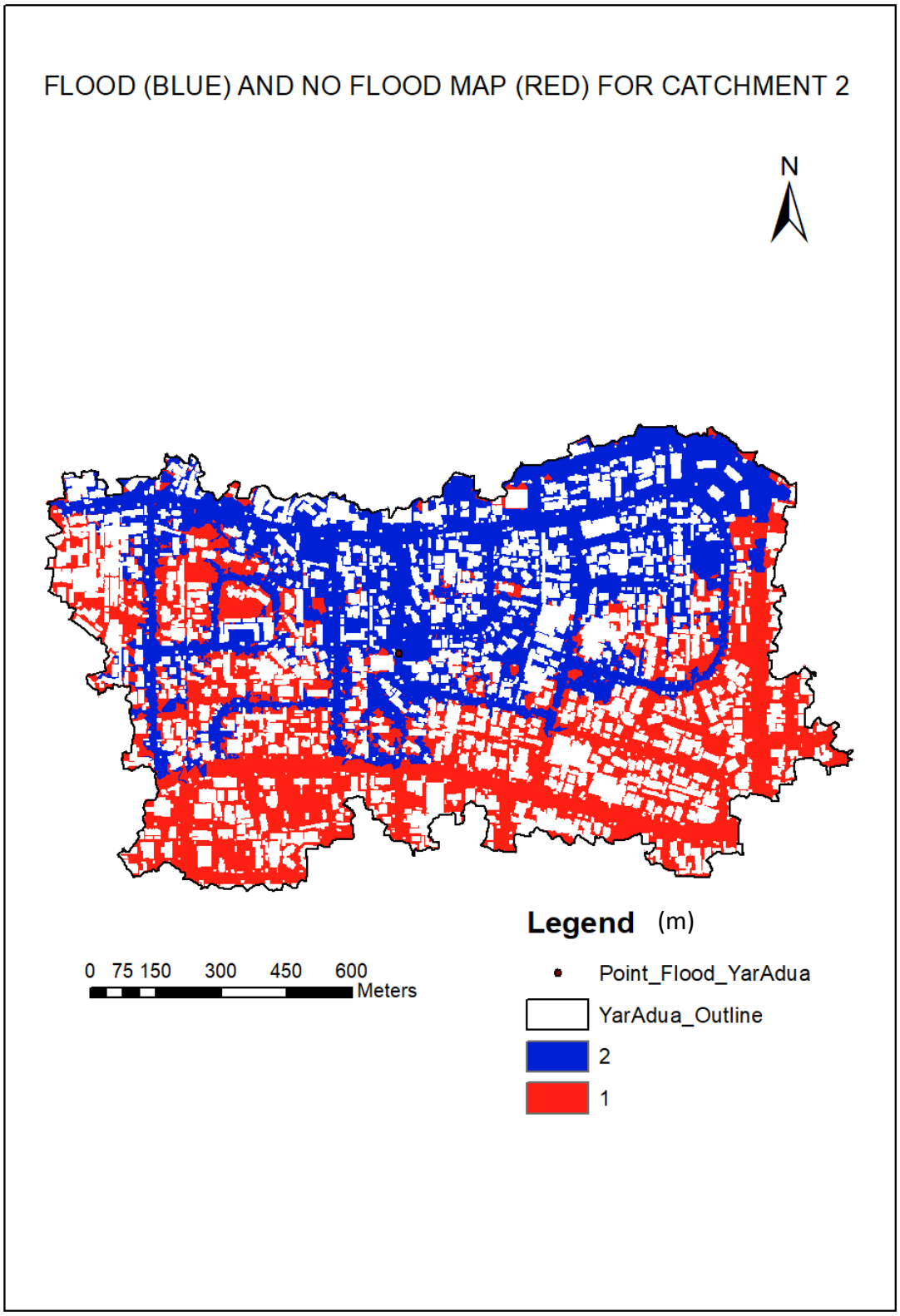


Appendix

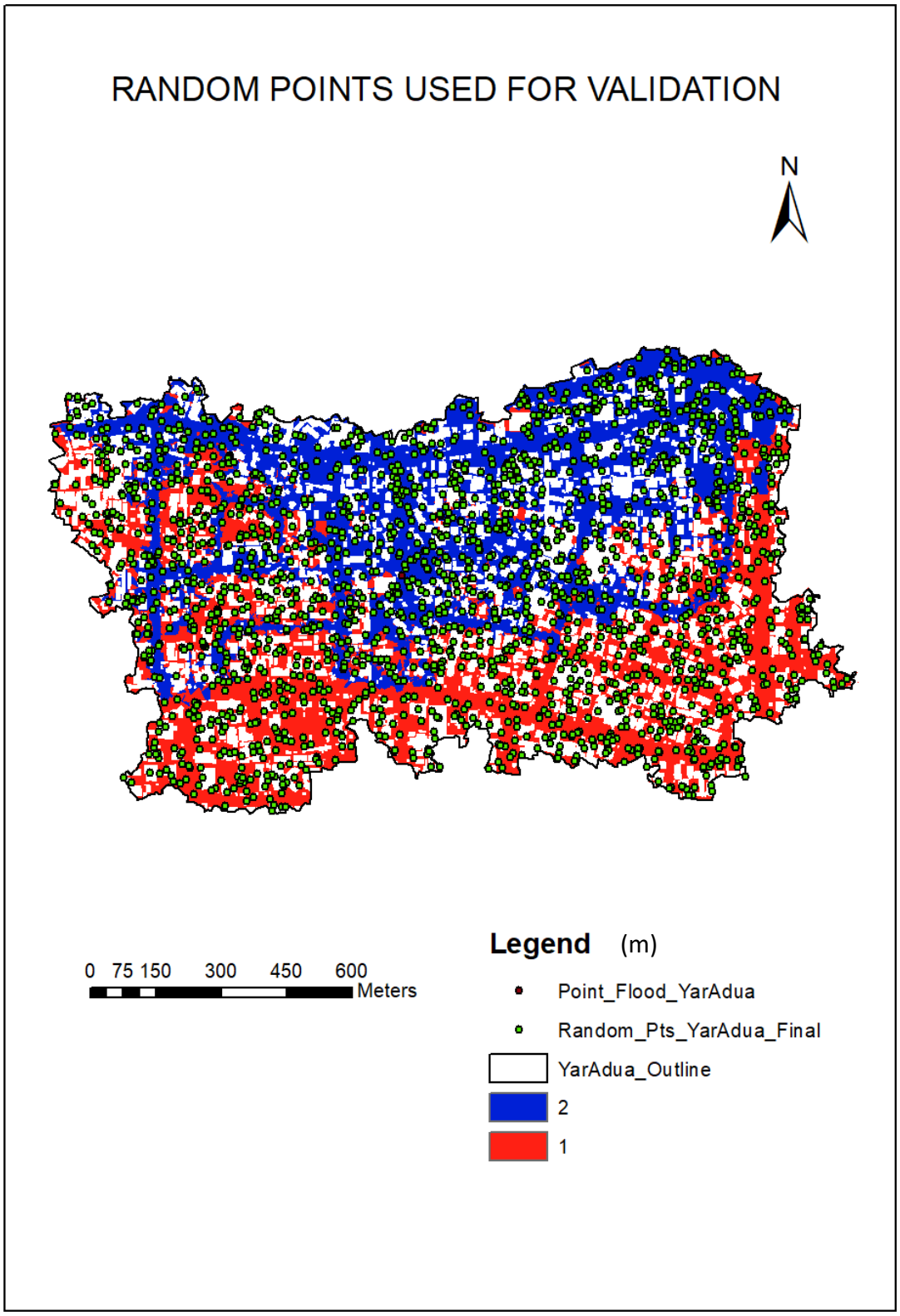
F4- Validation flood for sub-catchment 2



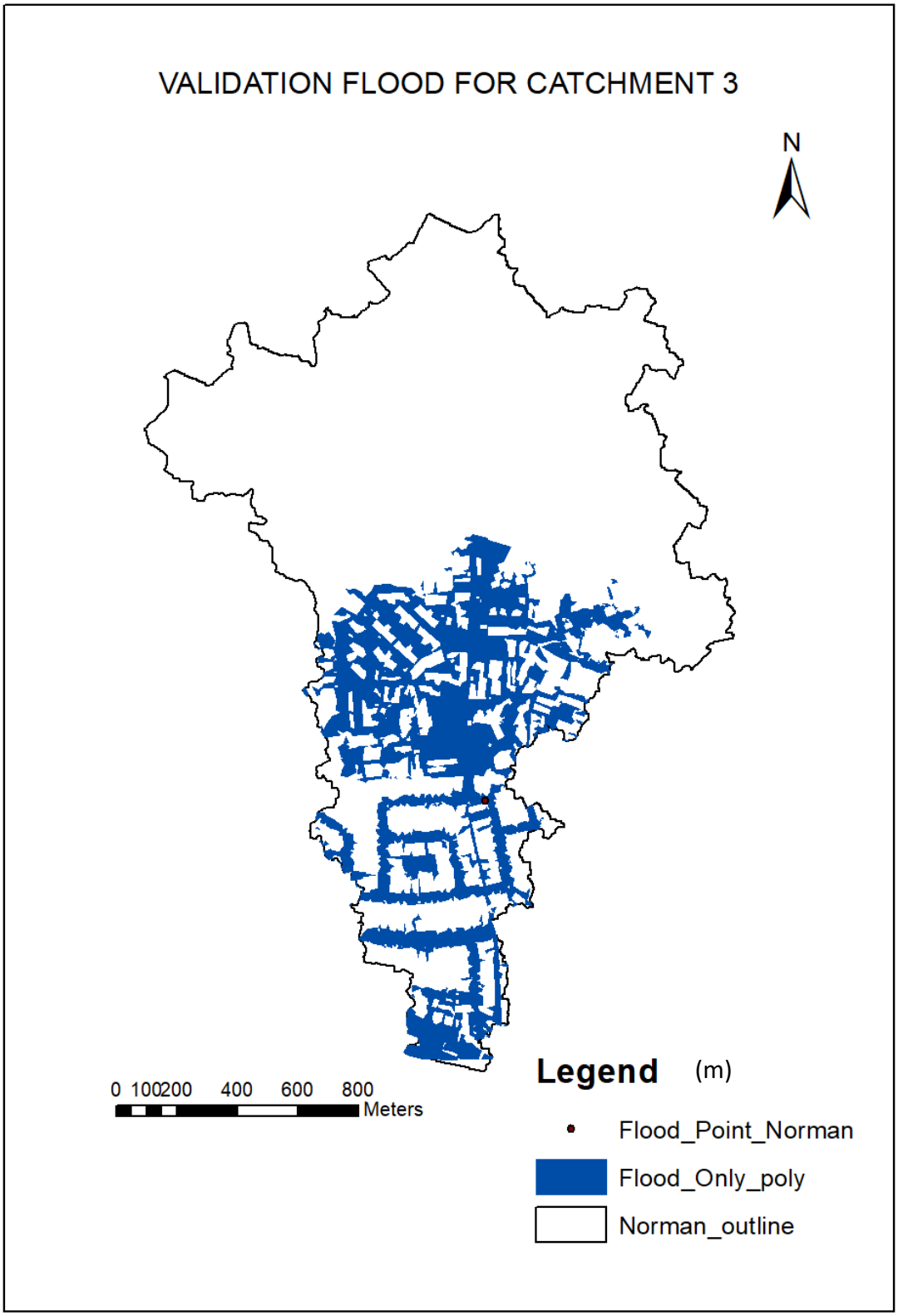
F5- Flood (blue) and no flood (red) Boolean classification of validation flood for sub-catchment 2



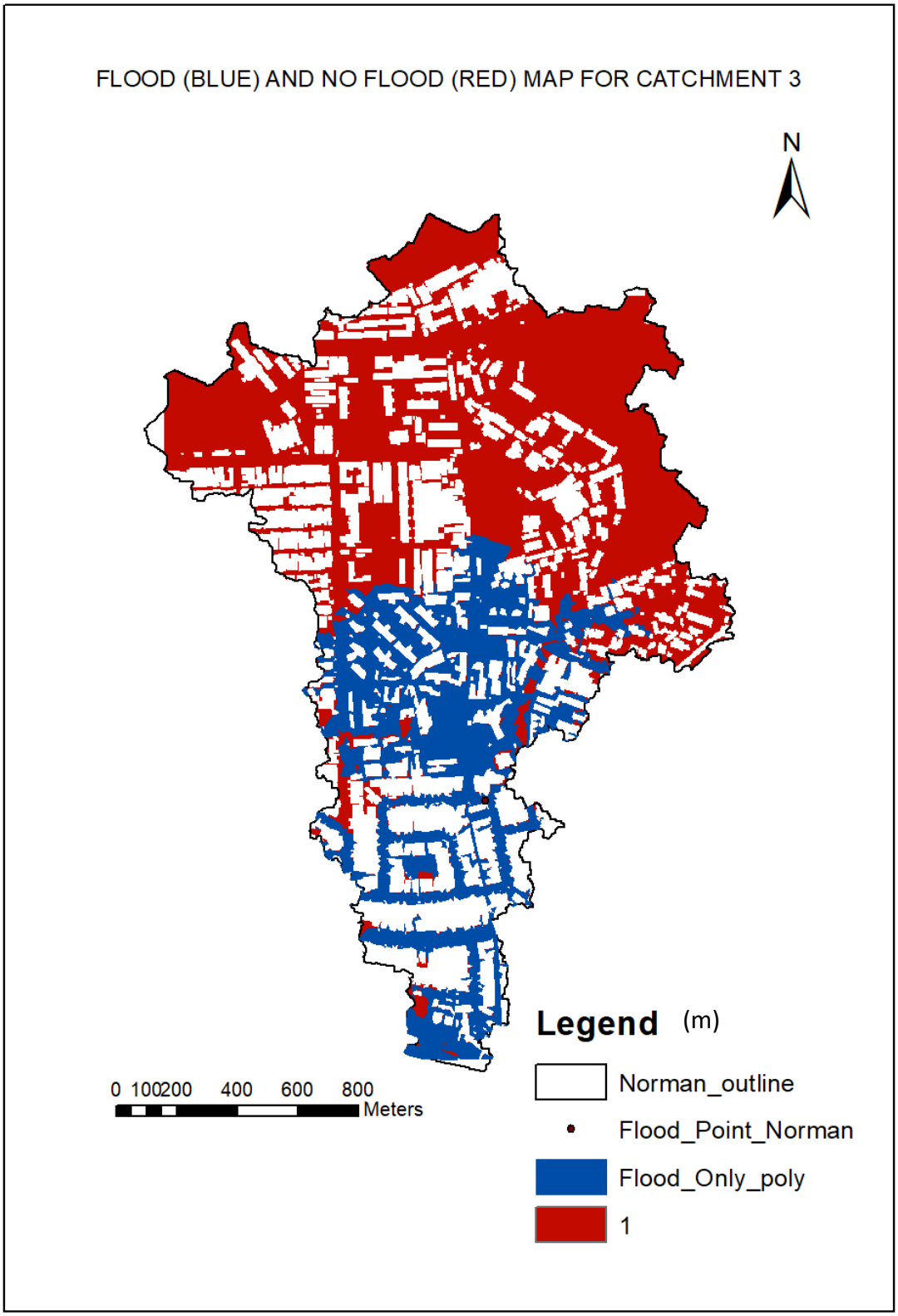
F6- Random points for analysis with predicted flood- sub-catchment 2



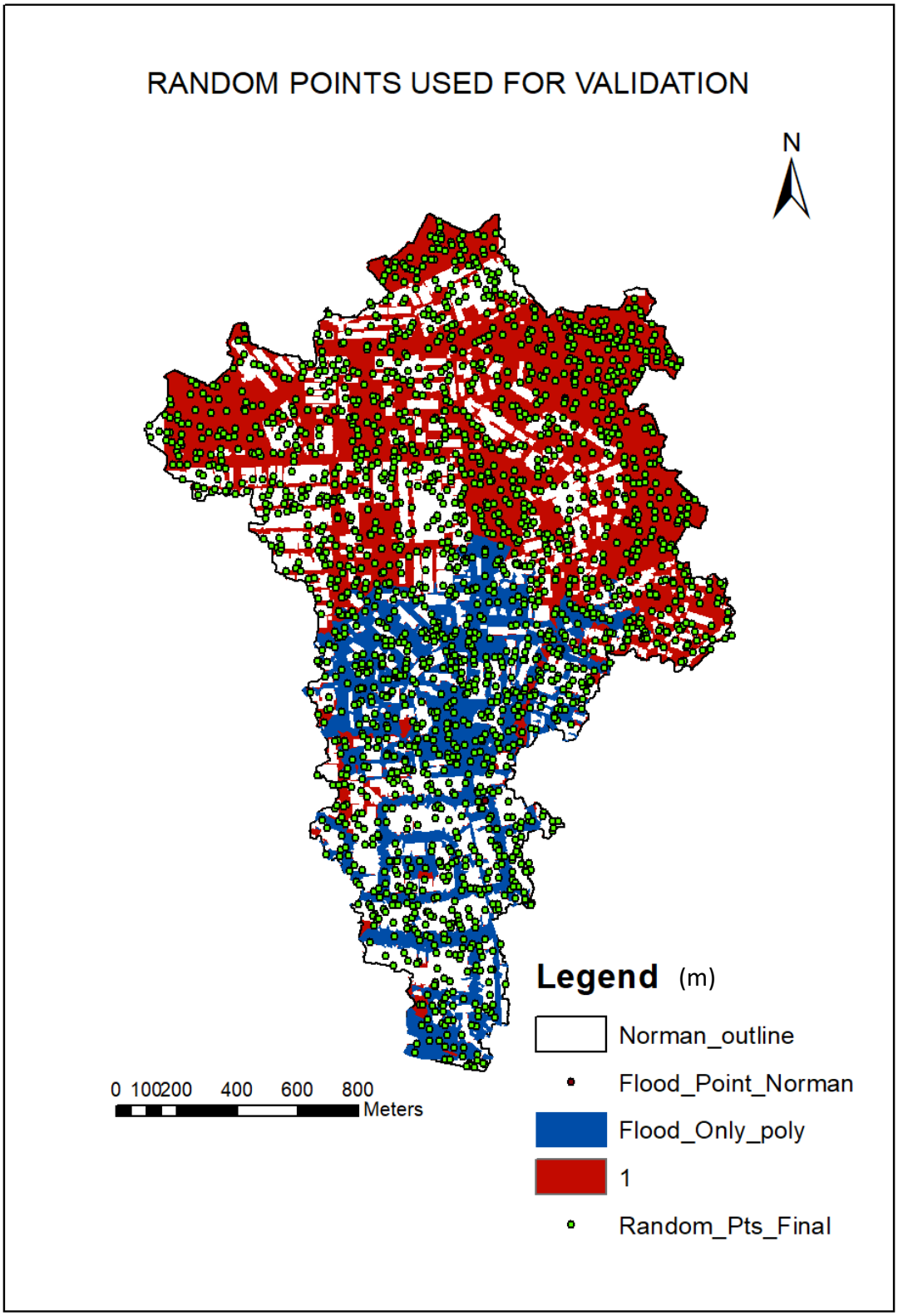
F7- Validation flood for sub-catchment 3



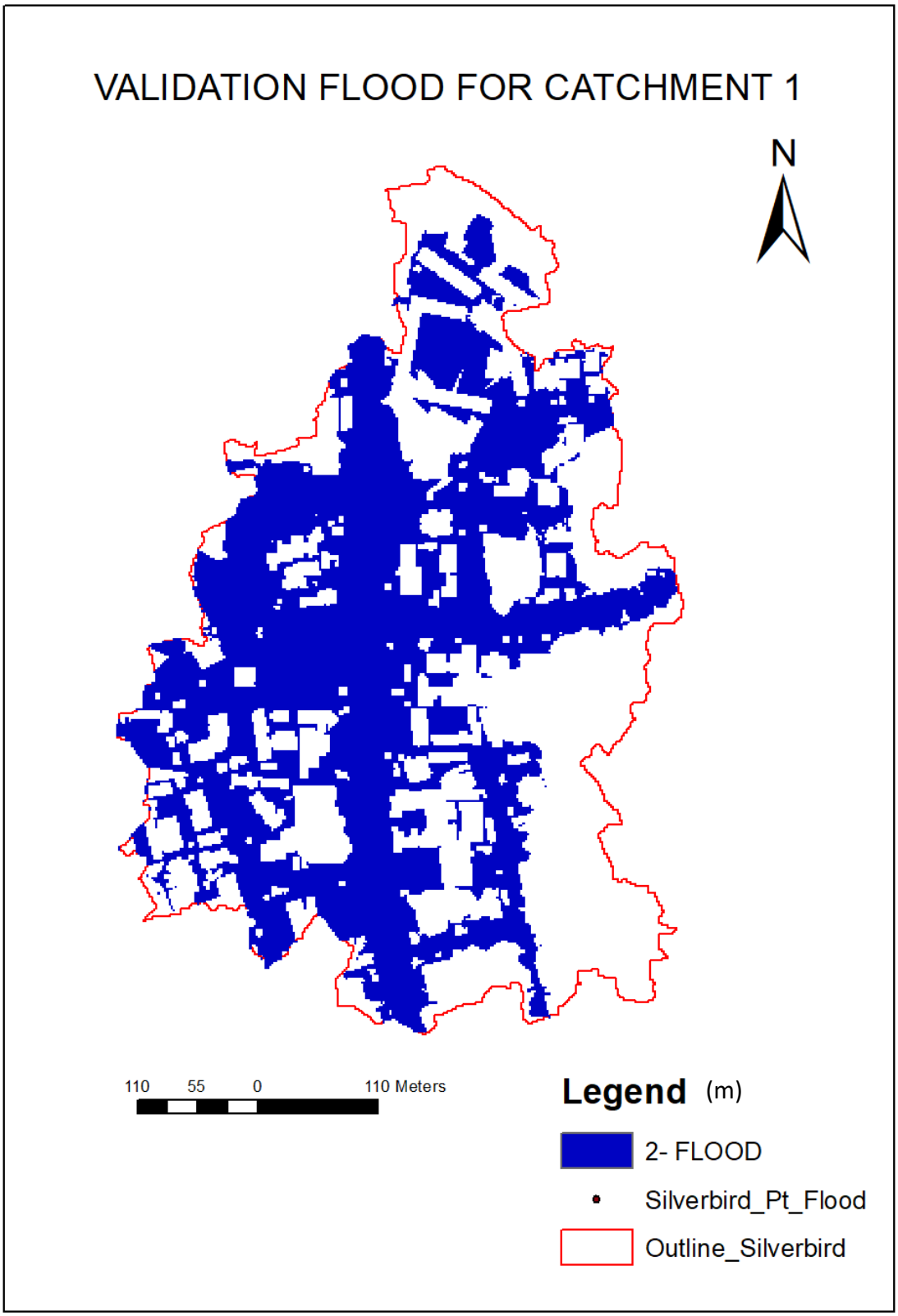
F8- Flood (blue) and no flood (red) Boolean classification of validation flood for sub-catchment 3



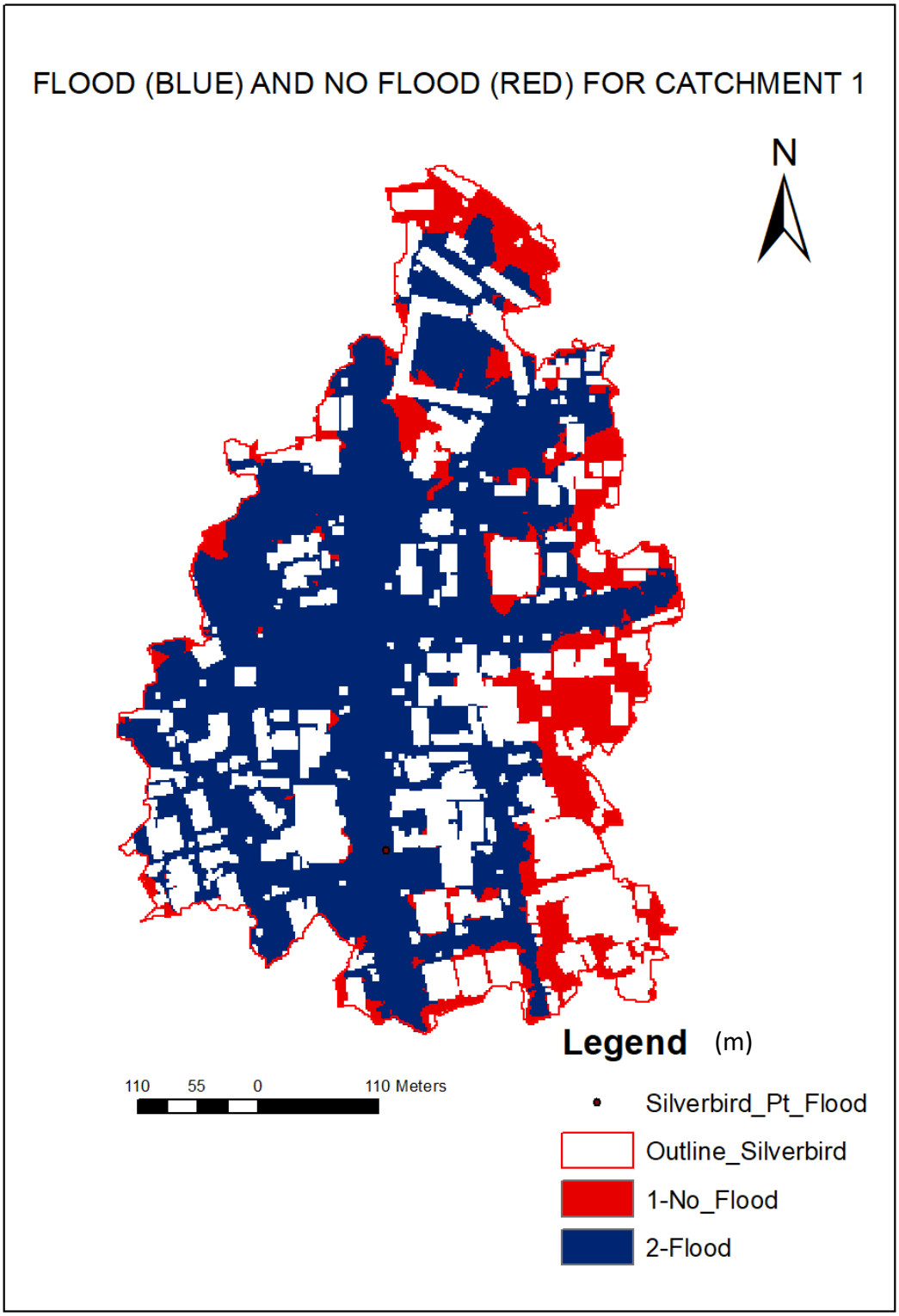
F9- Random points for analysis with predicted flood- sub-catchment 3



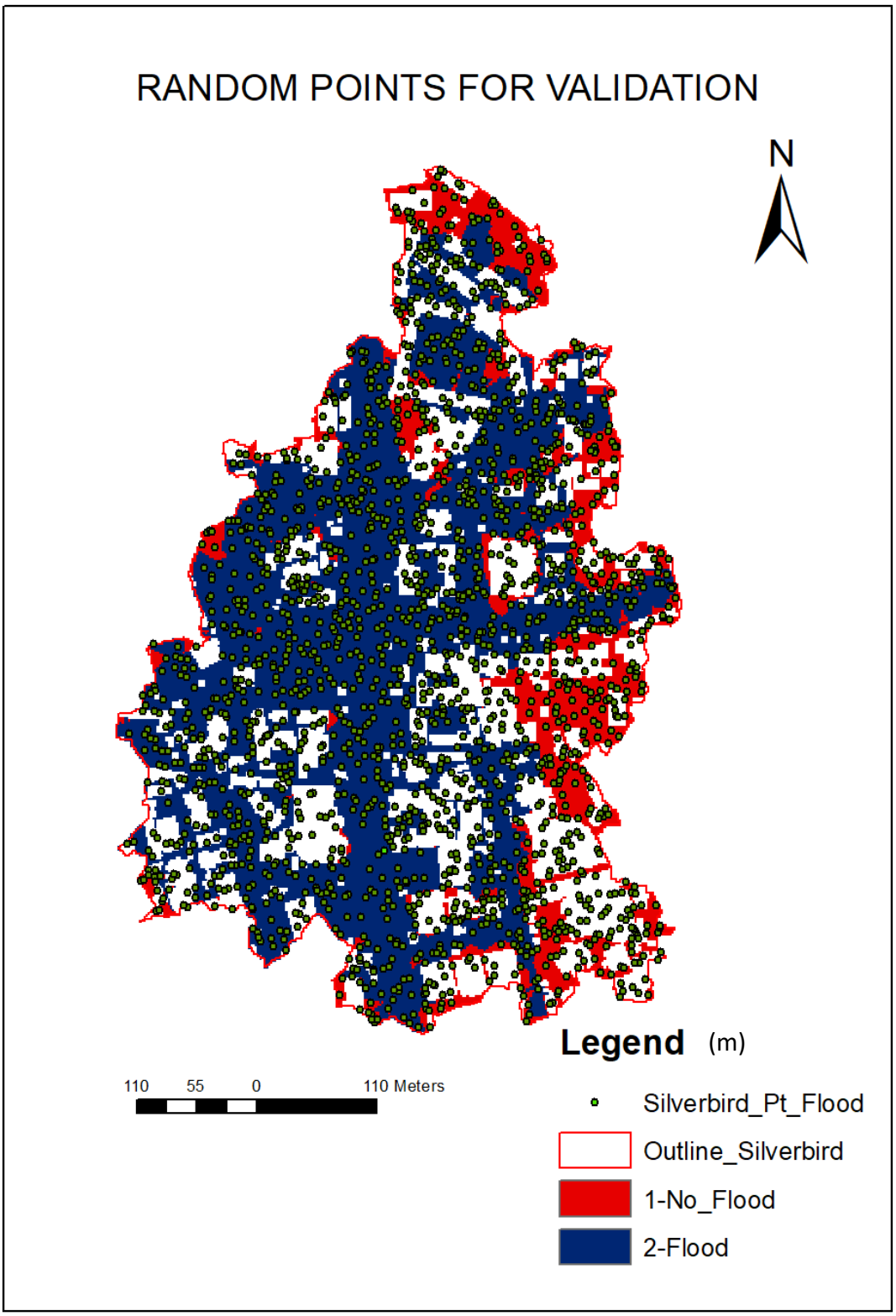
F10- Validation flood for sub-catchment 1



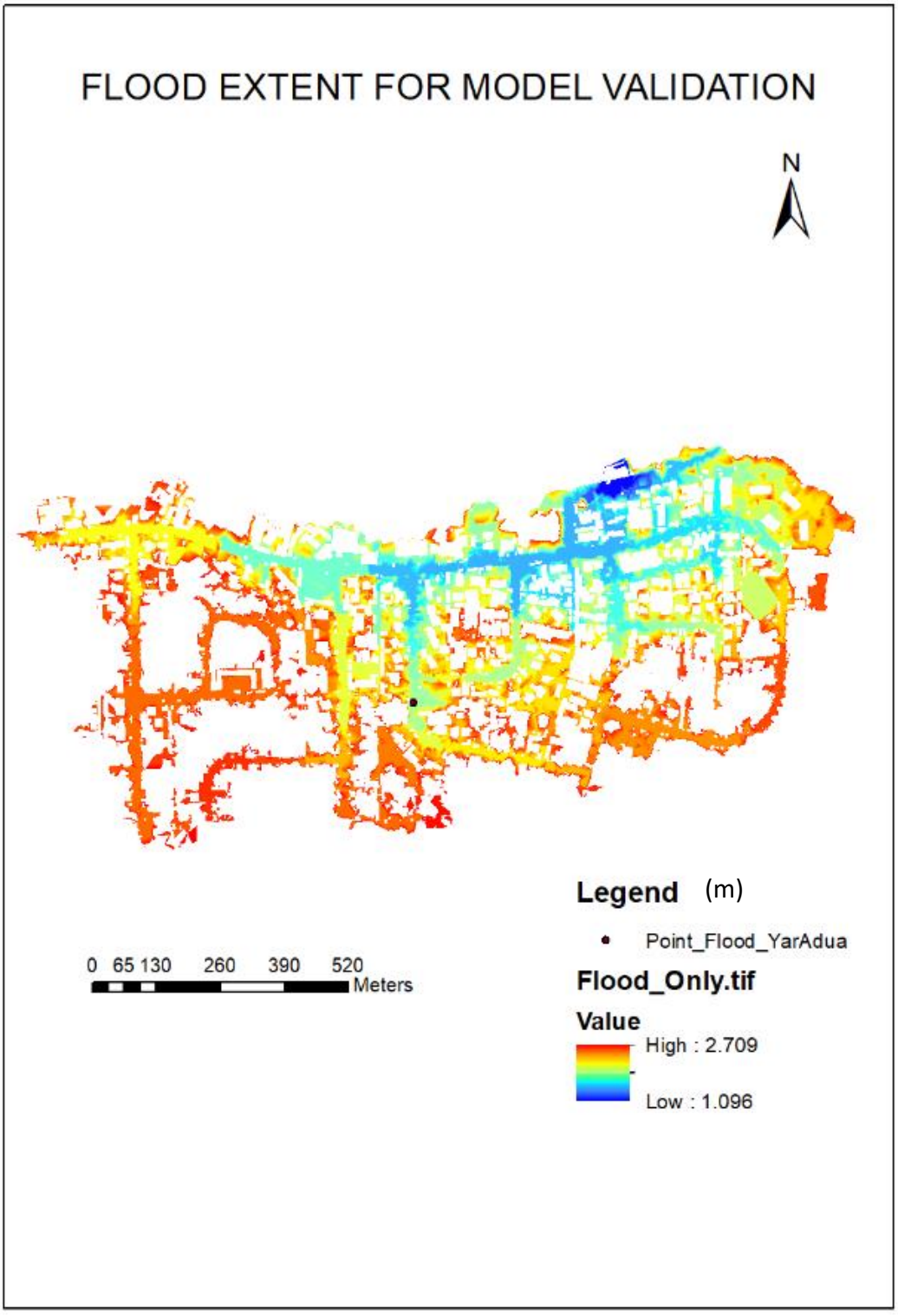
F11- Flood (blue) and no flood (red) Boolean classification of validation flood for sub-catchment 1



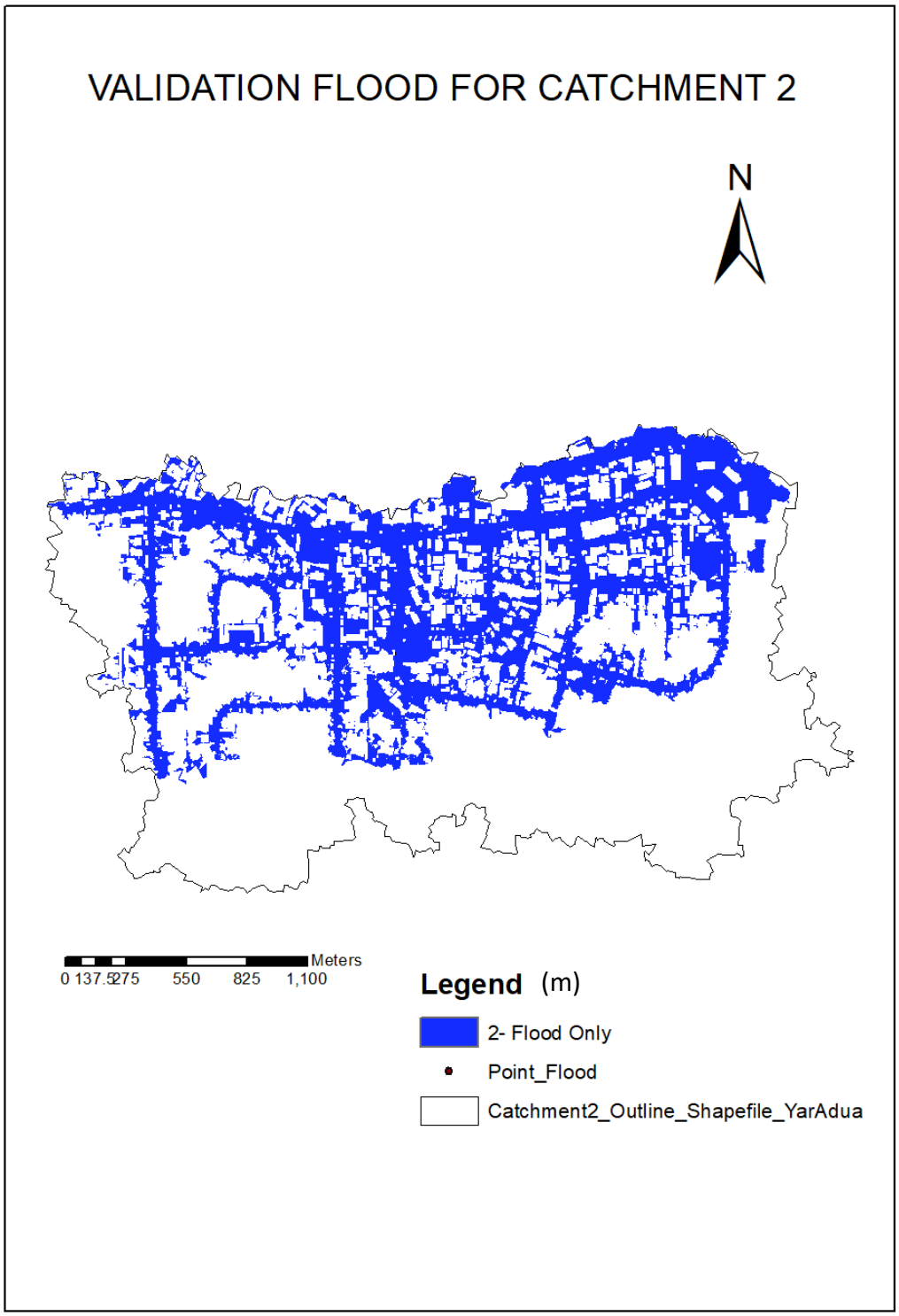
F12- Random points for analysis with predicted flood- sub-catchment 1



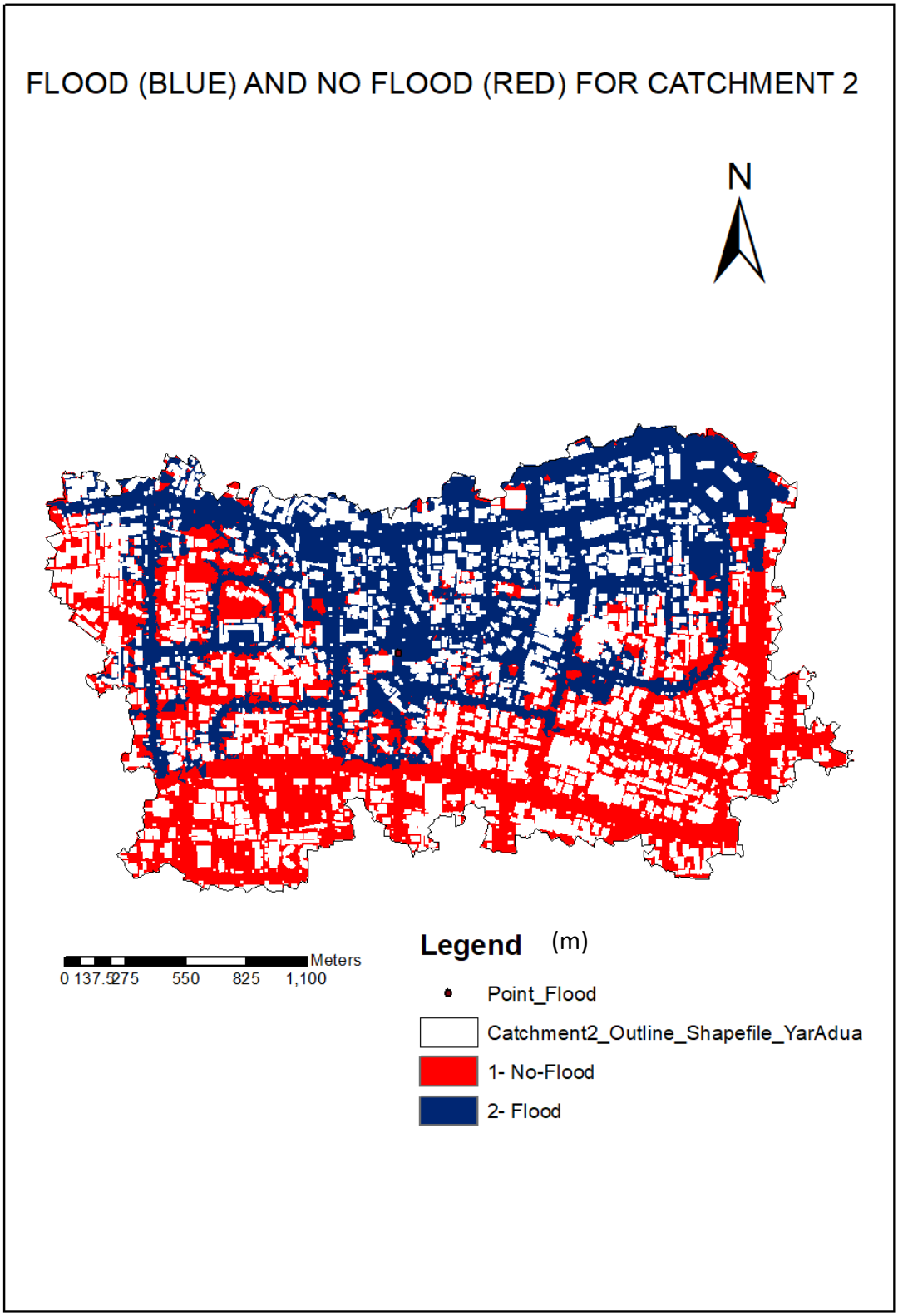
F14- Flood extent for validating sub-catchment 2



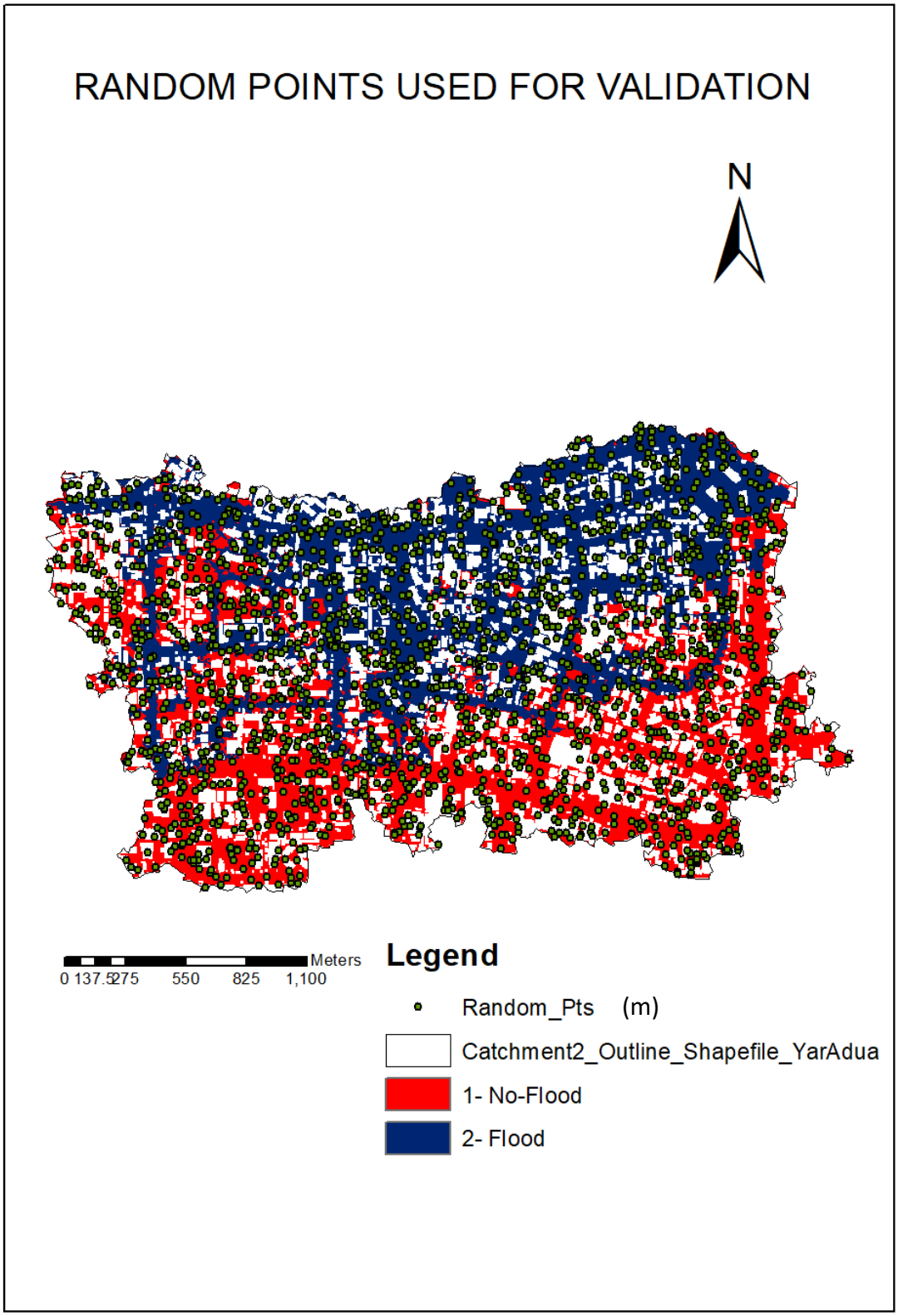
F15- Validation flood for sub-catchment 2



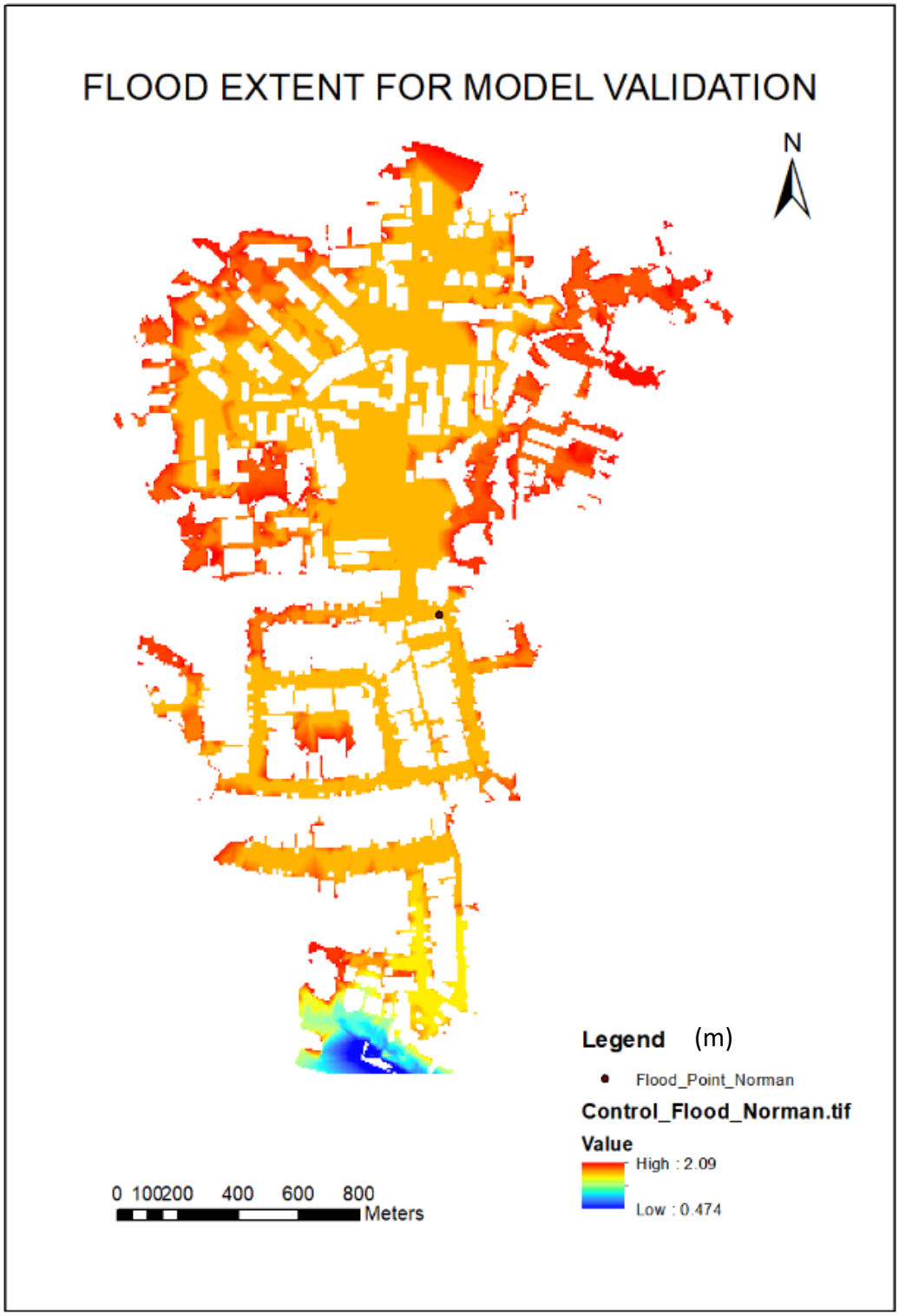
F16- Flood (blue) and no flood (red) Boolean classification of validation flood for Sub-catchment 2



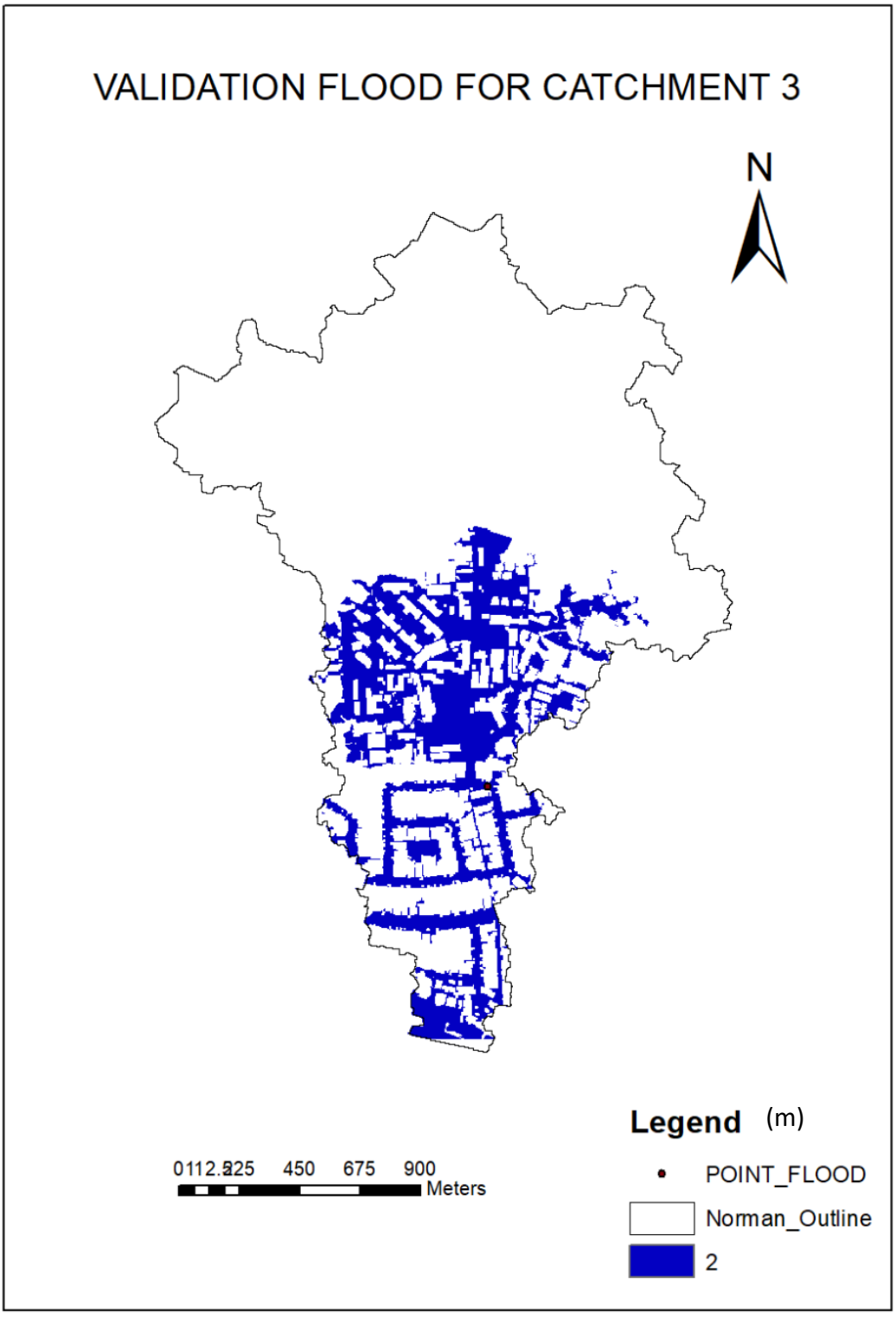
F17- Random points for analysis with predicted flood- Sub-catchment 2



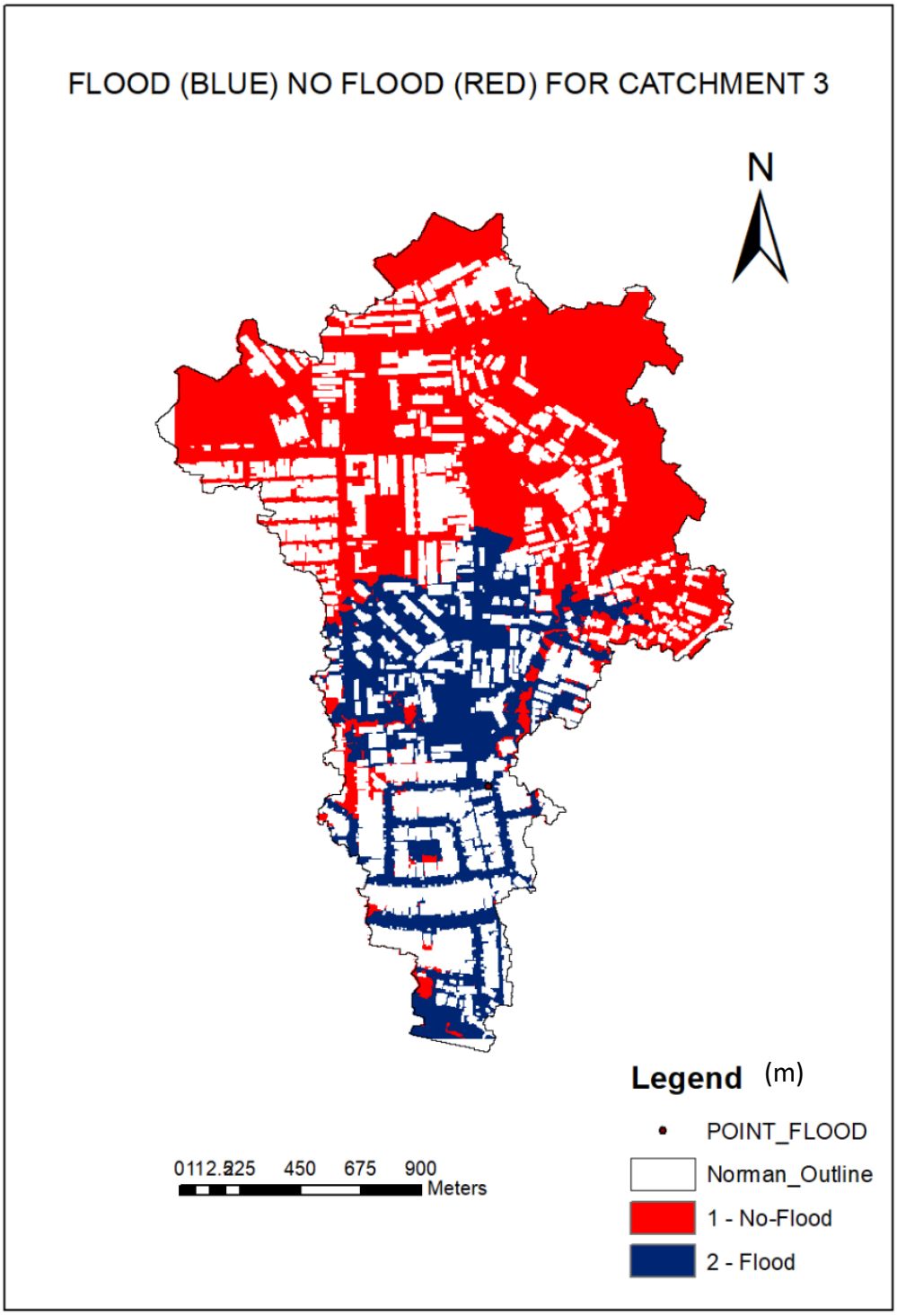
F18- Flood extent for validating Sub-catchment 3



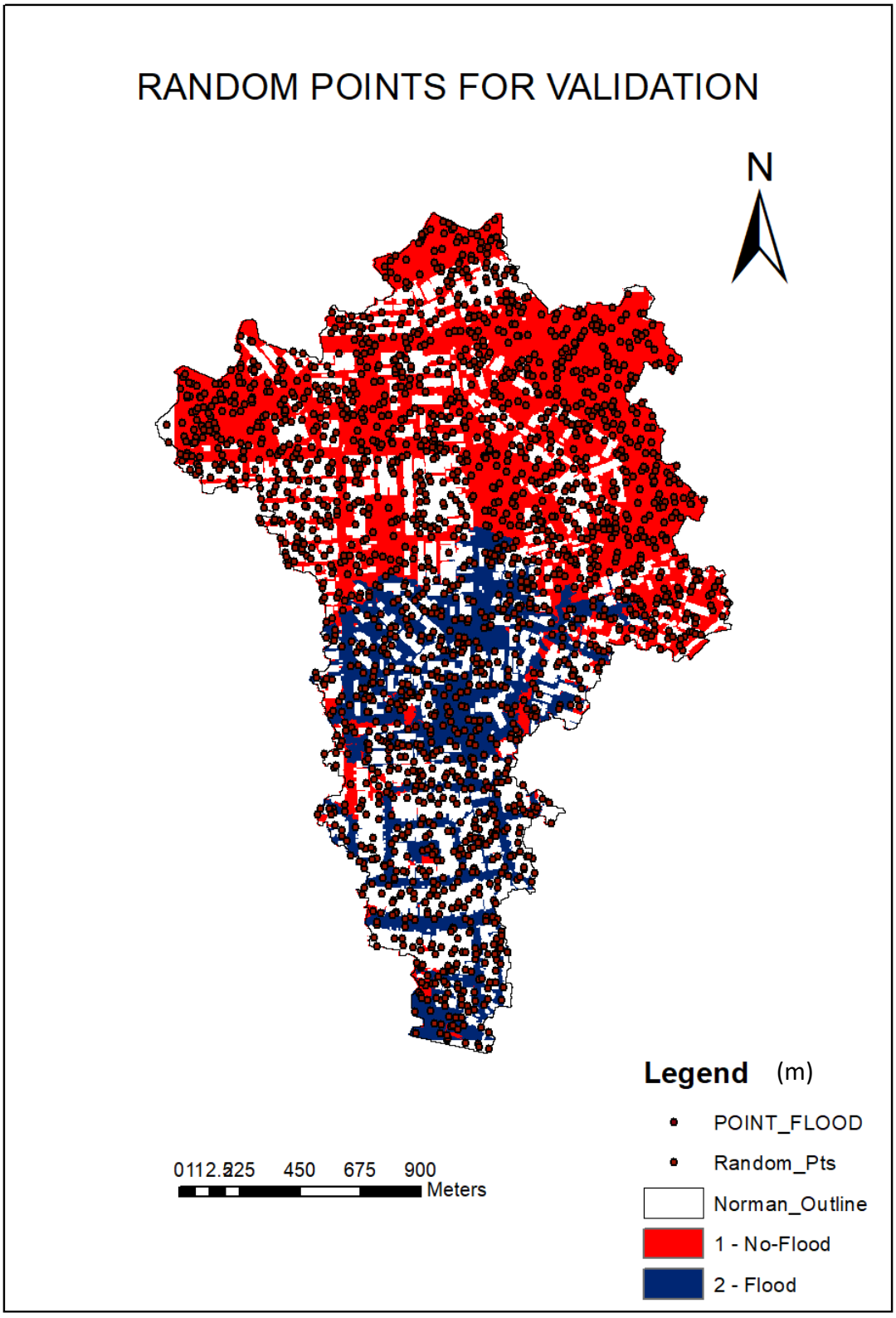
F19- Validation flood for sub-catchment 3



F20- Flood (blue) and no flood (red) Boolean classification of validation flood for sub-catchment 3



F21- Random points for analysis with predicted flood- sub-catchment 3



References

Abdi, M., Karimi, A., Navidbakhsh, M., Pirzad Jahromi, G., & Hassani, K. (2015). A lumped parameter mathematical model to analyze the effects of tachycardia and bradycardia on the cardiovascular system. *International Journal of Numerical Modelling: Electronic Networks, Devices and Fields, 28*(3), 346-357.

Acharya, A. S., Prakash, A., Saxena, P., & Nigam, A. (2013). Sampling: Why and how of it. *Indian Journal of Medical Specialties, 4*(2), 330-333.

Adams III, T. (2016). Flood forecasting in the United States NOAA/National Weather Service *Flood Forecasting* (pp. 249-310): Elsevier.

Adams, T. E., & Pagano, T. (2016). *Flood forecasting: A global perspective*: Academic Press.

Adefisoye, T. (2015). An Assessment of Nigeria's Institutional Capacity in Disaster Management. *Scientific Research Journal (SCIRJ), Volume III*(Issue I).

Adelekan, I. O. (2010). Vulnerability of poor urban coastal communities to flooding in Lagos, Nigeria. *Environment and Urbanization, 22*(2), 433-450.

Adnan, M. S. G., Abdullah, A. Y. M., Dewan, A., & Hall, J. W. (2020). The effects of changing land use and flood hazard on poverty in coastal Bangladesh. *Land use policy, 99*, 104868.

Aitamurto, T., & Saldivar, J. (2017). Motivating participation in crowdsourced policymaking: The interplay of epistemic and interactive aspects. *Proceedings of the ACM on Human-Computer Interaction, 1*(CSCW), 1-22.

Ajibola, Y. H., Gbenro, O. P., & Khadijah, L. A. (2018). Land use effects on soil erodibility and hydraulic conductivity in Akure, Nigeria. *African Journal of Agricultural Research, 13*(7), 329-337.

Aliyu, A., Liman-Hamza, K., & Lawal, A. (2023). Floods in Sub-Saharan Africa; Causes, Determinants and Health Consequences: Floods in Sub-Saharan Africa. *Nigerian Medical Journal, 64*(1), 13-24.

Anderson, J., French, D., Benton, J., & Dennis, M. (2020). The effects of the Grow Green urban greening improvements on physical health and wellbeing behaviours in Manchester UK: A natural experimental study.

Arshad, B., Ogie, R., Barthelemy, J., Pradhan, B., Verstaevel, N., & Perez, P. (2019). Computer vision and IoT-based sensors in flood monitoring and mapping: A systematic review. *Sensors, 19*(22), 5012.

Atufu, C. E., & Holt, C. P. (2018). Evaluating the impacts of flooding on the residents of Lagos, Nigeria. *WIT Transactions on the Built Environment, 184*, 81-90.

Awosika, L., & Folorunsho, R. (2005). *Natural and anthropogenic hazards in the african coastal and ocean environment: need for holistic and pragmatic early warning system and management approach.* Paper presented at the Proceedings of OCEANS 2005 MTS/IEEE.

Aziz, A., & Tanaka, S. (2011). Regional parameterization and applicability of Integrated Flood Analysis System (IFAS) for flood forecasting of upper-middle Indus River. *Pakistan Journal of Meteorology, 8*(15), 21-38.

Bai, T., Mayer, A. L., Shuster, W. D., & Tian, G. (2018). The hydrologic role of urban green space in mitigating flooding (Luohe, China). *Sustainability, 10*(10), 3584.

Barbedo, J., Miguez, M., van der Horst, D., & Marins, M. (2014). Enhancing ecosystem services for flood mitigation: a conservation strategy for peri-urban landscapes? *Ecology and Society, 19*(2). doi:10.5751/es-06482-190254

Bates, P. D., & De Roo, A. (2000). A simple raster-based model for flood inundation simulation. *Journal of Hydrology, 236*(1-2), 54-77.

Bates, P. D., Horritt, M. S., Aronica, G., & Beven, K. (2004). Bayesian updating of flood inundation likelihoods conditioned on flood extent data. *Hydrological Processes, 18*(17), 3347-3370.

Bates, P. D., Horritt, M. S., & Fewtrell, T. J. (2010). A simple inertial formulation of the shallow water equations for efficient two-dimensional flood inundation modelling. *Journal of Hydrology, 387*(1-2), 33-45.

Bellos, V., & Tsakiris, G. (2015). Comparing various methods of building representation for 2D flood modelling in built-up areas. *Water Resources Management, 29*(2), 379-397.

Bernhofen, M. V., Whyman, C., Trigg, M. A., Sleigh, P. A., Smith, A. M., Sampson, C. C., Yamazaki, D., Ward, P. J., Rudari, R., & Pappenberger, F. (2018). A first collective validation of global fluvial flood models for major floods in Nigeria and Mozambique. *Environmental Research Letters, 13*(10), 104007.

Bhola, P. K., Nair, B. B., Leandro, J., Rao, S. N., & Disse, M. (2019). Flood inundation forecasts using validation data generated with the assistance of computer vision. *Journal of Hydroinformatics, 21*(2), 240-256. doi:10.2166/hydro.2018.044

Boettle, M., Rybski, D., & Kropp, J. P. (2016). Quantifying the effect of sea level rise and flood defence-a point process perspective on coastal flood damage. *Natural Hazards and Earth System Sciences, 16*(2), 559-576. doi:10.5194/nhess-16-559-2016

Borga, M., Anagnostou, E., Blöschl, G., & Creutin, J.-D. (2011). Flash flood forecasting, warning and risk management: the HYDRATE project. *Environmental Science & Policy, 14*(7), 834-844.

Borsch, S., & Simonov, Y. (2016). Operational hydrologic forecast system in Russia *Flood Forecasting* (pp. 169-181): Elsevier.

Brasington, J., & Richards, K. (1998). Interactions between model predictions, parameters and DTM scales for TOPMODEL. *Computers & geosciences, 24*(4), 299-314.

Braud, I., Vincendon, B., Anquetin, S., Ducrocq, V., & Creutin, J.-D. (2018). The challenges of flash flood forecasting *Mobility in the Face of Extreme Hydrometeorological Events 1* (pp. 63-88): Elsevier.

Brears, R. C. (2018). Blue-green infrastructure in managing urban water resources *Blue and Green Cities* (pp. 43-61): Springer.

Brears, R. C. (2018). From traditional grey infrastructure to blue-green infrastructure *Blue and Green Cities* (pp. 1-41): Springer.

Bricker, S., & Bloomfield, J. (2014). Controls on the basin-scale distribution of hydraulic conductivity of superficial deposits: a case study from the Thames Basin, UK. *Quarterly Journal of Engineering Geology and Hydrogeology, 47*(3), 223-236.

Broadmeadow, S., & Nisbet, T. (2010). Opportunity Mapping for Woodland to Reduce Flooding in the River Derwent, Cumbria. *Farnham, Surrey, UK: Forest Research*.

Brussee, A. R., Bricker, J. D., De Bruijn, K. M., Verhoeven, G. F., Winsemius, H. C., & Jonkman, S. N. (2021). Impact of hydraulic model resolution and loss of life model modification on flood fatality risk estimation: Case study of the Bommelerwaard, The Netherlands. *Journal of Flood Risk Management, 14*(3), e12713.

Bruwier, M., Mustafa, A., Aliaga, D. G., Archambeau, P., Erpicum, S., Nishida, G., Zhang, X., Pirotton, M., Teller, J., & Dewals, B. (2018). Influence of urban pattern on inundation flow in floodplains of lowland rivers. *Science of the Total Environment, 622*, 446-458.

Budhathoki, N. R., & Haythornthwaite, C. (2013). Motivation for open collaboration: Crowd and community models and the case of OpenStreetMap. *American Behavioral Scientist, 57*(5), 548-575.

Burnham, K. P., & Anderson, D. R. (2002). A practical information-theoretic approach. *Model selection and multimodel inference, 2*.

Calder, I., Harding, R., & Rosier, P. (1983). An objective assessment of soil-moisture deficit models. *Journal of Hydrology, 60*(1-4), 329-355.

Cancado, V., Brasil, L., Nascimento, N., & Guerra, A. (2008). *Flood risk assessment in an urban area: Measuring hazard and vulnerability*. Retrieved from https://web.sbe.hw.ac.uk/staffprofiles/bdgsa/11th_International_Conference_on_Urban_Drainage_CD/ICUD08/pdfs/699.pdf

Cao, X., Qi, Y., & Ni, G. (2021). Significant impacts of rainfall redistribution through the roof of buildings on urban hydrology. *Journal of Hydrometeorology, 22*(4), 1007-1023.

Casado, M. R., & Leinster, P. (2020). Towards more effective strategies to reduce property level flood risk: Standardising the use of Unmanned Aerial Vehicles. *Journal of Water Supply: Research and Technology-Aqua, 69*(8), 807-818.

Chakraborty, A., Messias, J., Benevenuto, F., Ghosh, S., Ganguly, N., & Gummadi, K. (2017). *Who makes trends? understanding demographic biases in crowdsourced recommendations.* Paper presented at the Proceedings of the International AAAI Conference on Web and Social Media.

Chakravarty, S., Ghosh, S. K., Suresh, C. P., Dey, A. N., & Shukla, G. (2012). *Deforestation: Causes, Effects and Control Strategies*. Paper presented at the Global Perspectives on Sustainable Forest Management

https://cdn.intechopen.com/pdfs/36125/InTechDeforestation_causes_effects_and_control_strategies.pdf

Chang, F.-J., & Guo, S. (2020). Advances in hydrologic forecasts and water resources management (Vol. 12, pp. 1819): Multidisciplinary Digital Publishing Institute.

Chen, Gao, B., & Devereux, B. (2017). State-of-the-art: DTM generation using airborne LIDAR data. *Sensors, 17*(1), 150.

Chen, Z., Gao, B., & Devereux, B. (2017). State-of-the-art: DTM generation using airborne LIDAR data. *Sensors, 17*(1), 150.

Chow, V. (1959). T. 1959 Open-Channel Hydraulics. *MCGraw Hiu*.

Collins, E. L., Sanchez, G. M., Terando, A., Stillwell, C. C., Mitasova, H., Sebastian, A., & Meentemeyer, R. K. (2022). Predicting flood damage probability across the conterminous United States. *Environmental Research Letters, 17*(3), 034006.

Costa, U., Andrade Jr, J., Makse, H., & Stanley, H. (1999). The role of inertia on fluid flow through disordered porous media. *Physica A: Statistical Mechanics and its Applications, 266*(1-4), 420-424.

Courty, L. G., Rico-Ramirez, M. A., & Pedrozo-Acuna, A. (2018). The Significance of the Spatial Variability of Rainfall on the Numerical Simulation of Urban Floods. *Water, 10*(2). doi:10.3390/w10020207

CRED. (2020). *Human cost of disasters. An overview of the last 20 years 2000-2019*. Retrieved from https://reliefweb.int/sites/reliefweb.int/files/resources/CredCrunch61-Humancost.pdf

CRED. (2021). *Disaster Year in Review 2020: Global Trends and Perspectives*. Retrieved from https://reliefweb.int/report/world/cred-crunch-newsletter-issue-no-62-may-2021-disaster-year-review-2020-global-trends-and

CRED. (2022). *EM-DAT The International Disaster Database*. Retrieved from: https://public.emdat.be/data

Critchley, W., Siegert, K., Chapman, C., & Finket, M. (2013). *Water harvesting: A manual for the design and construction of water harvesting schemes for plant production*: Scientific Publishers.

Dai, C., Howat, I. M., Larour, E., & Husby, E. (2019). Coastline extraction from repeat high resolution satellite imagery. *Remote Sensing of Environment, 229*, 260-270.

Danlami, D., Idris, S., Thlakma, R. S., & Gwandum, G. S. (2019). THE SPATIO-TEMPORAL VARIATIONS OF WIND SPEED DURING HARMATTAN SEASON IN NORTHEASTERN NIGERIA. *Geosfera Indonesia, 4*(2), 105-123.

Das, B., Jain, S., Singh, S., & Thakur, P. (2019). Evaluation of multisite performance of SWAT model in the Gomti River Basin, India. *Applied Water Science, 9*(5). doi:10.1007/s13201-019-1013-x

Davis, M., & Naumann, S. (2017). Making the case for sustainable urban drainage systems as a nature-based solution to urban flooding. *Nature-Based Solutions to Climate Change Adaptation in Urban Areas: Linkages between Science, Policy and Practice*, 123-137.

de Almeida, G. A., Bates, P., & Ozdemir, H. (2018). Modelling urban floods at submetre resolution: challenges or opportunities for flood risk management? *Journal of Flood Risk Management, 11*, S855-S865.

De Bruijn, K. M. (2004). Resilience and flood risk management. *Water Policy, 6*(1), 53-66.

Devi, N. N., Sridharan, B., & Kuiry, S. N. (2019). Impact of urban sprawl on future flooding in Chennai city, India. *Journal of Hydrology, 574*, 486-496.

Dewan, T. H. (2015). Societal impacts and vulnerability to floods in Bangladesh and Nepal. *Weather and Climate Extremes, 7*(Supplement C), 36-42. doi:10.1016/j.wace.2014.11.001

Dhara, S., Dang, T., Parial, K., & Lu, X. X. (2020). Accounting for uncertainty and reconstruction of flooding patterns based on multi-satellite imagery and support vector machine technique: A case study of Can Tho City, Vietnam. *Water, 12*(6), 1543.

Di Baldassarre, G., Laio, F., & Montanari, A. (2009). Design flood estimation using model selection criteria. *Physics and Chemistry of the Earth, Parts A/B/C, 34*(10-12), 606-611.

Diebold, C. (1942). An interpretation of certain infiltration values in forest areas obtained with the type F and type FA infiltrometers. *Soil science society of America journal, 6*(C), 423-429.

Dumbser, M., & Toro, E. F. (2011). On universal Osher-type schemes for general nonlinear hyperbolic conservation laws. *Communications in Computational Physics, 10*(3), 635-671.

Ebrahimi, N. G., Fathi-Moghadam, M., Kashefipour, S., Saneie, M., & Ebrahimi, K. (2008). Effects of flow and vegetation states on river roughness coefficients. *Journal of Applied Sciences, 8*(11), 2118-2123.

Emerton, R., Cloke, H., Ficchi, A., Hawker, L., de Wit, S., Speight, L., Prudhomme, C., Rundell, P., West, R., & Neal, J. (2020). Emergency flood bulletins for Cyclones Idai and Kenneth: a critical evaluation of the use of global flood forecasts for international humanitarian preparedness and response. *International Journal of Disaster Risk Reduction, 50*, 101811.

Emerton, R. E., Stephens, E. M., Pappenberger, F., Pagano, T. C., Weerts, A. H., Wood, A. W., Salamon, P., Brown, J. D., Hjerdt, N., & Donnelly, C. (2016). Continental and global scale flood forecasting systems. *Wiley Interdisciplinary Reviews: Water, 3*(3), 391-418.

Engelbrecht, F. A., & Vogel, C. H. (2021). When early warning is not enough. *One Earth, 4*(8), 1055-1058.

EPA. (2012). Wetlands Overview: United States Environmental Protection Agency. Retrieved from https://nepis.epa.gov/Exe/ZyPDF.cgi/500025PY.PDF?Dockey=500025PY.PDF

Erdelj, M., & Natalizio, E. (2016). *UAV-assisted disaster management: Applications and open issues.* Paper presented at the 2016 international conference on computing, networking and communications (ICNC).

Escobar Villanueva, J. R., Iglesias Martínez, L., & Pérez Montiel, J. I. (2019). DEM generation from fixed-wing UAV imaging and LiDAR-derived ground control points for flood estimations. *Sensors, 19*(14), 3205.

Fakhruddin, S., Kawasaki, A., & Babel, M. S. (2015). Community responses to flood early warning system: Case study in Kaijuri Union, Bangladesh. *International Journal of Disaster Risk Reduction, 14*, 323-331.

Fatemi, M. N., Okyere, S. A., Diko, S. K., Kita, M., Shimoda, M., & Matsubara, S. (2020). Physical vulnerability and local responses to flood damage in peri-urban areas of Dhaka, Bangladesh. *Sustainability, 12*(10), 3957.

Fernandez-Diaz, J. C., Carter, W. E., Shrestha, R. L., & Glennie, C. L. (2014). Now you see it… now you don't: Understanding airborne mapping LiDAR collection and data product generation for archaeological research in Mesoamerica. *Remote Sensing, 6*(10), 9951-10001.

Fleischmann, A., Paiva, R., & Collischonn, W. (2019). Can regional to continental river hydrodynamic models be locally relevant? A cross-scale comparison. *Journal of Hydrology X, 3*, 100027.

Fohringer, J., Dransch, D., Kreibich, H., & Schroter, K. (2015). Social media as an information source for rapid flood inundation mapping. *Natural Hazards and Earth System Sciences, 15*(12), 2725-2738. doi:10.5194/nhess-15-2725-2015

Forecasting, F. (2020). Warning Centre (FFWC). *Hydrographs of monsoon water level*.

Francés, F., Vélez, J. J., Vélez, J., & Puricelli, M. (2002). *Distributed modelling of large basins for a real time flood forecasting system in Spain.* Paper presented at the Proceedings Second Federal Interagency Hydrologic Modelling Conference, Gan, TY and Biftu, Las Vegas.

Francisco, T. H., Menezes, O. V., Guedes, A. L., Maquera, G., Neto, D. C., Longo, O. C., Chinelli, C. K., & Soares, C. A. (2022). The Main Challenges for Improving Urban Drainage Systems from the Perspective of Brazilian Professionals. *Infrastructures, 8*(1), 5.

Freeze, R. A., & Cherry, J. A. (1979). *Groundwater*. Retrieved from

Fritz, H. M., Blount, C. D., Albusaidi, F. B., & Al-Harthy, A. H. M. (2010). Cyclone Gonu storm surge in Oman. *Estuarine, Coastal and Shelf Science, 86*(1), 102-106.

Gao, M., Hugenholtz, C. H., Fox, T. A., Kucharczyk, M., Barchyn, T. E., & Nesbit, P. R. (2021). Weather constraints on global drone flyability. *Scientific reports, 11*(1), 1-13.

Gebrehiwot, A. A., & Hashemi-Beni, L. (2021). Three-dimensional inundation mapping using UAV image segmentation and digital surface model. *ISPRS International Journal of Geo-Information, 10*(3), 144.

Gerritsen, H. (2005). What happened in 1953? The Big Flood in the Netherlands in retrospect. *Philos Trans A Math Phys Eng Sci, 363*(1831), 1271-1291. doi:10.1098/rsta.2005.1568

Giannasi, F., Lovett, P., & Godwin, A. N. (2001). Enhancing confidence in discrete event simulations. *Computers in Industry, 44*(2), 141-157.

Glenis, V., Kutija, V., & Kilsby, C., G. (2018). A fully hydrodynamic urban flood modelling system representing buildings, green space and interventions. *Environmental Modelling and Software*.

Glenis, V., Kutija, V., & Kilsby, C. G. (2018). A fully hydrodynamic urban flood modelling system representing buildings, green space and interventions. *Environmental Modelling & Software, 109*, 272-292.

Glenis, V., McGough, A. S., Kutija, V., Kilsby, C., G, & Woodman, S. (2013). Flood modelling for cities using Cloud computing. *Journal of Cloud Computing: Advances, Systems and Applications, 2*(1), 7.

Green, D., Yu, D., Pattison, I., Wilby, R., Bosher, L., Patel, R., Thompson, P., Trowell, K., Draycon, J., & Halse, M. (2017). City-scale accessibility of emergency responders operating during flood events. *Natural Hazards and Earth System Sciences, 17*(1), 1-16.

Green, W. H., & Ampt, G. A. (1911). Studies on Soil Phyics. *The Journal of Agricultural Science, 4*(1), 1-24.

Guest, J. K., & Prévost, J. H. (2007). Design of maximum permeability material structures. *Computer Methods in Applied Mechanics and Engineering, 196*(4-6), 1006-1017.

Gupta, A. K., & Nair, S. S. (2011). Urban floods in Bangalore and Chennai: risk management challenges and lessons for sustainable urban ecology. *Current Science*, 1638-1645.

Gupta, H. V., Beven, K. J., & Wagener, T. (2006). Model calibration and uncertainty estimation. *Encyclopedia of hydrological sciences*.

Hackl, J., Adey, B. T., Woźniak, M., & Schümperlin, O. (2018). Use of unmanned aerial vehicle photogrammetry to obtain topographical information to improve bridge risk assessment. *Journal of Infrastructure Systems, 24*(1), 04017041.

Haile, A. T., & Rientjes, T. (2005). Effects of LiDAR DEM resolution in flood modelling: a model sensitivity study for the city of Tegucigalpa, Honduras. *Isprs wg iii/3, iii/4, 3*, 12-14.

Hajian-Tilaki, K. (2013). Receiver operating characteristic (ROC) curve analysis for medical diagnostic test evaluation. *Caspian journal of internal medicine, 4*(2), 627.

Hamby, D. M. (1994). A review of techniques for parameter sensitivity analysis of environmental models. *Environmental monitoring and assessment, 32*(2), 135-154.

Hamby, D. M. (1995). A comparison of sensitivity analysis techniques. *Health Physics, 68*(2), 195-204.

Hankin, B., Lamb, R., Craigen, I., Page, T., Chappell, N., & Metcalfe, P. (2017). A whole catchment approach to improve flood resilience in the Eden, Winning entry to the Defra Flood Modelling Competition 2016 [Internet].

Hapuarachchi, H., Wang, Q., & Pagano, T. (2011). A review of advances in flash flood forecasting. *Hydrological Processes, 25*(18), 2771-2784.

Harrigan, S., Cloke, H., & Pappenberger, F. (2020). Innovating global hydrological prediction through an Earth system approach. *WMO Bull, 69*, 1.

Harun-ur-Rashid, M. (1990). Estimation of Manning's roughness coefficient for basin and border irrigation. *Agricultural water management, 18*(1), 29-33.

Hashemi-Beni, L., Jones, J., Thompson, G., Johnson, C., & Gebrehiwot, A. (2018). Challenges and opportunities for UAV-based digital elevation model generation for flood-risk management: A case of princeville, north carolina. *Sensors, 18*(11), 3843.

Helderop, E., & Grubesic, T. H. (2019). Social, geomorphic, and climatic factors driving US coastal city vulnerability to storm surge flooding. *Ocean & coastal management, 181*, 104902.

Helmrich, A. M., Ruddell, B. L., Bessem, K., Chester, M. V., Chohan, N., Doerry, E., Eppinger, J., Garcia, M., Goodall, J. L., & Lowry, C. (2021). Opportunities for crowdsourcing in urban flood monitoring. *Environmental Modelling & Software, 143*, 105124.

Henonin, J., Russo, B., Mark, O., & Gourbesville, P. (2013). Real-time urban flood forecasting and modelling–a state of the art. *Journal of Hydroinformatics, 15*(3), 717-736.

Hensen, B., Mackworth-Young, C., Simwinga, M., Abdelmagid, N., Banda, J., Mavodza, C., Doyle, A., Bonell, C., & Weiss, H. (2021). Remote data collection for public health research in a COVID-19 era: ethical implications, challenges and opportunities. *Health Policy and Planning, 36*(3), 360-368.

Hessel, R., Jetten, V., & Guanghui, Z. (2003). Estimating Manning's n for steep slopes. *Catena, 54*(1-2), 77-91.

Hettiachchi, D., Sanderson, M., Goncalves, J., Hosio, S., Kazai, G., Lease, M., Schaekermann, M., & Yilmaz, E. (2021). *Investigating and Mitigating Biases in Crowdsourced Data.* Paper presented at the Companion Publication of the 2021 Conference on Computer Supported Cooperative Work and Social Computing.

Hilft, B. E. (2017). World risk report. *Analysis and prospects 2017*.

Hope Sr, K. R. (2009). Climate change and poverty in Africa. *International Journal of Sustainable Development & World Ecology, 16*(6), 451-461.

Horritt, M. (2006). A methodology for the validation of uncertain flood inundation models. *Journal of Hydrology, 326*(1-4), 153-165.

Horton, R. E. (1939). Analysis of runoff-plat experiments with varying infiltration-capacity. *Eos, Transactions American Geophysical Union, 20*(4), 693-711.

Horton, R. E. (1941). An approach toward a physical interpretation of infiltration-capacity. *Soil science society of America journal, 5*(C), 399-417.

Horton, R. E. (1945). Erosional development of streams and their drainage basins; hydrophysical approach to quantitative morphology. *Geological society of America bulletin, 56*(3), 275-370.

Hu, C., Xia, J., She, D., Song, Z., Zhang, Y., & Hong, S. (2021). A new urban hydrological model considering various land covers for flood simulation. *Journal of Hydrology, 603*, 126833.

Huang, C.-J., Hsu, M.-H., Teng, W.-H., & Wang, Y.-H. (2014). The impact of building coverage in the metropolitan area on the flow calculation. *Water, 6*(8), 2449-2466.

Huizinga, F. (2012). *The economics of flood prevention, A Dutch perspective*. Retrieved from https://www.cpb.nl/sites/default/files/publicaties/download/economics-flood-prevention.pdf

Hung, K.-C., Kalantari, M., & Rajabifard, A. (2016). Methods for assessing the credibility of volunteered geographic information in flood response: A case study in Brisbane, Australia. *Applied Geography, 68*, 37-47.

Hutsul, T., & Smirnov, Y. (2017). Comparative accuracy assessment of global DTM and DTM generated from soviet topographic maps for the purposes of road planning. *Geodesy and Cartography, 43*(4), 173-181.

ICRC. (2011). Disaster Services revised plan *International federation of red Cross and Red Crescent Societies*.

Jain, S. K., Mani, P., Jain, S. K., Prakash, P., Singh, V. P., Tullos, D., Kumar, S., Agarwal, S., & Dimri, A. (2018). A Brief review of flood forecasting techniques and their applications. *International Journal of River Basin Management, 16*(3), 329-344.

Jenkins, K., Surminski, S., Hall, J and Crick, F (2016). Surface water flood risk and management strategies for London: An Agent-Based Model Approach. . *ES3 Web of Conferences. 3rd European Conference on Flood Risk Management. , 7*, 30.

Jenson, S. K., & Domingue, J. O. (1988). Extracting topographic structure from digital elevation data for geographic information system analysis. *Photogrammetric engineering and remote sensing, 54*(11), 1593-1600.

Jeziorska, J. (2019). UAS for wetland mapping and hydrological modeling. *Remote Sensing, 11*(17), 1997.

Jimme, M. A., Bashir, A., & Adebayo, A. A. (2016). Spatial distribution pattern and terrain analysis of urban flash floods and inundated areas in Maiduguri Metropolis, Borno State, Northeast, Nigeria. *Journal of Geographic Information System, 8*(01), 108.

Jochem, A., Höfle, B., Wichmann, V., Rutzinger, M., & Zipf, A. (2012). Area-wide roof plane segmentation in airborne LiDAR point clouds. *Computers, Environment and Urban Systems, 36*(1), 54-64.

Johnson, A. I. (1963). *A field method for measurement of infiltration*: US Government Printing Office.

Joseph, D. D., Nield, D. A., & Papanicolaou, G. (1982). Nonlinear equation governing flow in a saturated porous medium. *Water Resources Research, 18*(4), 1049-1052.

Kalyanapu, A. J., Burian, S. J., McPherson, T. N., & (2009). Effect of land use-based surface roughness on hydrologic model output. *Journal of Spatial hydrology, 9*(2).

Kapetas, L., & Fenner, R. (2020). Integrating blue-green and grey infrastructure through an adaptation pathways approach to surface water flooding. *Philosophical Transactions of the Royal Society A, 378*(2168), 20190204.

Kauffeldt, A., Wetterhall, F., Pappenberger, F., Salamon, P., & Thielen, J. (2016). Technical review of large-scale hydrological models for implementation in operational flood forecasting schemes on continental level. *Environmental Modelling & Software, 75*, 68-76.

Kemp, D. J. (2002). *The development of a rainfall-runoff-routing (RRR) model.*

Keyvanfar, A., Shafaghat, A., & Awanghamat, M. A. (2021). Optimization and Trajectory Analysis of Drone's Flying and Environmental Variables for 3D Modelling the Construction Progress Monitoring. *International Journal of Civil Engineering*, 1-26.

Knight, J., & Evans, M. (2017). The sediment stratigraphy of a flood event: An example from the Sabie River, South Africa. *Catena, 151*, 87-97.

Koenig, T. A., Bruce, J. L., O'Connor, J., McGee, B. D., Holmes Jr, R. R., Hollins, R., Forbes, B. T., Kohn, M. S., Schellekens, M., & Martin, Z. W. (2016). *Identifying and preserving high-water mark data* (2328-7055). Retrieved from

Kraus, K., & Pfeifer, N. (2001). Advanced DTM generation from LIDAR data. *International Archives Of Photogrammetry Remote Sensing And Spatial Information Sciences, 34*(3/W4), 23-30.

Krishi, M. A., & Sule, I. K. (2016). Nigeria: NEMA Rejects N1.3 Billion Budget, Appeals for N15 Billion. *Daily Trust*. Retrieved from https://allafrica.com/stories/201602160925.html

Krivtsov, V., Birkinshaw, S., Arthur, S., Knott, D., Monfries, R., Wilson, K., Christie, D., Chamberlain, D., Brownless, P., & Kelly, D. (2020). Flood resilience, amenity and biodiversity benefits of an historic urban pond. *Philosophical Transactions of the Royal Society A, 378*(2168), 20190389.

Krzhizhanovskaya, V. V., Shirshov, G., Melnikova, N. B., Belleman, R. G., Rusadi, F., Broekhuijsen, B., Gouldby, B. P., Lhomme, J., Balis, B., & Bubak, M. (2011). Flood early warning system:

design, implementation and computational modules. *Procedia Computer Science, 4*, 106-115.

Kumar, & Jain, A. K. (2012). Modified Design of Experimental Setup and Measurement of Permeability of the Sand by Using Darcy's Law.

Kumar, Jain, S. K., & Gurrapu, S. (2020). Challenges and recent developments in flood forecasting in india. *Roorkee Water Conclave*.

Kumar, Samaniego, L., & Attinger, S. (2013). Implications of distributed hydrologic model parameterization on water fluxes at multiple scales and locations. *Water Resources Research, 49*(1), 360-379. doi:10.1029/2012wr012195

Kurniyaningrum, E., Limantara, L. M., Suhartanto, E., & Sisinggih, D. (2019). Development Of Flood Early Warning System Based On The Geoinformatics System In The Krukut River, Jakarta, Indonesia. *Int. J. Civ. Eng. Technol, 10*(2), 1325-1735.

Kutija, V., Bertsch, R., Glenis, V., Alderson, D., Parkin, G., Walsh, C., Robinson, J., & Kilsby, C. (2014). Model validation using crowd-sourced data from a large pluvial flood.

Kvocka, D. (2017). *Modelling elevations, inundation extent and hazard risk for extreme flood events.* Cardiff University.

Leandro, J., Chen, A. S., Djordjević, S., & Savić, D. A. (2009). Comparison of 1D/1D and 1D/2D coupled (sewer/surface) hydraulic models for urban flood simulation. *Journal of Hydraulic Engineering, 135*(6), 495-504.

Lederle, R., Shepard, T., & Meza, V. D. L. V. (2020). Comparison of methods for measuring infiltration rate of pervious concrete. *Construction and Building Materials, 244*, 118339.

Li, G., Zheng, Y., Fan, J., Wang, J., & Cheng, R. (2017). *Crowdsourced data management: Overview and challenges.* Paper presented at the Proceedings of the 2017 ACM International Conference on Management of Data.

Li, X., & Willems, P. (2020). A hybrid model for fast and probabilistic urban pluvial flood prediction. *Water Resources Research, 56*(6), e2019WR025128.

Liao, K.-H. (2012). A theory on urban resilience to floods—a basis for alternative planning practices. *Ecology and Society, 17*(4).

Liu, Liu, Y., Wang, X., Yu, D., Liu, K., Huang, H., & Hu, G. (2015). Developing an effective 2-D urban flood inundation model for city emergency management based on cellular automata. *Nat. Hazards Earth Syst. Sci, 15*(3), 381-391.

Looper, J. P., & Vieux, B. E. (2012). An assessment of distributed flash flood forecasting accuracy using radar and rain gauge input for a physics-based distributed hydrologic model. *Journal of Hydrology, 412*, 114-132.

Macamo, C. (2021). After Idai: Insights from Mozambique for Climate Resilient Coastal Infrastructure. *Policy Insights: African perspectives-Global insights, 110*, 1-22.

Maidment, D. R. (1993). *Handbook of hydrology* (Vol. 9780070): McGraw-Hill New York.

Manfreda, S., Nardi, F., Samela, C., Grimaldi, S., Taramasso, A. C., Roth, G., & Sole, A. (2014). Investigation on the use of geomorphic approaches for the delineation of flood prone areas. *Journal of Hydrology, 517*, 863-876.

Manfreda, S., Samela, C., Gioia, A., Consoli, G. G., Iacobellis, V., Giuzio, L., Cantisani, A., & Sole, A. (2015). Flood-prone areas assessment using linear binary classifiers based on flood maps obtained from 1D and 2D hydraulic models. *Natural Hazards, 79*(2), 735-754.

Mani, M. M., Keen, M. M., & Freeman, M. P. K. (2003). *Dealing with increased risk of natural disasters: challenges and options*: International Monetary Fund.

Mark, O., Weesakul, S., Apirumanekul, C., Aroonnet, S. B., & Djordjević, S. (2004). Potential and limitations of 1D modelling of urban flooding. *Journal of Hydrology, 299*(3-4), 284-299.

Martins, S. M. (2006). Validation of Simulation Based Models A Theoretical Outlook. *The Electronic Journal of Business Research Methods, 4*(1), 39-46.

Martz, L. W., & Garbrecht, J. (1993). Automated extraction of drainage network and watershed data from digital elevation models 1. *JAWRA Journal of the American Water Resources Association, 29*(6), 901-908.

Martz, L. W., & Garbrecht, J. (1999). An outlet breaching algorithm for the treatment of closed depressions in a raster DEM. *Computers & geosciences, 25*(7), 835-844.

Mason, D. C., Bates, P., & Dall'Amico, J. (2009). Calibration of uncertain flood inundation models using remotely sensed water levels. *Journal of Hydrology, 368*(1-4), 224-236.

Mavandadi, S., Dimitrov, S., Feng, S., Yu, F., Yu, R., Sikora, U., & Ozcan, A. (2012). Crowd-sourced BioGames: managing the big data problem for next-generation lab-on-a-chip platforms. *Lab on a Chip, 12*(20), 4102-4106.

McClean, F., Dawson, R., & Kilsby, C. (2020). Implications of using global digital elevation models for flood risk analysis in cities. *Water Resources Research, 56*(10), e2020WR028241.

McCullough, C. M. (2011). *Building a replicable flood forecast mitigation support system to simplify emergency decision-making.* University of Toledo.

McLuckie, D., Kandasamy, J., & Sayers, P. (2018). Strategic management of flood risk to communities *Strategic Management of Flood Risk* (pp. 13-31): ICE Publishing.

McSharry, P. (2018). Parsimonious risk assessment and the role of transparent diverse models *Risk modeling for hazards and disasters* (pp. 263-269): Elsevier.

Md Ali, A., Solomatine, D., & Di Baldassarre, G. (2015). Assessing the impact of different sources of topographic data on 1-D hydraulic modelling of floods. *Hydrology and Earth System Sciences, 19*(1), 631-643.

Meek, S., Jackson, M. J., & Leibovici, D. G. (2014). A flexible framework for assessing the quality of crowdsourced data.

Mees, H., Crabbé, A., Alexander, M., Kaufmann, M., Bruzzone, S., Lévy, L., & Lewandowski, J. (2016). Coproducing flood risk management through citizen involvement: insights from cross-country comparison in Europe. *Ecology and Society, 21*(3).

Meierdiercks, K. L., Smith, J. A., Baeck, M. L., & Miller, A. J. (2010). Analyses of Urban Drainage Network Structure and its Impact on Hydrologic Response 1. *JAWRA Journal of the American Water Resources Association, 46*(5), 932-943.

Meijer, E. (2015). Structure from Motion as documentation technique for Rock Art. *Adoranten*, 66.

Metzakis, M. (2019). Drone Photography Part 2: Tips for Getting Started with Drone Photography. *PSA Journal, 85*(11), 34-38.

Miguez, M. G., Rezende, O. M., & Veról, A. P. (2015). City growth and urban drainage alternatives: Sustainability challenge. *Journal of Urban Planning and Development, 141*(3), 04014026.

Milanesi, L., Pilotti, M., Belleri, A., Marini, A., & Fuchs, S. (2018). Vulnerability to flash floods: a simplified structural model for masonry buildings. *Water Resources Research, 54*(10), 7177-7197.

Minh, Q. T., Pham-Nguyen, H.-N., Tan, H. M., & Long, N. X. (2019). *Traffic congestion estimation based on crowd-sourced data.* Paper presented at the 2019 International Conference on Advanced Computing and Applications (ACOMP).

Mizutori, M., & Guha-Sapir, D. (2020). Human Cost of Disasters: An Overview of the Last 20 years (2000-2019). *Centre for Research on the Epidemiology of Disasters (CRED) and United Nations Office for Disaster Risk Reduction (UNDRR), Belgium and Switzerland*.

Mollerup, M., & Hansen, S. (2007). Power series solution for falling head ponded infiltration with evaporation. *Water Resources Research, 43*(3).

Moore, I. D., Grayson, R., & Ladson, A. (1991). Digital terrain modelling: a review of hydrological, geomorphological, and biological applications. *Hydrological Processes, 5*(1), 3-30.

Moriasi, D. N., Arnold, J. G., Van Liew, M. W., Bingner, R. L., Harmel, R. D., & Veith, T. L. (2007). Model evaluation guidelines for systematic quantification of accuracy in watershed simulations. *Transactions of the Asabe, 50*(3), 885-900.

Morse, J. M. (2000). Determining sample size (Vol. 10, pp. 3-5): Sage Publications Sage CA: Thousand Oaks, CA.

Mousa, M., Zhang, X., & Claudel, C. (2016). Flash flood detection in urban cities using ultrasonic and infrared sensors. *IEEE Sensors Journal, 16*(19), 7204-7216.

Muhadi, N. A., Abdullah, A. F., Bejo, S. K., Mahadi, M. R., & Mijic, A. (2020). The use of LiDAR-derived DEM in flood applications: A review. *Remote Sensing, 12*(14), 2308.

Nash, J. E., & Sutcliffe, J. V. (1970). River flow forecasting through conceptual models part I — A discussion of principles. *Journal of Hydrology, 10*, 282-290.

Nasr, A., & Hynds, P. 10-SMALL CATCHMENT HYDRODYNAMIC MODELLING: COMPARING THREE MODELLING APPROACHES.

NBS. (2020). *Nigeria Bureau of Statistics Population of Nigeria*. Retrieved from https://nigerianstat.gov.ng/elibrary?queries=population

Nhangumbe, M., Nascetti, A., Georganos, S., & Ban, Y. (2023). Supervised and unsupervised machine learning approaches using Sentinel data for flood mapping and damage assessment in Mozambique. *Remote Sensing Applications: Society and Environment*, 101015.

Nkwunonwo, U., Whitworth, M., & Baily, B. (2016). A review and critical analysis of the efforts towards urban flood risk management in the Lagos region of Nigeria. *Natural Hazards and Earth System Sciences, 16*(2), 349-369.

NOAA. (2012). National Oceanic and Atmospheric Administration (NOAA) Coastal Services Center. 2012. "Lidar 101: An Introduction to Lidar Technology, Data, and Applications." Revised. Charleston, SC: NOAA Coastal Services Center. Retrieved from https://coast.noaa.gov/data/digitalcoast/pdf/lidar-101.pdf

Notti, D., Giordan, D., Calo, F., Pepe, A., Zucca, F., & Galve, J. P. (2018). Potential and Limitations of Open Satellite Data for Flood Mapping. *Remote Sensing, 10*(11). doi:10.3390/rs10111673

Obiefuna, J., Adeaga, O., Omojola, A., Atagbaza, A., & Okolie, C. (2021). Flood risks to urban development on a coastal barrier landscape of Lekki Peninsula in Lagos, Nigeria. *Scientific African, 12*, e00787.

Ojigi, M., Abdulkadir, F., & Aderoju, M. (2013). *Geospatial mapping and analysis of the 2012 flood disaster in central parts of Nigeria.* Paper presented at the 8th National GIS Symposium. Dammam. Saudi Arabia.

Olukanni, D. O., & Salami, A. W. (2012). Assessment of impact of hydropower dams reservoir outflow on the downstream river flood regime–Nigeria's experience. *Hydropower-practice and application, 36*, 61-82.

Onyutha, C. (2016). Influence of hydrological model selection on simulation of moderate and extreme flow events: a case study of the Blue Nile basin. *Advances in Meteorology, 2016*.

Orupabo, S. (2008). Coastline Migration in Nigeria. Retrieved 12 June 2019 from Hydro International: Surveying in all waters.

Ouarzeddine, M., & Belhadj-Aissa, A. (2004). Generation of digital elevation model using InSAR.
Ouarzeddine, M. S. (2002). *Generation of Digital Terrain Models using polarimetric SAR interferometry*.
Oudin, L., Kay, A., Andréassian, V., & Perrin, C. (2010). Are seemingly physically similar catchments truly hydrologically similar? *Water Resources Research, 46*(11).
Oudin, L., Salavati, B., Furusho-Percot, C., Ribstein, P., & Saadi, M. (2018). Hydrological impacts of urbanization at the catchment scale. *Journal of Hydrology, 559*, 774-786.
Pagano, T., Elliott, J., Anderson, B., & Perkins, J. (2016). Australian bureau of meteorology flood forecasting and warning *Flood Forecasting* (pp. 3-40): Elsevier.
Parker, Priest, S. J., & McCarthy, S. (2011). Surface water flood warnings requirements and potential in England and Wales. *Applied Geography, 31*(3), 891-900.
Parker, Tunstall, S., & Wilson, T. (2005). Socio-economic benefits of flood forecasting and warning. *Flood Hazard Research Centre, Middlesex University, Queensway, Enfield, London, UK*.
Parvin, G. A., Esraz-Ul-Zannat, M., Ahsan, R., & Islam, I. (2022). Disaster Risks and Resilience of Urban Bangladesh: Role of Blue-Green Infrastructure *Blue-Green Infrastructure Across Asian Countries: Improving Urban Resilience and Sustainability* (pp. 419-440): Springer.
Pender, G., & ELZ, S. N. (2011). 12 Flood Inundation Modelling to Support Flood Risk Management. *Flood risk science and management*, 234.
Pengel, B., Krzhizhanovskaya, V., Melnikova, N., Shirshov, G., Koelewijn, A., Pyayt, A., & Mokhov, I. (2013). Flood early warning system: sensors and internet. *IAHS Red Book, 357*, 445-453.
Petty, T. R., Noman, N., Ding, D., & Gongwer, J. B. (2016). Flood forecasting GIS water-flow visualization enhancement (WaVE): A case study. *Journal of Geographic Information System, 8*(06), 692.
Pfeifer, N., & Mandlburger, G. (2017). LiDAR data filtering and DTM generation *Topographic Laser Ranging and Scanning* (pp. 307-334): CRC Press.
Philip, J. R. (1969). Theory of infiltration *Advances in hydroscience* (Vol. 5, pp. 215-296): Elsevier.
Pina, R., Ochoa-Rodriguez, S., Simões, N., Mijic, A., Sa Marques, A., & Maksimovic, Č. (2014). Semi-distributed or fully distributed rainfall-runoff models for urban pluvial flood modelling?
Polat, & Uysal, M. (2017). Dtm Generation with Uav Based Photogrammetric Point Cloud. *ISPRS - International Archives of the Photogrammetry, Remote Sensing and Spatial Information Sciences, XLII-4/W6*, 77-79. doi:10.5194/isprs-archives-XLII-4-W6-77-2017
Polat, N., & Uysal, M. (2015). Investigating performance of Airborne LiDAR data filtering algorithms for DTM generation. *Measurement, 63*, 61-68.
Pratomo, R. (2016). *Sensitivity analysis of flash-flood modelling in Grenada, as a small island Caribbean states.* Paper presented at the AIP Conference Proceedings.
Prokic, M. N., Savić, S., & Pavić, D. (2019). Pluvial flooding in urban areas across the European continent. *Geographica Pannonica, 23*(4).
Qi, W., Ma, C., Xu, H., Chen, Z., Zhao, K., & Han, H. (2021). A review on applications of urban flood models in flood mitigation strategies. *Natural Hazards, 108*(1), 31-62.
Rahman, R., & Salehin, M. (2013). Flood risks and reduction approaches in Bangladesh. *Disaster risk reduction approaches in Bangladesh*, 65-90.
Rakotosaona, M. J., La Barbera, V., Guerrero, P., Mitra, N. J., & Ovsjanikov, M. (2020). *Pointcleannet: Learning to denoise and remove outliers from dense point clouds.* Paper presented at the Computer Graphics Forum.

Ramadas, M., Maity, R., Ojha, R., & Govindaraju, R. S. (2015). Predictor selection for streamflows using a graphical modeling approach. *Stochastic environmental research and risk assessment, 29*, 1583-1599.

Ramsbottom, D., & Wicks, J. (2003). Catchment Flood Management Plans: guidance on selection of appropriate hydraulic modelling methods. *Environment Agency, Bristol, UK*.

Reduction, U. O. f. D. R. (2020). The human cost of disasters—an overview of the last 20 years 2000–2019.

Reeves, G., Freidel, R., Chen, Y., Koller, J., & Henderson, M. (2008). *The Los Alamos. confEic Radiation Environment Assimilation Model (DREAM) for Space Weather Specification and Forecasting.* Paper presented at the Advanced Maui Optical and Space Surveillance Technologies Conference.

Reeves, G. D., Chen, Y., Cunningham, G., Friedel, R., Henderson, M. G., Jordanova, V., Koller, J., Morley, S., Thomsen, M., & Zaharia, S. (2012). Dynamic radiation environment assimilation model: DREAM. *Space Weather, 10*(3), 1-25.

Refsgaard, J. C. (1997). Parameterisation, calibration and validation of distributed hydrological models. *Journal of Hydrology, 198*, 69-97.

Restas, A. (2015). Drone applications for supporting disaster management. *World Journal of Engineering and Technology, 3*(03), 316.

Revilla-Romero, B., Beck, H. E., Burek, P., Salamon, P., de Roo, A., & Thielen, J. (2015). Filling the gaps: Calibrating a rainfall-runoff model using satellite-derived surface water extent. *Remote Sensing of Environment, 171*, 118-131. doi:10.1016/j.rse.2015.10.022

Ritter, A., & Munoz-Carpena, R. (2013). Performance evaluation of hydrological models: Statistical significance for reducing subjectivity in goodness-of-fit assessments. *Journal of Hydrology, 480*, 33-45. doi:10.1016/j.jhydrol.2012.12.004

Rizaldy, A., Persello, C., Gevaert, C., & Oude Elberink, S. (2018). FULLY CONVOLUTIONAL NETWORKS FOR GROUND CLASSIFICATION FROM LIDAR POINT CLOUDS. *ISPRS Annals of Photogrammetry, Remote Sensing & Spatial Information Sciences, 4*(2).

Roberts, N. M., Cole, S. J., Forbes, R. M., Moore, R. J., & Boswell, D. (2009). Use of high-resolution NWP rainfall and river flow forecasts for advance warning of the Carlisle flood, north-west England. *Meteorological Applications: A journal of forecasting, practical applications, training techniques and modelling, 16*(1), 23-34.

Rose, A., Shakurideen, O., Kolawole, M., Davies, N., Ayejuyo, O., Friday, A., & Ogbe, R. (2017). An investigation of the role of vegetation as a determinant of the vertical distribution of soil organic carbon. *Journal of Emerging Trends in Engineering and Applied Sciences, 8*(1), 43-53.

Roth, D., Warner, J., & Winnubst, M. (2021). Room for the river, no room for conflict: Narratives of participation, win-win, consensus, and co-creation in Dutch spatial flood risk management *Split Waters* (pp. 69-92): Routledge India.

Saksena, S., Dey, S., Merwade, V., & Singhofen, P. J. (2020). A computationally efficient and physically based approach for urban flood modeling using a flexible spatiotemporal structure. *Water Resources Research, 56*(1), e2019WR025769.

Sanders, B. F., Schubert, J. E., Goodrich, K. A., Houston, D., Feldman, D. L., Basolo, V., Luke, A., Boudreau, D., Karlin, B., & Cheung, W. (2020). Collaborative modeling with fine-resolution data enhances flood awareness, minimizes differences in flood perception, and produces actionable flood maps. *Earth's Future, 8*(1), e2019EF001391.

Sayers, P. B., Horritt, M., Penning-Rowsell, E., & Feith, J. (2017). Present and future flood vulnerability, risk and disadvantage: A UK scale assessment.

Schröter, K., Ostrowski, M., Gocht, M., Kahl, B., Nachtnebel, H., Corral, C., & Sempere-Torres, D. (2009). EWASE—early warning systems efficiency: evaluation of flood forecast reliability. *EWASE–Early Warning Systems Efficiency, CRUE*.

Schumann, G. P., Vernieuwe, H., De Baets, B., & Verhoest, N. (2014). ROC-based calibration of flood inundation models. *Hydrological Processes, 28*(22), 5495-5502.

Seleem, O., Ayzel, G., de Souza, A. C. T., Bronstert, A., & Heistermann, M. (2022). Towards urban flood susceptibility mapping using data-driven models in Berlin, Germany. *Geomatics, Natural Hazards and Risk, 13*(1), 1640-1662.

Serifoglu Yilmaz, C., & Gungor, O. (2018). Comparison of the performances of ground filtering algorithms and DTM generation from a UAV-based point cloud. *Geocarto International, 33*(5), 522-537.

Shean, D. E., Alexandrov, O., Moratto, Z. M., Smith, B. E., Joughin, I. R., Porter, C., & Morin, P. (2016). An automated, open-source pipeline for mass production of digital elevation models (DEMs) from very-high-resolution commercial stereo satellite imagery. *ISPRS Journal of Photogrammetry and Remote Sensing, 116*, 101-117.

Sholihah, Q., Kuncoro, W., Wahyuni, S., Suwandi, S. P., & Feditasari, E. D. (2020). *The analysis of the causes of flood disasters and their impacts in the perspective of environmental law.* Paper presented at the IOP Conference Series: Earth and Environmental Science.

Short, D., Dawes, W. R., & White, I. (1995). The practicability of using Richards' equation for general purpose soil-water dynamics models. *Environment International, 21*(5), 723-730.

Sithole, G., & Vosselman, G. (2004). Experimental comparison of filter algorithms for bare-Earth extraction from airborne laser scanning point clouds. *ISPRS Journal of Photogrammetry and Remote Sensing, 59*(1-2), 85-101.

Smith, M. J., Edwards, E. P., Priestnall, G., & Bates, P. (2006). Exploitation of new data types to create digital surface models for flood inundation modelling. *FRMRC Research Rep. UR3, 86*.

Solaimani, K. (2009). Flood forecasting based on geographical information system. *African Journal of Agricultural Research, 4*(10), 950-956.

Somerville, P. (2020). The continuing failure of UK climate change mitigation policy. *Critical Social Policy*, 0261018320961762.

Soram, R., Roy, S., Singh, S. R., Khomdram, M., Yaikhom, S., & Takhellambam, S. (2013). On the Rate of Convergence of Newton-Raphson Method. *The International Journal of Engineering and Science (IJES), 2*(11), 05-12.

Soz, S. A., Kryspin-Watson, J., & Stanton-Geddes, Z. (2016). The role of green infrastructure solutions in urban flood risk management.

Stamataki, I., & Kjeldsen, T. R. (2021). Reconstructing the peak flow of historical flood events using a hydraulic model: The city of Bath, United Kingdom. *Journal of Flood Risk Management, 14*(3), e12719.

Stephens, E., Bates, P., Freer, J., & Mason, D. (2012). Calibration of flood inundation models using uncertain satellite observed water levels. *J Hydrol. doi, 10*.

Su, W., Ye, G., Yao, S., & Yang, G. (2014). Urban land pattern impacts on floods in a new district of China. *Sustainability, 6*(10), 6488-6508.

Sukojo, B. M., Hayati, N., & Usriyah, B. S. a. (2021). *Comparative Analysis of DTM Results with Hydro Enforcement LiDAR Data Method and Interferometric Synthetic Aperture Radar (InSAR) from Radar Satellite Imagery (Case Study of Kebumen Regency).* Paper presented at the IOP Conference Series: Earth and Environmental Science.

Syme, B. (2011). *Pros and Cons of 1D and 2D Modelling*. Paper presented at the Floodplain Management Assocoation Conference, San Diego, USA. https://www.tuflow.com/Download/Presentations/Syme.Pros%20and%20Cons%20of%201D%20and%202D%20Modelling.FMA,%20San%20Diego,%202011.pdf

Takaku, J., Tadono, T., & Tsutsui, K. (2014). GENERATION OF HIGH RESOLUTION GLOBAL DSM FROM ALOS PRISM. *ISPRS Annals of Photogrammetry, Remote Sensing & Spatial Information Sciences, 2*(4).

Taylor, D. C., Pawar, V., Kruzikas, D., Gilmore, K. E., Pandya, A., Iskandar, R., & Weinstein, M. C. (2010). Methods of model calibration. *Pharmacoeconomics, 28*(11), 995-1000.

Theobald, D. M., Norman, J. B., Peterson, E., Ferraz, S., Wade, A., & Sherburne, M. (2006). Functional Linkage of Water basins and Streams (FLoWS) v1 User's Guide: ArcGIS tools for Network-based analysis of freshwater ecosystems. *Natural Resource Ecology Lab, Colorado State University, Fort Collins, CO, 43*.

Thorne, C. R. (2020). *Blue–Green Cities: Integrating urban flood risk management with green infrastructure*: ICE Publishing.

Tiwari, V., Kumar, V., Matin, M. A., Thapa, A., Ellenburg, W. L., Gupta, N., & Thapa, S. (2020). Flood inundation mapping-Kerala 2018; Harnessing the power of SAR, automatic threshold detection method and Google Earth Engine. *Plos one, 15*(8), e0237324.

Toté, C., Patricio, D., Boogaard, H., Van Der Wijngaart, R., Tarnavsky, E., & Funk, C. (2015). Evaluation of satellite rainfall estimates for drought and flood monitoring in Mozambique. *Remote Sensing, 7*(2), 1758-1776.

Tran, Dwelle, M. C., Sargsyan, K., Ivanov, V. Y., & Kim, J. (2020). A novel modeling framework for computationally efficient and accurate real-time ensemble flood forecasting with uncertainty quantification. *Water Resources Research, 56*(3), e2019WR025727.

Trepekli, K., Balstrøm, T., Friborg, T., Fog, B., Allotey, A. N., Kofie, R. Y., & Møller-Jensen, L. (2022). UAV-borne, LiDAR-based elevation modelling: a method for improving local-scale urban flood risk assessment. *Natural Hazards, 113*(1), 423-451.

Tsai, V. J. (1993). Delaunay triangulations in TIN creation: an overview and a linear-time algorithm. *International Journal of Geographical Information Science, 7*(6), 501-524.

TSM. (2009). *Traffic Signs manual: Chapter 8- Traffic Safety Measures and Signs for Road Works and Temporary Situations*. United Kingdom: Department for Transport/Highways Agency

Retrieved from https://assets.publishing.service.gov.uk/government/uploads/system/uploads/attachment_data/file/203669/traffic-signs-manual-chapter-08-part-01.pdf.

Ugwu, C. F., Ugwu, C. S., & Ogba, K. T. (2021). Institutional Response and Mechanisms to the Management of Natural Disaster in Nigeria *Economic Effects of Natural Disasters* (pp. 381-396): Elsevier.

Unduche, F., Tolossa, H., Senbeta, D., & Zhu, E. (2018). Evaluation of four hydrological models for operational flood forecasting in a Canadian Prairie watershed. *Hydrological Sciences Journal-Journal Des Sciences Hydrologiques, 63*(8), 1133-1149. doi:10.1080/02626667.2018.1474219

Urama, K. C., & Ozor, N. (2010). Impacts of climate change on water resources in Africa: the role of adaptation. *African Technology Policy Studies Network, 29*, 1-29.

Uysal, M., Toprak, A. S., & Polat, N. (2015). DEM generation with UAV Photogrammetry and accuracy analysis in Sahitler hill. *Measurement, 73*, 539-543.

Valette, G., Prévost, S., Lucas, L., & Léonard, J. (2006). SoDA project: A simulation of soil surface degradation by rainfall. *Computers & Graphics, 30*(4), 494-506.
Van Slobbe, E., de Vriend, H. J., Aarninkhof, S., Lulofs, K., de Vries, M., & Dircke, P. (2013). Building with Nature: in search of resilient storm surge protection strategies. *Natural Hazards, 66*, 1461-1480.
Vieux, B. E., & Bedient, P. B. (2004). Assessing urban hydrologic prediction accuracy through event reconstruction. *Journal of Hydrology, 299*(3-4), 217-236.
Vosselman, G. (2013). Point cloud segmentation for urban scene classification. *Int. Arch. Photogramm. Remote Sens. Spat. Inf. Sci, 1*(257-262), 1.
Vrugt, J. A., & de Oliveira, D. Y. (2022). Confidence intervals of the Kling-Gupta efficiency. *Journal of Hydrology, 612*, 127968.
Wahlstrom, M. (2015). *Sendai Framework for Action (2015-2030)* Retrieved from https://www.preventionweb.net/files/43291_sendaiframeworkfordrren.pdf
Wainwright, J., & Mulligan, M. (2013). *Environmental modelling: finding simplicity in complexity*: John Wiley & Sons.
Wallace, C. W., McCarty, G., Lee, S., Brooks, R. P., Veith, T. L., Kleinman, P. J., & Sadeghi, A. M. (2018). Evaluating concentrated flowpaths in riparian forest buffer contributing areas using LiDAR imagery and topographic metrics. *Remote Sensing, 10*(4), 614.
Wang, J., Xu, K., Liu, L., Cao, J., Liu, S., Yu, Z., & Gu, X. D. (2013). *Consolidation of low-quality point clouds from outdoor scenes.* Paper presented at the Computer Graphics Forum.
Werner, M., Reggiani, P., Roo, A. D., Bates, P., & Sprokkereef, E. (2005). Flood forecasting and warning at the river basin and at the European scale. *Natural Hazards, 36*(1), 25-42.
Wijayarathne, D. B., & Coulibaly, P. (2020). Identification of hydrological models for operational flood forecasting in St. John's, Newfoundland, Canada. *Journal of Hydrology: Regional Studies, 27*, 100646.
Williams, J., Jose, R., Moobela, C., Hutchinson, D., Wise, R., & Gaterell, M. (2019). Residents' perceptions of sustainable drainage systems as highly functional blue green infrastructure. *Landscape and Urban Planning, 190*, 103610.
Wing, O. E., Bates, P. D., Neal, J. C., Sampson, C. C., Smith, A. M., Quinn, N., Shustikova, I., Domeneghetti, A., Gilles, D. W., & Goska, R. (2019). A new automated method for improved flood defense representation in large-scale hydraulic models. *Water Resources Research, 55*(12), 11007-11034.
WMO. (1992). International glossary of hydrology.
WMO. (2011). Manual on Flood Forecasting and Warning *WMO*.
Wu, Y., Peng, F., Peng, Y., Kong, X., Liang, H., & Li, Q. (2019). Dynamic 3D Simulation of Flood Risk Based on the Integration of Spatio-Temporal GIS and Hydrodynamic Models. *ISPRS International Journal of Geo-Information, 8*(11), 520.
Xie, J., Wu, C., Li, H., & Chen, G. (2017). Study on storm-water management of grassed swales and permeable pavement based on SWMM. *Water, 9*(11), 840.
Xu, Z., Wu, L., Shen, Y., Li, F., Wang, Q., & Wang, R. (2014). Tridimensional reconstruction applied to cultural heritage with the use of camera-equipped UAV and terrestrial laser scanner. *Remote Sensing, 6*(11), 10413-10434.
Yaseen, A., Lu, J., & Chen, X. (2022). Flood susceptibility mapping in an arid region of Pakistan through ensemble machine learning model. *Stochastic environmental research and risk assessment, 36*(10), 3041-3061.
Yazdi, J. (2018). Rehabilitation of urban drainage systems using a resilience-based approach. *Water Resources Management, 32*, 721-734.

Ye, C., Xu, Z., Lei, X., Liao, W., Ding, X., & Liang, Y. (2022). Assessment of urban flood risk based on data-driven models: A case study in Fuzhou City, China. *International Journal of Disaster Risk Reduction, 82*, 103318.

Yin, J., Yu, D., & Wilby, R. (2016). Modelling the impact of land subsidence on urban pluvial flooding: A case study of downtown Shanghai, China. *Science of the Total Environment, 544*, 744-753.

Yu, & Coulthard, T. J. (2015). Evaluating the importance of catchment hydrological parameters for urban surface water flood modelling using a simple hydro-inundation model. *Journal of Hydrology, 524*, 385-400.

Yu, & Lane, S. N. (2006). Urban fluvial flood modelling using a two-dimensional diffusion-wave treatment, part 2: development of a sub-grid-scale treatment. *Hydrological Processes: An International Journal, 20*(7), 1567-1583.

Yu, & Lane, S. N. (2011). Interactions between subgrid-scale resolution, feature representation and grid-scale resolution in flood inundation modelling. *Hydrological Processes, 25*(1), 36-53. doi:10.1002/hyp.7813

Yu, Yin, J., & Liu, M. (2016). Validating city-scale surface water flood modelling using crowd-sourced data. *Environmental Research Letters, 11*(12), 124011. doi:10.1088/1748-9326/11/12/124011

Yu, D., Guan, M., Wilby, R., Bruce, W., & Szegner, M. (2017). *Piloting a real-time surface water flood nowcasting system for enhancing operational resilience of emergency responders.* Paper presented at the EGU General Assembly Conference Abstracts.

Yu, D., Yin, J., & Liu, M. (2016). Validating city-scale surface water flood modelling using crowd-sourced data. *Environmental Research Letters, 11*(12), 124011.

Zanardi, R. P., Rolim, S. B., De Souza, S. F., Maranhão, M. R., & De Souza Filho, C. R. (2011). DTM generation from a stereo pair acquired by the China–Brazilian Earth Resources Satellite (CBERS-2) and quality control of the altimetric information. *International Journal of Remote Sensing, 32*(16), 4683-4694.

Zhang, Gerke, M., Vosselman, G., & Yang, M. (2018). FILTERING PHOTOGRAMMETRIC POINT CLOUDS USING STANDARD LIDAR FILTERS TOWARDS DTM GENERATION. *ISPRS Annals of Photogrammetry, Remote Sensing & Spatial Information Sciences, 4*(2).

Zhang, Zhao, D., Chen, J., Wang, H., & Wang, H. (2008). Application of Chicago rainfall process line model in the simulation of drainage system. *Water and Wastewater Engineering, 34*, 354.

Zhao, G., Pang, B., Xu, Z., Peng, D., & Xu, L. (2019). Assessment of urban flood susceptibility using semi-supervised machine learning model. *Science of the Total Environment, 659*, 940-949.

Zwęgliński, T. (2020). The use of drones in disaster aerial needs reconnaissance and damage assessment–three-dimensional modeling and orthophoto map study. *Sustainability, 12*(15), 6080.